Fractional Stochastic Dynamics in Structural Stability Analysis

by

Jian Deng

A thesis
presented to the University of Waterloo
in fulfilment of the
thesis requirement for the degree of
Doctor of Philosophy
in
Civil Engineering

Waterloo, Ontario, Canada, 2013

Author's Declaration

I hereby declare that I am the sole author of this thesis. This is a true copy of the thesis, including any required final revisions, as accepted by my examiners.

I understand that my thesis may be made electronically available to the public.

Abstract

The objective of this thesis is to develop a novel methodology of fractional stochastic dynamics to study stochastic stability of viscoelastic systems under stochastic loadings.

Numerous structures in civil engineering are driven by dynamic forces, such as seismic and wind loads, which can be described satisfactorily only by using probabilistic models, such as white noise processes, real noise processes, or bounded noise processes. Viscoelastic materials exhibit time-dependent stress relaxation and creep; it has been shown that fractional calculus provide a unique and powerful mathematical tool to model such a hereditary property. Investigation of stochastic stability of viscoelastic systems with fractional calculus frequently leads to a parametrized family of fractional stochastic differential equations of motion. Parametric excitation may cause parametric resonance or instability, which is more dangerous than ordinary resonance as it is characterized by exponential growth of the response amplitudes even in the presence of damping.

The Lyapunov exponents and moment Lyapunov exponents provide not only the information about stability or instability of stochastic systems, but also how rapidly the response grows or diminishes with time. Lyapunov exponents characterizes sample stability or instability. However, this sample stability cannot assure the moment stability. Hence, to obtain a complete picture of the dynamic stability, it is important to study both the top Lyapunov exponent and the moment Lyapunov exponent. Unfortunately, it is very difficult to obtain the accurate values of theses two exponents. One has to resort to numerical and approximate approaches.

The main contributions of this thesis are: (1) A new numerical simulation method is proposed to determine moment Lyapunov exponents of fractional stochastic systems, in which three steps are involved: discretization of fractional derivatives, numerical solution of the fractional equation, and an algorithm for calculating Lyapunov exponents from small data sets. (2) Higher-order stochastic averaging method is developed and applied to investigate stochastic stability of fractional viscoelastic single-degree-of-freedom structures under white noise, real noise, or bounded noise excitation. (3) For two-degree-of-freedom coupled non-gyroscopic and gyroscopic viscoelastic systems under random excitation, the

Stratonovich equations of motion are set up, and then decoupled into four-dimensional Itô stochastic differential equations, by making use of the method of stochastic averaging for the non-viscoelastic terms and the method of Larionov for viscoelastic terms. An elegant scheme for formulating the eigenvalue problems is presented by using Khasminskii and Wedig's mathematical transformations from the decoupled Itô equations. Moment Lyapunov exponents are approximately determined by solving the eigenvalue problems through Fourier series expansion. Stability boundaries, critical excitations, and stability index are obtained. The effects of various parameters on the stochastic stability of the system are discussed. Parametric resonances are studied in detail. Approximate analytical results are confirmed by numerical simulations.

Acknowledgments

First and foremost, I like to express my sincere appreciation to my supervisors, Professor Wei-Chau Xie and Professor Mahesh D Pandey, for their valuable advice, support and encouragement. I wish to thank them for introducing me to Waterloo, to the famous "Waterloo School", and to the novel, exciting, and challenging field of research.

I would like to extend my sincere gratitude to my committee members, Professor Scott Walbridge, Professor Jeffrey West, Professor Xinzhi Liu, and Professor Lei Xu, for their insightful comments and cares for my research. I am grateful to Professor N. Sri Namachchivaya from the University of Illinois at Urbana-Champaign, for agreeing to serve on my thesis committee as an external examiner and for carefully reading my thesis and making some encouraging comments. I also wish to thank Professors Robert Gracie, Sriram Narasimhan, Bryan Tolson, John Shortreed, and Arnold Yuan for their comments and cares for my research.

Thanks also go to my friends in the mechanics and structural engineering group, with whom I shared many unforgettable days.

The financial support by the Natural Sciences and Engineering Research Council of Canada (NSERC) and the University Network of Excellence in Nuclear Engineering (UNENE) in the form of a Research Assistantship is greatly appreciated.

TO

My Family

Contents

List of Figures xv

1 Introduction 1

1.1 Stochastic Stability of Structures 1

1.1.1 Motivations 1

1.1.2 Gyroscopic Systems 2

1.1.3 Stochastic Stability 4

1.1.4 Lyapunov Exponents and Moment Lyapunov Exponents 7

1.2 Noise Models and Stochastic Differential Equations 10

1.2.1 Noise Models 10

1.2.2 Stochastic Differential Equations 13

1.2.3 Approximation of a Physical Process by a Diffusion Process 16

1.2.4 Numerical Methods for Solving SDEs 17

1.2.5 Stochastic Averaging Method for Approximating SDEs 18

1.3 Ordinary Viscoelasticity & Fractional Viscoelasticity 22

1.3.1 Fractional Calculus 22

1.3.2 Viscoelasticity 24

1.4 Scopes of the Research 29

2 A Numerical Method for Moment Lyapunov Exponents of Fractional Systems **31**

2.1 Exponential Kernel and Power Kernel 31

2.2 Numerical Determination of Moment Lyapunov Exponents of Fractional Systems 33

2.2.1 Numerical Discretization of Fractional Derivatives 33
2.2.2 Determination of the pth Moment of Response Variables 35
2.2.3 Determination of the pth Moment Lyapunov Exponent 37
2.2.4 Procedure for Numerical Determination of Moment Lyapunov Exponents of Fractional Systems 40
2.3 Summary 42

3 Higher-Order Stochastic Averaging Analysis of SDOF Fractional Viscoelastic Systems 44
3.1 Formulation 44
3.2 Stochastic Averaging Method for Fractional Differential Equations 46
3.3 Fractional Viscoelastic Systems Under Wide-band Noise 48
3.3.1 First-Order Averaging Analysis 48
3.3.2 Second-Order Stochastic Averaging 52
3.3.3 Higher-Order Stochastic Averaging 59
3.3.4 Numerical Results and Discussion 67
3.3.5 Ordinary Viscoelastic Systems 75
3.4 Lyapunov Exponents of Fractional Viscoelastic Systems under Bounded Noise Excitation 78
3.4.1 Lyapunov Exponents 78
3.4.2 Numerical Determination of Lyapunov Exponents 84
3.4.3 Results and Discussion 85
3.5 Moment Lyapunov Exponents of Fractional Systems under Bounded Noise Excitation 89
3.5.1 First-Order Stochastic Averaging 89
3.5.2 Second-Order Stochastic Averaging 93
3.5.3 Higher-Order Stochastic Averaging 94
3.5.4 Results and Discussion 94

3.6 Summary 101

4 Stochastic Stability of Coupled Non-Gyroscopic Viscoelastic Systems . . . 103

4.1 Coupled Systems Excited by Wide-Band Noises 103

4.1.1 Formulation 103

4.1.2 Moment Lyapunov Exponents of 4-D Systems 108

4.1.3 Stability Boundary 118

4.1.4 Simulation 122

4.1.5 Stability Index 126

4.1.6 Application: Flexural-Torsional Stability of a Rectangular Beam 127

4.1.7 Results and Discussion 130

4.2 Coupled Systems Excited by Bounded Noise 135

4.2.1 Formulation 135

4.2.2 Parametric Resonances 139

4.3 Summary 154

5 Stochastic Stability of Gyroscopic Viscoelastic Systems . . . 156

5.1 Vibration of a Rotating Shaft 156

5.2 Gyroscopic Systems Excited by Wide-band Noise 159

5.2.1 Formulation 159

5.2.2 Moment Lyapunov Exponents 165

5.2.3 Stability Boundary 167

5.2.4 Stability Index 169

5.2.5 Simulation 170

5.2.6 Results and Discussion 172

5.3 Gyroscopic Systems Excited by Bounded Noise 178

5.3.1 Stochastic Averaging 178

5.3.2 Parametric Resonances 184
5.3.3 Effect of Viscoelasticity 194
5.4 Summary 198

6 Conclusions and Future Research **210**
6.1 Contributions 210
6.2 Future Research 213

Bibliography **215**

List of Figures

1.1 Illustration of Lyapunov stability 5

1.2 Seismic waves and power spectral densities (El-Centro, U.S.A., 1940) 11

1.3 Power spectral density of a real noise process 11

1.4 Power spectral density of a bounded noise process 14

1.5 Fractional calculus of a function 25

1.6 Creep and recovery for a fractional viscoelastic material 28

3.1 Comparison of simulation and approximate results for fractional SDOF viscoelastic system under white noise excitation 69

3.2 Effect of damping (β) on Moment Lyapunov exponents under Gaussian white noise excitation 69

3.3 Effect of elastic modulus (E) on Moment Lyapunov exponents of fractional SDOF viscoelastic system under white noise excitation 70

3.4 Effect of viscosity (η) on moment Lyapunov exponents of fractional SDOF viscoelastic system under white noise excitation 71

3.5 Effect of retardation (τ_ε) on moment Lyapunov exponents of fractional SDOF viscoelastic system under white noise excitation 71

3.6 Effect of fractional order μ on moment Lyapunov exponents under Gaussian white noise excitation 72

3.7 Effect of white noise intensity σ on moment Lyapunov exponents under Gaussian white noise excitation 72

3.8 Comparison of simulation and approximate results for fractional SDOF viscoelastic system under real noise excitation 74

3.9 Effect of parameter α on moment Lyapunov exponents under real noise excitation 75

3.10 Moment Lyapunov exponents for SDOF systems of ordinary viscoelasticity with white noise 77

3.11 Moment Lyapunov exponents for ordinary viscoelasticity under real noise excitation 79

3.12 Moment Lyapunov exponents for ordinary viscoelasticity under real noise excitation 79

3.13 Moment Lyapunov exponents under real noise for various σ for ordinary viscoelasticity 80

3.14 Moment Lyapunov exponents under real noise for various α for ordinary viscoelasticity 80

3.15 Stability boundaries of the viscoelastic system under bounded noise 87

3.16 Lyapunov exponents of a viscoelastic system under bounded noise 87

3.17 Lyapunov exponents of SDOF viscoelastic system 88

3.18 Effect of fractional order μ on system stability under bounded noise 88

3.19 Effect of damping on stability boundaries under bounded noise 89

3.20 Comparison of simulation and approximation results for SDOF system under bounded noises 95

3.21 Effect of σ of bounded noises on moment Lyapunov exponents of SDOF systems 96

3.22 Parametric resonance of SDOF fractional viscoelastic system 97

3.23 Parametric resonance of SDOF fractional viscoelastic system 98

3.24 Largest Lyapunov exponents of SDOF fractional systems 99
3.25 Effect of noise amplitude ζ of bounded noises on moment Lyapunov exponents of SDOF systems 99
3.26 Parametric resonance of SDOF fractional viscoelastic system 100
4.1 Moment Lyapunov exponents of coupled system for Kth order Fourier expansion 117
4.2 Comparison of Lyapunov exponents of coupled system under white noise 122
4.3 Lyapunov exponents of couple system excited by white noise 125
4.4 Stability index of coupled system under white noise 126
4.5 Flexural-torsional vibration of a rectangular beam 127
4.6 Almost-sure and pth moment stability boundaries of coupled system under white noise 130
4.7 Critical excitation and pseudo-damping of coupled system under white noise 131
4.8 Effect of fractional order on fractional coupled system under white noise excitation 132
4.9 Effect of damping on fractional coupled system under white noise excitation 133
4.10 Effect of τ_ε on fractional coupled system under white noise excitation 133
4.11 Effect of viscosity γ on coupled system under white noise excitation 134
4.12 Effect of viscosity κ on coupled system under white noise excitation 134
4.13 Effect of σ on coupled system under real noise excitation 135
4.14 Effect of α on coupled system under real noise excitation 136
4.15 Effect of damping on coupled system under white noise excitation 136
4.16 Largest Lyapunov exponents of coupled system for subharmonic resonance 143

4.17 Parametric subharmonic resonance of Lyapunov exponents for coupled system 144

4.18 Effects of viscosity γ on coupled system for subharmonic resonance 144

4.19 Effects of fractional order μ on coupled system for subharmonic resonance 145

4.20 Stability boundaries of coupled system for subharmonic resonance 146

4.21 Stability boundaries of coupled system for subharmonic resonance 146

4.22 Moment Lyapunov exponents of coupled system for subharmonic resonance 147

4.23 Lyapunov exponents of coupled system for combination additive resonance 150

4.24 Lyapunov exponents of coupled system for combination additive resonance 150

4.25 Stability boundaries of coupled system for combination additive resonance 151

4.26 Moment Lyapunov exponents of coupled system for combination additive resonance 151

4.27 Moment Lyapunov exponents of coupled system for combination additive resonance 152

4.28 Moment Lyapunov exponents of fractional coupled system for combination additive resonance 152

5.1 Vibration of a rotating shaft 157

5.2 Stability index for gyroscopic system under white noises 170

5.3 Effect of fractional order μ on Moment Lyapunov exponents of fractional gyroscopic systems under Gaussian white noise excitation 173

5.4 Effect of damping on Moment Lyapunov exponents of fractional gyroscopic systems under Gaussian white noise excitation 173

5.5 Largest Lyapunov exponents of gyroscopic system under white noise excitation 174

5.6 Stability boundaries of gyroscopic elastic system with white noise excitation 174

5.7 Stability boundaries of gyroscopic viscoelastic system with white noise excitation 175

5.8 Stability boundaries of gyroscopic elastic system with white noise excitation (3D) 176

5.9 Stability boundaries of gyroscopic viscoelastic system with white noise excitation (3D) 177

5.10 Instability regions for subharmonic resonance with $\omega_0 = 2\omega_1$ 187

5.11 Instability regions for subharmonic resonance with $\omega_0 = 2\omega_2$ 188

5.12 Effect of ζ on Lyapunov exponents for subharmonic resonance 189

5.13 Effect of σ on Lyapunov exponents for subharmonic resonance 189

5.14 Moment Lyapunov exponents for subharmonic resonance 200

5.15 Effect of ζ on Lyapunov exponents for combination additive resonance 201

5.16 Effect of σ on Lyapunov exponents for combination additive resonance 201

5.17 Stability boundaries for gyroscopic systems under bounded noises with combination additive resonance 202

5.18 Effect of σ on Lyapunov exponents for gyroscopic systems under bounded noises with combination additive resonance 202

5.19 Instability regions for gyroscopic systems under bounded noises with combination additive resonance 203

5.20 Moment Lyapunov exponents for gyroscopic systems under bounded noise with combination additive resonance 204

5.21 Instability regions for gyroscopic systems under bounded noise with combination differential resonance 204

5.22 Instability regions for fractional gyroscopic systems under bounded noise for subharmonic resonance with $\omega_0 = 2\omega_1$ 205

5.23 Instability regions for fractional gyroscopic systems under bounded noise for subharmonic resonance with $\omega_0 = 2\omega_2$ 206

5.24 Effect of μ on fractional gyroscopic systems under bounded noise for subharmonic resonance 207

5.25 Effect of μ on fractional gyroscopic systems under bounded noise for combination additive resonance 207

5.26 Instability regions for fractional gyroscopic systems under bounded noise with combination additive resonance 208

5.27 Instability regions for fractional gyroscopic systems under bounded noise with combination differential resonance 209

5.28 Effect of μ on fractional gyroscopic systems under bounded noise for combination differential resonance 209

CHAPTER 1

Introduction

1.1 Stochastic Stability of Structures

1.1.1 Motivations

In the study of structures under dynamic loadings, one may distinguish two broadly distinct streams. On the one hand, there is the endeavor to obtain the definite response of structures, i.e., an exact or approximate solution (Ibrahim, 1985; Clough and Penzien, 2003; Chopra, 2007). On the other hand, one strives to obtain information about the whole class of solutions, i.e., the problems of dynamic stability of structures (Bolotin, 1964; Herrmann, 1967; Huseyin, 1978; Xie, 2006).

The collapse of original Takoma Narrows Bridge caused by wind gusts provides convincing evidence in favor of the intensive research on dynamic stability of structures. Provided that the wind load is taken as a stochastic process, the equation of motion can be derived as a stochastic differential equation with parametric excitations, upon which motion stability analysis is based (Lin and Ariaratnam, 1980; Pandey and Ariaratnam, 1998, 1999).

Parametric stochastic stability problems can also occur in structural systems subject to vertical ground motion (Lin and Shih, 1982), in aircraft structures and helicopter rotor blades subject to turbulent flow (Lin and Prussing, 1982), in a ship's roll motion due to the time-dependent restoring moment (Shlesinger and Swean, 1998), and in machine and structure components subjected to parametric excitation (Ibrahim, 1985; Xie, 2006). Some other examples include liquid sloshing in rocket tanks subjected to longitudinal excitation generated from the rocket engines (Ibrahim and Soundararajan, 1983). New areas finding application of stability analysis continue to unfold, such as mining engineering.

1.1.2 Gyroscopic Systems

For many engineering structures under dynamic loadings, the motions are mathematically governed by partial differential equations. Using an appropriate discretization technique in the spatial variables, such as Galerkin's method, the equations of motion may be approximated by a system of differential equations of the form (Inman, 2006)

$$\mathbf{M}\ddot{\mathbf{x}}(t)+(\mathbf{D}+\mathbf{G})\dot{\mathbf{x}}(t)+(\mathbf{K}+\mathbf{C})\mathbf{x}(t)=\mathbf{f}(t), \tag{1.1.1}$$

where $\mathbf{x}(t)$ is a vector of state variables or generalized coordinates. $\mathbf{f}(t)$ denotes a vector of external loadings. $\mathbf{M}$ and $\mathbf{D}$ are the inertia matrix and the viscous damping matrix, respectively. $\mathbf{G}$ is the skew symmetric gyroscopic matrix, $\mathbf{G}^T=-\mathbf{G}$, $\mathbf{K}$ is the stiffness matrix, which is symmetric $\mathbf{K}^T=\mathbf{K}$ or skew symmetric $\mathbf{K}^T=-\mathbf{K}$, and $\mathbf{C}$ is the circulatory matrix.

When the externally applied loads appear in the form of coefficient or parameter matrix, e.g., in matrix $\mathbf{K}$, the systems are called parametrically excited systems and the instability is referred as parametric resonance or parametric instability. Parametric resonance is more dangerous than ordinary resonance as it is characterized by exponential growth of the response amplitudes even in the presence of damping. It has been shown that Lyapunov exponents and moment Lyapunov exponents provide ideal avenues to study parametric instability (Xie, 2006).

In equation (1.1.1), two or more coordinates are usually coupled in matrix $\mathbf{G}$ or $\mathbf{K}$. A system with stiffness matrix $\mathbf{K}$ but without gyroscopic matrix $\mathbf{G}$ may be called a coupled non-gyroscopic system. A typical example problem of coupled non-gyroscopic systems is the flexural-torsional stability of a rectangular beam.

A system with gyroscopic matrix $\mathbf{G}$ is called a gyroscopic system. The gyroscopic matrix is often due to gyroscopic forces which may arise from, for example, Coriolis effect or Lorentz effect. A force is called gyroscopic if the work it does during an actual infinitesimal displacement of the system is equal to zero. Typical examples of gyroscopic systems include rotating and hydroelastic systems, such as rotating shafts under pulsating axial thrust and pipes conveying fluid in pulsating flow.

Gyroscopic systems are an essential component in some civil engineering structures. Merkin (1956) is among the earliest who studied the linear gyroscopic systems. Later, Mettler (1966) investigated the dynamic stability in the case of harmonic excitations. Linear or nonlinear autonomous gyroscopic systems were studied in detail (Chetaev, 1961; Dimentberg, 1961; Huseyin, 1978). The stability of linear and nonlinear gyroscopic systems with harmonically varying parameters was considered and analytical results for stability boundaries were studied (Ariaratnam and Namachchivaya, 1986a,b). More recently, Lingala (2010) discussed the dynamics and stability of nonlinear delay gyroscopic systems with periodically varying delay. Investigation of the stability properties of rotating shafts is of great importance in the design and safe operation of rotating machines. The effect of parametric periodic excitations on stability of rotating shafts was well investigated (Parszewski, 1984). However, studies have shown that it is more realistic to describe parametric loadings as stochastic processes (Namachchivaya and Ariaratnam, 1987), which turn equation (1.1.1) into stochastic differential equations. Yin (1991) obtained analytical expressions for Lyapunov exponents of linear gyroscopic systems. Nagata and Namachchivaya (1998) studied the global dynamics of autonomous gyroscopic systems near both a $0:1$ resonance and a Hamiltonian Hopf bifurcation. Nolan and Namachchivaya (1999) investigated the stability behaviour of a linear gyroscopic system parametrically perturbed by a (multiplicative) real noise of small intensity and the maximal Lyapunov exponent is calculated using the perturbation method. This perturbation method was also used to obtain asymptotic approximations for the moment Lyapunov exponent and the Lyapunov exponent for a gyroscopic system close to a double zero resonance and subjected to small damping and noisy disturbances (Vedula and Namachchivaya, 2002). Abdelrahman (2002) investigated the almost-sure stochastic stability of various kinds of parametrically excited dynamical systems by using the concept of Lyapunov exponent. By examining the local dynamics of a nearly symmetric shaft, concentrating on the combination resonance case, it was shown that the addition of forcing can extend the stability region of this system (McDonald and

Namachchivaya, 2002). Vedula (2005) systematically investigated dynamics and stochastic stability of nonlinear gyroscopic systems and nonlinear delay gyroscopic systems.

1.1.3 Stochastic Stability

The dynamic stability is often concerned with the following question: Given a solution (the trivial solution or zero equilibrium point), what is its relation to its neighbors? One asks then whether the trajectories starting near the trivial solution do tend to remain near zero (the equilibrium point is then stable), to approach zero (the equilibrium point is then asymptotic stable), or to depart from zero (the equilibrium point is then unstable).

This problem may also be represented graphically. The three different paths of the two dimensional example in Figure 1.1 represent all three cases: asymptotic stability, stability, and instability in the sense of Lyapunov.

The dynamic stability of structures under deterministic loadings has been extensively investigated (Bolotin, 1964). However, the loadings imposed on the structures are quite often random forces, such as those arising from earthquakes, wind, explosive vibration and ocean waves, which can be characterized satisfactorily only in probabilistic terms, such as white noises, real noises, or bounded noises. This results in stochastic stability of structures which is a very intensive research topic (Ariaratnam *et al.*, 1988; Kliemann and Namachchivaya, 1995; Lin and Cai, 1995; Zhu, 2003; Xie, 2006). Professors S.T. Ariaratnam and his associates at the University of Waterloo have made extraordinary contributions in the areas of random vibration, stochastic mechanics, dynamic stability of structures, and nonlinear vibrations (Kliemann and Namachchivaya, 1995), which is called ‘‘Waterloo school" by Kliemann (2008).

The most frequently used stochastic stability concepts are almost-sure stability and moment stability, the definitions of which follow Khasminskii (1980) and Arnold (1998).

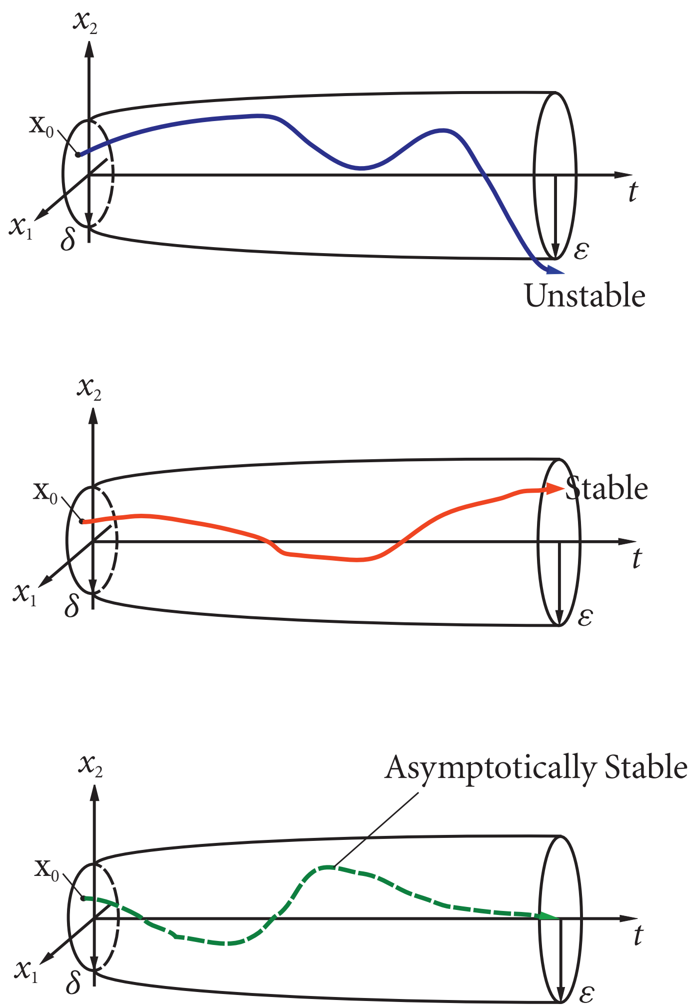

Figure 1.1 Illustration of Lyapunov stability

Almost-Sure (a.s.) Stability or Stability with Probability One (w.p.1)

The equilibrium point $\mathbf{x}(t) = \mathbf{0}$ is stable with probability 1 (w.p.1) if, for any $\varepsilon > 0$ and $\rho > 0$, there exists $\delta(\varepsilon, \rho) > 0$ such that

$$\mathcal{P}\left\{ \sup_{t \geqslant 0} \left\| \mathbf{x}(t) \right\| \geqslant \varepsilon \right\} < \rho, \tag{1.1.2}$$

whenever $\left\| \mathbf{x}(0) \right\| < \delta$, where $\mathcal{P}\{\cdot\}$ denotes the probability, $\| \cdot \|$ denotes a suitable vector norm.

In engineering language, if the system starts with an initial condition $\|\mathbf{x}(0)\|$ inside the $\delta(\varepsilon)$ region, then almost any maximum solution $\|\mathbf{x}(t;\mathbf{x}(0))\|$ of the system will remain inside the ε region for all time t if the system is stable. In other words, for almost any realization of the process $\mathbf{x}(t)$, the maximum value of the norm $\|\mathbf{x}(t;\mathbf{x}(0))\|$ can be controlled within a value ε, if the starting point $\|\mathbf{x}(0)\|$ is in a certain value δ where δ depends on ε.

Almost-Sure Asymptotic Stability

The equilibrium point $\mathbf{x}(t)=\mathbf{0}$ is asymptotically stable w.p.1 if and only if it is stable w.p.1 and

$$P\left\{\lim_{t\to\infty}\|\mathbf{x}(t)\|=0\right\}=1. \tag{1.1.3}$$

In engineering language, for almost any realization of the process $\mathbf{x}(t)$, the long-run value of the norm $\|\mathbf{x}(t)\|$ goes to zero.

Moment Stability

The equilibrium point $\mathbf{x}(t)=\mathbf{0}$ is stable in the pth moment if, for any $\varepsilon>0$, there exists $\delta>0$ such that $\mathsf{E}\left[\|\mathbf{x}(t)\|^p\right]<\varepsilon$, for all $t\geqslant 0$ and $\|\mathbf{x}(0)\|<\delta$, where $\mathsf{E}[\,\cdot\,]$ denotes the expectation.

In engineering language, for any realization of the process $\mathbf{x}(t)$, the pth moment of $\|\mathbf{x}(t)\|$ can be controlled within a value ε if the starting point $\|\mathbf{x}(0)\|$ is in a certain value δ, where δ depends on ε.

It can be seen that higher moment stability implies lower moment stability and mean square stability implies almost-sure stability.

These definitions on stochastic stability are general enough to apply to both linear and nonlinear systems. It can be shown that if a linearized system is asymptotically stable then the full nonlinear system is also asymptotically stable (see Hagedorn, 1978, pages 84-93). Unfortunately if a linearized system is stable but not asymptotically stable, the stability of the original nonlinear system cannot be determined. In this situation the nonlinear terms in the system need to be included in the stability analysis.

In practice, it is very difficult, if not impossible, to determine stochastic stability directly from the definitions. Instead, more direct methods, such as determining the Lyapunov exponents and the moment Lyapunov exponents of stochastic dynamical systems, are exploited.

The modern theory of stochastic stability is founded on two characteristic numbers: Lyapunov exponents and moment Lyapunov exponents. These two indexes are used to indicate stability status.

1.1.4 Lyapunov Exponents and Moment Lyapunov Exponents

Lyapunov Exponent

Lyapunov exponents were first introduced by Lyapunov (1892) for investigating the stability of dynamical systems described by nonlinear ordinary differential equations. The theory of Lyapunov exponents was further advanced by Oseledec (1968) in the well-known *Multiplicative Ergodic Theorem*. Oseledec showed that for continuous dynamical systems, both deterministic and stochastic, there exist *deterministic, real* numbers characterizing the average exponential rates of growth or decay of the solution for large time and called them *Lyapunov exponents*. Since then, Lyapunov exponents have been applied in a variety of branches of science and engineering.

For a linear stochastic system

$$\dot{\mathbf{x}}(t) = \mathbf{A}\big(\boldsymbol{\xi}(t)\big)\,\mathbf{x}(t), \qquad \mathbf{x}(0) = \mathbf{x}_0 \in \mathcal{R}^n, \tag{1.1.4}$$

where $\mathbf{A} : \mathcal{M} \to \mathcal{R}^{(n,n)}$ is an analytic function from a compact connected smooth manifold $\mathcal{M}$ into the space $\mathcal{R}^{(n,n)}$, and $\boldsymbol{\xi}(t) = \{\xi_1, \xi_2, \cdots, \xi_d\}^T$ is a stationary ergodic diffusion process. By assuming that $\boldsymbol{\xi}(t)$ is strongly elliptic and satisfies other non-degenerate conditions, one has, for any $\mathbf{x}_0 \neq \mathbf{0}$,

$$\lambda = \lim_{t \to \infty} \frac{1}{t} \log \big\| \mathbf{x}(t; \mathbf{x}_0) \big\|, \qquad \text{almost surely,} \tag{1.1.5}$$

where $\big\|\mathbf{x}(t)\big\| = \big(\mathbf{x}(t)^T \mathbf{x}(t)\big)^{1/2}$ is the Euclidean norm. λ is deterministic and equal to the largest Lyapunov exponent from the *Multiplicative Ergodic Theorem*. A n-dimensional system (i.e., one defined by n first-order differential equation of motion) will have n Lyapunov exponents, each representing the rate of growth or decay of small perturbations along each of the principal axes in that system's state space. If the Lyapunov exponent λ is negative, the solutions of system (1.1.4) decay exponentially as $t \to \infty$ and the system is stable almost-surely or with probability 1; otherwise, the system is unstable w.p.1.

Moment Lyapunov Exponent

Lyapunov exponents characterize sample stability or instability. However, this sample stability cannot assure the moment stability, due to the theory of large deviation (Baxendale, 1985; Arnold and Kliemann, 1987). Hence, to obtain a complete picture of the dynamic stability, it is important to study both the top Lyapunov exponent and the moment Lyapunov exponent.

The connection between moment stability and almost-sure stability for an undamped linear two-dimensional system under real noise excitation was established by Molchanov (1998). These results were extended for an arbitrary n-dimensional linear stochastic system by Arnold (1984), in which a formula connecting moment and sample stability was formulated. A systematic study of moment Lyapunov exponents is presented by Arnold *et al.* (1984b) for linear Itô systems and by Arnold *et al.* (1984a) for linear stochastic systems under real noise excitations.

The stability of the pth moment $\mathsf{E}[\,\|\mathbf{x}(t)\|^p\,]$ of the solution of system (1.1.4) is governed by the pth moment Lyapunov exponent defined by

$$\Lambda(p) = \lim_{t\to\infty} \frac{1}{t} \log \mathsf{E}[\,\|\mathbf{x}(t)\|^p\,], \tag{1.1.6}$$

where $\mathsf{E}[\cdot]$ denotes the expected value. The pth moments are asymptotically stable if $\Lambda(p) < 0$.

The moment Lyapunov exponent $\Lambda(p)$ possesses the following properties:

1. $\Lambda\big(p, \mathbf{x}(0)\big) = \Lambda(p)$, for all initial conditions $\mathbf{x}(0)$ in the n-dimensional vector space excluding the origin.

2. For all real values of p, $\Lambda(p)$ is real, analytic, and convex.

3. $\Lambda(p)/p$ is increasing and $\Lambda(p)$ passes the origin, $\Lambda(0) = 0$, and

$$\lambda = \Lambda'(0) = \lim_{p\to 0} \frac{\partial \Lambda(p)}{\partial p}, \tag{1.1.7}$$

i.e., the slope of $\Lambda(p)$ at the origin is equal to the Lyapunov exponent given by equation (1.1.6).

4. The pth moment Lyapunov exponent $\Lambda(p)$ is the principal eigenvalue of the differential eigenvalue problem

$$\mathscr{L}(p)T(p) = \Lambda(p)T(p), \tag{1.1.8}$$

with non-negative eigenfunction $T(p)$.

Equation (1.1.7) is the most concise relationship between the almost-sure stability and the moment stability of linear system (1.1.4). $\mathscr{L}(p)$ in equation (1.1.8) can be derived from equation (1.1.4) by making use of the Khasminskii's transformation (Arnold *et al.*, 1984a,b). The operator $\mathscr{L}$ can also be obtained in a more straight-forward way which was first used by Wedig (1988).

Although Oseledec's Multiplicative Ergodic Theorem established the existence of the Lyapunov exponents, it is very difficult to accurately evaluate the Lyapunov exponents. The procedure proposed by Khasminskii (1967) is often used to obtain the approximate results of the largest Lyapunov exponents for Itô stochastic differential equations. Using the method of stochastic averaging, Ariaratnam (1996) and Xie (2006) obtained the Lyapunov exponents of a viscoelastic system.

Despite the importance of the moment Lyapunov exponents, publications are limited because of the difficulties in their actual determination. Furthermore, almost all of the research on the moment Lyapunov exponents is on the determination of approximate results of a single oscillator or two coupled oscillators under weak-noise excitations using perturbation methods. Using the analytic property of the moment Lyapunov exponents, Arnold *et al.* (1997) obtained weak-noise expansions of the moment Lyapunov exponents of a two dimensional system in terms of εp, where ε is a small parameter, under both white-noise and real-noise excitations. Khasminskii and Moshchuk (1998) obtained an asymptotic expansion of the moment Lyapunov exponent of a two-dimensional system under white-noise parametric excitation in terms of the small fluctuation parameter ε, from which the stability index was obtained. Namachchivaya and Vedula (2000) obtained general asymptotic approximation of the moment Lyapunov exponent and the Lyapunov exponent for a four-dimensional system with one critical mode and another asymptotically stable mode driven by a small intensity stochastic process. Namachchivaya and Roessel (2001) studied the moment Lyapunov exponents of two coupled oscillators driven by real noise. Xie

(2006) obtained weak-noise expansions of the moment Lyapunov exponent, the Lyapunov exponent, and the stability index of a two-dimensional system under real-noise excitation and bounded-noise excitation in terms of the small fluctuation parameter.

There are several numerical algorithms to simulate Lyapunov exponents (Wolf *et al.*, 1985; Rosenstein *et al.*, 1993). Gram-Schmidt orthornormalization is performed after each iteration in Wolf's algorithm. On the other hand, there seems to be only one numerical algorithm for determining the moment Lyapunov exponents using Monte-Carlo simulation (Xie, 2005). In this algorithm, the critical step is the periodic normalization of the pth moment in order to avoid numerical overflow and underflow. This unique algorithm has been successfully used to numerical determination of moment Lyapunov exponents of various dynamic systems (Kozic *et al.*, 2007).

1.2 Noise Models and Stochastic Differential Equations

1.2.1 Noise Models

Numerous structures in civil engineering are driven by dynamic forces, such as seismic and wind loads, which can be described satisfactorily only by using probabilistic models. Figure 1.2 illustrates three real seismic wave records and corresponding power spectral densities. Mathematically, these excitations on structures can be described as stochastic processes. Different random excitations may have different forms of power spectral densities. For engineering applications, the random excitation has been modeled as a Gaussian white noise process, a real noise process, or a bounded noise process.

Gaussian white noise process is a weakly stationary process that is delta-correlated and mean zero. This process is formally the derivative of the Wiener process given by

$$\xi(t) = \sigma \dot{W}(t), \tag{1.2.1}$$

with constant cosine and sine power spectral density over the entire frequency range as follows, which is obviously an idealization,

$$S(\omega) = \sigma^2, \quad \Psi(\omega) = 0. \tag{1.2.2}$$

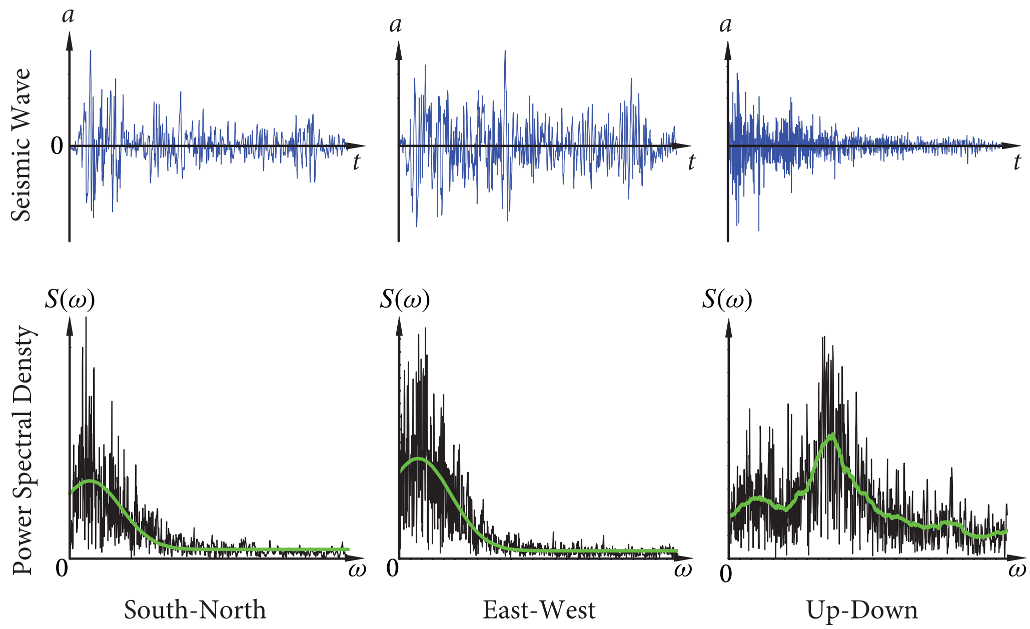

Figure 1.2 Seismic waves and power spectral densities (El-Centro, U.S.A., 1940)

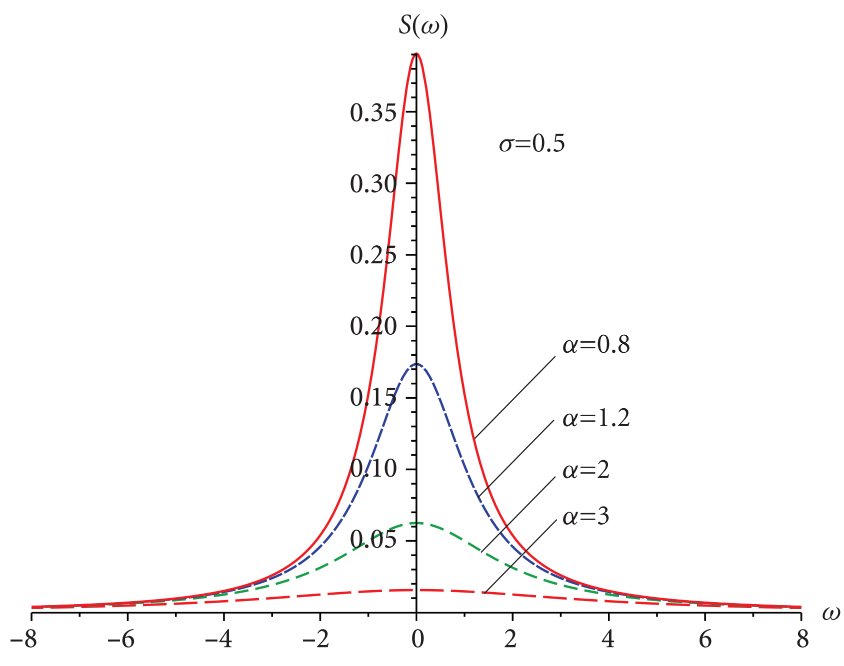

Figure 1.3 Power spectral density of a real noise process

A white noise process is frequently adopted as a model for wide-band noise with very short memory because of the availability of mathematical theory, such as Itô calculus, in dealing with white noise processes. The use of the white noise model simplifies the analysis significantly. Moreover, filtered or transformed white noise processes, such as real noises or bounded noises, can provide satisfactorily approximation to excitations with almost any spectral characteristics.

Another important noise is called real noise, which is synonymously named an Ornstein-Uhlenbeck process and is given by

$$\mathrm{d}X(t) = -\alpha X(t)\mathrm{d}t + \sigma \,\mathrm{d}W(t), \tag{1.2.3}$$

with cosine and sine power spectral density

$$S(\omega) = \frac{\sigma^2}{\alpha^2+\omega^2} = \frac{\sigma^2}{\alpha^2}\frac{1}{1+\left(\frac{\omega}{\alpha}\right)^2}, \quad \Psi(\omega) = \frac{\omega\sigma^2}{\alpha(\alpha^2+\omega^2)}, \tag{1.2.4}$$

where $W(t)$ is a standard Wiener process. Ornstein-Uhlenbeck process is stationary and Gaussian. The power spectral density function $S(\omega)$ mainly concentrates in lower frequency band, as can be seen from equation (1.2.4) and Figure 1.3. When α is increased, $S(\omega)$ becomes flat in a wide frequency range. For large values of α, real noise's power will spread over a wide frequency band; thus, by suitably selecting the parameter α, a real noise may be used as the mathematical model of a wide-band noise. For the special case when $\sigma = \alpha\sqrt{S_0} \to \infty$, the Ornstein-Uhlenbeck process $X(t)$ approaches Gaussian white noise process with constant spectral density $S(\omega) = S_0$, i.e., the Ornstein-Uhlenbeck process $X(t) = \sqrt{S_0}\,\xi(t)$, where $\xi(t)$ is a unit Gaussian white noise process.

A bounded noise $\eta(t)$ is a realistic and versatile model of stochastic fluctuation in engineering applications and is normally represented as

$$\eta(t) = \zeta \cos\left[\nu t + \sigma W(t) + \theta\right], \tag{1.2.5}$$

where ζ is the noise amplitude, σ is the noise intensity, $W(t)$ is the standard Wiener process, and θ is a random variable uniformly distributed in the interval $[0, 2\pi]$. The inclusion of the phase angle θ makes the bounded noise $\eta(t)$ a weakly stationary process. Equation (1.2.5) may be written as

$$\eta(t) = \zeta \cos Z(t), \quad \mathrm{d}Z(t) = \nu t + \sigma \circ \mathrm{d}W(t), \tag{1.2.6}$$

where the initial condition of $Z(t)$ is $Z(0)=\theta$, the small circle denotes the term in the sense of Stratonovich. This process is of course bounded between $-\zeta$ and $+\zeta$ for all time t and hence is a bounded stochastic process. The auto-correlation function of $\eta(t)$ is given by

$$R(\tau)=\mathrm{E}[\eta(t)\eta(t+\tau)]=\frac{1}{2}\zeta^2\cos\nu\tau\,\exp\Big(-\frac{\sigma^2}{2}|\tau|\Big), \tag{1.2.7}$$

and the spectral density function of $\eta(t)$ is

$$S(\omega)=\int_{-\infty}^{+\infty}R(\tau)\mathrm{e}^{-\mathrm{i}\omega\tau}\mathrm{d}\tau=\frac{\zeta^2\sigma^2\big(\omega^2+\nu^2+\frac{1}{4}\sigma^4\big)}{2\big[(\omega+\nu)^2+\frac{1}{4}\sigma^4\big]\big[(\omega-\nu)^2+\frac{1}{4}\sigma^4\big]}, \tag{1.2.8}$$

which is shown in Figure 1.4.

When the noise intensity σ is small, the bounded noise can be used to model a narrow-band process about frequency ν. In the limit as σ approaches zero, the bounded noise reduces to a deterministic sinusoidal function. On the other hand, in the limit as σ approaches infinite, the bounded noise becomes a white noise of constant spectral density. However, since the mean-square value is fixed at $\frac{1}{2}$, this constant spectral density level reduces to zero in the limit. Bounded noise therefore presents an ideal model for use as a structural loading because it may be used to represent varying types of loads. The bounded noise process was first used by Stratonovich (1967) and has since been applied in various areas (Ariaratnam, 1996), such as the ground acceleration in earthquake engineering (Lin and Cai, 1995).

1.2.2 Stochastic Differential Equations

As ordinary differential equations are based on ordinary calculus, stochastic differential equations (SDE) are rooted in stochastic calculus. There are two dominating versions of stochastic calculus, the Itô stochastic calculus and the Stratonovich stochastic calculus. Accordingly, stochastic differential equations are categorized as Itô SDEs and Stratonovich SDEs.

The Stratonovich stochastic differential equation satisfied by a Markov diffusion process $X(t)$ is given by

$$\mathrm{d}X(t)=m^*(X,t)\mathrm{d}t+\sigma^*(X,t)\circ\mathrm{d}W(t), \tag{1.2.9}$$

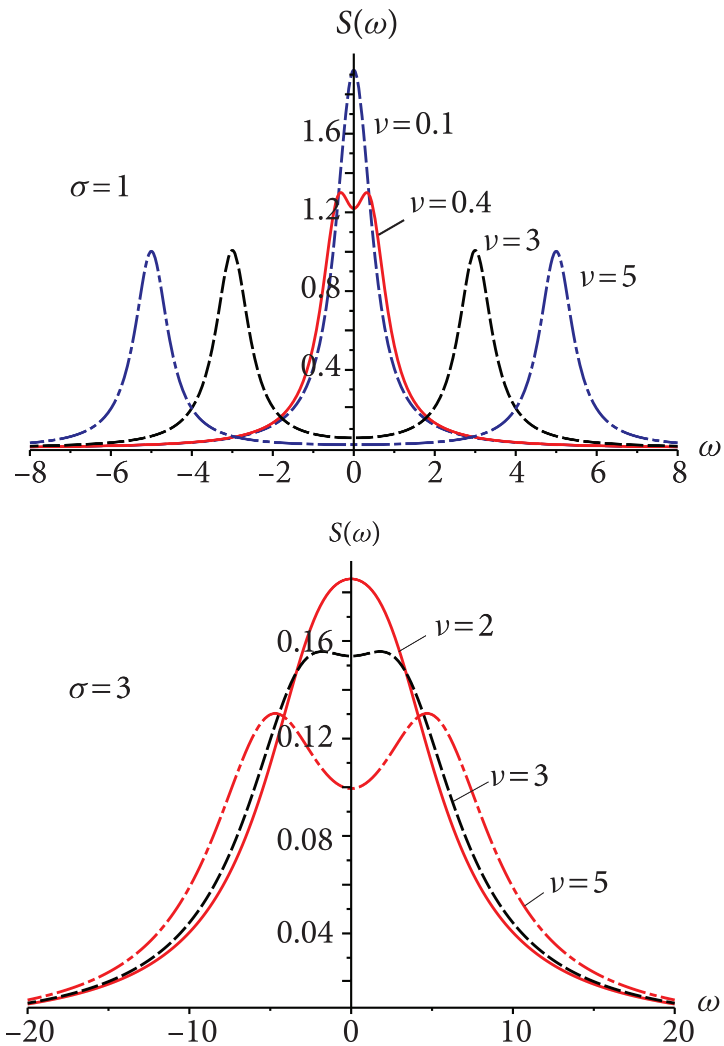

Figure 1.4 Power spectral density of a bounded noise process

which implies the stochastic integral equation

$$X(t)=X(t_0)+\int_{t_0}^{t} m^*(X(s),s)\mathrm{d}s+\int_{t_0}^{t} \sigma^*(X(s),s)\circ \mathrm{d}W(s), \tag{1.2.10}$$

where $W(t)$ is a unit Wiener process or Brown motion. The second integral is called Stratonovich integral defined as

$$\int_{t_0}^{t} \sigma^*(X(s),s)\circ \mathrm{d}W(s)=\lim_{n\to\infty}\sum_{j=0}^{n-1}\sigma^*\Big(\frac{X(t_j)+X(t_{j+1})}{2},t_j\Big)\big[X(t_{j+1})-X(t_j)\big]. \tag{1.2.11}$$

On the other hand, the Markov diffusion process $X(t)$ may also be defined by Itô stochastic differential equation

$$\mathrm{d}X(t) = m(X,t)\mathrm{d}t + \sigma(X,t)\mathrm{d}W(t), \tag{1.2.12}$$

with the initial condition $X(0) = x_0$, w.p.1, stands for the integral equation

$$X(t) = X(t_0) + \int_{t_0}^{t} m(X(s),s)\mathrm{d}s + \int_{t_0}^{t} \sigma(X(s),s)\mathrm{d}W(s), \tag{1.2.13}$$

where the second integral is called Stratonovich integral defined as

$$\int_{t_0}^{t} \sigma(X(s),s)\mathrm{d}W(s) = \lim_{n\to\infty} \sum_{j=0}^{n-1} \sigma\big(X(t_j),t_j\big)\big[X(t_{j+1}) - X(t_j)\big]. \tag{1.2.14}$$

It can be shown that there exists a unique Markov process $X(t)$, a solution to the Itô SDE (1.2.12) on $[t_0, T]$, if the following two conditions are satisfied, for a constant $C > 0$

$$\begin{aligned} &(a)\ \big|m(X,t) - m(Y,t)\big| + \big|\sigma(X,t) - \sigma(Y,t)\big| \leqslant C\big|X - Y\big|, \quad \text{for } X, Y \in R \text{ and } t \in [t_0, T] \\ &(b)\ \big|m(X,t)\big|^2 + \big|\sigma(X,t)\big|^2 \leqslant C\big(1 + |X|^2\big), \quad \text{for } X \in R \text{ and } t \in [t_0, T]. \end{aligned} \tag{1.2.15}$$

Actually, condition (a) ensures that solutions $X(t)$ do not explode, i.e., become infinite in finite time, and condition (b) ensures that solutions are pathewise unique. Further, $a = m(X,t)$ and $b = \sigma^2(X,t)$ are called the drift and diffusion coefficients, respectively.

The transition probability density $q\big(\xi, t \,|\, \xi_0, t_0\big)$ of the diffusion process $X(t)$ satisfies the equations:

$$\begin{aligned} &\left(\frac{\partial}{\partial t_0} + \mathscr{L}_{\xi_0}\right) q(\xi, t \,|\, \xi_0, t_0) = 0, && \text{Backward Kolmogorov equation,} \\ &\left(-\frac{\partial}{\partial t} + \mathscr{L}_{\xi}^{*}\right) q(\xi, t \,|\, \xi_0, t_0) = 0, && \text{Forward Kolmogorov equation or Fokker-Planck equation,} \end{aligned} \tag{1.2.16}$$

where

$$\mathscr{L}_{\xi_0}(\cdot) = m(\xi_0, t_0)\frac{\partial(\cdot)}{\partial \xi_0} + \frac{1}{2}\sigma^2(\xi_0, t_0)\frac{\partial^2(\cdot)}{\partial \xi_0^2},$$

$$\mathscr{L}_{\xi}^{*}(\cdot) = -\frac{\partial}{\partial \xi}\big[m(\xi,t)(\cdot)\big] + \frac{1}{2}\frac{\partial^2}{\partial \xi^2}\big[\sigma^2(\xi,t)(\cdot)\big].$$

One can readily convert an Itô SDE to an equivalent Stratonovich SDE and back again.

Itô's Lemma

Suppose $\mathbf{X}(t)$ is a vector of diffusion process governed by the Itô stochastic differential equations

$$\mathrm{d}X_j = m_j(\mathbf{X}, t)\mathrm{d}t + \sum_{l=1}^{d} \sigma_{jl}(\mathbf{X}, t)\mathrm{d}W_l(t), \quad j = 1, 2, \cdots, n, \tag{1.2.17}$$

and let $\phi(\mathbf{X}, t)$ be any scalar function differentiable once with respect to t and twice with respect to X_j. Then the Itô differential of $\phi(\mathbf{X}, t)$ is given by

$$\mathrm{d}\phi(\mathbf{X}, t) = \mathcal{A}_{t,\mathbf{X}}\mathrm{d}t + \sum_{j=1}^{n}\sum_{l=1}^{d} \sigma_{jl}\frac{\partial \phi}{\partial X_j}\mathrm{d}W_l, \tag{1.2.18}$$

$$\frac{\mathrm{d}}{\mathrm{d}t}\mathsf{E}[\phi(\mathbf{X}, t)] = \mathsf{E}[\mathcal{A}_{t,\mathbf{X}}], \tag{1.2.19}$$

where

$$\mathcal{A}_{t,\mathbf{X}} = \frac{\partial}{\partial t} + \sum_{j=1}^{n} m_j(\mathbf{X}, t)\frac{\partial}{\partial X_j} + \frac{1}{2}\sum_{j=1}^{n}\sum_{k=1}^{n} b_{jk}(\mathbf{X}, t)\frac{\partial^2}{\partial X_j \partial X_k}, \quad \mathbf{b}(\mathbf{X}, t) = \sigma\sigma^T.$$

Thus, Itô's Lemma is used to find the differential of a time-dependent function of a stochastic process; it serves as the stochastic calculus counterpart of the chain rule in ordinary calculus.

1.2.3 Approximation of a Physical Process by a Diffusion Process

Consider a physical system described by a first-order differential equation

$$\frac{\mathrm{d}}{\mathrm{d}t}X(t) = f(X, t) + g(X, t)\xi(t), \tag{1.2.20}$$

where $f(X, t)$ and $g(X, t)$ are deterministic functional forms which can be nonlinear, and $\xi(t)$ is a stationary wide-band process.

If $\xi(t)$ is approximated by a white noise, then $X(t)$ tends to be a diffusion process governed by the Stratonovich stochastic differential equation

$$\mathrm{d}X(t) = f(X, t)\mathrm{d}t + g(X, t) \circ \mathrm{d}W(t), \tag{1.2.21}$$

whose equivalent Itô equation is

$$\mathrm{d}X(t) = \left[f(X, t) + \frac{1}{2}g(X, t)\frac{\partial g(X, t)}{\partial X}\right]\mathrm{d}t + g(X, t)\mathrm{d}W(t). \tag{1.2.22}$$

This is to say, the physical process is approximated by a diffusion process, which is governed by the Itô stochastic differential equation in (1.2.22) converted from the physical equation in (1.2.20), by using theory of Wong and Zakai (1965).

By using Itô's Lemma or by solving the deterministic Fokker-Plank equations for the transition probability density functions, only few stochastic differential equations (SDE) can be explicitly solved (Pandey and Ariaratnam, 1996). For most cases, one has to resort to numerical methods such as Euler's method in Section 1.2.4, or approximate analytical methods such as stochastic averaging method in Section 1.2.5.

1.2.4 Numerical Methods for Solving SDEs

A detailed source of numerical solutions of stochastic differential equations is given by Kloeden and Platen (1992). A single realization of a numerical solution approximates a sample path. Let's discuss Euler's method, as it is a simple and the straight-forward method to implement.

Consider the Itô SDE in equation (1.2.12). It is assumed that the initial condition is $X(0)=X_0$ and $X(t)$ is the solution on the time interval $[0, T]$. The interval $[0, T]$ is discretized into k segments of equal length: $t_0=0$, t_1, t_2, $\ldots$, t_{k-1}, $t_k=T$, where the length of each subinterval is $\Delta t=t_{i+1}-t_i=T/K$, $i=0,1,\ldots,k-1$. Then $t_{i+1}=t_i+\Delta t=(i+1)\Delta t$ and $\Delta W_i=\Delta W(t_i)=W(t_i+\Delta t)-W(t_i)$.

In Euler's method, the differential $\mathrm{d}X(t_i)$ is approximated by $\Delta X(t_i)=X(t_{i+1})-X(t_i)$. For each sample path, the value of $X(t_{i+1})$ is approximated using only the value at the previous time step, $X(t_i)$. Let X_i denote the approximation to the solution at t_i, $X(t_i)$. Then Euler's method for equation (1.2.12) is given by the recursive formula:

$$X_{i+1}=X_i+m(X_i,t_i)\Delta t+\sigma(X_i,t_i)\Delta W_i, \quad i=0,1,\cdots,k-1, \tag{1.2.23}$$

where $\Delta W_i \sim N(0,\Delta t)$, from the definition of Weiner process. Let η be a random variable with a standard normal distribution, $\eta \sim N(0,1)$, then $\sqrt{\Delta t}\,\eta \sim N(0,\Delta t)$. To generate sample paths by numerical methods, random values from standard normal distribution are needed. Euler's method for equation (1.2.12) is given by:

$$X_{i+1}=X_i+m(X_i,t_i)\Delta t+\sigma(X_i,t_i)\sqrt{\Delta t}\,\eta_i, \quad i=0,1,\cdots,k-1, \quad X_0=X(0). \tag{1.2.24}$$

It can be shown that Euler's method converges on the condition of equation (1.2.15) and

$$\left|m(X,t_1)-m(Y,t_2)\right|+\left|\sigma(X,t_1)-\sigma(Y,t_2)\right|\leqslant C\left|X-Y\right|^{1/2}, \tag{1.2.25}$$

for all $t_1, t_2 \in [t_0, T]$ and $X \in \mathbf{R}$. Then the numerical approximation given by Euler's method X_i and the exact solution $X(t_i)$ satisfy

$$\begin{aligned} &\mathsf{E}\left[\left|X(t_i)-X_i\right|^2 \,\middle|\, X(t_{i-1})=X_{i-1}\right]=\mathcal{O}[(\Delta t)^2], \\ &\mathsf{E}\left[\left|X(t_i)-X_i\right|^2 \,\middle|\, X(t_0)=X_0\right]=\mathcal{O}(\Delta t), \end{aligned} \tag{1.2.26}$$

which show that in each step, Euler's method has an error that is of order $(\Delta t)^2$ and over the entire interval $[0, T]$, the error is of the order Δt. One may come to the conclusion that if Δt is reduced, then the approximation improves. However, if Δt is too small, there will be rounding error in a computer's simulation, which will accumulate due to the large number of calculations.

1.2.5 Stochastic Averaging Method for Approximating SDEs

The ordinary averaging method, originally developed by Bogoliubov and Mitropolskii (1961), has proven to be a very powerful approximate tool for investigating deterministic dynamic problems which are weakly nonlinear, i.e., for linear systems perturbed by nonlinear effects. Later, Stratonovich (1963) extended the ordinary averaging method to stochastic averaging method based on physical and mathematical arguments, and Khasminskii (1966b) provided a rigorous mathematical proof.

The basic idea of stochastic averaging method was to approximate the original stochastic system by an averaged stochastic system, which is presumably easier to study, and infer properties of the dynamics of the original system by the understanding of the dynamics of the averaged system. Thus, the response state vector or response process of the original system is approximated by a new process which is a diffusive Markov vector with the probability density governed by a partial differential equation, called the Fokker-Planck equation. Then the properties of the approximate solution can be readily determined. The method was devised to obtain the coefficient functions in this equation.

The appeal of stochastic averaging methods lies in the fact that they often reduce the dimensionality of the problem and significantly simplify the solution procedures while keep the basic behaviors of the original system, so they are widely used in various problems of stochastic mechanics such as response, stability, reliability, bifurcation, optical control, and the first passage and fatigue failure analyses (Ibrahim, 1985; Namachchivaya and Ariaratnam, 1987; Zhu, 1988; Lin and Cai, 1995; Ariaratnam, 1996; Zhu, 2003; Xie, 2006). Recently, Onu completed his doctoral thesis entitled *Stochastic averaging for mechanical systems* (Onu, 2010).

Consider a stochastic system

$$\dot{\mathbf{x}}(t)=\varepsilon\,\mathbf{F}(t,\mathbf{x},\boldsymbol{\xi}(t),\varepsilon),\qquad \mathbf{x}(0)=\mathbf{x}_0, \tag{1.2.27}$$

where

$$\mathbf{x}(t)=\{X_1,X_2,\cdots,X_n\}^T,\qquad \boldsymbol{\xi}(t)=\{\xi_1,\xi_2,\cdots,\xi_n\}^T, \tag{1.2.28}$$

and $0<\varepsilon\ll 1$ is a small parameter, $\boldsymbol{\xi}(t)$ is a zero mean value, stationary stochastic process vector. If as $\varepsilon\to 0$, $\mathbf{F}(t,\mathbf{x},\boldsymbol{\xi}(t),\varepsilon)$ can be expressed uniformly in $t,\mathbf{x},\boldsymbol{\xi}$ as

$$\mathbf{F}(t,\mathbf{x},\boldsymbol{\xi}(t),\varepsilon)=\mathbf{F}^{(0)}(t,\mathbf{x},\boldsymbol{\xi}(t))+\varepsilon\,\mathbf{F}^{(1)}(t,\mathbf{x})+o(\varepsilon), \tag{1.2.29}$$

where $\mathbf{F}^{(0)}$, $\mathbf{F}^{(1)}$ and their first- and second-order derivatives with respect to $\mathbf{x}$ are smooth and bounded functions, $\mathbf{F},\mathbf{F}^{(0)}$ and $\mathbf{F}^{(1)}$ are measurable for fixed $\mathbf{x}$ and ε, and the correlation function $\mathrm{E}[\boldsymbol{\xi}(t)\boldsymbol{\xi}(t+\tau)]$ decays to zero fast enough as τ increases, or $\boldsymbol{\xi}(t)$ is a wide-band process, then system (1.2.27) can be approximated uniformly in weak sense (e.g., Khasminskii, 1966a) by a Markov diffusion process $\bar{\mathbf{x}}(t)$ satisfying

$$\mathrm{d}\bar{\mathbf{x}}(t)=\varepsilon\,\mathbf{m}(\bar{\mathbf{x}})\,\mathrm{d}t+\varepsilon^{1/2}\boldsymbol{\sigma}(\bar{\mathbf{x}})\,\mathrm{d}\mathbf{W}(t), \tag{1.2.30}$$

provided that the following limits exist uniformly in $\mathbf{x}$ and t:

$$\begin{aligned}\mathbf{m}(\bar{\mathbf{x}})&=\underset{t}{\mathscr{M}}\left\{\mathbf{F}^{(1)}+\int_{-\infty}^{0}\mathrm{E}\left[\frac{\partial\mathbf{F}^{0}}{\partial\mathbf{x}}\mathbf{F}_{\tau}^{(0)}\right]\mathrm{d}\tau\right\},\\ \mathbf{b}(\bar{\mathbf{x}})&=\boldsymbol{\sigma}(\bar{\mathbf{x}})\boldsymbol{\sigma}^{T}(\bar{\mathbf{x}})=\underset{t}{\mathscr{M}}\left\{\int_{-\infty}^{\infty}\mathrm{E}\left[\mathbf{F}^{0}\left(\mathbf{F}_{\tau}^{(0)}\right)^{T}\right]\mathrm{d}\tau\right\},\end{aligned} \tag{1.2.31}$$

where $\mathbf{W}(t)=\{W_1,W_2,\cdots,W_n\}^T$ denotes an n-dimensional vector of mutually independent standard Wiener processes, $\mathbf{F}_{\tau}^{(0)}=\mathbf{F}_0[t+\tau,\mathbf{x},\boldsymbol{\xi}(t+\tau)]$, and $\mathbf{b}(\bar{\mathbf{x}})$ is the $n\times n$ diffusion matrix. $\underset{t}{\mathscr{M}}\{\cdot\}$ is the averaging operator defined by

$$\underset{t}{\mathscr{M}}\{\cdot\} = \lim_{T\to\infty}\frac{1}{T}\int_{\tau}^{\tau+T}\{\cdot\}\,\mathrm{d}t, \tag{1.2.32}$$

where the integration is performed over an explicitly appearing time parameter t in the integrand. In the elemental form, equation (1.2.31) can be written as

$$\begin{aligned} m_j(\bar{\mathbf{x}}) &= \underset{t}{\mathscr{M}}\left\{F_j^{(1)} + \int_{-\infty}^{0}\mathrm{E}\Big[\sum_{k=1}^{n}\frac{\partial F_j^0}{\partial x_k}F_{k\tau}^{(0)}\Big]\mathrm{d}\tau\right\}, \\ \left[\boldsymbol{\sigma}(\bar{\mathbf{x}})\boldsymbol{\sigma}^T(\bar{\mathbf{x}})\right]_{jk} &= \underset{t}{\mathscr{M}}\left\{\int_{-\infty}^{\infty}\mathrm{E}\Big[F_j^0F_{k\tau}^{(0)}\Big]\mathrm{d}\tau\right\}. \end{aligned} \tag{1.2.33}$$

Although stochastic averaging principle only ensures that the approximate solution given by equation (1.2.30) converges in distribution to the true solution of equation (1.2.27) over a finite time interval, it still provides a useful approach when the true solution is difficult to obtain. The attractiveness of the method lies in its applicability, subject to certain restrictions, to a wide variety of systems, including those which are nonlinear, or parametrically excited, or both. A physical interpretation of this method, which is more appealing to engineers, was given by Lin and Cai (1995).

However, the major limitation of this ordinary averaging method is the assumption of quasi-linearity. Some terms in the original equation of motion, such as nonlinear restoring forces, may disappear in the first-order averaged equations (Mickens, 1981). Thus, the effects of those terms on the stochastic response of the system cannot be investigated by using the ordinary stochastic averaging method (Zhu, 1988). Various averaging procedures for obtaining approximate solutions have been presented (Sanders and Verhulst, 1985; Anh and Tinh, 2001; Hijawi *et al.*, 1997). It is possible to combine the equivalent linearization method with stochastic averaging (Iwan and Spanos, 1978). A similar attempt has also been reported by Naprstek (1976). However, there are also theoretical difficulties associated with this approach (Ariaratnam, 1978). A comprehensive literature review on stochastic averaging was made by Roberts and Spanos (1986); Lin and Cai (2000); Zhu (1988).

The nonlinearity in weak-linear terms can be considered in ordinary averaging methods which include higher-order terms, i.e., second-order or higher-order averaging methods.

Actually, it is illustrated that the effect of the weak nonlinearity in certain cases shows up only in the higher-order approximations (see Mickens, 1981, page 63).

The Lagrange Standard Form

In practice, the equation of motion is usually given as:

$$\dot{\mathbf{x}}(t)=\mathbf{A}(t)\mathbf{x}+\varepsilon\,\mathbf{g}(t,\mathbf{x},\boldsymbol{\xi}(t),\varepsilon),\quad \mathbf{x}(0)=\mathbf{x}_0, \tag{1.2.34}$$

where $\mathbf{A}(t)$ is a continuous $n\times n$ matrix. It is obvious that equation (1.2.34) is not the same form as (1.2.27). This case can be treated by the method of "variation of parameters" as follows.

The unperturbed ($\varepsilon=0$) equation is linear and it has n independent solutions which are used to compose a fundamental matrix $\Phi(t)$. Introducing the co-moving coordinates as:

$$\mathbf{x}=\Phi(t)\mathbf{y},\quad \dot{\mathbf{x}}(t)=\dot{\Phi}(t)\mathbf{y}+\Phi(t)\dot{\mathbf{y}}. \tag{1.2.35}$$

Substitution into equation (1.2.34) yields

$$\dot{\Phi}(t)\mathbf{y}+\Phi(t)\dot{\mathbf{y}}=\mathbf{A}(t)\Phi(t)\mathbf{y}+\varepsilon\,\mathbf{g}(t,\Phi(t)\mathbf{y},\boldsymbol{\xi}(t),\varepsilon). \tag{1.2.36}$$

Since $\Phi(t)$ is chosen to be the fundamental matrix of the unperturbed system, i.e., to satisfy the unperturbed equation, $\dot{\Phi}(t)=\mathbf{A}(t)\Phi(t)$, one obtains

$$\Phi(t)\dot{\mathbf{y}}=\varepsilon\,\mathbf{g}(t,\Phi(t)\mathbf{y},\boldsymbol{\xi}(t),\varepsilon), \tag{1.2.37}$$

i.e.,

$$\dot{\mathbf{y}}=\varepsilon\Phi^{-1}(t)\ \mathbf{g}(t,\Phi(t)\mathbf{y},\boldsymbol{\xi}(t),\varepsilon), \tag{1.2.38}$$

with the initial values follow from

$$\mathbf{y}(0)=\Phi^{-1}(0)x(0).$$

Writing down the equations for the components of $\dot{\mathbf{y}}$ while using Cramer's rule, one has

$$\dot{y}_i=\varepsilon\frac{W_i(t,\mathbf{y},\xi)}{W(t)},\quad i=1,\cdots,n, \tag{1.2.39}$$

with $W(t)=|\Phi(t)|$, the determinant of $\Phi(t)$, $W_i(t,\mathbf{y},\xi)$ is the determinant of the matrix which one obtains by replacing the ith column of $\Phi(t)$ by $\mathbf{g}$ (Verhulst, 1996). Equation

(1.2.38) is said to have the Lagrange standard form of stochastic version. More generally, the standard form is

$$\dot{\mathbf{y}} = \varepsilon \mathbf{F}(t, \Phi(t)\mathbf{y}, \boldsymbol{\xi}(t), \varepsilon). \tag{1.2.40}$$

Thus, without loss of generality, we discuss the weakly nonlinear differential equations in Lagrange standard form, which is exact in the form of (1.2.27).

If the unperturbed equation is nonlinear or coupled, the variation of parameters technique still applies. Such case is sometimes called strong nonlinear differential equation (Zhu, 2003), as compared to the weakly nonlinear equation where a small parameter ε is placed before the nonlinear term. In practice, however, there are usually many technical obstructions while carrying out the procedure (Rand and Armbruster, 1987; Sachdev, 1991). For example, nonlinear systems, where the unperturbed system is already nonlinear, were investigated by using elliptic functions (Coppola, 1997) and by using generalized harmonic functions (Xu and Cheung, 1994; Zhu, 2003). The unperturbed gyroscopic system is coupled, which will be treated by the method of operator in Chapter 5.

1.3 Ordinary Viscoelasticity & Fractional Viscoelasticity

1.3.1 Fractional Calculus

Unification of integration and differentiation notions

Consider the infinite sequence of integrals and derivatives

$$\cdots, \quad \int_a^t \mathrm{d}\tau_2 \int_a^{\tau_2} f(\tau_1)\mathrm{d}\tau_1, \quad \int_a^t f(\tau_1)\mathrm{d}\tau_1, \quad f(t), \quad \frac{\mathrm{d}f(t)}{\mathrm{d}t}, \quad \frac{\mathrm{d}^2 f(t)}{\mathrm{d}t^2}, \quad \cdots, \tag{1.3.1}$$

or

$$\cdots, \quad \frac{\mathrm{d}^{(-2)}f(t)}{\mathrm{d}t^{(-2)}}, \quad \frac{\mathrm{d}^{(-1)}f(t)}{\mathrm{d}t^{(-1)}}, \quad f(t), \quad \frac{\mathrm{d}f(t)}{\mathrm{d}t}, \quad \frac{\mathrm{d}^2 f(t)}{\mathrm{d}t^2}, \quad \cdots. \tag{1.3.2}$$

The nth repeated integration is given by

$$f^{(-n)}(t) = \frac{\mathrm{d}^{(-n)}f(t)}{\mathrm{d}t^{(-n)}} = \int_a^t \mathrm{d}t_1 \int_a^{t_1} \mathrm{d}t_2 \cdots \int_a^{t_{n-1}} f(t_n)\mathrm{d}t_n. \tag{1.3.3}$$

From Cauchy formula for repeated integration, applying the induction hypothesis and switching the order of integration, one can compress the repeated integration (1.3.3) into a single integral

$$f^{(-n)}(t)=\frac{1}{(n-1)!}\int_a^t(t-\tau)^{n-1}f(\tau)\mathrm{d}\tau,\quad n\in\mathcal{N}^+,\tag{1.3.4}$$

for almost all x with $-\infty\leqslant a<t\leqslant\infty$, and $\mathcal{N}^+$ is the set of positive integers.

Supposing that $n\geqslant 1$ is fixed and taking integer $m\geqslant 0$, one obtains

$$f^{(-m-n)}(t)=\frac{1}{\Gamma(n)}\mathcal{D}^{-m}\int_a^t(t-\tau)^{n-1}f(\tau)\mathrm{d}\tau,\tag{1.3.5}$$

where the symbol $\mathcal{D}^{-m}(m\geqslant 0)$ denotes the mth iterated integration.

On the other hand, for a fixed $n\geqslant 1$ and integer $m\geqslant n$ the $(m-n)$th derivative of the function $f(t)$ can be written as

$$f^{(m-n)}(t)=\frac{1}{\Gamma(n)}\mathcal{D}^{m}\int_a^t(t-\tau)^{n-1}f(\tau)\mathrm{d}\tau,\quad m\in\mathcal{N}^+,\tag{1.3.6}$$

where the symbol $\mathcal{D}^{m}(m\geqslant 0)$ denotes the mth iterated differentiation.

It is of interest to note that equations (1.3.5) and (1.3.6) are equivalent. This is the so-called unification of the notions of integer-order integration and differentiation (Podlubny, 1999).

Fractional calculus

A natural extension of Cauchy formula for repeated integration is to define Riemann-Liouville (RL) fractional integral heuristically from equation (1.3.4)

$$f^{(-\alpha)}(t)={}_a^{\mathrm{RL}}\mathcal{D}_t^{-\alpha}[f(t)]=\frac{1}{\Gamma(\alpha)}\int_a^t(t-\tau)^{\alpha-1}f(\tau)\mathrm{d}\tau,\quad \alpha\in\mathcal{R}^+,\tag{1.3.7}$$

where ${}_a^{\mathrm{RL}}\mathcal{D}_t^{-\alpha}[f(t)]$ denotes the symbol of Riemann-Liouville (RL) fractional integral of function $f(t)$. α is a coefficient of "fractance" (Rand, 2012), $\mathcal{R}^+$ is positive real numbers, and $\Gamma(\alpha)$ is the gamma function

$$\Gamma(\alpha)=\int_0^\infty \mathrm{e}^{-t}t^{\alpha-1}\mathrm{d}t.\tag{1.3.8}$$

For most engineering problems, $f(t)$ vanishes for $t<0$; hence $a=0$ for equation (1.3.7). If α is a positive integer, then $\Gamma(\alpha)=(\alpha-1)!$, so this definition of $f^{(-\alpha)}(t)$ agrees with (1.3.4) when α is a positive integer.

Substituting equation (1.3.7) into (1.3.6) leads to

$$ {}^{\mathrm{RL}}_{0}\mathcal{D}^{m-\alpha}_{t}[f(t)] = \frac{1}{\Gamma(\alpha)} \frac{\mathrm{d}^m}{\mathrm{d}t^m} \int_0^t (t-\tau)^{\alpha-1} f(\tau)\mathrm{d}\tau. \tag{1.3.9} $$

Denoting $\mu = m - \alpha$, one can write Riemann-Liouville (RL) fractional derivative as

$$ {}^{\mathrm{RL}}_{0}\mathcal{D}^{\mu}_{t}[f(t)] = \frac{1}{\Gamma(m-\mu)} \frac{\mathrm{d}^m}{\mathrm{d}t^m} \int_0^t \frac{f(\tau)}{(t-\tau)^{-(m-\mu)+1}}\mathrm{d}\tau, \quad m-1 \leqslant \mu \leqslant m, \tag{1.3.10} $$

where ${}^{\mathrm{RL}}_{a}\mathcal{D}^{\mu}_{t}[f(t)]$ denotes the symbol of Riemann-Liouville (RL) fractional derivative of function $f(t)$.

It can be seen that ${}^{\mathrm{RL}}_{0}\mathcal{D}^{0}_{t}[f(t)] = f(t)$ and ${}^{\mathrm{RL}}_{0}\mathcal{D}^{m}_{t}[f(t)] = f^{(m)}(t)$ (Podlubny, 1999). Specifically, for $0 \leqslant \mu \leqslant 1$, assuming $f(t)$ is absolutely continuous for $t > 0$, one has (see Kilbas *et al.*, 2006, equation (2.1.28))

$$ {}^{\mathrm{RL}}_{0}\mathcal{D}^{\mu}_{t}[f(t)] = \frac{1}{\Gamma(1-\mu)} \frac{\mathrm{d}}{\mathrm{d}t} \int_0^t \frac{f(\tau)}{(t-\tau)^{\mu}}\mathrm{d}\tau = \frac{1}{\Gamma(1-\mu)} \left[\frac{f(0)}{t^{\mu}} + \int_0^t \frac{f'(\tau)}{(t-\tau)^{\mu}}\mathrm{d}\tau \right]. \tag{1.3.11} $$

It is interesting to note that this is actually the solution of Abel's integral equation (Kilbas *et al.*, 2006). Further assuming $f(0) = 0$ gives the fractional derivative in Caputo (C) form

$$ {}^{\mathrm{C}}_{0}\mathcal{D}^{\mu}_{t}[f(t)] = \frac{1}{\Gamma(1-\mu)} \int_0^t \frac{f'(\tau)}{(t-\tau)^{\mu}}\mathrm{d}\tau = \frac{1}{\Gamma(1-\mu)} \int_0^t \frac{f'(t-\tau)}{\tau^{\mu}}\mathrm{d}\tau. \tag{1.3.12} $$

The fractional calculus of arbitrary real order α can be considered as an interpolation of the sequence of integer-order calculus in equation (1.3.2), which is the same as fractional moments (Deng and Pandey, 2008; Deng *et al.*, 2009). Figure 1.5 provides a sense of fractional calculus of a simple function $f(x) = x$. Inherently, fractional derivatives take into account the memory of the past evolution of the response, i.e., from the start time $\tau = 0$ to the present time $\tau = t$, in contrast with the standard integer-order differential operator that considers only the local time history.

1.3.2 Viscoelasticity

Viscoelasticity has been observed in many engineering materials, such as polymers, concrete, metals at elevated temperatures, and rocks, which have been used extensively in industrial applications, such as nuclear power plants and space shuttles.

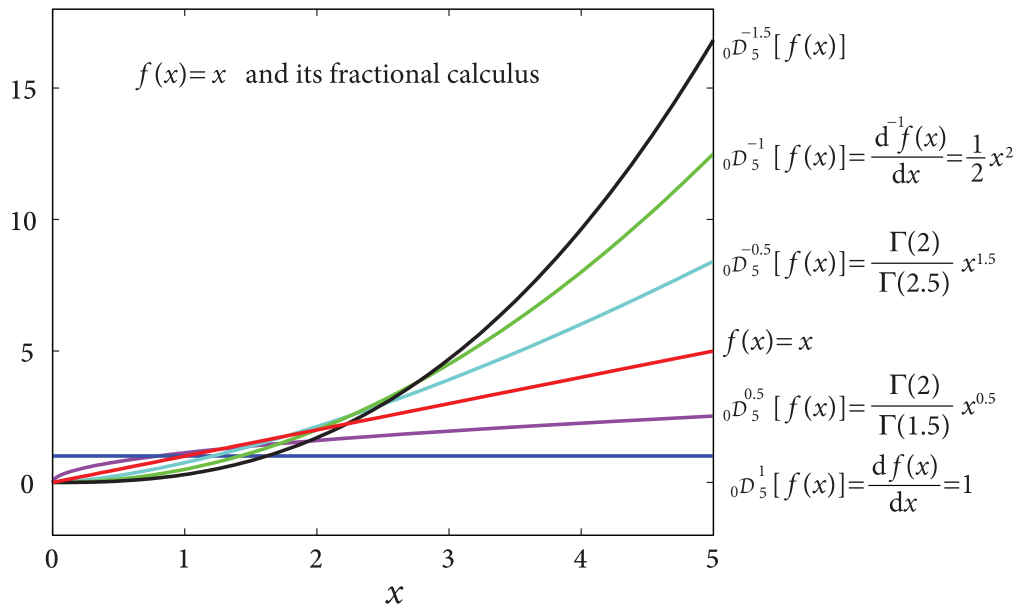

Figure 1.5 Fractional calculus of a function

The time-dependent behavior and strain rate effects of viscoelastic materials have been described by constitutive equations, which include time as a variable in addition to the stress and strain variables and their integer-order differentials or integrals. Viscoelastic materials exhibit stress relaxation and creep, with the former characterized by a decrease of the stress with time for a fixed strain and the latter characterized by a growth of the strain under a constant stress. Several mechanical models for ordinary viscoelasticity were reviewed (Findley *et al.*, 1976). These models involve exponential strain creeps or exponential stress relaxations, e.g., Kelvin-Voigt model exhibiting an exponential strain creep. These exponential laws are due to the integer-order differential equation form of constitutive models for viscoelasticity.

The Kelvin-Voigt model, which simply consists of a spring and a dashpot connected in parallel, is often used to characterize the viscoelasticity. This model can be used to form more complicated models (Ahmadi and Glocker, 1983; Floris, 2011). The constitutive equation of Kelvin-Voigt model is

$$\sigma(t)=E\varepsilon(t)+\eta\frac{\mathrm{d}\varepsilon(t)}{\mathrm{d}t}, \tag{1.3.13}$$

where $\sigma(t)$ and $\varepsilon(t)$ are the stress and strain, respectively, E is the spring constant or modulus, η is the Newtonian viscosity or the coefficient of viscosity. Supposing $\varepsilon(t) = H(t)$ and $\sigma(t) = H(t)$, respectively, and using the Laplace transform and inverse Laplace transform lead to the material functions for Kelvin-Voigt model

$$G(t) = E + \eta\delta(t), \quad J(t) = \frac{1}{E}\left(1 - e^{-\frac{t}{\tau_\varepsilon}}\right), \tag{1.3.14}$$

where $\tau_\varepsilon = \eta/E$ is referred to as the retardation time, $\delta(t)$ is the Dirac delta function, and $H(t)$ is the Heaviside step function.

For a constant applied stress σ_0, the creep function is

$$\varepsilon(t) = \frac{\sigma_0}{E}\left(1 - e^{-t/\tau_\varepsilon}\right), \tag{1.3.15}$$

where $\tau_\varepsilon = \eta/E$ is called the retardation time. When the stress is removed, the recovery function $\varepsilon_R(t)$ is

$$\varepsilon_R(t) = \varepsilon_0 e^{-t/\tau_\varepsilon}, \tag{1.3.16}$$

where ε_0 is the initial strain at the time of stress removal.

The Maxwell model consists of a spring (E) and a dashpot (η) connected in series, which the constitutive relation is described as

$$\sigma(t) + \frac{\eta}{E}\frac{d\sigma}{dt} = \eta\frac{d\varepsilon}{dt}. \tag{1.3.17}$$

The material functions for Maxwell model can be obtained by assuming $\varepsilon(t) = H(t)$ and $\sigma(t) = H(t)$, respectively, and taking the Laplace transform

$$G(t) = Ee^{-\frac{t}{\tau_\sigma}}, \quad J(t) = \frac{1}{E} + \frac{1}{\eta}t, \tag{1.3.18}$$

where $\tau_\sigma = \eta/E$ is referred to as the relaxation time.

Recently, an increasing interest has been directed to non-integer or fractional viscoelastic constitutive models (Debnath, 2003; Paola and Pirrotta, 2009; Mainardi, 2010). In contrast to the well-established mechanical models based on Hookean springs and Newtonian dashpots, which result in exponential decays of the relaxation functions, the fractional models accommodate non-exponential relaxations, making them capable of modelling hereditary phenomena with long memory. Fractional constitutive models lead to power law behavior in linear viscoelasticity asymptotically (Bagley and Torvik, 1983). It can also result in non-exponential relaxation behavior typical of numerous experimental observations (Glockle and Nonnenmacher, 1994). Fractional viscoelasticity allows creep and relaxation processes to be described adequately by means of simple and concise relationships between stresses and strains with a relatively small number of adjustable parameters, without using a relaxation (or retardation) spectrum (Glockle and Nonnenmacher, 1991; Heymans and Bauwens, 1994). There is a theoretical reason for using fractional calculus in viscoelasticity (Bagley and Torvik, 1983): the molecular theory of Rouse (1953) gives stress and strain relationship with fractional derivative of strain. Experiments also revealed that the viscous damping behaviour can be described satisfactorily by the introduction of fractional derivatives in stress-strain relations (Koh and Kelly, 1990; Pfitzenreiter, 2004, 2008).

The fractional viscoelastic mechanical models are fractional generalizations of the conventional constitutive models, by replacing the derivative of order 1 with the fractional derivative of order μ ($0 \leqslant \mu \leqslant 1$) in the Rieman-Liouville sense in their constitutive models. The fractional Kelvin-Voigt constitutive equation is defined as

$$\sigma(t) = E\varepsilon(t) + \eta \frac{\mathrm{d}^{\mu}\varepsilon(t)}{\mathrm{d}t^{\mu}} = E\varepsilon(t) + \eta \, {}^{\mathrm{RL}}_{0}\mathcal{D}^{\mu}_{t}[\varepsilon(t)], \tag{1.3.19}$$

where ${}^{\mathrm{RL}}_{0}\mathcal{D}^{\mu}_{t}[\,\cdot\,]$ is an operator for Riemann-Liouville (RL) fractional derivative of order μ.

For a constant applied stress σ_0, the creep function is

$$\varepsilon(t) = \frac{\sigma_0}{E}\left\{1 - \mathcal{E}_{\mu}\left[-\left(\frac{t}{\tau_{\varepsilon}}\right)^{\mu}\right]\right\}, \quad \tau_{\varepsilon} = \frac{\eta}{E}. \tag{1.3.20}$$

When the stress is removed, the recovery function $\varepsilon_R(t)$ is

$$\varepsilon_R(t) = \varepsilon_0 \mathcal{E}_{\mu}\left[-\left(\frac{t}{\tau_{\varepsilon}}\right)^{\mu}\right], \tag{1.3.21}$$

where $\mathcal{E}_{\alpha}(z)$ is the Mittag-Leffler function defined by

$$\mathcal{E}_{\alpha}(z) = \sum_{n=0}^{\infty} \frac{z^n}{\Gamma(\alpha n + 1)}. \tag{1.3.22}$$

It is seen that when $\mu = 1$, the Mittag-Leffler function $E_\mu(z)$ reduces to the exponential function

$$E_1(z) = \sum_{m=0}^{\infty} \frac{z^m}{\Gamma(m+1)} = \sum_{m=0}^{\infty} \frac{z^m}{m!} = e^z. \tag{1.3.23}$$

The fractional Kelvin-Voigt model in equation (1.3.19) can be separated into two parts: Hooke element $E\varepsilon(t)$ and fractional Newton (Scott-Blair) element $\eta\ {}_{0}^{\mathrm{RL}}D_t^{\mu}[\varepsilon(t)]$.

When $\mu = 0$, the fractional Newton part becomes a constant η, which is the case for the Hooke model. It is further observed that, only when $\mu = 0$, this model exhibits transient elasticity at $t = 0$.

When $\mu = 1$, the relaxation modulus of the fractional Newton part becomes a Dirac delta function, i.e., $G(t) = \eta\delta(t)$, which is the case of the integer Newton model.

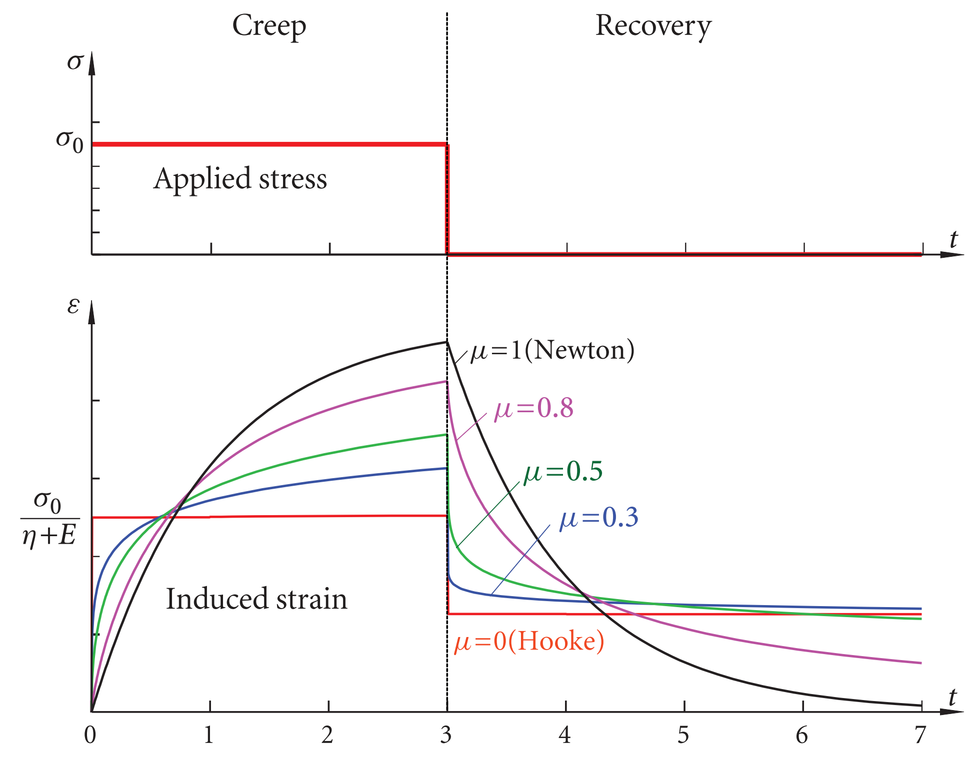

Figure 1.6 Creep and recovery for a fractional viscoelastic material

Hence, the fractional Newton element is a continuum between the spring model and the Newton model. A typical relationship of creep and recovery for a fractional viscoelastic material is displayed in Figure 1.6, which clearly shows that the extra degree-of-freedom from using the fractional order can improve the performance of traditional viscoelastic elements. Specifically, when $\mu = 1$, this fractional model reduces to the ordinary integer Kelvin-Voigt model.

The fractional-order operator in equation (1.3.10) is a *global* operator having a memory of all past events, making it adequate for modeling the memory and hereditary effects in most materials, as the operator consider the whole time history from the start $\tau = 0$ to the present time $\tau = t$. However, this requirement of all historic values would sometimes cause computational difficulties.

1.4 Scopes of the Research

Problems to be addressed and solutions in this thesis are outlined as follows:

1. How to effectively describe the long history-dependent properties of viscoelastic materials?

   In this thesis, fractional derivatives are used to describe constitutive relations of viscoelastic materials with time-dependent properties. Chapter 1 also provides preliminary background knowledge and literature reviews.

2. How to perform numerical simulation for fractional stochastic systems?

   In this thesis, a new numerical method for determining moment Lyapunov exponents of fractional stochastic systems is proposed in Chapter 2. It can be used to obtain simulation results or to verify approximate results.

3. How to consider weak nonlinearity in stochastic averaging method?

   In this thesis, higher-order stochastic averaging method is developed to capture the influence of weak nonlinearities in equations of motion, which were lost in the first-order averaging method. Chapter 3 first justifies stochastic averaging method for fractional differential equations. Then stochastic stability is studied for fractional viscoelastic single-degree-of-freedom systems under the excitation of wide-band and bounded noises, by using the method of higher-order stochastic averaging. These approximate analytical solutions are compared with simulation results.

4. How to efficiently study stochastic stability of coupled non-gyroscopic systems?

   In this thesis, an elegant algorithm is proposed to determine moment Lyapunov exponents of four-dimensional systems. Chapter 4 deals with stochastic stability of coupled non-gyroscopic viscoelastic systems. Flexural-torsional stability of a rectangular beam is taken as an example. Parametric resonance is studied in detail.

5. How to efficiently obtain the Lyapunov exponents and moment Lyapunov exponents of gyroscopic systems?

   In this thesis, gyroscopic systems excited by wide-band noises and by bounded noises are investigated by stochastic averaging method and parametric resonance is studied in Chapter 5. A typical example of gyroscopic systems is the vibration of a rotating shaft.

On the basis of theories of structural dynamics, fractional calculus, stochastic differential equations, viscoelastic mechanics, and random vibration, this thesis is aimed to formulate a novel methodology of fractional stochastic dynamics to study stochastic stability of viscoelastic systems under stochastic loadings. The viscoelastic structures includes single-degree-of-freedom systems, coupled non-gyroscopic systems, and gyroscopic systems. It is expected to improve or to optimize the dynamic stability by adjusting structural parameters after the Lyapunov exponents and moment Lyapunov exponents are obtained.

It is noted that the equations of motion for viscoelastic structures usually appear to be fractional equations. Such equations originate not only in structural dynamics, but also in other areas such as biophysics and population dynamics (Cushing, 1977). Hence, research on the stability of viscoelastic structures may help to advance research in other areas.

CHAPTER 2

A Numerical Method for Moment Lyapunov Exponents of Fractional Systems

This chapter proposes a numerical method for determining both the Lyapunov moments and the pth moment Lyapunov exponents of stochastic systems containing fractional derivatives. Section 2.1 gives the reasons why a new numerical simulation method for fractional systems is needed. Section 2.2 proposes the new numerical method. Discussion is made in Section 2.3.

2.1 Exponential Kernel and Power Kernel

Consider the fractional stochastic differential equation of motion

$$\ddot{\mathbf{x}}(t) = \mathbf{f}\left(\mathbf{x}(t), \dot{\mathbf{x}}(t), {}_0\mathcal{D}_t^{\mu}[\mathbf{x}(\mathbf{t})], \boldsymbol{\xi}(\mathbf{t})\right), \tag{2.1.1}$$

where ${}_0\mathcal{D}_t^{\mu}[\mathbf{x}(\mathbf{t})]$ denotes a fractional derivative. The most commonly used fractional derivatives is the Rieman-Liouville fractional derivatives, $0 \leqslant \mu \leqslant 1$. $\mathbf{x}(t)$ is the response vector, $\boldsymbol{\xi}(t)$ denotes a vector of the loadings.

To illustrate the characteristics of fractional systems, one can compare the viscoelastic equations of motion with exponential kernels and power kernels. The exponential kernel function comes from the ordinary Maxwell model (Findley *et al.*, 1976)

$$\mathcal{H}(t) = \gamma \mathrm{e}^{-\kappa t}, \tag{2.1.2}$$

the derivative of which is also an exponential function. Considering the ordinary viscoelastic term

$$x(t) = \int_0^t \mathcal{H}(t-s)q(s)\mathrm{d}s = \int_0^t \gamma\, \mathrm{e}^{-\kappa(t-s)} q(s)\,\mathrm{d}s, \tag{2.1.3}$$

the derivative $\dot{x}(t)$ can be expressed as a function of $x(t)$ and $q(t)$,

$$\dot{x}(t) = \gamma\, q(t) - \kappa x(t). \tag{2.1.4}$$

This feature is crucial in Monte Carlo simulation of moment Lyapunov exponents, because the integro-differential equation of motion can then be readily and accurately transformed into a set of first-order differential equations without memory, which assure periodic normalization affordable and therefore guarantees Xie's algorithm applicable. Here "without memory" means in the iteration equations, the variable values in $(k+1)$th iteration depend on values of previous kth iteration only.

However, this is not the case for power kernel function, which comes from fractional derivatives. Consider the fractional term in equation (1.3.11)

$$x(t) = \int_0^t \frac{q'(\tau)}{(t-\tau)^{\mu}}\mathrm{d}\tau. \tag{2.1.5}$$

It can be found that the derivative $\dot{x}(t)$ seems not able to be readily expressible as a function of $x(t)$ and $\dot{q}(t)$ or $q(t)$, which in turn leads to the fact that the fractional stochastic differential equation of motion in equation (2.1.1) cannot be readily and accurately converted into a system of first-order differential equations without memory. On the contrary, $x(t)$ depends on all the historical values. Thus, any normalization during the simulation iteration will distort the fractional derivative and result in an error in the discretization of fractional derivatives. Consequently, Xie's algorithm with periodic normalization (Xie, 2005) is unapplicable to numerical simulation of moment Lyapunov exponents, and Wolf et al's method with Gram-Schmidt orthornormalization (Wolf *et al.*, 1985) cannot be applied to numerical simulation of Lyapunov exponents of fractional differential equations of motion.

It should be noted that the fractional differential equation governing the dynamics of a system has been approximately discretized into a set of differential equations without fractional derivative terms and without memory (Yuan and Agrawal, 2002; Atanackovic and Stankovic, 2008). This scheme involves a physical background, for it is equivalent to a classical spring-dashpot representation, but it does not imply the benefits derived from fractional-derivative models. In addition, it is less flexible and incorrectly predicts the asymptotic behavior (Schmidt and Gaul, 2006). Relatively large errors may be incurred during these transformations with the purpose of obtaining moment Lyapunov exponents. This is probably due to the fact that it is necessary to store the entire response history of the system due to the non-local character of the fractional derivatives. However, the entire response history is transformed into systems of several variables without memory and this inevitably incurs errors. It is acknowledged that more research is needed in this area.

2.2 Numerical Determination of Moment Lyapunov Exponents of Fractional Systems

2.2.1 Numerical Discretization of Fractional Derivatives

In order to discretize the fractional stochastic equation of motion (2.1.1), Rieman-Liouville fractional derivative must be simulated numerically. Suppose the time interval concerned is $[0, t]$ and the step time length is h, then one has $t = t_n = nh$ and $t_{n-k} = (n-k)h,\ k = 0, 1, \cdots, n$. Since the fractional derivative in equation (1.3.11) is a convolution integral, it can also be written as

$$
\begin{aligned}
{}_0^{\mathrm{RL}}\mathcal{D}_{t_n}^{\mu}[q(t)] &= \frac{1}{\Gamma(1-\mu)}\Big[\frac{q(0)}{t_n^{\mu}} + \int_0^{t_n} \frac{q'(t_n-\tau)}{\tau^{\mu}}\mathrm{d}\tau\Big] \\
&= \frac{1}{\Gamma(1-\mu)}\Big[\frac{q(0)}{(nh)^{\mu}} + \sum_{j=0}^{n-1}\int_{jh}^{(j+1)h} \frac{q'(t_n-\tau)}{\tau^{\mu}}\mathrm{d}\tau\Big].
\end{aligned}
\tag{2.2.1}
$$

This discretization is described in more detail below for the two assumed local response $q(t)$ distributions.

1. **Piecewise linear method**

   The response $q(t)$ over a given interval is approximated by:

$$
q(t) = a_0 + a_1 t, \tag{2.2.2}
$$

The fitting constants for the interval $[t_j, t_{j+1}]$ are give by

$$a_0 = q(t_{j+1}) - \frac{t_{j+1}[q(t_{j+1}) - q(t_j)]}{t_{j+1} - t_j}, \quad a_1 = \frac{q(t_{j+1}) - q(t_j)}{t_{j+1} - t_j}. \tag{2.2.3}$$

The first-order derivative in the interval $jh \leqslant \tau \leqslant (j+1)h$

$$\dot{q}(t_n - \tau) = \dot{q}(nh - \tau) = \frac{q[(n-j)h] - q[(n-j-1)h]}{h}, \tag{2.2.4}$$

and

$$\int_{jh}^{(j+1)h} \frac{1}{\tau^\mu} \mathrm{d}\tau = \frac{1}{1-\mu} h^{1-\mu} [(j+1)^{1-\mu} - j^{1-\mu}] \tag{2.2.5}$$

leads to

$$\begin{aligned} {}_0^{\mathrm{RL}}\mathcal{D}_{t_n}^{\mu}[q(t)] &= \frac{1}{\Gamma(1-\mu)} \left\{ \frac{q(0)}{(nh)^\mu} \right. \\ &\quad \left. + \frac{1}{1-\mu} \frac{1}{h^\mu} \sum_{j=0}^{n-1} [q[(n-j)h] - q[(n-j-1)h]][(j+1)^{1-\mu} - j^{1-\mu}] \right\} \\ &= \kappa \left[\frac{(1-\mu)q(0)}{n^\mu} + \sum_{j=0}^{n-1} a_j \right], \end{aligned} \tag{2.2.6}$$

where

$$\kappa = \frac{1}{h^\mu \Gamma(2-\mu)}, \quad a_j = \{q[(n-j)h] - q[(n-j-1)h]\}[(j+1)^{1-\mu} - j^{1-\mu}], \tag{2.2.7}$$

or in the quadrature form

$${}_0^{\mathrm{RL}}\mathcal{D}_{t_n}^{\mu}[q(t)] = \frac{1}{h^\mu} \sum_{j=0}^{n} w_j q(jh), \tag{2.2.8}$$

where the abscissae are jh and the weights of the quadrature (w_j) are

$$\begin{aligned} w_0 &= \frac{1}{\Gamma(2-\mu)} [(n-1)^{1-\mu} - n^{1-\mu} + (1-\mu)n^{-\mu}], \quad w_n = \frac{1}{\Gamma(2-\mu)}, \\ w_j &= \frac{1}{\Gamma(2-\mu)} [(n-j+1)^{1-\mu} - 2(n-j)^{1-\mu} + (n-j-1)^{1-\mu}], \quad 1 \leqslant j \leqslant n-1. \end{aligned} \tag{2.2.9}$$

2. **Piecewise quadratic method**

An improvement in accuracy may be achieved by assuming that the response $q(t)$ over a given interval is approximated a quadratic polynomial:

$$q(t)=a_0+a_1 t+a_2 t^2. \tag{2.2.10}$$

Since there are three constants in the above expression, it must be fit over the interval $[t_{j-1}, t_{j+1}]$. The fitting constants for the polynomial are given by

$$\begin{aligned}
a_0 &= \frac{q(t_{j-1})\big(t_j^2 t_{j+1}-t_j t_{j+1}^2\big)+q(t_j)\big(t_{j-1}t_{j+1}^2-t_{j-1}^2 t_{j+1}\big)+q(t_{j+1})\big(t_{j-1}^2 t_j-t_{j-1}t_j^2\big)}{t_{j-1}\big(t_{j+1}^2-t_j^2\big)+t_j\big(t_{j-1}^2-t_{j+1}^2\big)+t_{j+1}\big(t_j^2-t_{j-1}^2\big)},\\
a_1 &= \frac{q(t_{j-1})\big(t_{j+1}^2-t_j^2\big)+q(t_j)\big(t_{j-1}^2-t_{j+1}^2\big)+q(t_{j+1})\big(t_j^2-t_{j-1}^2\big)}{\big(t_{j-1}-t_j\big)\big(t_{j-1}-t_{j+1}\big)\big(t_j-t_{j+1}\big)},\\
a_2 &= \frac{q(t_{j-1})\big(t_j-t_{j+1}\big)+q(t_j)\big(t_{j+1}-t_{j-1}\big)+q(t_{j+1})\big(t_{j-1}-t_j\big)}{t_{j-1}\big(t_{j+1}^2-t_j^2\big)+t_j\big(t_{j-1}^2-t_{j+1}^2\big)+t_{j+1}\big(t_j^2-t_{j-1}^2\big)}.
\end{aligned} \tag{2.2.11}$$

For equally divided interval, one has $t_{j+1}=(j+1)h, t_j=jh, t_{j-1}=(j-1)h$, then the coefficients a_1 and a_2 can be simplified by

$$\begin{aligned}
a_1 &= -\frac{q(t_{j-1})(2j+1)-4jq(t_j)+q(t_{j+1})(2j-1)}{2h},\\
a_2 &= -\frac{-q(t_{j-1})+2q(t_j)-q(t_{j+1})}{2h^2}.
\end{aligned} \tag{2.2.12}$$

This method is more efficient than the piecewise linear approach because the integration interval is twice as large. Accuracy may also be improved because the quadratic method provides a better representation of a smoothly varying response field.

2.2.2 Determination of the pth Moment of Response Variables

In this section, the pth moment of the response variables is determined through numerical solution of stochastic differential equation of motion in which fractional derivatives have been discretized.

The state vector of system (2.1.1) is augmented to rewrite the system as an N-dimensional system of autonomous Itô stochastic differential equations

$$\mathrm{d}Y_j = m_j(\mathbf{Y}, \mathbf{U})\,\mathrm{d}t + \sum_{l=1}^{d} \sigma_{jl}(\mathbf{Y}, \mathbf{U})\,\mathrm{d}W_l, \qquad j = 1, 2, \cdots, N, \tag{2.2.13}$$

where $\mathbf{U} = \{U_1, U_2, \cdots, U_M\}^T$, in which

$$U_r = \frac{1}{h^{\mu}} \sum_{j=0}^{n} \omega_j Y_r(jh) \tag{2.2.14}$$

is discretization of the rth fractional derivative, for $r = 1, 2, \cdots, M$, $M \leqslant N$, and $\mathbf{Y} = \{Y_1, Y_2, \cdots, Y_N\}^T$, where $Y_j = X_j$, for $j = 1, 2, \cdots, n$, $n \leqslant N$ and n is the discretization number of intervals in $[0, t]$. In the remainder of this chapter, vector $\mathbf{X}$ and the vector containing the first n elements of vector $\mathbf{Y}$ are interchangeable for the ease of presentation.

Since the moment Lyapunov exponent is related to the exponential rate of growth or decay of the pth moment, only the numerical approximation of the pth moment of the solution of system (2.1.1) or (2.2.13) is of interest in the Monte Carlo simulation. As a result, pathwise approximations of the solutions of the stochastic differential equations (2.1.1) or (2.2.13) are not necessary. Only a much weaker form of convergence in probability distribution is required. For the numerical solutions of the stochastic differential equations (2.2.13), weak Euler approximations may be applied. To evaluate the pth moment $\mathsf{E}[\|\mathbf{X}\|^p]$, S samples of the solutions of equations (2.2.13) are generated.

If the functions $m_j(\mathbf{Y}, \mathbf{U})$ and $\sigma_{jl}(\mathbf{Y}, \mathbf{U})$, $j = 1, 2, \cdots, N$, $l = 1, 2, \cdots, d$, are four times continuously differentiable, the order 1.0 Euler scheme of the sth realization of equations (2.2.13) at the kth iteration with $t_k - t_{k-1} = \Delta$, where Δ is the time step of integration, is given by

$$Y_{j,s}^{k} = Y_{j,s}^{k-1} + m_{j,s}^{k-1} \cdot \Delta + \sum_{l=1}^{d} \sigma_{jl,s}^{k-1} \cdot \Delta W_{l,s}^{k-1}, \quad j = 1, 2, \cdots, N, \tag{2.2.15}$$

where the subscript "s" stands for the sth sample, $s = 1, 2, \cdots, S$, the superscript "k" stands for the value at time t_k. $\Delta W_{l,s}^{k-1}$ can be taken as a normally distributed random number with mean 0 and standard deviation $\sqrt{\Delta}$

$$\Delta W_{l,s}^{k-1} = n_{l,s}^{k-1} \sqrt{\Delta}, \tag{2.2.16}$$

where $n_{l,s}^{k-1}$ is a standard normal random number $N(0,1)$.

If the drift $m_j(\mathbf{Y},\mathbf{U})$ and diffusion $\sigma_{jl}(\mathbf{Y},\mathbf{U})$ are six times continuously differentiable, the simplified order 2.0 weak Taylor scheme of the sth realization of equations (2.2.13) at the kth iteration may be used (Xie, 2006).

Having obtained S samples of the solutions of the stochastic differential equations, the pth moment can be determined as follows

$$\mathsf{E}[\|\mathbf{X}(t_k)\|^p] = \frac{1}{S}\sum_{s=1}^{S}\|\mathbf{X}_s^k\|^p, \qquad \|\mathbf{X}_s^k\| = \sqrt{(\mathbf{X}_s^k)^T\mathbf{X}_s^k}, \tag{2.2.17}$$

where $X_{j,s}^k = Y_{j,s}^k$, for $j=1,\ 2,\cdots,\ n$. From the definitions of Lyapunov exponent in (1.1.6), when $p=1$, it is the sample from which Lyapunov exponent is determined. The pth moment Lyapunov exponent is the Lyapunov exponent of pth moment.

2.2.3 Determination of the pth Moment Lyapunov Exponent

In this section, the pth moment Lyapunov exponent is determined by using the numerical procedure proposed by Rosenstein *et al.* (1993), which is especially suitable for problems with small data sets.

Having obtained the pth moment $\mathsf{E}[\|\mathbf{X}\|^p]$ at any time instance t using equation (2.2.17), one can determine the moment Lyapunov exponent $\Lambda_{\mathbf{X}}(p)$ using equation (1.1.6). However, since the pth moment grows or decays exponentially in time, numerical overflow or underflow must be found in a long time instance. To avoid this computational difficulty, periodic normalization of the pth moment was proposed (Xie, 2005).

From equation (2.2.14), it is clearly seen that the difficulty in Monte Carlo simulation of the pth moment Lyapunov exponent for fractional systems lies in the fact that the state variables in each iteration are all history dependent. This means that we must store all the values in history without any distortion. However, data normalization during the iterations will mutilate the historical values of state variables and then cannot obtain the correct fractional derivatives, which in turn leads to erroneous estimation of moment Lyapunov exponents. Hence, any methods with normalization can not be applied to fractional systems.

One approach to alleviate this situation is to use the short memory principle, which assumes that for large time t the role of the "history" of the behaviour of the state variable

Y_r near the lower terminal (the "starting point") $t=0$ can be neglected under certain conditions, i.e.,

$$ {}_0^{\mathrm{RL}}\mathcal{D}_t^{\mu}[q(t)] \approx {}_{t-L}^{\mathrm{RL}}\mathcal{D}_t^{\mu}[q(t)], \tag{2.2.18}$$

where L is the memory length. In other words, according to the short-memory principle (2.2.18), the fractional derivative with the lower limit 0 is approximated by the fractional derivative with moving lower limit $t-L$. Due to this approximation, the number of addends in approximation (2.2.14) is always no greater than L/h. However, this simple implementation will of course result in some inaccuracy, especially for long time-dependent materials. Furthermore, although in this simplification the memory is short, the fractional derivatives is still time-dependent, thus any normalization in the iterations still cannot be allowed for the fractional systems in order to correctly determine moment Lyapunov exponents.

Since all the historical data need to be stored during the computation of fractional derivatives and the data increases or decreases exponentially, the time considered cannot be very long, due to the limited capacity of computer storage. To avoid computational difficulties (e.g., overflow) and any data transformation (e.g., normalization), a data set with small size must be considered. Hence, determination of moment Lyapunov exponents of fractional systems is a problem of small data sets.

The numerical procedure for determination of Lyapunov exponents from small data sets, which takes advantage of all the available data (Rosenstein *et al.*, 1993; Becks *et al.*, 2005), can be readily extended to calculate moment Lyapunov exponents if a time series of pth moment $\mathsf{E}[\|\mathbf{X}\|^p]$ is available. The procedure is described as follows.

From equation (2.2.17), a single time series of the pth moment $\mathsf{E}[\|\mathbf{X}\|^p]$ is attained. The first step to estimate the largest Lyapunov exponent involves reconstructing the attractor dynamics from a single time series. The delay embedding theorem of Takens (1981) can be used for this purpose, because it guarantees that an attractor can be reconstructed whose Lyapunov spectrum is identical to that of the original attractor, from discrete time samples of almost any dynamical observable. Recently, Takens theory was extended to infinite-dimensional dynamical systems (Robinson, 2005).

The reconstructed trajectory, **E**, can be expressed as a matrix where each row is a phase-space vector,

$$\mathbf{E} = (\mathbf{E}_1, \mathbf{E}_2, \cdots, \mathbf{E}_R)^T, \tag{2.2.19}$$

where $\mathbf{E}_i$ is the state of the system at discrete time i. For an K-point time series, $\mathrm{e}_1, \mathrm{e}_2, \cdots, \mathrm{e}_K$, each $\mathbf{E}_i$ is given by

$$\mathbf{E}_i = (\mathrm{e}_i, \mathrm{e}_{i+J}, \cdots, \mathrm{e}_{i+(r-1)J})^T, \tag{2.2.20}$$

where J is the lag or reconstruction delay which can be chosen by many methods such as the fast Fourier transform, r is the embedding dimension which is usually estimated in accordance with Takens' theorem, i.e., $r > 2K$, and R is the number of reconstructed points, $R = K - (r-1)J$.

After the reconstruction of the dynamics, the nearest neighbor of each point on the trajectory is located. The nearest neighbor, $E_{\hat{j}}$, is determined by searching for the point that minimizes the distance to the particular reference point,E_j as follows

$$d_j(0) = \min_{E_{\hat{j}}} \left\| E_j - E_{\hat{j}} \right\|, \tag{2.2.21}$$

where $d_j(0)$ is the initial distance from the jth point to its nearest neighbor. The additional constraint is imposed that nearest neighbors have a temporal separation greater than the mean period of the time series (Rosenstein *et al.*, 1993), i.e., $|j - \hat{j}| >$ mean period. The largest Lyapunov exponent is then estimated as the mean rate of separation of the nearest neighbors as follows, according to Sato *et al.* (1987),

$$\lambda_{\max}(i) = \frac{1}{i\Delta t} \frac{1}{(R-i)} \sum_{j=1}^{R-i} \ln\left(\frac{d_j(i)}{d_j(0)}\right), \tag{2.2.22}$$

where Δt is the sampling period of the time series, and $d_j(i)$ is the distance between the jth pair of nearest neighbors after i discrete-time steps, i.e., $i\Delta t$ seconds. In order to improve convergence (with respect to i), Sato *et al.* (1987) further give an alternate form of equation (2.2.22)

$$\lambda_{\max}(i,k) = \frac{1}{k\Delta t} \frac{1}{(R-k)} \sum_{j=1}^{R-k} \ln\left(\frac{d_j(i+k)}{d_j(i)}\right), \tag{2.2.23}$$

where k is held constant, and $\lambda_{\max}$ is extracted by locating the plateau of $\lambda_{\max}(i,k)$ with respect to i. From the definition of $\lambda_{\max}$ (Rosenstein *et al.*, 1993), one can assume the jth pair of nearest neighbors diverge approximately at a rate given by the largest Lyapunov exponent

$$d_j(i) \approx C_j e^{\lambda_{\max}(i\Delta t)}, \tag{2.2.24}$$

where C_j is the initial separation. Taking logarithm of equation (2.2.24) yields

$$\ln d_j(i) \approx \ln C_j + \lambda_{\max}(i\Delta t). \tag{2.2.25}$$

The largest Lyapunov exponent is calculated using a least-squares fit to the average line given by

$$y(i) = \frac{1}{\Delta t}\langle \ln d_j(i)\rangle, \tag{2.2.26}$$

where $\langle\cdot\rangle$ denotes the average over all values of j. This process of averaging is the key to calculating accurate values of $\lambda_{\max}$ using noisy data sets.

2.2.4 Procedure for Numerical Determination of Moment Lyapunov Exponents of Fractional Systems

The results presented in Sections 2.2.1 to 2.2.3 are summarized in the following procedure for the numerical determination of the pth moment Lyapunov exponent of fractional systems.

1. **Setting the Initial Conditions**

   For the sth sample, $s=1, 2, \cdots, S$, set the initial conditions of the first n elements of the state vector $\mathbf{Y}_s$ as

   $$Y_{j,s}(0) = \frac{1}{\sqrt{n}}, \qquad i=1, 2, \cdots, n.$$

   $Y_{j,s}(0)$, $j=n+1, n+2, \cdots, N$, can be set to any values; for simplicity of implementation, they may also be set to $1/\sqrt{n}$.

2. **Monte Carlo Simulation of the pth Moment of Response Variables**

   (a) For $k=1, 2, \cdots, K$, and sample $s=1, 2, \cdots, S$, perform the numerical solution of the stochastic differential equations, by using discretization of fractional derivatives in equation (2.2.8) and the Euler scheme in equation (2.2.15). For each increment in k, the increment in time is Δ.

i. Generate $3d$ standard normally distributed random numbers to evaluate $\Delta W_{l,s}^{k-1}$, $\Delta W_{l_1,s}^{k-1}$, $\Delta W_{l_2,s}^{k-1}$, for $l,\ l_1,\ l_2=1,\ 2,\cdots,\ d$, using equation (2.2.16).

ii. Evaluate $\mathbf{Y}_s(k\Delta)$ in time step Δ using the iterative equation (2.2.15).

(b) For all values of p of interest and sample $s=1,\ 2,\cdots,\ S$, determine the pth norms $\|\mathbf{X}_s(k\Delta)\|^p$ using $\|\mathbf{X}_s\|=(\mathbf{X}_s^T\mathbf{X}_s)^{1/2}$, where $X_{j,s}=Y_{j,s}$, $j=1,\ 2,\cdots,\ n$, $k=1,\ 2,\cdots,\ K$.

(c) Determine the pth moments $\mathsf{E}[\|\mathbf{X}(k\Delta)\|^p]$ using equation (2.2.17) for all values of p of interest. The pth moments $\mathsf{E}[\|\mathbf{X}(k\Delta)\|^p]$ for $k=1\ 2,\cdots,\ K$ forms a time series.

3. **Determining the pth Moment Lyapunov Exponent**

(a) From the time series of the pth moments $\mathsf{E}[\|\mathbf{X}(k\Delta)\|^p]$, $k=1,\ 2,\cdots,\ K$, estimate the reconstruction delay J and mean period using the fast Fourier transform, and the embedding dimension r by Takens' theorem.

(b) Reconstruct the attractor dynamics, $\mathbf{E}=(\mathbf{E}_1,\mathbf{E}_2,\cdots,\mathbf{E}_R)^T$, using the method of delays.

(c) Find the nearest neighbors using equation (2.2.21) and constrain temporal separation.

(d) Calculate the distance between the jth pair of nearest neighbors after i discrete time steps, i.e., $i\Delta t$,

$$d_j(i)=\|E_{j+i}-E_{\hat{j}+i}\|,\quad i=1,\ 2,\cdots,\min(R-j,R-\hat{j}),\quad R=K-(r-1)\,J. \tag{2.2.27}$$

(e) Measure average separation of neighbors using equation (2.2.26). Do not normalize.

(f) Use least squares to fit a line to the data $y(i)$. The largest Lyapunov exponent is the slope of the least-squares fitted line.

2.3 Summary

A numerical method for determining both the Lyapunov moments and the pth moment Lyapunov exponents of fractional stochastic systems, which governs the almost sure stability and the pth moment stability, has been developed.

The main steps of this method include discretization of fractional derivatives, numerical solution of the stochastic differential equation, and the algorithm for calculating the largest Lyapunov exponents from small data sets. The determination of both Lyapunov exponents and the pth moment Lyapunov exponents is put into the same algorithm, for both exponents are deduced from a time series from equation (2.2.17).

Xie's algorithm (Xie, 2005) depends upon two large numbers: a large number of samples of the solutions of the stochastic differential equations needed for the evaluation of the pth moment $\mathsf{E}[\,\|\mathbf{X}\|^{p}]$ and a large time t required for the determination of pth moment Lyapunov exponent. The method in this chapter is characterized by requirement for small data sets and without any normalization. The possibility that the method does not necessarily need a large time t yet still has acceptable accurate results is due to the fact that this method takes advantage of all the available data. However, we have to keep the other large number, i.e., the number of samples of the solutions of the stochastic differential equations needed for the evaluation of the pth moment. In this chapter, S samples of solutions of the fractional stochastic differential equations are taken to calculate the pth moment. From the Central Limit Theorem, it is well known that the estimated pth moment Lyapunov exponent is a random number, with the mean being the true value of the pth moment Lyapunov exponent and standard deviation equal to $s_p/\sqrt{S}$, where s_p is the sample standard deviation determined from the S samples. The standard deviation of the estimated pth moment Lyapunov exponent can be reduced by increasing the number of samples S. Because the proposed method for fractional systems is based on Rosenstein *et al.* (1993), it should be noted that the proposed method is not as accurate as the methods with periodic normalization in most cases, due to that only small data sets or only a short time t is considered.

Examples to apply the numerical method will be presented in later chapters, e.g., in Figures 3.1, 3.8, and 3.20. The method can be easily applied for higher dimensional systems and any noise excitations.

CHAPTER 3

Higher-Order Stochastic Averaging Analysis of SDOF Fractional Viscoelastic Systems

Section 3.1 sets up the fractional stochastic differential equation of motion for systems with single-degree-of-freedom (SDOF). Stochastic averaging method for fractional differential equations is developed in Section 3.2. The ordinary first-order stochastic averaging method is extended to higher-order and applied to the stochastic stability analysis of fractional viscoelastic systems under wide-band noise excitation in Section 3.3 and under bounded noise excitation in Section 3.5. In Section 3.4, exact analytical Lyapunov exponent is determined for fractional viscoelastic systems driven by bounded noises.

3.1 Formulation

Consider the stability of a column of uniform cross-section under dynamic axial compressive load $F(t)$. The equation of motion is given by (Xie, 2006)

$$\frac{\partial^2 M(x,t)}{\partial x^2} = \rho A \frac{\partial^2 v(x,t)}{\partial t^2} + \beta_0 \frac{\partial v(x,t)}{\partial t} + F(t)\frac{\partial^2 v(x,t)}{\partial x^2}, \tag{3.1.1}$$

where ρ is the mass density per unit volume of the column, A is the cross-sectional area, $v(x,t)$ is the transverse displacement of the central axis, β_0 is the damping constant. The moment $M(x,t)$ at the cross-section x and the geometry relation are

$$M(x,t) = \int_A \sigma(x,t)\, z \, \mathrm{d}A, \quad \varepsilon(x,t) = -\frac{\partial^2 v(x,t)}{\partial x^2} z. \tag{3.1.2}$$

The viscoelastic material is supposed to follow fractional constitutive model in equation (1.3.19), which can be recast as

$$\sigma(t) = \left[E + \eta \, {}^{\mathrm{RL}}_{0}\mathcal{D}^{\mu}_{t}\right] \varepsilon(t). \tag{3.1.3}$$

Substituting equation (3.1.3) into (3.1.2) and (3.1.1) yields

$$\rho A \frac{\partial^2 v(x,t)}{\partial t^2} + \beta_0 \frac{\partial v(x,t)}{\partial t} + EI \frac{\partial^4 v(x,t)}{\partial x^4} + I\eta \, {}^{\mathrm{RL}}_{0}\mathcal{D}^{\mu}_{t} \left[\frac{\partial^4 v(x,t)}{\partial x^4}\right] + F(t) \frac{\partial^2 v(x,t)}{\partial x^2} = 0. \tag{3.1.4}$$

If the column of length L is simply supported, the transverse deflection can be expressed as

$$v(x,t) = \sum_{n=1}^{\infty} q_n(t) \sin \frac{n\pi x}{L}. \tag{3.1.5}$$

Substituting equation (3.1.5) into (3.1.4) leads to the equations of motion

$$\ddot{q}_n(t) + 2\beta \dot{q}_n(t) + \omega_n^2 \left[1 - \frac{F(t)}{P_n} + \frac{\eta}{E} \, {}^{\mathrm{RL}}_{0}\mathcal{D}^{\mu}_{t}\right] q_n(t) = 0, \tag{3.1.6}$$

where

$$\beta = \frac{\beta_0}{2\rho A}, \quad \omega_n^2 = \frac{EI}{\rho A} \left(\frac{n\pi}{L}\right)^4, \quad P_n = EI \left(\frac{n\pi}{L}\right)^2. \tag{3.1.7}$$

If only the nth mode is considered, and the damping, viscoelastic effect, and the amplitude of load are all small, and if the function $F(t)/P_n$ is taken to be a stochastic process $\xi(t)$, the equation of motion of a single-degree-of-freedom system can be written as, by introducing a small parameter $0 < \varepsilon \ll 1$,

$$\ddot{q}(t) + 2\varepsilon\beta \dot{q}(t) + \omega^2 \left[1 + \varepsilon \xi(t) + \varepsilon \tau_\varepsilon \, {}^{\mathrm{RL}}_{0}\mathcal{D}^{\mu}_{t}\right] q(t) = 0, \quad \tau_\varepsilon = \frac{\eta}{E}. \tag{3.1.8}$$

The presence of small parameter ε is reasonable, since damping and noise perturbation are small in many engineering applications. Here the viscoelasticity is also considered to be a kind of weak damping.

3.2 Stochastic Averaging Method for Fractional Differential Equations

The equation of motion for simply supported column with fractional constitutive relations has been obtained in equation (3.1.8) or

$$\ddot{q}(t)+2\varepsilon\beta\dot{q}(t)+\omega^2[1-\varepsilon^{1/2}\xi(t)]q(t)+\omega^2\frac{\varepsilon\tau_\varepsilon}{\Gamma(1-\mu)}\int_0^t\frac{q'(\tau)}{(t-\tau)^\mu}\mathrm{d}\tau=0. \tag{3.2.1}$$

The averaging method for integro-differential equations was originally put forward by Larionov (1969). It provides a rigorous foundation to apply the averaging principle to problems with integro-differential equations for deterministic systems with both finite and infinite time intervals. However, it is noted that the kernel in the viscoelastic term of equation (3.2.1) is not the same kernel form as $\mathbf{H}(t,\tau,\mathbf{X}(\tau))$ discussed by Larionov (1969). The averaging method of Larionov can be extended to deal with fractional stochastic differential equations as follows.

The fractional stochastic system of equation (3.2.1) can be transformed into the following general system of stochastic integro-differential equations

$$\dot{\mathbf{X}}=\varepsilon^{1/2}\Big[\mathbf{F}^{(0)}(t,\mathbf{X},\boldsymbol{\xi}(t))+\varepsilon^{1/2}\mathbf{F}(t,\mathbf{X})+\varepsilon^{1/2}\int_0^t\mathbf{H}(t,\tau,\mathbf{X}'(\tau))\mathrm{d}\tau\Big], \tag{3.2.2}$$

where $\mathbf{X}$ is an n-dimensional vector, $\mathbf{F}^{(0)}(t,\mathbf{X},\boldsymbol{\xi}(t))$, $\mathbf{F}(t,\mathbf{X})$ and $\mathbf{H}(t,\tau,\mathbf{X}'(\tau))$ are n-dimensional continuous functions defined for all $t,s\geqslant 0$ and $\mathbf{X}\in D\subset\mathbf{E}^n$, where $\mathbf{E}^n$ is an n-dimensional Euclidean space. The first- and second-order derivatives of $\mathbf{F}^{(0)}(t,\mathbf{X},\boldsymbol{\xi}(t))$ are bounded. $\boldsymbol{\xi}(t)$ is a zero mean value, stationary stochastic process vector, $\boldsymbol{\xi}(t)=\{\xi_1,\xi_2,\cdots,\xi_n\}^T$.

Supposing that $\underset{t}{\mathscr{M}}\{\cdot\}$ is an averaging operator and

$$\begin{aligned}
&\underset{t}{\mathscr{M}}\left\{\mathbf{F}(t,\mathbf{X})+\int_0^t\mathbf{H}(t,\tau,\mathbf{X}'(\tau))\mathrm{d}\tau\right\}=\mathbf{f}\,(\mathbf{X}),\\
&\underset{t}{\mathscr{M}}\left\{\int_{-\infty}^0\mathsf{E}\Big[\frac{\partial\mathbf{F}^0}{\partial\mathbf{X}}\mathbf{F}_\tau^{(0)}\Big]\mathrm{d}\tau\right\}=\mathbf{a}(\mathbf{X}),\\
&\underset{t}{\mathscr{M}}\left\{\int_{-\infty}^\infty\mathsf{E}\big[\mathbf{F}^0\big(\mathbf{F}_\tau^{(0)}\big)^T\big]\mathrm{d}\tau\right\}=\boldsymbol{\sigma}(\mathbf{X})\boldsymbol{\sigma}^T(\mathbf{X})
\end{aligned} \tag{3.2.3}$$

exist for any $\mathbf{X}\in D$, where $\mathbf{F}_\tau^{(0)}=\mathbf{F}^0(t+\tau,\mathbf{X},\boldsymbol{\xi}(t+\tau))$, and $\boldsymbol{\sigma}(\mathbf{X})$ is the $n\times n$ diffusion matrix.

Then, over a time interval of order $1/\varepsilon^{1/2}$, the system of integro-differential equations (3.2.2) can be approximated uniformly by the averaged stochastic system of Itô stochastic differential equations

$$\mathrm{d}\mathbf{Y}=\varepsilon\big[\mathbf{f}\,(\mathbf{Y})+\mathbf{a}(\mathbf{Y})\big]\mathrm{d}t+\varepsilon^{1/2}\boldsymbol{\sigma}(\mathbf{Y})\mathrm{d}\mathbf{W}(t), \tag{3.2.4}$$

where $\mathbf{W}(t)=\{W_1, W_2, \cdots, W_n\}^T$ denotes an n-dimensional vector of mutually independent standard Wiener processes, on the condition that the following conditions are also satisfied

1. The correlation function $\mathsf{E}\big[\boldsymbol{\xi}(t)\boldsymbol{\xi}(t+\tau)\big]$ of a stochastic process $\boldsymbol{\xi}(t)$ decays to zero fast enough as τ increases, or $\boldsymbol{\xi}(t)$ is a wide-band process.
2. The function $\mathbf{F}(t,\mathbf{X})$ and $\mathbf{H}(t,\tau,\mathbf{X}')$ satisfy with respect to $\mathbf{X}$ Lipschitz condition with constants μ_1 and μ_2, respectively, i.e.,

$$\big|\mathbf{F}(t,\mathbf{X}_1)-\mathbf{F}(t,\mathbf{X}_2)\big|\leqslant\mu_1\big|\mathbf{X}_1-\mathbf{X}_2\big|,\quad \big|\mathbf{H}(t,\tau,\mathbf{X}_1')-\mathbf{H}(t,\tau,\mathbf{X}_2')\big|\leqslant\mu_2\big|\mathbf{X}_1-\mathbf{X}_2\big|$$

   holds for $\mathbf{X}_1\in D$ and $\mathbf{X}_2\in D$.
3. The solution of $\mathbf{Y}=\mathbf{Y}(t)$ of system (3.2.4) with $\mathbf{Y}(0)=\mathbf{X}(0)$ is defined for $t\geqslant 0$ and lies in the region D and its neighborhood.
4. In the region D, the limit $\mathbf{f}\,(\mathbf{X})$ satisfies a Lipschitz condition with constant μ_3

$$\big|\mathbf{f}\,(\mathbf{X}_1)-\mathbf{f}\,(\mathbf{X}_2)\big|\leqslant\mu_3\big|\mathbf{X}_1-\mathbf{X}_2\big|, \tag{3.2.5}$$

   and along the trajectory $\mathbf{Y}(t)$, the following relation

$$\left|\int_{t_1}^{t_2}\mathbf{f}\,\big(\mathbf{Y}(\tau)\big)\mathrm{d}\tau\right|\leqslant M\big|t_1-t_2\big| \tag{3.2.6}$$

   holds for some constant M.

This stochastic averaging method for fractional differential equations is a combination of the averaging method of Larionov (1969) for deterministic system and the method of stochastic averaging by Khasminskii (1966a).

3.3 Fractional Viscoelastic Systems Under Wide-band Noise

This section develops the method of higher-order stochastic averaging. Stochastic stability of a column with material of fractional constitutive relation is investigated, of which results from first-order, second-order, and higher-order stochastic averaging are compared.

3.3.1 First-Order Averaging Analysis

Rearranging equation (3.1.8) by moving the terms with ε to the right hand side

$$\ddot{q}(t)+\omega^2 q(t) = -2\varepsilon\beta\dot{q}(t)+\omega^2\Big[\varepsilon^{1/2}\xi(t)-\varepsilon\tau_\varepsilon\, {}^{\mathrm{RL}}_{0}\mathcal{D}^{\mu}_{t}\Big]q(t). \tag{3.3.1}$$

Equation (3.3.1) admits the trivial solution $q(t)=0$. However, it is not the Lagrange standard form given in equation (1.2.27) or (1.2.40), hence the variation of parameters has to be used. Suppose the homogeneous solution to the system is of the form

$$q(t)=a\cos\Phi(t), \quad \dot{q}(t)=-\omega a\sin\Phi(t), \quad \Phi(t)=\omega t+\varphi(t), \tag{3.3.2}$$

a particular solution can be given by using the method of variation of parameters

$$q(t)=a(t)\cos\Phi(t), \quad \dot{q}(t)=-\omega a(t)\sin\Phi(t), \quad \Phi(t)=\omega t+\varphi(t). \tag{3.3.3}$$

Taking derivative of the first equation of (3.3.3) and equating to the second equation, one has

$$\dot{a}(t)\cos\Phi(t)-a(t)\dot{\varphi}(t)\sin\Phi(t)=0. \tag{3.3.4}$$

Taking derivative of the second equation of (3.3.3) and substituting it into system (3.3.1) yields, together with (3.3.3),

$$\begin{aligned}&\dot{a}(t)\sin\Phi(t)+a(t)\dot{\varphi}(t)\cos\Phi(t)\\&=-2\varepsilon\beta a(t)\sin\Phi(t)-\omega\varepsilon^{1/2}\xi(t)a(t)\cos\Phi(t)+\omega\varepsilon\tau_\varepsilon\, {}^{\mathrm{RL}}_{0}\mathcal{D}^{\mu}_{t}\big[a(s)\cos\Phi(s)\big].\end{aligned} \tag{3.3.5}$$

Solving equations (3.3.4) and (3.3.5) leads to the equation of motion as a system of equations for amplitude $a(t)$ and phase angle $\varphi(t)$,

$$\dot{a}(t)=-2\varepsilon\beta a(t)\sin^2\Phi(t)-\frac{1}{2}\omega a(t)\sin 2\Phi(t)\varepsilon^{1/2}\xi(t)+\omega\varepsilon\sin\Phi(t)\tau_\varepsilon\, {}^{\mathrm{RL}}_{0}\mathcal{D}^{\mu}_{t}\big[a(s)\cos\Phi(s)\big],$$

$$\dot{\varphi}(t) = -\varepsilon\beta \sin 2\Phi(t) - \omega \cos^2 \Phi(t)\varepsilon^{1/2}\xi(t) + \frac{1}{a(t)}\omega \cos \Phi(t)\varepsilon\tau_\varepsilon \, {}^{\mathrm{RL}}_{0}\mathcal{D}^{\mu}_{t}\big[a(s) \cos \Phi(s)\big]. \tag{3.3.6}$$

To calculate the pth moment Lyapunov exponents, letting $P = a^p$, the pth norm of system (3.3.1), one can obtain

$$\dot{P}(t) = -2\varepsilon\beta pP \sin^2 \Phi(t) - \frac{1}{2}\omega pP \sin 2\Phi(t)\varepsilon^{1/2}\xi(t) + \frac{pP\omega\varepsilon}{a(t)} \sin \Phi(t)\tau_\varepsilon \, {}^{\mathrm{RL}}_{0}\mathcal{D}^{\mu}_{t}\big[a(s) \cos \Phi(s)\big]. \tag{3.3.7}$$

The equations for pth norm and phase angle can written in the matrix form

$$\begin{Bmatrix} \dot{P}(t) \\ \dot{\varphi}(t) \end{Bmatrix} = \varepsilon \mathbf{F}^{(1)}(P, \varphi, t) + \varepsilon^{1/2} \mathbf{F}^{(0)}(P, \varphi, \xi, t), \tag{3.3.8}$$

where $\mathbf{F}^{(1)}(P, \varphi, t)$ stand for drift terms, while the functions $\mathbf{F}^{(0)}(P, \varphi, \xi, t)$ are associated with diffusion terms, which are

$$\mathbf{F}^{(1)}(P, \varphi, t) = \begin{Bmatrix} -2\beta pP \sin^2 \Phi(t) + pP\omega\tau_\varepsilon I^{sc} \\ -\beta \sin 2\Phi(t) + \omega\tau_\varepsilon I^{cc} \end{Bmatrix} = \begin{Bmatrix} F_1^{(1)}(P, \varphi, t) \\ F_2^{(1)}(P, \varphi, t) \end{Bmatrix},$$

$$\mathbf{F}^{(0)}(P, \varphi, \xi, t) = \begin{Bmatrix} -\frac{1}{2}\omega pP \sin 2\Phi(t)\xi(t) \\ -\omega \cos^2 \Phi(t)\xi(t) \end{Bmatrix} = \begin{Bmatrix} F_1^{(0)}(P, \varphi, \xi, t) \\ F_2^{(0)}(P, \varphi, \xi, t) \end{Bmatrix},$$

$$I^{sc} = \sin \Phi(t) \, {}^{\mathrm{RL}}_{0}\mathcal{D}^{\mu}_{t} \left\{ \left[\frac{P(s)}{P(t)}\right]^{1/p} \cos \Phi(s) \right\}, \quad I^{cc} = \cos \Phi(t) \, {}^{\mathrm{RL}}_{0}\mathcal{D}^{\mu}_{t} \left\{ \left[\frac{P(s)}{P(t)}\right]^{1/p} \cos \Phi(s) \right\}. \tag{3.3.9}$$

Equations (3.3.8) are still too complex to solve analytically. It is fortunate, however, that the right hand side is small because of the presence of the small parameter ε. This means that both P and φ change slowly. Therefore one can expect to obtain reasonably accurate results by averaging the response over one period. The system (3.3.1) can be approximated by the method of stochastic averaging, which leads to Itô stochastic differential equations

$$\mathrm{d}\begin{Bmatrix} \bar{P}(t) \\ \bar{\varphi}(t) \end{Bmatrix} = \varepsilon \begin{Bmatrix} \bar{m}_P \\ \bar{m}_\varphi \end{Bmatrix} \mathrm{d}t + \varepsilon^{1/2} \bar{\boldsymbol{\sigma}} \, \mathrm{d}\mathbf{W}(t), \tag{3.3.10}$$

where $\mathbf{W}(t)$ are standard Wiener processes, and

$$\bar{m}_P = \mathop{\mathcal{M}}_t \left\{ F_1^{(1)}(P,\varphi,t) + \int_{-\infty}^{0} \mathrm{E}\Big[\frac{\partial F_1^{(0)}}{\partial P} F_{1\tau}^{(0)} + \frac{\partial F_1^{(0)}}{\partial \varphi} F_{2\tau}^{(0)} \Big] \mathrm{d}\tau \right\},$$

$$\bar{m}_\varphi = \mathop{\mathcal{M}}_t \left\{ F_2^{(1)}(P,\varphi,t) + \int_{-\infty}^{0} \mathrm{E}\Big[\frac{\partial F_2^{(0)}}{\partial P} F_{1\tau}^{(0)} + \frac{\partial F_2^{(0)}}{\partial \varphi} F_{2\tau}^{(0)} \Big] \mathrm{d}\tau \right\}, \tag{3.3.11}$$

$$[\bar{\boldsymbol{\sigma}}\bar{\boldsymbol{\sigma}}^T]_{ij} = \mathop{\mathcal{M}}_t \left\{ \int_{-\infty}^{\infty} \mathrm{E}\big[F_i^{(0)} F_{j\tau}^{(0)} \big] \mathrm{d}\tau \right\}, \quad i,j=1,\ 2,$$

$$F_{j\tau}^{(0)} = F_j^{(0)}\big(P,\varphi,\xi(t+\tau),t+\tau\big), \quad j=1,\ 2.$$

The averaging method for fractional differential equations due to Larionov (1969) is used to obtain the approximate drift terms in the Itô equations in which the viscoelastic terms are involved, while the diffusion terms are averaged according to the well-known method of Stratonovich (1963). When applying the averaging operation, $P(t)$ and $\varphi(t)$ are treated as unchanged, i.e., they are replaced by $\bar{P}$ and $\bar{\varphi}$ directly. By substituting in the corresponding terms one has

$$\bar{m}_P = -\beta p \bar{P} + p\bar{P}\omega\tau_\varepsilon \mathop{\mathcal{M}}_t \left\{ I^{sc} \right\} + \frac{1}{4}\omega^2 p \bar{P} \mathop{\mathcal{M}}_t \left\{ J_1 \right\}, \tag{3.3.12}$$

where

$$J_1 = \int_{-\infty}^{0} R(\tau) \Big\{ p \sin 2\Phi(t) \sin 2\Phi(t+\tau) + 2\cos 2\Phi(t)\big[1 + \cos 2\Phi(t+\tau)\big] \Big\} \mathrm{d}\tau,$$

and $R(\tau) = \mathrm{E}\big[\xi(t)\xi(t+\tau)\big]$ is the correlation function of the wide-band noise $\xi(t)$. It can be obtained that

$$\begin{aligned} \mathop{\mathcal{M}}_t \{J_1\} &= \int_{-\infty}^{0} R(\tau)\Big[\frac{p}{2}\cos(2\omega\tau) + \cos(2\omega\tau)\Big] \mathrm{d}\tau \\ &= \frac{p+2}{2} \int_{-\infty}^{0} R(\tau)\cos 2\omega\tau \, \mathrm{d}\tau = \frac{p+2}{4} S(2\omega), \end{aligned} \tag{3.3.13}$$

where the cosine and sine power spectral density functions of noise $\xi(t)$ are given by

$$S(\omega) = \int_{-\infty}^{\infty} R(\tau)\cos\omega\tau\,\mathrm{d}\tau = 2\int_{0}^{\infty} R(\tau)\cos\omega\tau\,\mathrm{d}\tau = 2\int_{-\infty}^{0} R(\tau)\cos\omega\tau\,\mathrm{d}\tau,$$

$$\Psi(\omega) = 2\int_{0}^{\infty} R(\tau)\sin\omega\tau\,\mathrm{d}\tau = -2\int_{-\infty}^{0} R(\tau)\sin\omega\tau\,\mathrm{d}\tau,$$

$$\int_{-\infty}^{\infty} R(\tau)\sin\omega\tau\,\mathrm{d}\tau=0, \tag{3.3.14}$$

and the averaging results are used

$$\underset{t}{\mathscr{M}}\Big\{\cos(\omega t+\varphi)\cos\omega t\Big\}=\underset{t}{\mathscr{M}}\Big\{\sin(\omega t+\varphi)\sin\omega t\Big\}=\frac{1}{2}\cos\varphi. \tag{3.3.15}$$

On the other hand, applying the transformation $s=t-\tau$ and changing the order of integration lead to

$$\begin{aligned}\underset{t}{\mathscr{M}}\left\{I^{sc}\right\}&=\frac{-\omega}{\Gamma(1-\mu)}\lim_{T\to\infty}\frac{1}{T}\int_{t=0}^{T}\int_{\tau=0}^{t}(t-\tau)^{-\mu}\sin\Phi(\tau)\sin\Phi(t)\,\mathrm{d}\tau\,\mathrm{d}t\\&=\frac{-\omega}{\Gamma(1-\mu)}\lim_{T\to\infty}\frac{1}{T}\int_{t=0}^{T}\int_{s=0}^{t}s^{-\mu}\sin\Phi(t)\sin\Phi(t-s)\,\mathrm{d}s\mathrm{d}t\\&=\frac{-\omega}{2\Gamma(1-\mu)}\int_{0}^{\infty}s^{-\mu}\cos\omega s\,\mathrm{d}s=-\frac{1}{2}\mathcal{H}^{c}(\omega),\end{aligned} \tag{3.3.16}$$

where for ease of presentation, the fractional derivative is rewritten as

$${}_{0}^{\mathrm{RL}}\mathcal{D}_{t}^{\mu}[f(\tau)g(t)]=\frac{g(t)}{\Gamma(1-\mu)}\int_{0}^{t}\frac{f'(\tau)}{(t-\tau)^{\mu}}\mathrm{d}\tau. \tag{3.3.17}$$

When averaged, $P(s)$ and $P(t)$ in equations (3.3.9) are taken as constants and then canceled out.

Similarly, it can be shown that

$$\underset{t}{\mathscr{M}}\left\{I^{cc}\right\}=\underset{t}{\mathscr{M}}\Big\{\cos\Phi(t)\;{}_{0}^{\mathrm{RL}}\mathcal{D}_{t}^{\mu}\cos\Phi(s)\Big\}=\frac{1}{2}\mathcal{H}^{s}(\omega), \tag{3.3.18}$$

where

$$\begin{aligned}\mathcal{H}^{c}(\omega)&=\frac{\omega}{\Gamma(1-\mu)}\int_{0}^{\infty}\tau^{-\mu}\cos\omega\tau\,\mathrm{d}\tau=\omega^{\mu}\sin\frac{\mu\pi}{2},\\\mathcal{H}^{s}(\omega)&=\frac{\omega}{\Gamma(1-\mu)}\int_{0}^{\infty}\tau^{-\mu}\sin\omega\tau\,\mathrm{d}\tau=\omega^{\mu}\cos\frac{\mu\pi}{2}.\end{aligned} \tag{3.3.19}$$

Substituting equations (3.3.13) and (3.3.16) into (3.3.12) gives

$$\bar{m}_{P}=p\bar{P}\left\{-\beta-\frac{\omega\tau_{\varepsilon}}{2}\mathcal{H}^{c}(\omega)+\frac{p+2}{16}\omega^{2}S(2\omega)\right\}, \tag{3.3.20}$$

and in a similar way, one obtains

$$\bar{m}_{\varphi}=\frac{\omega}{4}\left\{\tau_{\varepsilon}\mathcal{H}^{s}(\omega)+\frac{\omega}{2}\Psi(2\omega)\right\}, \tag{3.3.21}$$

$$[\bar{\boldsymbol{\sigma}}\bar{\boldsymbol{\sigma}}^T]_{11} = b_{11} = \frac{1}{8}\omega^2 p^2 \bar{P}^2 S(2\omega), \quad [\bar{\boldsymbol{\sigma}}\bar{\boldsymbol{\sigma}}^T]_{12} = [\bar{\boldsymbol{\sigma}}\bar{\boldsymbol{\sigma}}^T]_{21} = 0,$$

$$[\bar{\boldsymbol{\sigma}}\bar{\boldsymbol{\sigma}}^T]_{22} = b_{22} = \frac{1}{8}\omega^2[2S(0) + S(2\omega)].$$

It is noted that $\bar{m}_P$, $\bar{m}_\varphi$, and the diffusion matrix $[\bar{\boldsymbol{\sigma}}\bar{\boldsymbol{\sigma}}^T]$ do not involve the phase angle $\varphi(t)$. The averaged Itô equations are reduced to

$$\mathrm{d}\bar{P} = \varepsilon p\bar{P}\left\{-\beta - \frac{\omega\tau_\varepsilon}{2}\mathcal{H}^c(\omega) + \frac{p+2}{16}\omega^2 S(2\omega)\right\}\mathrm{d}t + \varepsilon^{1/2}\omega p\bar{P}\sqrt{\frac{S(2\omega)}{8}}\mathrm{d}W_1(t), \quad (3.3.22)$$

$$\mathrm{d}\bar{\varphi} = \varepsilon\frac{\omega}{4}\left\{\tau_\varepsilon\mathcal{H}^s(\omega) + \frac{\omega}{2}\Psi(2\omega)\right\}\mathrm{d}t + \varepsilon^{1/2}\omega\sqrt{\frac{2S(0)+S(2\omega)}{8}}\mathrm{d}W_2(t). \quad (3.3.23)$$

Equations (3.3.22) and (3.3.23) are decoupled, then the averaged transformed amplitude $\bar{P}$ and phase processes form independent Markov processes. Noting that the property of independent increment of Wiener process indicates that the expectation of the second term in equation (3.3.22) is zero (Parzen, 1999). Taking the expected value on both sides of equation (3.3.22) leads to

$$\mathrm{d}\mathrm{E}[\bar{P}] = \varepsilon p\Big[-\beta - \frac{\omega\tau_\varepsilon}{2}\mathcal{H}^c(\omega) + \frac{p+2}{16}\omega^2 S(2\omega)\Big]\mathrm{E}[\bar{P}]\,\mathrm{d}t. \quad (3.3.24)$$

The moment Lyapunov exponents from the first-order averaging can be obtained as

$$\Lambda(p) = \lim_{t\to\infty}\frac{\log\mathrm{E}[\bar{P}]}{t} \approx \varepsilon p\Big[-\beta - \frac{\omega\tau_\varepsilon}{2}\mathcal{H}^c(\omega) + \frac{p+2}{16}\omega^2 S(2\omega)\Big], \quad (3.3.25)$$

where the sign "$\approx$" is used because stochastic averaging is just an approximation. Using the relation between the moment Lyapunov exponent and the Lyapunov exponent yields

$$\lambda = \Lambda'(0) \approx \varepsilon\Big[-\beta - \frac{\omega\tau_\varepsilon}{2}\mathcal{H}^c(\omega) + \frac{1}{8}\omega^2 S(2\omega)\Big]. \quad (3.3.26)$$

3.3.2 Second-Order Stochastic Averaging

The original equation of motion (3.3.1) has been transformed into an equivalent system of differential equations in equation (3.3.8)

$$\begin{Bmatrix}\dot{P}(t)\\ \dot{\varphi}(t)\end{Bmatrix} = \varepsilon\begin{Bmatrix}f_1(P,\varphi,t)\\ f_2(P,\varphi,t)\end{Bmatrix} + \varepsilon^{1/2}\begin{Bmatrix}g_1(P,\varphi,\xi,t)\\ g_2(P,\varphi,\xi,t)\end{Bmatrix}, \quad (3.3.27)$$

where

$$
\begin{aligned}
f_1(P,\varphi,t) &= -2\beta pP\sin^2(\omega t+\varphi)+pP\omega\tau_\varepsilon I^{sc},\\
f_2(P,\varphi,t) &= -\beta\sin 2(\omega t+\varphi)+\omega\tau_\varepsilon I^{cc},\\
g_1(P,\varphi,\xi,t) &= -\omega pP\xi(t)\sin(\omega t+\varphi)\cos(\omega t+\varphi),\\
g_2(P,\varphi,\xi,t) &= -\omega\xi(t)\cos^2(\omega t+\varphi).
\end{aligned}
\tag{3.3.28}
$$

To formulate a second-order stochastic averaging, the near-identity transformation is introduced

$$
P(t)=\bar{P}(t)+\varepsilon P_1(\bar{P},\bar{\varphi},t),\qquad \varphi(t)=\bar{\varphi}(t)+\varepsilon\varphi_1(\bar{P},\bar{\varphi},t),
\tag{3.3.29}
$$

where $\bar{P}(t)$ and $\bar{\varphi}(t)$ stand for nonoscillatory amplitude and phase angle, respectively.

It is reasonable to treat the oscillatory effects of terms containing excitation functions $\xi(t)$ separately from the oscillatory effects of the nonexcitation terms and to consider only the deterministic part of equation (3.3.27) at this moment (The contribution of the diffusion term is considered in equation (3.3.45)). Differentiating equation (3.3.29) with respect to t and equating each result with the corresponding drift functions from (3.3.27) give

$$
\begin{Bmatrix}\dot{\bar{P}}\\ \dot{\bar{\varphi}}\end{Bmatrix}+\varepsilon\begin{Bmatrix}\dfrac{\partial P_1}{\partial\bar{P}}\dot{\bar{P}}+\dfrac{\partial P_1}{\partial\bar{\varphi}}\dot{\bar{\varphi}}+\dfrac{\partial P_1}{\partial t}\\ \dfrac{\partial\varphi_1}{\partial\bar{P}}\dot{\bar{P}}+\dfrac{\partial\varphi_1}{\partial\bar{\varphi}}\dot{\bar{\varphi}}+\dfrac{\partial\varphi_1}{\partial t}\end{Bmatrix}=\varepsilon\begin{Bmatrix}f_1\big(\bar{P}+\varepsilon P_1,\bar{\varphi}+\varepsilon\varphi_1,t\big)\\ f_2\big(\bar{P}+\varepsilon P_1,\bar{\varphi}+\varepsilon\varphi_1,t\big)\end{Bmatrix}.
\tag{3.3.30}
$$

Substituting the Taylor expansion

$$
f_j\big(\bar{P}+\varepsilon P_1,\bar{\varphi}+\varepsilon\varphi_1,t\big)=f_j\big(\bar{P},\bar{\varphi},t\big)+\varepsilon P_1\frac{\partial f_j}{\partial\bar{P}}+\varepsilon\varphi_1\frac{\partial f_j}{\partial\bar{\varphi}}+o(\varepsilon),\quad j=1,\ 2,
\tag{3.3.31}
$$

and the inverse matrix

$$
\mathbf{A}=\begin{bmatrix}1+\varepsilon\dfrac{\partial P_1}{\partial\bar{P}} & \varepsilon\dfrac{\partial P_1}{\partial\bar{\varphi}}\\ \varepsilon\dfrac{\partial\varphi_1}{\partial\bar{P}} & 1+\varepsilon\dfrac{\partial\varphi_1}{\partial\bar{\varphi}}\end{bmatrix},\quad
\mathbf{A}^{-1}=\begin{bmatrix}1-\varepsilon\dfrac{\partial P_1}{\partial\bar{P}} & -\varepsilon\dfrac{\partial P_1}{\partial\bar{\varphi}}\\ -\varepsilon\dfrac{\partial\varphi_1}{\partial\bar{P}} & 1-\varepsilon\dfrac{\partial\varphi_1}{\partial\bar{\varphi}}\end{bmatrix}+o(\varepsilon)
\tag{3.3.32}
$$

into equation (3.3.30) yields

$$
\dot{\bar{P}}=\varepsilon\bar{u}_1+\varepsilon^2\bar{u}_2+o(\varepsilon^2),\quad \dot{\bar{\varphi}}=\varepsilon\bar{v}_1+\varepsilon^2\bar{v}_2+o(\varepsilon^2),
\tag{3.3.33}
$$

where

$$\bar{u}_1 = f_1 - \frac{\partial P_1}{\partial t}, \quad \bar{u}_2 = \frac{\partial f_1}{\partial \bar{P}} P_1 + \frac{\partial f_1}{\partial \bar{\varphi}} \varphi_1 - \frac{\partial P_1}{\partial \bar{P}} f_1 - \frac{\partial P_1}{\partial \bar{\varphi}} f_2 + \frac{\partial P_1}{\partial t}\frac{\partial P_1}{\partial \bar{P}} + \frac{\partial \varphi_1}{\partial t}\frac{\partial P_1}{\partial \bar{\varphi}},$$
$$\bar{v}_1 = f_2 - \frac{\partial \varphi_1}{\partial t}, \quad \bar{v}_2 = \frac{\partial f_2}{\partial \bar{P}} P_1 + \frac{\partial f_2}{\partial \bar{\varphi}} \varphi_1 - \frac{\partial \varphi_1}{\partial \bar{P}} f_1 - \frac{\partial \varphi_1}{\partial \bar{\varphi}} f_2 + \frac{\partial P_1}{\partial t}\frac{\partial \varphi_1}{\partial \bar{P}} + \frac{\partial \varphi_1}{\partial t}\frac{\partial \varphi_1}{\partial \bar{\varphi}}. \tag{3.3.34}$$

The following two terms can be expanded by using f_1 and f_2 in equation (3.3.28)

$$\frac{\partial f_1}{\partial \bar{P}} P_1 + \frac{\partial f_1}{\partial \bar{\varphi}} \varphi_1 = P_1\Big[\omega\tau_\varepsilon p I^{sc} + \omega\tau_\varepsilon \bar{P} J^{sc} - 2\beta p \sin^2(\omega t + \bar{\varphi})\Big]$$
$$+\varphi_1\Big[\omega p \bar{P}\tau_\varepsilon (I^{cc} - I^{ss}) - 2\beta p \bar{P} \sin(2\omega t + 2\bar{\varphi})\Big], \tag{3.3.35}$$
$$\frac{\partial f_2}{\partial \bar{P}} P_1 + \frac{\partial f_2}{\partial \bar{\varphi}} \varphi_1 = P_1 \frac{\omega\tau_\varepsilon J^{cc}}{p} + \varphi_1\Big[-\omega\tau_\varepsilon (I^{cs} + I^{sc}) - 2\beta \cos(2\omega t + 2\bar{\varphi})\Big],$$

where

$$I^{ss} = {}_0^{\mathrm{RL}}\mathcal{D}_t^{\mu}\left\{\left[\frac{\bar{P}(s)}{\bar{P}(t)}\right]^{1/p} \sin(\omega t + \bar{\varphi}) \sin(\omega s + \bar{\varphi})\right\},$$
$$I^{cs} = {}_0^{\mathrm{RL}}\mathcal{D}_t^{\mu}\left\{\left[\frac{\bar{P}(s)}{\bar{P}(t)}\right]^{1/p} \cos(\omega t + \bar{\varphi}) \sin(\omega s + \bar{\varphi})\right\},$$
$$J^{cc} = {}_0^{\mathrm{RL}}\mathcal{D}_t^{\mu}\left\{\left[\frac{\bar{P}(s)}{\bar{P}(t)}\right]^{1/p}\left[\frac{1}{\bar{P}(s)} - \frac{1}{\bar{P}(t)}\right] \cos(\omega t + \bar{\varphi}) \cos(\omega s + \bar{\varphi})\right\},$$
$$J^{sc} = {}_0^{\mathrm{RL}}\mathcal{D}_t^{\mu}\left\{\left[\frac{\bar{P}(s)}{\bar{P}(t)}\right]^{1/p}\left[\frac{1}{\bar{P}(s)} - \frac{1}{\bar{P}(t)}\right] \sin(\omega t + \bar{\varphi}) \cos(\omega s + \bar{\varphi})\right\},$$

and

$$\frac{\partial I^{sc}}{\partial \bar{P}} = \frac{J^{sc}}{p}, \quad \frac{\partial I^{cc}}{\partial \bar{P}} = \frac{J^{cc}}{p}, \quad \frac{\partial I^{cc}}{\partial \bar{\varphi}} = -I^{sc} - I^{cs}, \quad \frac{\partial I^{sc}}{\partial \bar{\varphi}} = I^{cc} - I^{ss}. \tag{3.3.36}$$

A key issue arises on how to determine the functions P_1 and φ_1. It is assumed that

$$\frac{\partial P_1}{\partial t} = f_1 - \mathscr{M}_t\{f_1\}, \quad \frac{\partial \varphi_1}{\partial t} = f_2 - \mathscr{M}_t\{f_2\}, \tag{3.3.37}$$

then the terms $f_1 - (\partial P_1/\partial t)$ and $f_2 - (\partial \varphi_1/\partial t)$ contain only nonoscillatory terms. It also suggests that P_1 and φ_1 are oscillatory functions. Taking averaging on the first two equations of equation (3.3.28) and using (3.3.16) and (3.3.18) yield

$$\mathscr{M}_t\{f_1\} = -\beta p \bar{P} - \frac{1}{2} p \bar{P} \omega\tau_\varepsilon \mathcal{H}^c(\omega), \quad \mathscr{M}_t\{f_2\} = \frac{1}{2}\omega\tau_\varepsilon \mathcal{H}^s(\omega). \tag{3.3.38}$$

Substituting equations (3.3.28) and (3.3.38) into (3.3.37) leads to

$$\begin{aligned}\frac{\partial P_1}{\partial t} &= \beta p\bar{P}\cos(2\omega t+2\bar{\varphi})+\omega\tau_\varepsilon p\bar{P}\Big[I^{sc}+\frac{1}{2}\mathcal{H}^c(\omega)\Big],\\ \frac{\partial \varphi_1}{\partial t} &= -\beta\sin(2\omega t+2\bar{\varphi})+\omega\tau_\varepsilon\Big[I^{cc}-\frac{1}{2}\mathcal{H}^s(\omega)\Big],\end{aligned}\tag{3.3.39}$$

where $\bar{P}$ is treated as a constant under the averaging operation. Meanwhile, it can be shown that

$$\begin{aligned}I^{sc} &= -\frac{\omega}{\Gamma(1-\mu)}\int_0^t \frac{\sin(\omega t+\bar{\varphi})\sin(\omega s+\bar{\varphi})}{(t-s)^\mu}\mathrm{d}s\\ &= -\frac{\omega}{\Gamma(1-\mu)}\Bigg[\int_0^\infty \frac{\sin(\omega t+\bar{\varphi})\sin(\omega t-\omega\tau+\bar{\varphi})}{\tau^\mu}\mathrm{d}\tau\\ &\quad -\int_t^\infty \frac{\sin(\omega t+\bar{\varphi})\sin(\omega t-\omega\tau+\bar{\varphi})}{\tau^\mu}\mathrm{d}\tau\Bigg]\\ &= \frac{\omega}{2\Gamma(1-\mu)}\int_0^\infty \frac{\cos(2\omega t-\omega\tau+2\bar{\varphi})}{\tau^\mu}\mathrm{d}\tau-\frac{1}{2}\mathcal{H}^c(\omega) \qquad (3.3.40)\\ &= -\frac{1}{2}\mathcal{H}^c(\omega)+\frac{1}{2}\big[\cos(2\omega t+2\bar{\varphi})\mathcal{H}^c(\omega)+\sin(2\omega t+2\bar{\varphi})\mathcal{H}^s(\omega)\big]. \qquad (3.3.41)\end{aligned}$$

Equation (3.3.40) exists when $t\to\infty$. Similarly, one may obtain

$$\begin{aligned}I^{cc} &= \frac{1}{2}\mathcal{H}^s(\omega)-\frac{1}{2}\big[\sin(2\omega t+2\bar{\varphi})\mathcal{H}^c(\omega)-\cos(2\omega t+2\bar{\varphi})\mathcal{H}^s(\omega)\big],\\ I^{ss} &= \frac{1}{2}\mathcal{H}^s(\omega)+\frac{1}{2}\big[\sin(2\omega t+2\bar{\varphi})\mathcal{H}^c(\omega)-\cos(2\omega t+2\bar{\varphi})\mathcal{H}^s(\omega)\big],\\ I^{cs} &= \frac{1}{2}\mathcal{H}^c(\omega)+\frac{1}{2}\big[\cos(2\omega t+2\bar{\varphi})\mathcal{H}^c(\omega)+\sin(2\omega t+2\bar{\varphi})\mathcal{H}^s(\omega)\big].\end{aligned}\tag{3.3.42}$$

Substituting equation (3.3.41) into (3.3.39) and solving this ordinary first-order differential equation result in

$$P_1=\frac{1}{2\omega}\beta p\bar{P}\sin(2\omega t+2\bar{\varphi})+\frac{1}{4}\tau_\varepsilon p\bar{P}\big[\mathcal{H}^c(\omega)\sin(2\omega t+2\bar{\varphi})-\mathcal{H}^s(\omega)\cos(2\omega t+2\bar{\varphi})\big],\tag{3.3.43}$$

where the constant of integration is taken as zero. Similarly, it can be set approximately

$$\varphi_1=\frac{\beta}{2\omega}\cos(2\omega t+2\bar{\varphi})+\frac{1}{4}\tau_\varepsilon\big[\mathcal{H}^c(\omega)\cos(2\omega t+2\bar{\varphi})+\mathcal{H}^s(\omega)\sin(2\omega t+2\bar{\varphi})\big].\tag{3.3.44}$$

Having obtained functions for P_1 and φ_1, one has

$$\bar{u}_1 = f_1 - \frac{\partial P_1}{\partial t} = \underset{t}{\mathscr{M}}\{f_1\} = -\beta p \bar{P} - \frac{1}{2}\omega p \bar{P}\tau_\varepsilon H^c(\omega),$$

$$\begin{aligned}
\bar{u}_2 &= \frac{\partial f_1}{\partial \bar{P}} P_1 + \frac{\partial f_1}{\partial \bar{\varphi}}\varphi_1 - \frac{\partial P_1}{\partial \bar{P}}\underset{t}{\mathscr{M}}\{f_1\} - \frac{\partial P_1}{\partial \bar{\varphi}}\underset{t}{\mathscr{M}}\{f_2\} \\
&= P_1\left[\omega\tau_\varepsilon p I^{sc} + \omega\tau_\varepsilon \bar{P} J^{sc} - 2\beta p \sin^2(\omega t + \bar{\varphi})\right] \\
&\quad + \varphi_1\left[\omega\tau_\varepsilon p\bar{P}(I^{cc} - I^{ss}) - 2\beta p \bar{P}\sin(2\omega t + 2\bar{\varphi})\right] \\
&\quad - \left\{\frac{\beta p}{2\omega}\sin(2\omega t + 2\bar{\varphi}) + \frac{\tau_\varepsilon p}{4}\left[H^c(\omega)\sin(2\omega t + 2\bar{\varphi}) - H^s(\omega)\cos(2\omega t + 2\bar{\varphi})\right]\right\}\underset{t}{\mathscr{M}}\{f_1\} \\
&\quad - \left\{\frac{1}{\omega}\beta p \bar{P}\cos(2\omega t + 2\bar{\varphi})\right. \\
&\quad \left. + \frac{1}{2}\tau_\varepsilon p \bar{P}\left[H^c(\omega)\cos(2\omega t + 2\bar{\varphi}) + H^s(\omega)\sin(2\omega t + 2\bar{\varphi})\right]\right\}\underset{t}{\mathscr{M}}\{f_2\},
\end{aligned}$$

$$\bar{v}_1 = f_2 - \frac{\partial \varphi_1}{\partial t} = \underset{t}{\mathscr{M}}\{f_2\} = \frac{1}{2}\omega\tau_\varepsilon H^s(\omega),$$

$$\begin{aligned}
\bar{v}_2 &= \frac{\partial f_2}{\partial \bar{P}} P_1 + \frac{\partial f_2}{\partial \bar{\varphi}}\varphi_1 - \frac{\partial \varphi_1}{\partial \bar{P}}\underset{t}{\mathscr{M}}\{f_1\} - \frac{\partial \varphi_1}{\partial \bar{\varphi}}\underset{t}{\mathscr{M}}\{f_2\} \\
&= P_1\frac{\omega\tau_\varepsilon J^{cc}}{p} + \varphi_1\left[-\omega\tau_\varepsilon(I^{cs} + I^{sc}) - 2\beta\cos(2\omega t + 2\bar{\varphi})\right] \\
&\quad + \left\{\frac{\beta}{\omega}\sin(2\omega t + 2\bar{\varphi}) + \frac{1}{2}\tau_\varepsilon\left[H^c(\omega)\sin(2\omega t + 2\bar{\varphi}) - H^s(\omega)\cos(2\omega t + 2\bar{\varphi})\right]\right\}\underset{t}{\mathscr{M}}\{f_2\},
\end{aligned}$$

where $\underset{t}{\mathscr{M}}\{f_1\}$ and $\underset{t}{\mathscr{M}}\{f_2\}$ have been given in equation (3.3.38).

Note that equation (3.3.33) includes only the contribution of the drift terms, as can be seen from (3.3.30). The contribution of the diffusion terms should be added as follows: substituting P and φ in terms of relations (3.3.29) into the diffusion terms in (3.3.27), expanding functions g_j in a Taylor series

$$g_j\big(\bar{P} + \varepsilon P_1, \bar{\varphi} + \varepsilon\varphi_1, t\big) = g_j(\bar{P}, \bar{\varphi}, t) + \varepsilon\frac{\partial g_j}{\partial \bar{P}} P_1 + \varepsilon\frac{\partial g_j}{\partial \bar{\varphi}}\varphi_1 + o(\varepsilon^2), \quad j = 1,\ 2,$$

multiplying the diffusion matrix by the inverse matrix (3.3.32), and adding the contribution of the diffusion term to (3.3.33). This process results in two equations

$$\dot{\bar{P}} = \varepsilon\bar{u}_1 + \varepsilon^2\bar{u}_2 + \varepsilon^{1/2} g_1(\bar{P}, \bar{\varphi}, \xi, t) + \varepsilon^{3/2}\left[-g_1\frac{\partial P_1}{\partial \bar{P}} - g_2\frac{\partial P_1}{\partial \bar{\varphi}} + P_1\frac{\partial g_1}{\partial \bar{P}} + \varphi_1\frac{\partial g_1}{\partial \bar{\varphi}}\right] + o(\varepsilon^2),$$

$$\dot{\bar{\varphi}} = \varepsilon\bar{v}_1 + \varepsilon^2\bar{v}_2 + \varepsilon^{1/2}g_2(\bar{P},\bar{\varphi},\xi,t) + \varepsilon^{3/2}\left[-g_1\frac{\partial\varphi_1}{\partial\bar{P}} - g_2\frac{\partial\varphi_1}{\partial\bar{\varphi}} + P_1\frac{\partial g_2}{\partial\bar{P}} + \varphi_1\frac{\partial g_2}{\partial\bar{\varphi}}\right] + o(\varepsilon^2), \tag{3.3.45}$$

where $\bar{u}_1$, $\bar{u}_2$, $\bar{v}_1$, and $\bar{v}_2$ are expressed in equation (3.3.34). Equation (3.3.45) can be simplified to a standard form for stochastic averaging,

$$\begin{Bmatrix} \dot{\bar{P}}(t) \\ \dot{\bar{\varphi}}(t) \end{Bmatrix} = \begin{Bmatrix} F_1^{(1)}(\bar{P},\bar{\varphi},t) \\ F_2^{(1)}(\bar{P},\bar{\varphi},t) \end{Bmatrix} + \begin{Bmatrix} F_1^{(0)}(\bar{P},\bar{\varphi},\xi,t) \\ F_2^{(0)}(\bar{P},\bar{\varphi},\xi,t) \end{Bmatrix}, \tag{3.3.46}$$

where

$$\begin{aligned}
&F_1^{(1)}(\bar{P},\bar{\varphi},t) = \varepsilon\bar{u}_1 + \varepsilon^2\bar{u}_2, \quad F_2^{(1)}(\bar{P},\bar{\varphi},t) = \varepsilon\bar{v}_1 + \varepsilon^2\bar{v}_2, \\
&F_1^{(0)}(\bar{P},\bar{\varphi},\xi,t) = \varepsilon^{1/2}g_1(\bar{P},\bar{\varphi},\xi,t) + \varepsilon^{3/2}\left[-g_1\frac{\partial P_1}{\partial\bar{P}} - g_2\frac{\partial P_1}{\partial\bar{\varphi}} + P_1\frac{\partial g_1}{\partial\bar{P}} + \varphi_1\frac{\partial g_1}{\partial\bar{\varphi}}\right], \\
&F_2^{(0)}(\bar{P},\bar{\varphi},\xi,t) = \varepsilon^{1/2}g_2(\bar{P},\bar{\varphi},\xi,t) + \varepsilon^{3/2}\left[-g_1\frac{\partial\varphi_1}{\partial\bar{P}} - g_2\frac{\partial\varphi_1}{\partial\bar{\varphi}} + P_1\frac{\partial g_2}{\partial\bar{P}} + \varphi_1\frac{\partial g_2}{\partial\bar{\varphi}}\right].
\end{aligned} \tag{3.3.47}$$

Substituting equation (3.3.28) into (3.3.47) yields

$$\begin{aligned}
&P_1\frac{\partial g_1}{\partial\bar{P}} + \varphi_1\frac{\partial g_1}{\partial\bar{\varphi}} = \omega p\xi(t)\left[\frac{P_1}{2}\sin(2\omega t + 2\bar{\varphi}) + \bar{P}\varphi_1\cos(2\omega t + 2\bar{\varphi})\right], \\
&P_1\frac{\partial g_2}{\partial\bar{P}} + \varphi_1\frac{\partial g_2}{\partial\bar{\varphi}} = \omega\varphi_1\xi(t)\sin(2\omega t + 2\bar{\varphi}).
\end{aligned}$$

Substituting equations (3.3.45) and (3.3.28) into (3.3.47) results in

$$\begin{aligned}
F_1^{(1)}(\bar{P},\bar{\varphi},t) &= \varepsilon\left[-\beta p\bar{P} - \frac{1}{2}\omega p\bar{P}\tau_\varepsilon\mathcal{H}^c(\omega)\right] + \varepsilon^2\bar{u}_2, \\
F_2^{(1)}(\bar{P},\bar{\varphi},t) &= \varepsilon\left[\frac{1}{2}\omega\tau_\varepsilon\mathcal{H}^s(\omega)\right] + \varepsilon^2\bar{v}_2, \\
F_1^{(0)}(\bar{P},\bar{\varphi},\xi,t) &= \varepsilon^{1/2}\left[\frac{1}{2}\omega p\bar{P}\xi(t)\sin(2\omega t + 2\bar{\varphi})\right] \\
&\quad + \varepsilon^{3/2}\left[-g_1\frac{\partial P_1}{\partial\bar{P}} - g_2\frac{\partial P_1}{\partial\bar{\varphi}} + P_1\frac{\partial g_1}{\partial\bar{P}} + \varphi_1\frac{\partial g_1}{\partial\bar{\varphi}}\right], \\
F_2^{(0)}(\bar{P},\bar{\varphi},\xi,t) &= \varepsilon^{1/2}\left\{-\frac{1}{2}\omega\xi(t)\left[1 + \cos(2\omega t + 2\bar{\varphi})\right]\right\} \\
&\quad + \varepsilon^{3/2}\left[-g_1\frac{\partial\varphi_1}{\partial\bar{P}} - g_2\frac{\partial\varphi_1}{\partial\bar{\varphi}} + P_1\frac{\partial g_2}{\partial\bar{P}} + \varphi_1\frac{\partial g_2}{\partial\bar{\varphi}}\right].
\end{aligned} \tag{3.3.48}$$

Substituting equations (3.3.43) and (3.3.44) into (3.3.46) and then using the stochastic averaging method result in the averaged Itô stochastic differential equations:

$$\mathrm{d}\bar{P}=\bar{m}_{\bar{P}}\mathrm{d}t+\bar{\sigma}_{11}^{*}\mathrm{d}W_1+\bar{\sigma}_{12}^{*}\mathrm{d}W_2,\quad \mathrm{d}\bar{\varphi}=\bar{m}_{\bar{\varphi}}\mathrm{d}t+\bar{\sigma}_{21}^{*}\mathrm{d}W_1+\bar{\sigma}_{22}^{*}\mathrm{d}W_2, \tag{3.3.49}$$

where $W_1(t)$ and $W_2(t)$ are two independent standard Wiener processes, and

$$\begin{aligned}
\bar{m}_{\bar{P}}&=\underset{t}{\mathscr{M}}\left\{F_1^{(1)}(\bar{P},\bar{\varphi},t)+\int_{-\infty}^{0}\mathrm{E}\Big[\frac{\partial F_1^{(0)}}{\partial\bar{P}}F_{1\tau}^{(0)}+\frac{\partial F_1^{(0)}}{\partial\bar{\varphi}}F_{2\tau}^{(0)}\Big]\mathrm{d}\tau\right\},\\
\bar{m}_{\bar{\varphi}}&=\underset{t}{\mathscr{M}}\left\{F_2^{(1)}(\bar{P},\bar{\varphi},t)+\int_{-\infty}^{0}\mathrm{E}\Big[\frac{\partial F_2^{(0)}}{\partial\bar{P}}F_{1\tau}^{(0)}+\frac{\partial F_2^{(0)}}{\partial\bar{\varphi}}F_{2\tau}^{(0)}\Big]\mathrm{d}\tau\right\},\\
[\bar{\boldsymbol{\sigma}}\bar{\boldsymbol{\sigma}}^T]_{ij}^{*}&=\underset{t}{\mathscr{M}}\left\{\int_{-\infty}^{\infty}\mathrm{E}[F_i^{(0)}F_{j\tau}^{(0)}]\mathrm{d}\tau\right\},\quad i,j=1,\ 2,\\
F_{j\tau}^{(0)}&=F_j^{(0)}\big(\bar{P},\bar{\varphi},\xi(t+\tau),t+\tau\big),\qquad j=1,\ 2,
\end{aligned} \tag{3.3.50}$$

where $F_j^{(0)}$ and $F_j^{(1)}$ are functions in equation (3.3.48). Substituting equation (3.3.48) into (3.3.50) and neglecting higher-order terms result in

$$\begin{aligned}
\bar{m}_{\bar{P}}&=\varepsilon p\bar{P}\Big[-\beta-\frac{\omega\tau_\varepsilon}{2}H^c(\omega)+\frac{p+2}{16}\omega^2S(2\omega)\Big]-\frac{\varepsilon^2}{16}p(p+2)\bar{P}\tau_\varepsilon H^s(\omega)\omega^2S(2\omega),\\
\bar{m}_{\bar{\varphi}}&=-\frac{\varepsilon}{8}\omega[\omega\Psi(2\omega)-4\tau_\varepsilon H^s(\omega)]\\
&\quad-\frac{\varepsilon^2}{8}\left\{\frac{4\beta^2}{\omega}-\omega^2\tau_\varepsilon H^s(\omega)\Psi(2\omega)+4\beta\tau_\varepsilon H^c(\omega)+\omega{\tau_\varepsilon}^2\Big[(H^c(\omega))^2+(H^s(\omega))^2\Big]\right\},\\
\bar{\sigma}_{11}^{*}&=[\bar{\boldsymbol{\sigma}}^{*}\bar{\boldsymbol{\sigma}}^{*T}]_{11}=\omega p\bar{P}\sqrt{\frac{1}{8}S(2\omega)\ [\varepsilon-\varepsilon^2\tau_\varepsilon H^s(\omega)]},\\
\bar{\sigma}_{12}^{*}&=\bar{\sigma}_{21}^{*}=[\bar{\boldsymbol{\sigma}}^{*}\bar{\boldsymbol{\sigma}}^{*T}]_{21}=0,\\
\bar{\sigma}_{22}^{*}&=\bar{\sigma}_{22}^{*}=\omega\sqrt{\frac{1}{8}\ [S(2\omega)+2S(0)]\ [\varepsilon-\varepsilon^2\tau_\varepsilon H^s(\omega)]}.
\end{aligned}$$

Taking the expected value on both sides of equation (3.3.49) leads to

$$\mathrm{dE}[\bar{P}]=\left\{\varepsilon p\Big[-\beta-\frac{\omega\tau_\varepsilon}{2}H^c(\omega)+\frac{p+2}{16}\omega^2S(2\omega)\Big]-\frac{\varepsilon^2}{16}p(p+2)\tau_\varepsilon H^s(\omega)\omega^2S(2\omega)\right\}\mathrm{E}[\bar{P}]\mathrm{d}t,$$

and the pth moment Lyapunov exponent, including the second-order term, is

$$\Lambda(p)=\lim_{t\to\infty}\frac{\log\mathrm{E}[\bar{P}]}{t}$$

$$\approx \varepsilon p\Big[-\beta-\frac{\omega\tau_\varepsilon}{2}\mathcal{H}^c(\omega)+\frac{p+2}{16}\omega^2 S(2\omega)\Big]\boxed{-\tfrac{\varepsilon^2}{16}p(p+2)\tau_\varepsilon\mathcal{H}^s(\omega)\omega^2 S(2\omega)}. \quad (3.3.51)$$

Comparing equation (3.3.51) with (3.3.25), one may find that moment Lyapunov exponent of second-order averaging adds a term of order ε^2 on the result of first-order averaging, highlighted in the frame box. Hence, the second-order averaging method can be reduced to first-order averaging if the functions P_1 and φ_1 are set to be zero.

From the relation in equation (1.1.7), the largest Lyapunov exponent from the second-order averaging is given by

$$\lambda \approx \varepsilon\Big[-\beta-\frac{\omega\tau_\varepsilon}{2}\mathcal{H}^c(\omega)+\frac{1}{8}\omega^2 S(2\omega)\Big]\boxed{-\tfrac{\varepsilon^2}{8}\tau_\varepsilon\mathcal{H}^s(\omega)\omega^2 S(2\omega)}, \quad (3.3.52)$$

where the difference between the first-order and second-order averaging is framed.

3.3.3 Higher-Order Stochastic Averaging

Following the procedure of Section 3.3.2, higher-order stochastic averaging analysis can be carried out. Let's take the third-order stochastic averaging as an example of higher-order method. Introducing a near-identity transformation as in equation (3.3.29), but up to order ε^2

$$P(t)=\bar{P}(t)+\varepsilon P_1+\varepsilon^2 P_2, \quad \varphi(t)=\bar{\varphi}(t)+\varepsilon\varphi_1+\varepsilon^2\varphi_2, \quad (3.3.53)$$

where $P_1=P_1(\bar{P},\bar{\varphi},t)$, $P_2=P_2(\bar{P},\bar{\varphi},t)$, $\varphi_1=\varphi_1(\bar{P},\bar{\varphi},t)$, and $\varphi_2=\varphi_2(\bar{P},\bar{\varphi},t)$ are unknown functions. When $P_2=0$ and $\varphi_2=0$, it is reduced to second-order averaging.

Differentiating equation (3.3.53) with respect to t and equating each result with the corresponding drift functions from (3.3.27) gives

$$\begin{Bmatrix}\dot{\bar{P}}\\ \dot{\bar{\varphi}}\end{Bmatrix}+\varepsilon\begin{Bmatrix}\dfrac{\partial P_1}{\partial\bar{P}}\dot{\bar{P}}+\dfrac{\partial P_1}{\partial\bar{\varphi}}\dot{\bar{\varphi}}+\dfrac{\partial P_1}{\partial t}\\ \dfrac{\partial\varphi_1}{\partial\bar{P}}\dot{\bar{P}}+\dfrac{\partial\varphi_1}{\partial\bar{\varphi}}\dot{\bar{\varphi}}+\dfrac{\partial\varphi_1}{\partial t}\end{Bmatrix}+\varepsilon^2\begin{Bmatrix}\dfrac{\partial P_2}{\partial\bar{P}}\dot{\bar{P}}+\dfrac{\partial P_2}{\partial\bar{\varphi}}\dot{\bar{\varphi}}+\dfrac{\partial P_2}{\partial t}\\ \dfrac{\partial\varphi_2}{\partial\bar{P}}\dot{\bar{P}}+\dfrac{\partial\varphi_2}{\partial\bar{\varphi}}\dot{\bar{\varphi}}+\dfrac{\partial\varphi_2}{\partial t}\end{Bmatrix}$$

$$=\varepsilon\begin{Bmatrix}f_1\big(\bar{P}+\varepsilon P_1+\varepsilon^2 P_2,\bar{\varphi}+\varepsilon\varphi_1+\varepsilon^2\varphi_2,t\big)\\ f_2\big(\bar{P}+\varepsilon P_1+\varepsilon^2 P_2,\bar{\varphi}+\varepsilon\varphi_1+\varepsilon^2\varphi_2,t\big)\end{Bmatrix}, \quad (3.3.54)$$

or in the matrix form

$$\mathbf{A}\begin{Bmatrix}\dot{\bar{P}}\\ \dot{\bar{\varphi}}\end{Bmatrix}=\varepsilon\begin{Bmatrix}f_1\big(\bar{P}+\varepsilon P_1+\varepsilon^2P_2,\bar{\varphi}+\varepsilon\varphi_1+\varepsilon^2\varphi_2,t\big)-\dfrac{\partial P_1}{\partial t}\\ f_2\big(\bar{P}+\varepsilon P_1+\varepsilon^2P_2,\bar{\varphi}+\varepsilon\varphi_1+\varepsilon^2\varphi_2,t\big)-\dfrac{\partial\varphi_1}{\partial t}\end{Bmatrix}-\varepsilon^2\begin{Bmatrix}\dfrac{\partial P_2}{\partial t}\\ \dfrac{\partial\varphi_2}{\partial t}\end{Bmatrix},\qquad(3.3.55)$$

where

$$\mathbf{A}=\begin{bmatrix}1+\varepsilon\dfrac{\partial P_1}{\partial\bar{P}}+\varepsilon^2\dfrac{\partial P_2}{\partial\bar{P}} & \varepsilon\dfrac{\partial P_1}{\partial\bar{\varphi}}+\varepsilon^2\dfrac{\partial P_2}{\partial\bar{\varphi}}\\ \varepsilon\dfrac{\partial\varphi_1}{\partial\bar{P}}+\varepsilon^2\dfrac{\partial\varphi_2}{\partial\bar{P}} & 1+\varepsilon\dfrac{\partial\varphi_1}{\partial\bar{\varphi}}+\varepsilon^2\dfrac{\partial\varphi_2}{\partial\bar{\varphi}}\end{bmatrix}.\qquad(3.3.56)$$

Using the expansion of $1/|\mathbf{A}|$ to the order of ε^2, the inverse matrix of $\mathbf{A}$ is obtained as

$$\mathbf{A}^{-1}=\frac{1}{|\mathbf{A}|}\begin{bmatrix}1+\varepsilon\dfrac{\partial\varphi_1}{\partial\bar{\varphi}}+\varepsilon^2\dfrac{\partial\varphi_2}{\partial\bar{\varphi}} & -\varepsilon\dfrac{\partial P_1}{\partial\bar{\varphi}}-\varepsilon^2\dfrac{\partial P_2}{\partial\bar{\varphi}}\\ -\varepsilon\dfrac{\partial\varphi_1}{\partial\bar{P}}-\varepsilon^2\dfrac{\partial\varphi_2}{\partial\bar{P}} & 1+\varepsilon\dfrac{\partial P_1}{\partial\bar{P}}+\varepsilon^2\dfrac{\partial P_2}{\partial\bar{P}}\end{bmatrix}=\begin{bmatrix}A_{11} & A_{12}\\ A_{21} & A_{22}\end{bmatrix},\qquad(3.3.57)$$

where

$$A_{11}=1-\varepsilon\frac{\partial P_1}{\partial\bar{P}}+\varepsilon^2\Big[\frac{\partial P_1}{\partial\bar{\varphi}}\frac{\partial\varphi_1}{\partial\bar{P}}-\frac{\partial P_2}{\partial\bar{P}}+\Big(\frac{\partial P_1}{\partial\bar{P}}\Big)^2\Big],$$

$$A_{12}=-\varepsilon\frac{\partial P_1}{\partial\bar{\varphi}}+\varepsilon^2\Big[\frac{\partial P_1}{\partial\bar{\varphi}}\frac{\partial\varphi_1}{\partial\bar{\varphi}}-\frac{\partial P_2}{\partial\bar{\varphi}}+\frac{\partial P_1}{\partial\bar{P}}\frac{\partial P_1}{\partial\bar{\varphi}}\Big],$$

$$A_{21}=-\varepsilon\frac{\partial\varphi_1}{\partial\bar{P}}+\varepsilon^2\Big[\frac{\partial\varphi_1}{\partial\bar{P}}\frac{\partial\varphi_1}{\partial\bar{\varphi}}-\frac{\partial\varphi_2}{\partial\bar{P}}+\frac{\partial P_1}{\partial\bar{P}}\frac{\partial\varphi_1}{\partial\bar{P}}\Big],$$

$$A_{22}=1-\varepsilon\frac{\partial\varphi_1}{\partial\bar{\varphi}}+\varepsilon^2\Big[\frac{\partial P_1}{\partial\bar{\varphi}}\frac{\partial\varphi_1}{\partial\bar{P}}-\frac{\partial\varphi_2}{\partial\bar{\varphi}}+\Big(\frac{\partial\varphi_1}{\partial\bar{\varphi}}\Big)^2\Big].$$

Taylor expansion of a function with multi-variables is given by

$$\begin{aligned}f_j\big(\bar{P}+\varepsilon P_1+\varepsilon^2P_2,\bar{\varphi}+\varepsilon\varphi_1+\varepsilon^2\varphi_2,t\big)&=f_j\big(\bar{P},\bar{\varphi},t\big)+\varepsilon\Big\{P_1\frac{\partial f_j\big(\bar{P},\bar{\varphi},t\big)}{\partial\bar{P}}+\varphi_1\frac{\partial f_j\big(\bar{P},\bar{\varphi},t\big)}{\partial\bar{\varphi}}\Big\}\\ &+\varepsilon^2\Big\{P_2\frac{\partial f_j\big(\bar{P},\bar{\varphi},t\big)}{\partial\bar{P}}+\varphi_2\frac{\partial f_j\big(\bar{P},\bar{\varphi},t\big)}{\partial\bar{\varphi}}+\frac{1}{2}P_1^2\frac{\partial^2f_j\big(\bar{P},\bar{\varphi},t\big)}{\partial\bar{P}^2}\\ &+\frac{1}{2}\varphi_1^2\frac{\partial^2f_j\big(\bar{P},\bar{\varphi},t\big)}{\partial\bar{\varphi}^2}+P_1\varphi_1\frac{\partial^2f_j\big(\bar{P},\bar{\varphi},t\big)}{\partial\bar{P}\partial\bar{\varphi}}\Big\}+o(\varepsilon^2),\quad j=1,\ 2.\end{aligned}\qquad(3.3.58)$$

Substituting equations (3.3.57) and (3.3.58) into (3.3.55) yields

$$\dot{\bar{P}} = \varepsilon\overline{\mu}_1 + \varepsilon^2\overline{\mu}_2 + \varepsilon^3\overline{\mu}_3 + o(\varepsilon^3), \quad \dot{\bar{\varphi}} = \varepsilon\overline{\nu}_1 + \varepsilon^2\overline{\nu}_2 + \varepsilon^3\overline{\nu}_3 + o(\varepsilon^3), \tag{3.3.59}$$

where

$$\begin{aligned}
\overline{\mu}_1 &= f_1 - \frac{\partial P_1}{\partial t}, \ \overline{\mu}_2 = \frac{\partial f_1}{\partial \bar{P}} P_1 + \frac{\partial f_1}{\partial \bar{\varphi}}\varphi_1 - \frac{\partial P_1}{\partial \bar{P}}\left(f_1 - \frac{\partial P_1}{\partial t}\right) - \frac{\partial P_1}{\partial \bar{\varphi}}\left(f_2 - \frac{\partial \varphi_1}{\partial t}\right) - \frac{\partial P_2}{\partial t}, \\
\overline{\mu}_3 &= \frac{\partial f_1}{\partial \bar{P}} P_2 + \frac{\partial f_1}{\partial \bar{\varphi}}\varphi_2 + \frac{P_1^2}{2}\frac{\partial^2 f_1}{\partial \bar{P}^2} + \frac{\varphi_1^2}{2}\frac{\partial^2 f_1}{\partial \bar{\varphi}^2} + P_1\varphi_1\frac{\partial^2 f_1}{\partial \bar{P}\partial \bar{\varphi}} \\
&\quad - \frac{\partial P_1}{\partial \bar{P}}\left(P_1\frac{\partial f_1}{\partial \bar{P}} + \varphi_1\frac{\partial f_1}{\partial \bar{\varphi}} - \frac{\partial P_2}{\partial t}\right) - \frac{\partial P_1}{\partial \bar{\varphi}}\left(P_1\frac{\partial f_2}{\partial \bar{P}} + \varphi_1\frac{\partial f_2}{\partial \bar{\varphi}} - \frac{\partial \varphi_2}{\partial t}\right) \\
&\quad + \left(f_1 - \frac{\partial P_1}{\partial t}\right)\left[\frac{\partial P_1}{\partial \bar{\varphi}}\frac{\partial \varphi_1}{\partial \bar{P}} - \frac{\partial P_2}{\partial \bar{P}} + \left(\frac{\partial P_1}{\partial \bar{P}}\right)^2\right] + \left(f_2 - \frac{\partial \varphi_1}{\partial t}\right)\left(\frac{\partial P_1}{\partial \bar{\varphi}}\frac{\partial \varphi_1}{\partial \bar{\varphi}} - \frac{\partial P_2}{\partial \bar{\varphi}} + \frac{\partial P_1}{\partial \bar{P}}\frac{\partial P_1}{\partial \bar{\varphi}}\right), \\
\overline{\nu}_1 &= f_2 - \frac{\partial \varphi_1}{\partial t}, \quad \overline{\nu}_2 = \frac{\partial f_2}{\partial \bar{P}} P_1 + \frac{\partial f_2}{\partial \bar{\varphi}}\varphi_1 - \frac{\partial \varphi_1}{\partial \bar{P}}\left(f_1 - \frac{\partial P_1}{\partial t}\right) - \frac{\partial \varphi_1}{\partial \bar{\varphi}}\left(f_2 - \frac{\partial \varphi_1}{\partial t}\right) - \frac{\partial \varphi_2}{\partial t}, \\
\overline{\nu}_3 &= \frac{\partial f_2}{\partial \bar{P}} P_2 + \frac{\partial f_2}{\partial \bar{\varphi}}\varphi_2 + \frac{P_1^2}{2}\frac{\partial^2 f_2}{\partial \bar{P}^2} + \frac{\varphi_1^2}{2}\frac{\partial^2 f_2}{\partial \bar{\varphi}^2} + P_1\varphi_1\frac{\partial^2 f_2}{\partial \bar{P}\partial \bar{\varphi}} \\
&\quad - \frac{\partial \varphi_1}{\partial \bar{P}}\left(P_1\frac{\partial f_1}{\partial \bar{P}} + \varphi_1\frac{\partial f_1}{\partial \bar{\varphi}} - \frac{\partial P_2}{\partial t}\right) - \frac{\partial \varphi_1}{\partial \bar{\varphi}}\left(P_1\frac{\partial f_2}{\partial \bar{P}} + \varphi_1\frac{\partial f_2}{\partial \bar{\varphi}} - \frac{\partial \varphi_2}{\partial t}\right) \\
&\quad + \left(f_2 - \frac{\partial \varphi_1}{\partial t}\right)\left[\frac{\partial P_1}{\partial \bar{\varphi}}\frac{\partial \varphi_1}{\partial \bar{P}} - \frac{\partial \varphi_2}{\partial \bar{\varphi}} + \left(\frac{\partial \varphi_1}{\partial \bar{\varphi}}\right)^2\right] + \left(f_1 - \frac{\partial P_1}{\partial t}\right)\left(\frac{\partial P_1}{\partial \bar{P}}\frac{\partial \varphi_1}{\partial \bar{P}} - \frac{\partial \varphi_2}{\partial \bar{P}} + \frac{\partial \varphi_1}{\partial \bar{P}}\frac{\partial \varphi_1}{\partial \bar{\varphi}}\right).
\end{aligned} \tag{3.3.60}$$

Since the third-order averaging can be reduced to second-order averaging, it is natural to assume that P_1 and φ_1 have the same forms as in equation (3.3.43) and (3.3.44), respectively. Following the same idea of deriving equations (3.3.43) and (3.3.44), one can integrate $\overline{\mu}_2$ with respect to t, solve the result for P_2, and remove any terms from P_2 that are linear in $\bar{\varphi}$ (in order for the near-identity transformation (3.3.53) to be uniformly valid in the large t limit). Assuming

$$\frac{\partial P_2}{\partial t} = \overline{u}_2 - \underset{t}{\mathscr{M}}\{\overline{u}_2\}, \tag{3.3.61}$$

where $\overline{u}_2$ is given in equation (3.3.34), and solving this differential equation, one can obtain function P_2. Similarly, φ_2 can be obtained.

Now, consider the contribution of terms containing excitation function. Substitute P and φ in terms of relations (3.3.53) into the diffusion terms in (3.3.27), then expand functions g_j in a Taylor series,

$$g_j(\bar{P}+\varepsilon P_1+\varepsilon^2 P_2, \bar{\varphi}+\varepsilon\varphi_1+\varepsilon^2\varphi_2, t) = g_j(\bar{P}, \bar{\varphi}, t) + \varepsilon\left\{P_1\frac{\partial g_j}{\partial \bar{P}} + \varphi_1\frac{\partial g_j}{\partial \bar{\varphi}}\right\} + \cdots, \quad j=1,\ 2, \tag{3.3.62}$$

multiply the diffusion matrix by the inverse matrix (3.3.57), and add the contribution of the diffusion term to (3.3.59). This process results in two equations

$$\begin{aligned}\dot{\bar{P}} &= F_1^{(1)} + F_1^{(0)}\xi(t) = (\varepsilon\overline{\mu}_1+\varepsilon^2\overline{\mu}_2+\varepsilon^3\overline{\mu}_3) + (\varepsilon^{1/2}g_1+\varepsilon^{3/2}g_3+\varepsilon^{5/2}g_5)\xi(t),\\ \dot{\bar{\varphi}} &= F_2^{(1)} + F_2^{(0)}\xi(t) = (\varepsilon\overline{\nu}_1+\varepsilon^2\overline{\nu}_2+\varepsilon^3\overline{\nu}_3) + (\varepsilon^{1/2}h_1+\varepsilon^{3/2}h_3+\varepsilon^{5/2}h_5)\xi(t),\end{aligned} \tag{3.3.63}$$

where

$$\begin{aligned} F_1^{(1)} &= \varepsilon\overline{\mu}_1+\varepsilon^2\overline{\mu}_2+\varepsilon^3\overline{\mu}_3, \quad F_1^{(0)} = \varepsilon^{1/2}g_1+\varepsilon^{3/2}g_3+\varepsilon^{5/2}g_5,\\ F_2^{(1)} &= \varepsilon\overline{\nu}_1+\varepsilon^2\overline{\nu}_2+\varepsilon^3\overline{\nu}_3, \quad F_2^{(0)} = \varepsilon^{1/2}h_1+\varepsilon^{3/2}h_3+\varepsilon^{5/2}h_5,\end{aligned} \tag{3.3.64}$$

and $\overline{\mu}_1, \overline{\mu}_2, \overline{\mu}_3, \overline{\nu}_1, \overline{\nu}_2$, and $\overline{\nu}_3$ are given in equation (3.3.60), g_i and h_i $(i=3,\ 5)$ are complicated functions of P_j, φ_j $(j=1,\ 2,\ 3)$ and g_1 and h_1 as follows

$$\begin{aligned} g_3 &= -g_1\frac{\partial P_1}{\partial \bar{P}} - h_1\frac{\partial P_1}{\partial \bar{\varphi}} + P_1\frac{\partial g_1}{\partial \bar{P}} + \varphi_1\frac{\partial g_1}{\partial \bar{\varphi}},\\ g_5 &= -\frac{\partial P_1}{\partial \bar{P}}(P_1\frac{\partial g_1}{\partial \bar{P}} + \varphi_1\frac{\partial g_1}{\partial \bar{\varphi}}) - \frac{\partial P_1}{\partial \bar{\varphi}}(P_1\frac{\partial h_1}{\partial \bar{P}} + \varphi_1\frac{\partial h_1}{\partial \bar{\varphi}})\\ &\quad + g_1(\frac{\partial P_1}{\partial \bar{\varphi}}\frac{\partial \varphi_1}{\partial \bar{P}} - \frac{\partial P_2}{\partial \bar{P}} + \frac{\partial P_1}{\partial \bar{P}}\frac{\partial P_1}{\partial \bar{P}}) + h_1(\frac{\partial P_1}{\partial \bar{\varphi}}\frac{\partial \varphi_1}{\partial \bar{\varphi}} - \frac{\partial P_2}{\partial \bar{\varphi}} + \frac{\partial P_1}{\partial \bar{P}}\frac{\partial P_1}{\partial \bar{\varphi}}),\\ h_3 &= P_1\frac{\partial h_1}{\partial \bar{P}} + \varphi_1\frac{\partial h_1}{\partial \bar{\varphi}} - h_1\frac{\partial \varphi_1}{\partial \bar{\varphi}} - g_1\frac{\partial \varphi_1}{\partial \bar{P}},\\ h_5 &= -\frac{\partial \varphi_1}{\partial \bar{\varphi}}(P_1\frac{\partial h_1}{\partial \bar{P}} + \varphi_1\frac{\partial h_1}{\partial \bar{\varphi}}) - \frac{\partial \varphi_1}{\partial \bar{P}}(P_1\frac{\partial g_1}{\partial \bar{P}} + \varphi_1\frac{\partial g_1}{\partial \bar{\varphi}})\\ &\quad + h_1(\frac{\partial P_1}{\partial \bar{\varphi}}\frac{\partial \varphi_1}{\partial \bar{P}} - \frac{\partial \varphi_2}{\partial \bar{\varphi}} + \frac{\partial \varphi_1}{\partial \bar{\varphi}}\frac{\partial \varphi_1}{\partial \bar{\varphi}}) + g_1(\frac{\partial \varphi_1}{\partial \bar{\varphi}}\frac{\partial \varphi_1}{\partial \bar{P}} - \frac{\partial \varphi_2}{\partial \bar{P}} + \frac{\partial P_1}{\partial \bar{P}}\frac{\partial \varphi_1}{\partial \bar{P}}).\end{aligned} \tag{3.3.65}$$

The stochastic averaging method can be used to obtain the averaged Itô stochastic differential equations:

$$\mathrm{d}\bar{P} = \bar{m}_P^*\mathrm{d}t + \bar{\sigma}_{11}^*\mathrm{d}W_1 + \bar{\sigma}_{12}^*\mathrm{d}W_2, \quad \mathrm{d}\bar{\varphi} = \bar{m}_\varphi^*\mathrm{d}t + \bar{\sigma}_{21}^*\mathrm{d}W_1 + \bar{\sigma}_{22}^*\mathrm{d}W_2, \tag{3.3.66}$$

where $W_1(t)$ and $W_2(t)$ are two independent standard Wiener processes, and equation (3.3.50) still holds but $F_j^{(1)}$ and $F_j^{(0)}$ are functions in equation (3.3.64).

On solving the function P_2 in equation (3.3.61), one is able to obtain the averaging value of $\bar{u}_2$. This can be done by considering equation (3.3.45), $\underset{t}{\mathscr{M}}\{f_1\}$ and $\underset{t}{\mathscr{M}}\{f_2\}$ in equation (3.3.38) and

$$\begin{aligned}
&\underset{t}{\mathscr{M}}\left\{I^{cc}\cos(2\omega t+2\bar{\varphi})\right\}\\
&\quad=-\frac{\omega}{\Gamma(1-\mu)}\underset{t}{\mathscr{M}}\left\{\frac{1}{2}\left[\cos(\omega t+\bar{\varphi})+\cos(3\omega t+3\bar{\varphi})\right]\int_0^t\frac{\sin(\omega s+\bar{\varphi})}{(t-s)^{\mu}}\mathrm{d}s\right\}=\frac{1}{4}\mathcal{H}^s(\omega),\\
&\underset{t}{\mathscr{M}}\left\{I^{cc}\sin(2\omega t+2\bar{\varphi})\right\}=-\frac{1}{4}\mathcal{H}^c(\omega),\quad \underset{t}{\mathscr{M}}\left\{I^{sc}\sin(2\omega t+2\bar{\varphi})\right\}=\frac{1}{4}\mathcal{H}^s(\omega),\\
&\underset{t}{\mathscr{M}}\left\{I^{sc}\cos(2\omega t+2\bar{\varphi})\right\}=\frac{1}{4}\mathcal{H}^c(\omega),\quad \underset{t}{\mathscr{M}}\left\{I^{ss}\cos(2\omega t+2\bar{\varphi})\right\}=-\frac{1}{4}\mathcal{H}^s(\omega),\\
&\underset{t}{\mathscr{M}}\left\{I^{cs}\cos(2\omega t+2\bar{\varphi})\right\}=\frac{1}{4}\mathcal{H}^c(\omega),\quad \underset{t}{\mathscr{M}}\left\{I^{cs}\sin(2\omega t+2\bar{\varphi})\right\}=\frac{1}{4}\mathcal{H}^s(\omega),\\
&\underset{t}{\mathscr{M}}\left\{I^{ss}\sin(2\omega t+2\bar{\varphi})\right\}=\frac{1}{4}\mathcal{H}^c(\omega).
\end{aligned}\tag{3.3.67}$$

Then, from differential equation equation (3.3.61), P_2 can be solved as

$$\begin{aligned}
P_2=&-\frac{p\bar{P}\tau_\varepsilon\mathcal{H}^s(\omega)}{8\omega}\left[\omega\tau_\varepsilon\mathcal{H}^c(\omega)+2\beta\right]\sin 2\phi(t)\\
&+\frac{p\bar{P}\mathcal{H}^s(\omega)}{32\omega}\left[2\beta(\tau_\varepsilon+1)+2\tau_\varepsilon\omega\mathcal{H}^c(\omega)-2p\tau_\varepsilon\beta-\omega p{\tau_\varepsilon}^2\mathcal{H}^c(\omega)\right]\sin 4\phi(t)\\
&+\frac{p\bar{P}}{8}\left[\tau_\varepsilon\mathcal{H}^s(\omega)\right]^2\cos 2\phi(t)\\
&+\frac{p\bar{P}}{64\omega^2}\Big\{(2-p\tau_\varepsilon)\tau_\varepsilon\omega^2\left[\mathcal{H}^s(\omega)^2-\mathcal{H}^c(\omega)^2\right]+4\omega\beta\mathcal{H}^c(\omega)\left[(p-1)\tau_\varepsilon-1\right]\\
&+4(p-2)\beta^2\Big\}\cos 4\phi(t).
\end{aligned}\tag{3.3.68}$$

Similarly, φ_2 can be given by

$$\begin{aligned}
\varphi_2=&-\frac{1}{8}\left[\tau_\varepsilon\mathcal{H}^s(\omega)\right]^2\sin 2\phi(t)\\
&-\frac{1}{32\omega^2}\left[2\beta+\omega\tau_\varepsilon\left(\mathcal{H}^c(\omega)+\mathcal{H}^s(\omega)\right)\right]\left[2\beta+\omega\tau_\varepsilon\left(\mathcal{H}^c(\omega)-\mathcal{H}^s(\omega)\right)\right]\sin 4\phi(t)
\end{aligned}$$

$$-\frac{\tau_\varepsilon \mathcal{H}^s(\omega)}{8\omega}\big[\omega\tau_\varepsilon \mathcal{H}^c(\omega)+2\beta\big]\cos 2\phi(t)+\frac{1}{16\omega}\tau_\varepsilon \mathcal{H}^s(\omega)\big[2\beta+\omega\tau_\varepsilon \mathcal{H}^c(\omega)\big]\cos 4\phi(t). \tag{3.3.69}$$

To obtain $\bar{\mu}_3$ and $\bar{\nu}_3$ in equation (3.3.59), the following two terms can be simplified by using f_1 and f_2 in equation (3.3.28)

$$\begin{aligned}\frac{\partial f_1}{\partial \bar{P}}P_2+\frac{\partial f_1}{\partial \bar{\varphi}}\varphi_2 &= P_2\big[\omega\tau_\varepsilon p I^{sc}+\omega\tau_\varepsilon \bar{P} J^{sc}-2\beta p\sin^2(\omega t+\bar{\varphi})\big]\\ &\quad+\varphi_2\big[\omega p\bar{P}\tau_\varepsilon(I^{cc}-I^{ss})-2\beta p\bar{P}\sin(2\omega t+2\bar{\varphi})\big],\\ \frac{\partial f_2}{\partial \bar{P}}P_2+\frac{\partial f_2}{\partial \bar{\varphi}}\varphi_2 &= P_2\frac{\omega\tau_\varepsilon J^{cc}}{p}+\varphi_2\big[-\omega\tau_\varepsilon(I^{cs}+I^{sc})-2\beta\cos(2\omega t+2\bar{\varphi})\big],\end{aligned} \tag{3.3.70}$$

and some useful derivatives must be used,

$$\begin{aligned}\frac{\partial^2 f_1}{\partial \bar{P}^2} &= \frac{\partial}{\partial \bar{P}}\big[\omega\tau_\varepsilon p I^{sc}+\omega\tau_\varepsilon \bar{P} J^{sc}-2\beta p\sin^2(\omega t+\bar{\varphi})\big]=2\omega\tau_\varepsilon J^{sc}+\omega\tau_\varepsilon\bar{P}\frac{\partial J^{sc}}{\partial \bar{P}},\\ \frac{\partial^2 f_1}{\partial \bar{P}\partial\bar{\varphi}} &= \frac{\partial}{\partial \bar{\varphi}}\big[\omega\tau_\varepsilon p I^{sc}+\omega\tau_\varepsilon \bar{P} J^{sc}-2\beta p\sin^2(\omega t+\bar{\varphi})\big]\\ &= \omega\tau_\varepsilon p(I^{cc}-I^{ss})+\omega\tau_\varepsilon\bar{P}(J^{cc}-J^{ss})-2\beta p\sin 2(\omega t+\bar{\varphi}),\\ \frac{\partial^2 f_1}{\partial \bar{\varphi}^2} &= \frac{\partial}{\partial \bar{\varphi}}\big[\omega p\bar{P}\tau_\varepsilon(I^{cc}-I^{ss})-2\beta p\bar{P}\sin(2\omega t+2\bar{\varphi})\big]\\ &= -2\omega\tau_\varepsilon p\bar{P}(I^{sc}+I^{cs})-4\beta p\bar{P}\cos(2\omega t+2\bar{\varphi}),\end{aligned}$$

and

$$\begin{aligned}\frac{\partial^2 f_2}{\partial \bar{P}^2} &= \frac{\partial}{\partial \bar{P}}\Big[\frac{\omega\tau_\varepsilon J^{cc}}{p}\Big]\\ &= \frac{\omega\tau_\varepsilon}{p}\int_0^t \mathcal{H}(t-s)\Big[\frac{\bar{P}(s)}{\bar{P}(t)}\Big]^{1/p}\Big[\Big(\frac{1}{p}-1\Big)\frac{1}{\bar{P}(s)^2}-\frac{2}{p}\frac{1}{\bar{P}(t)\bar{P}(s)}+\Big(\frac{1}{p}+1\Big)\frac{1}{\bar{P}(t)^2}\Big]\\ &\quad \cos(\omega t+\bar{\varphi})\cos(\omega s+\bar{\varphi})\,\mathrm{d}s,\\ \frac{\partial^2 f_2}{\partial \bar{P}\partial\bar{\varphi}} &= \frac{\partial}{\partial \bar{\varphi}}\Big[\frac{\omega\tau_\varepsilon J^{cc}}{p}\Big]=-\frac{\omega\tau_\varepsilon}{p}\big(J^{sc}+J^{cs}\big),\\ \frac{\partial^2 f_2}{\partial \bar{\varphi}^2} &= \frac{\partial}{\partial \bar{\varphi}}\big[-\omega\tau_\varepsilon(I^{cs}+I^{sc})-2\beta\cos(2\omega t+2\bar{\varphi})\big]\\ &= -2\omega\tau_\varepsilon(I^{cc}-I^{ss})+4\beta\sin(2\omega t+2\bar{\varphi}),\end{aligned}$$

where

$$
\begin{aligned}
&\frac{\partial I^{sc}}{\partial \bar{P}} = \frac{\partial}{\partial \bar{P}} \int_0^t \mathcal{H}(t-s)\left[\frac{\bar{P}(s)}{\bar{P}(t)}\right]^{1/p} \sin(\omega t+\bar{\varphi})\cos(\omega s+\bar{\varphi})\,\mathrm{d}s = \frac{J^{sc}}{p},\\
&\frac{\partial I^{cc}}{\partial \bar{P}} = \frac{J^{cc}}{p}, \quad \frac{\partial I^{cc}}{\partial \bar{\varphi}} = -I^{sc} - I^{cs}, \quad \frac{\partial I^{ss}}{\partial \bar{\varphi}} = I^{cs} + I^{sc},\\
&\frac{\partial I^{sc}}{\partial \bar{\varphi}} = \frac{\partial}{\partial \bar{\varphi}} \int_0^t \mathcal{H}(t-s)\left[\frac{\bar{P}(s)}{\bar{P}(t)}\right]^{1/p} \sin(\omega t+\bar{\varphi})\cos(\omega s+\bar{\varphi})\,\mathrm{d}s = I^{cc} - I^{ss},\\
&\frac{\partial I^{cs}}{\partial \bar{\varphi}} = -I^{ss} + I^{cc}, \quad \frac{\partial J^{sc}}{\partial \bar{\varphi}} = J^{cc} - J^{ss}, \quad \frac{\partial J^{cc}}{\partial \bar{\varphi}} = -J^{sc} - J^{cs}.
\end{aligned}
\tag{3.3.71}
$$

Substituting P_1, φ_1, P_2 in equation (3.3.68) and φ_2 in equation (3.3.69) into (3.3.60) yields the values of $\overline{\mu}_1$, $\overline{\mu}_2$, $\overline{\mu}_3$, and $\overline{\nu}_1$, $\overline{\nu}_2$, $\overline{\nu}_3$. The first two variables are simple, $\overline{\mu}_1 = \overline{u}_1$ and $\overline{\nu}_1 = \overline{v}_1$. However, $\overline{\mu}_2$, $\overline{\mu}_3$, $\overline{\nu}_2$, and $\overline{\nu}_3$ are too tedious to present here. In the same way, substituting P_1, φ_1, P_2 in equation (3.3.68) and φ_2 in equation (3.3.69) into (3.3.65) yields the values of g_i and h_i $(i=3,5)$.

Following the same procedure as the second-order averaging, the averaged Itô stochastic differential equations of equation (3.3.63) are obtained as, based on equation (3.3.66),

$$
\mathrm{d}\bar{P} = \bar{m}_P^* \mathrm{d}t + \bar{\sigma}_{11}^* \mathrm{d}W_1 + \bar{\sigma}_{12}^* \mathrm{d}W_2, \quad \mathrm{d}\bar{\varphi} = \bar{m}_\varphi^* \mathrm{d}t + \bar{\sigma}_{21}^* \mathrm{d}W_1 + \bar{\sigma}_{22}^* \mathrm{d}W_2, \tag{3.3.72}
$$

and

$$
\begin{aligned}
\bar{m}_P^* = {}& \varepsilon p\bar{P}\left[-\beta - \frac{\omega\tau_\varepsilon}{2}\mathcal{H}^c(\omega) + \frac{p+2}{16}\omega^2 S(2\omega)\right] - \frac{\varepsilon^2}{16} p(p+2)\bar{P}\tau_\varepsilon \mathcal{H}^s(\omega)\omega^2 S(2\omega)\\
& - \frac{1}{1024}\varepsilon^3 p\bar{P}\Big\{ S(2\omega)\Big[(-48-22p+3p^2+p^3)\omega^2{\tau_\varepsilon}^2\big(\mathcal{H}^c(\omega)\big)^2\\
& \qquad + (-192-88p+12p^2+4p^3)\beta(\beta+\omega\tau_\varepsilon \mathcal{H}^c(\omega))\\
& \qquad - (144+74p+p^3+3p^2)\omega^2{\tau_\varepsilon}^2\big(\mathcal{H}^s(\omega)\big)^2\Big]\\
& \qquad + 2\Psi(2\omega)\omega\tau_\varepsilon p(p+2)\mathcal{H}^s(\omega)\big[2\beta + \tau_\varepsilon\omega \mathcal{H}^c(\omega)\big]\Big\},
\end{aligned}
$$

$$
\begin{aligned}
b_{11}^* = {}& \varepsilon\frac{1}{8}\omega^2 p^2\bar{P}^2 S(2\omega) - \varepsilon^2\frac{1}{8}\omega^2 p^2\bar{P}^2 S(2\omega)\mathcal{H}^s(\omega)\\
& - \varepsilon^3\frac{1}{512} p^2\bar{P}^2 S(2\omega)\Big\{\big(2p+p^2-24\big)\big[\omega\tau_\varepsilon \mathcal{H}^c(\omega) + 2\beta\big]^2
\end{aligned}
$$

$$-\left(72+2p+p^2\right)\left[\omega\tau_\varepsilon \mathcal{H}^s(\omega)\right]^2\Big\},$$

$$b_{12}^* = b_{21}^* = o(\varepsilon^3) \approx 0. \tag{3.3.73}$$

It is not surprising to find that the first two terms of drift coefficients and diffusion coefficients in equation (3.3.72) are identical to those in the second-order averaging, as the third-order averaging add one more term over the second-order averaging. The first equation in equation (3.3.72) is decoupled from the second equation. Focus is turned to the Itô differential equation:

$$\mathrm{d}\bar{P} = \bar{m}_P^* \mathrm{d}t + \bar{\sigma}_{11}^* \mathrm{d}W_1, \quad \bar{\sigma}_{11}^* = \sqrt{b_{11}^*}, \tag{3.3.74}$$

where the term with $\bar{\sigma}_{12}^*$ is dropped because it is very small from equation (3.3.73). Taking the expected value on both sides of equation (3.3.74) leads to

$$\mathrm{dE}[\bar{P}] = \frac{\bar{m}_P^*}{\bar{P}} \mathrm{E}[\bar{P}]\mathrm{d}t,$$

and the pth moment Lyapunov exponent, including the third-order term, is

$$\begin{aligned}\Lambda(p) =& \lim_{t\to\infty} \frac{\log \mathrm{E}[\bar{P}]}{t} \\ \approx& \varepsilon p\Big[-\beta - \frac{\omega\tau_\varepsilon}{2}\mathcal{H}^c(\omega) + \frac{p+2}{16}\omega^2 S(2\omega)\Big] \boxed{-\tfrac{\varepsilon^2}{16}p(p+2)\tau_\varepsilon \mathcal{H}^s(\omega)\omega^2 S(2\omega)} \\ & -\tfrac{1}{1024}\varepsilon^3 p\Big\{S(2\omega)\Big[(-48-22p+3p^2+p^3)\omega^2{\tau_\varepsilon}^2\left(\mathcal{H}^c(\omega)\right)^2 \\ & +(-192-88p+12p^2+4p^3)\beta(\beta+\omega\tau_\varepsilon \mathcal{H}^c(\omega)) \\ & -(144+74p+p^3+3p^2)\omega^2{\tau_\varepsilon}^2\left(\mathcal{H}^s(\omega)\right)^2\Big] \\ & +2\Psi(2\omega)\omega\tau_\varepsilon p(p+2)\mathcal{H}^s(\omega)\left[2\beta+\tau_\varepsilon\omega \mathcal{H}^c(\omega)\right]\Big\}.\end{aligned} \tag{3.3.75}$$

Comparing equation (3.3.75) with (3.3.51), one may find that moment Lyapunov exponent of third-order averaging adds a term of order ε^3 on the result of second-order averaging, highlighted in the grey box. Hence, the third-order averaging method can be reduced to second-order averaging if the functions P_2 and φ_2 are set to zero.

From the relation in equation (1.1.7), the largest Lyapunov exponent from the third-order averaging is given by

$$\lambda \approx \varepsilon\Big[-\beta-\frac{\omega}{2}H^s(\omega)+\frac{1}{8}\omega^2 S(2\omega)\Big]\boxed{-\tfrac{1}{8}\varepsilon^2\omega^2\tau_\varepsilon S(2\omega)H^s(\omega)}$$
$$+\tfrac{1}{512}\varepsilon^3 p\Big\{S(2\omega)\Big[11\big(\omega\tau_\varepsilon H^c(\omega)\big)^2+44\beta\big(\beta+\omega\tau_\varepsilon H^c(\omega)\big)+37\big(\omega\tau_\varepsilon H^s(\omega)\big)^2\Big]$$
$$-2\Psi(2\omega)\omega\tau_\varepsilon H^s(\omega)\big[2\beta+\tau_\varepsilon\omega H^c(\omega)\big]\Big\}, \tag{3.3.76}$$

where the grey part denotes the difference between the third-order and second-order averaging in equation (3.3.52).

3.3.4 Numerical Results and Discussion

This section provides some numerical results of stochastic averaging analysis in the preceding three sections and simulation is used to check the averaging results.

Case 1: Under Gaussian white noise excitation

Substituting the power spectral density of white in equation (1.2.2) and the terms in equation (3.3.19) into (3.3.25), (3.3.51) and (3.3.75), respectively, yields the moment Lyapunov exponents of first order, second-order and third-order stochastic averaging,

$$\Lambda_1(p)=\varepsilon p\left\{-\beta-\frac{\omega^{\mu+1}\tau_\varepsilon}{2}\sin\frac{\mu\pi}{2}+\frac{p+2}{16}\omega^2\sigma^2\right\},$$
$$\Lambda_2(p)=\varepsilon p\Big[-\beta-\frac{\omega^{1+\mu}\tau_\varepsilon}{2}\sin\frac{\mu\pi}{2}+\frac{p+2}{16}\omega^2\sigma^2\Big]\boxed{-\tfrac{\varepsilon^2}{16}p(p+2)\tau_\varepsilon\omega^{2+\mu}\sigma^2\cos\tfrac{\mu\pi}{2}},$$
$$\Lambda_3(p)=\varepsilon p\Big[-\beta-\frac{\omega^{1+\mu}\tau_\varepsilon}{2}\sin\frac{\mu\pi}{2}+\frac{p+2}{16}\omega^2\sigma^2\Big]\boxed{-\tfrac{\varepsilon^2}{16}p(p+2)\tau_\varepsilon\omega^{2+\mu}\sigma^2\cos\tfrac{\mu\pi}{2}}$$
$$-\tfrac{\varepsilon^3}{1024}p\sigma^2\Big[(-48-22p+3p^2+p^3)\omega^{2+2\mu}\tau_\varepsilon{}^2\sin^2\tfrac{\mu\pi}{2}$$
$$+(-192-88p+12p^2+4p^3)\beta\big(\beta+\omega^{1+\mu}\tau_\varepsilon\sin\tfrac{\mu\pi}{2}\big)$$
$$-(144+74p+p^3+3p^2)\omega^{2+2\mu}\tau_\varepsilon{}^2\cos^2\tfrac{\mu\pi}{2}\Big], \tag{3.3.77}$$

where the framed part and grey part denote the difference between the first-order and second-order averaging and between the second-order and third-order averaging, respectively.

In order to check these approximate analytical results, the method for numerical determination of moment Lyapunov exponents in Section 2.2 is adopted. Letting

$$q_1(t) = q(t), \quad q_2(t) = \dot{q}(t), \quad Q(t) = {}_0^{\mathrm{RL}}\mathcal{D}_t^{\mu}[q(t)], \tag{3.3.78}$$

the equation of motion (3.1.8) can be written as a two-dimensional system

$$\dot{q}_1(t) = q_2, \quad \dot{q}_2(t) = -2\varepsilon\beta q_2 - \omega^2\big[\big(1-\varepsilon^{1/2}\xi(t)\big)q_1 + \varepsilon\tau_\varepsilon Q\big]. \tag{3.3.79}$$

When the excitation is white noise in equation (1.2.1), this equation can be discretized using the Euler scheme:

$$\begin{aligned} q_1^{k+1} &= q_1^k + q_2^k \cdot \Delta t, \\ q_2^{k+1} &= q_2^k - \big[2\varepsilon\beta q_2^k + \omega^2\big(q_1^k + \varepsilon\tau_\varepsilon Q^k\big)\big] \cdot \Delta t + \omega^2\varepsilon^{1/2} q_1^k \sigma \cdot \Delta W^k, \\ Q^k &= \frac{1}{h^\mu}\sum_{j=1}^{n+1} \omega_j q_1^j. \end{aligned} \tag{3.3.80}$$

After this discretization, a time series of the response variable $q(t)$ can be obtained under certain initial conditions. Having obtained S samples of the solutions to fractional stochastic differential equations, the pth moment can be determined as in equation (2.2.17).

Figure 3.1 compares the approximate analytical moment Lyapunov exponents given by equation (3.3.77) and the numerical results for various values of β. The good agreement between analytical and numerical methods implies that the numerical algorithm works well as expected. With the increase of the damping coefficient β from 0.01 to 0.15, the system changes from unstable to stable. The stabilizing effect of damping β is also shown in Figures 3.2 three dimensionally. With the increase of β, the stability index, i.e., $\Lambda(p) = 0$, also increases, which suggests the system becomes more stable.

The elastic modulus E plays a destabilizing role, for with the increase of E, the system becomes unstable, as shown in Figure 3.3. However, Figure 3.4 depicts that viscosity η stabilizes the system. The boundaries for pth moment stability are determined by $\Lambda(p) = 0$.

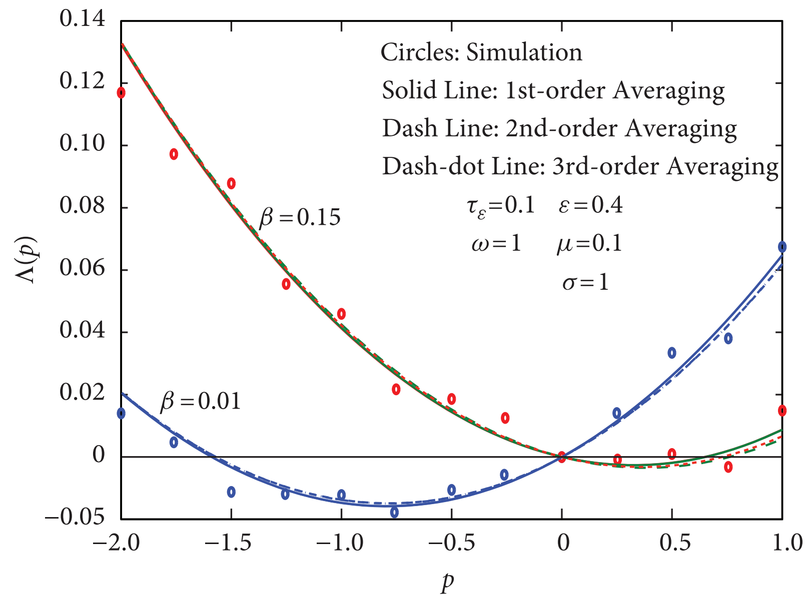

Figure 3.1 Comparison of simulation and approximate results for fractional SDOF viscoelastic system under white noise excitation

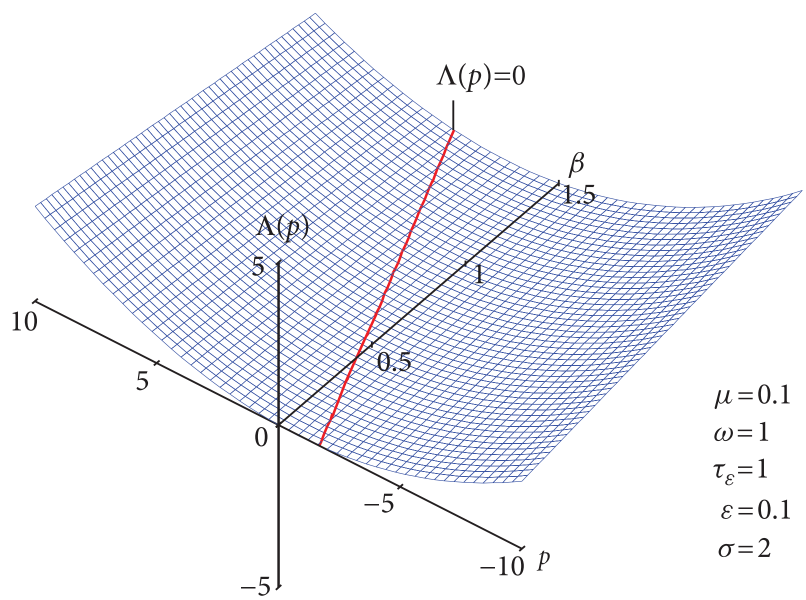

Figure 3.2 Effect of damping (β) on Moment Lyapunov exponents under Gaussian white noise excitation

The retardation $\tau_\varepsilon = \eta/E$ is a combination of these two material parameters. From this relation, one can predict the stabilizing effect of τ_ε, which is confirmed in Figure 3.5. The reason is when E decreases or η increases, the relaxation time of viscoelasticity decreases, then the system is more stable.

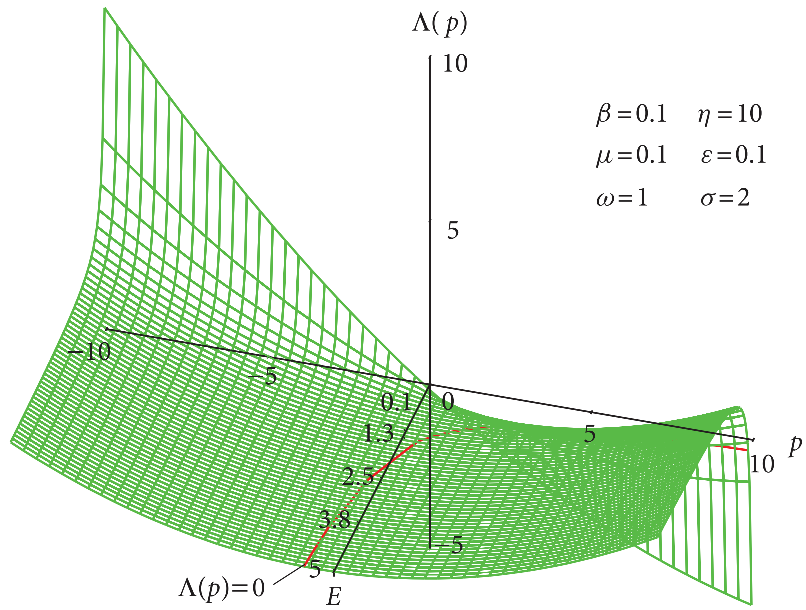

Figure 3.3 Effect of elastic modulus (E) on Moment Lyapunov exponents of fractional SDOF viscoelastic system under white noise excitation

Figure 3.6 shows that the fractional order μ plays an important role in the system stability. The increase of the parameter μ would enhance the system stability. When μ changes from 0 to 1, the system gradually becomes stabilized. As indicated in Figure 1.6, when μ shifts from 0 to 1, the fractional Newton element in a fractional Kelvin-Voigt model moves from a Hooke element to an integer-value Newton element, i.e., from elasticity to total viscosity. Therefore, the fractional order μ enables a subtle and smooth transition from elasticity to viscosity in one element, which abandons the conventional binary theory that only allow an element either to function totally elastic (a spring) or perform perfect viscosity (a dashpot). Many real-world elements in engineering are composed of multi-state components that have different performance levels and several viscoelastic modes. Figure 3.6 clearly shows fractional components have vital effects on the entire system's performance. The effect of

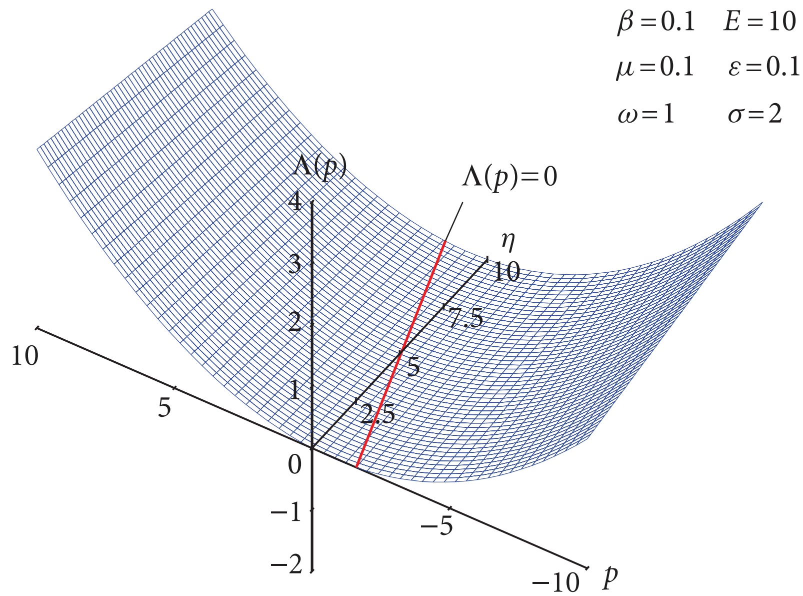

Figure 3.4 Effect of viscosity (η) on moment Lyapunov exponents of fractional SDOF viscoelastic system under white noise excitation

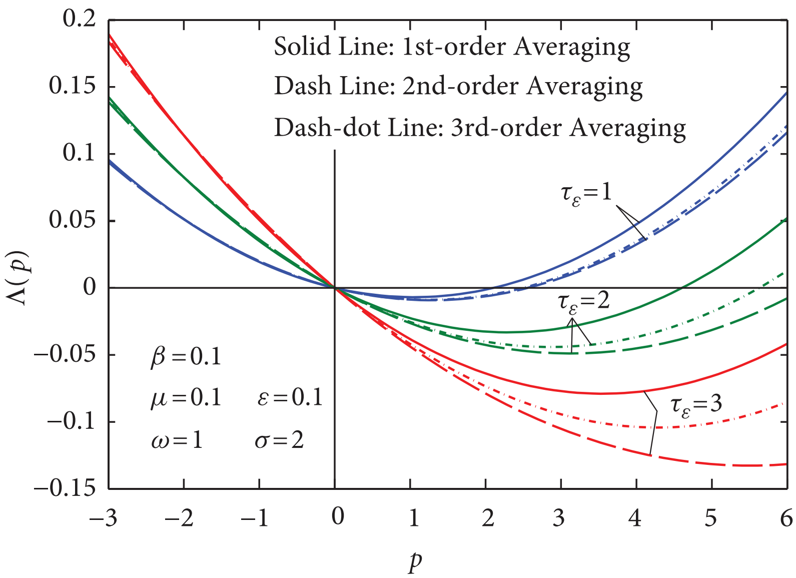

Figure 3.5 Effect of retardation (τ_ε) on moment Lyapunov exponents of fractional SDOF viscoelastic system under white noise excitation

parameters of white noise is shown in Figure 3.7. With the increase of the noise intensity factor σ, the system becomes more and more unstable.

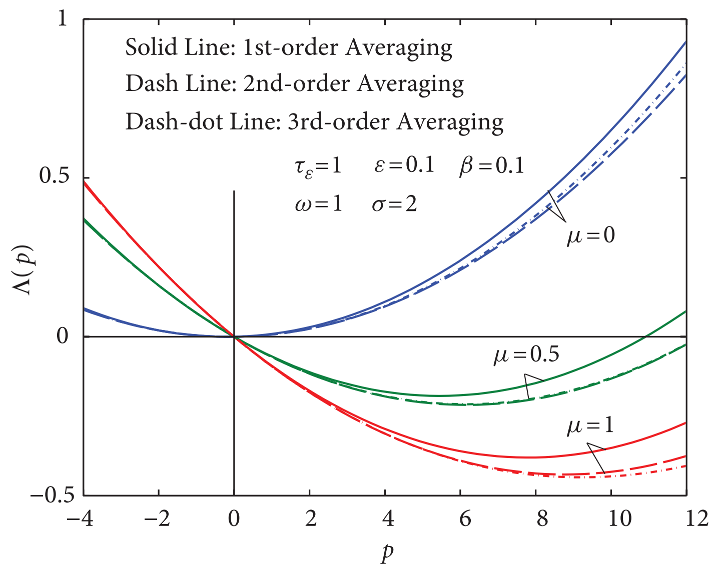

Figure 3.6 Effect of fractional order μ on moment Lyapunov exponents under Gaussian white noise excitation

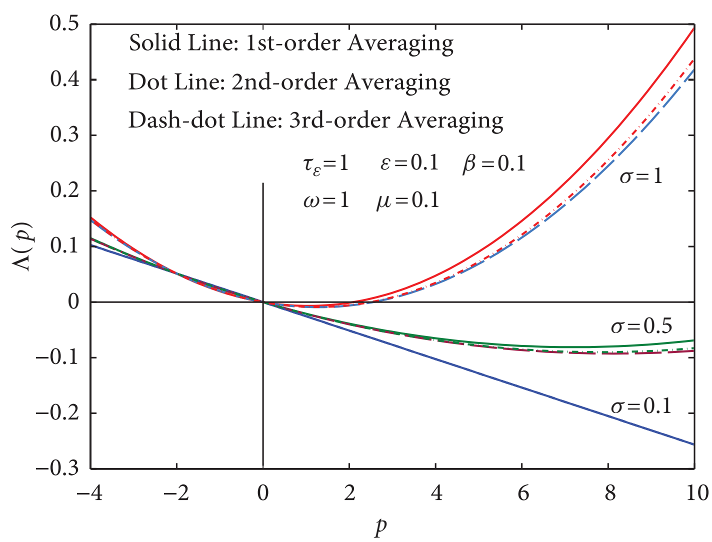

Figure 3.7 Effect of white noise intensity σ on moment Lyapunov exponents under Gaussian white noise excitation

It can be seen that when the moment order p is relatively small, first-order averaging agrees well with second-order averaging. The bigger the absolute value of p, the larger difference between the first and second-order averaging. The second-order averaging is almost overlapped by the third-order averaging.

Case 2: Under real noise excitation

When the excitation is real noise, the equation of motion can be discretized using the Euler scheme as follows:

$$
\begin{aligned}
q_1^{k+1} &= q_1^k + q_2^k \cdot \Delta t, \\
q_2^{k+1} &= q_2^k - \Big\{2\varepsilon\beta q_2^k + \omega^2\big[\big(1-\varepsilon^{1/2}q_3^k\big)q_1^k + \varepsilon\tau_\varepsilon Q^k\big]\Big\} \cdot \Delta t, \\
q_3^{k+1} &= q_3^k - \alpha q_3^k \cdot \Delta t + \sigma \cdot \Delta W^k, \\
Q^k &= \frac{1}{h^\mu}\sum_{j=1}^{n+1}\omega_j q_1^j,
\end{aligned}
\tag{3.3.81}
$$

where $q_3 = \xi(t)$ and q_1, q_2 are used to calculated the pth norm of the state vector of the system $\|\mathbf{q}\|^p = [(q_1)^2 + (q_2)^2]^{p/2}$.

Substituting the power spectral density of real noise in equation (1.2.4) and the terms in equation (3.3.19) into (3.3.25), (3.3.51) and (3.3.75), respectively, yields the moment Lyapunov exponents of first order, second-order and third-order stochastic averaging,

$$
\Lambda_1(p) = \varepsilon p\Big(-\beta - \frac{\tau_\varepsilon\omega^{1+\mu}}{2}\sin\frac{\mu\pi}{2} + \frac{p+2}{16}\omega^2\frac{\sigma^2}{\alpha^2+4\omega^2}\Big),
$$

$$
\Lambda_2(p) = \varepsilon p\Big(-\beta - \frac{\omega^{1+\mu}\tau_\varepsilon}{2}\sin\frac{\mu\pi}{2} + \frac{p+2}{16}\omega^2\frac{\sigma^2}{\alpha^2+4\omega^2}\Big)
\boxed{-\frac{\varepsilon^2}{16}p(p+2)\tau_\varepsilon\cos\frac{\mu\pi}{2}\omega^{2+\mu}\frac{\sigma^2}{\alpha^2+4\omega^2}},
$$

$$
\Lambda_3(p) = \varepsilon p\Big(-\beta - \frac{\omega^{1+\mu}\tau_\varepsilon}{2}\sin\frac{\mu\pi}{2} + \frac{p+2}{16}\omega^2\frac{\sigma^2}{\alpha^2+4\omega^2}\Big)
\boxed{-\frac{\varepsilon^2}{16}p(p+2)\tau_\varepsilon\cos\frac{\mu\pi}{2}\omega^{2+\mu}\frac{\sigma^2}{\alpha^2+4\omega^2}}
$$

$$-\frac{1}{1024}\varepsilon^3 p\left\{\frac{\sigma^2}{\alpha^2+4\omega^2}\left[(-48-22p+3p^2+p^3)\omega^{2+2\mu}{\tau_\varepsilon}^2\sin^2\frac{\mu\pi}{2}\right.\right.$$

$$+(-192-88p+12p^2+4p^3)\beta(\beta+\omega^{1+\mu}\tau_\varepsilon\sin\frac{\mu\pi}{2})$$

$$\left.-(144+74p+p^3+3p^2)\omega^{2+2\mu}{\tau_\varepsilon}^2\cos^2\frac{\mu\pi}{2}\right]$$

$$\left.+2\frac{\sigma^2}{\alpha(\alpha^2+4\omega^2)}\omega^{2+\mu}\tau_\varepsilon p(p+2)\cos\frac{\mu\pi}{2}\left[2\beta+\tau_\varepsilon\omega^{1+\mu}\sin\frac{\mu\pi}{2}\right]\right\}. \tag{3.3.82}$$

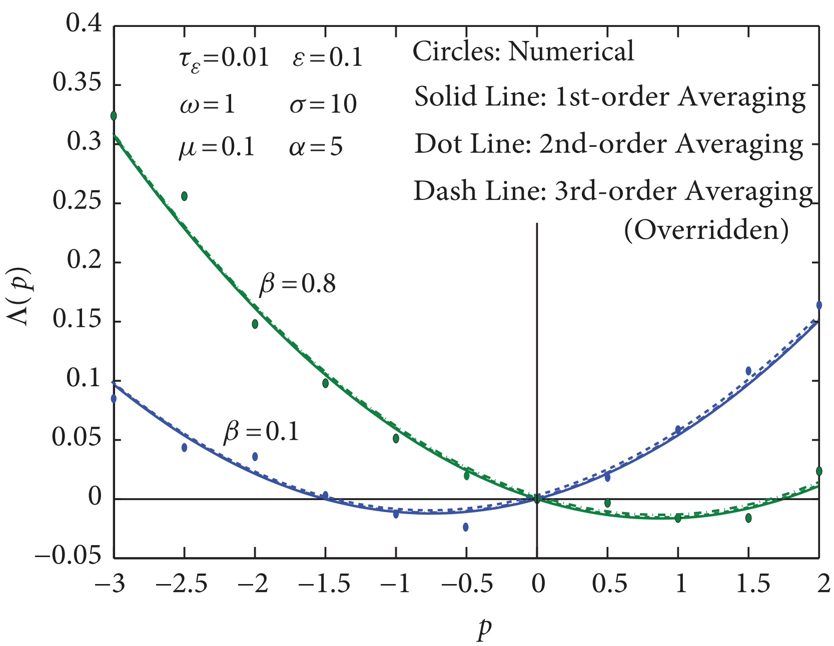

Figure 3.8 Comparison of simulation and approximate results for fractional SDOF viscoelastic system under real noise excitation

Figure 3.8 compares the approximate analytical moment Lyapunov exponents given by equation (3.3.82) and the numerical results for various values of β. Again,the good agreeable results between analytical and numerical methods are observed.

Comparing equations (3.3.82) with (3.3.77), one finds that parameters β, τ_ε, σ and μ affect the system under real noise in the same way as those under white noise. The additional parameter α of real noise plays a stabilizing role, as shown in figure 3.9. From equation

(1.2.4), it is seen that larger α would make the power of noise spread over a wider frequency band, which reduces the power of the noise in the neighborhood of resonance, and then stabilizes the system. However, larger σ may cause the noise's power more concentrated and prominent effect of resonance would de-stabilize the system.

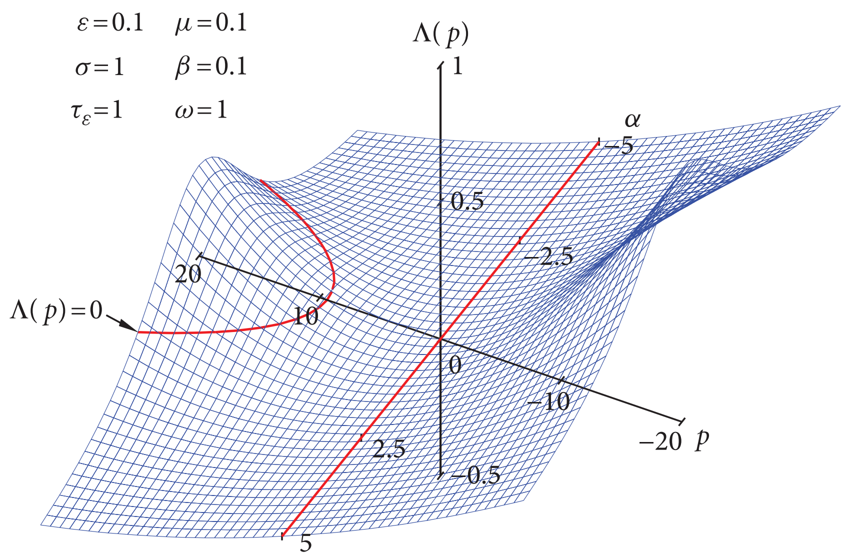

Figure 3.9 Effect of parameter α on moment Lyapunov exponents under real noise excitation

3.3.5 Ordinary Viscoelastic Systems

The equation of motion in equation (3.1.8) can be rewritten as

$$\ddot{q}(t)+2\varepsilon\beta\dot{q}(t)+\omega_n^2\left\{\left[1-\varepsilon^{1/2}\xi(t)\right]q(t)-\varepsilon\int_0^t \mathcal{H}(t-s)q(s)\mathrm{d}s\right\}=0, \tag{3.3.83}$$

where $\mathcal{H}(t)$ is the viscoelastic kernel function and ordinary Maxwell constitutive relation is taken in equation (3.3.84), so system (3.3.83) is ordinary viscoelastic systems,

$$\mathcal{H}(t)=\sum_{j=1}^{M}\gamma_j \mathrm{e}^{-\kappa_j t}, \tag{3.3.84}$$

where M is the number of Maxwell units in parallel chain. Its sine and cosine transformations are given by

$$\begin{aligned} \mathcal{H}^{s}(\omega) &= \int_0^\infty \mathcal{H}(\tau)\sin\omega\tau\,\mathrm{d}\tau = \sum_{j=1}^{M}\frac{\omega\gamma_j}{\kappa_j^2+\omega^2}, \\ \mathcal{H}^{c}(\omega) &= \int_0^\infty \mathcal{H}(\tau)\cos\omega\tau\,\mathrm{d}\tau = \sum_{j=1}^{M}\frac{\gamma_j\kappa_j}{\kappa_j^2+\omega^2}. \end{aligned} \tag{3.3.85}$$

One reason to use ordinary Maxwell model to illustrate higher-order stochastic averaging is that it can be used as an approximation to most linear viscoelastic behaviour as closely as possible if enough number of Maxwell units are arranged in parallel. More importantly, Maxwell kernel function possesses a unique characteristics to enable the original integro-differential equation of motion to be readily and accurately transformed into a set of first-order differential equations as shown in Section 2.1.

Case 1: The wide-band noise is taken as Gaussian white noise

Suppose that the excitation is approximated by a Gaussian white noise with spectral density $S(\omega)=\sigma^2=\text{constant}$ for all ω, and $\xi(t)\mathrm{d}t=\sigma\,\mathrm{d}W(t)$. Let

$$x_1(t)=q(t),\quad x_2(t)=\dot{q}(t),\quad x_{j+2}(t)=\int_0^t \gamma_j \mathrm{e}^{-\kappa_j(t-s)}q(s)\,\mathrm{d}s,\quad j=1,\,2. \tag{3.3.86}$$

Equation (3.3.83) can be discretized by using the Euler scheme,

$$\begin{aligned} x_1^{k+1} &= x_1^k + x_2^k\cdot h, \\ x_2^{k+1} &= x_2^k + \Big(-\omega^2 x_1^k - 2\varepsilon\beta x_2^k + \varepsilon\omega^2\sum_{j=3}^{4}x_j^k\Big)h - \varepsilon^{1/2}\sigma\omega^2 x_1^k\cdot\Delta W^k, \\ x_j^{k+1} &= x_j^k + \big(\gamma_j x_1^k - \kappa_j x_{j+2}^k\big)h, \qquad j=3,4, \end{aligned} \tag{3.3.87}$$

with h being the time step and k denoting the kth iteration.

Moment Lyapunov moments are illustrated in Figure 3.10 by using first-order, second-order and third-order stochastic averaging methods, which are compared with results from Monte-Carlo simulation. In Monte Carlo simulation, the sample size for estimating the expected value is $N=5000$, time step is $h=0.001$, and the total length of time for simulation is $T=1000$, i.e., the number of iteration is 5×10^4.

It is seen that the first-order averaging results agree with the simulation results very well when p and σ are small. As expected, the second-order averaging gives a better approximation. Results of third-order averaging are almost overridden by those of second-order averaging, although third-order averaging makes somewhat of an improvement. When the intensity of noise σ increases, the system becomes more and more unstable in the sense that the largest Lyapunov exponents and moment Lyapunov exponents (for $p>0$) increase.

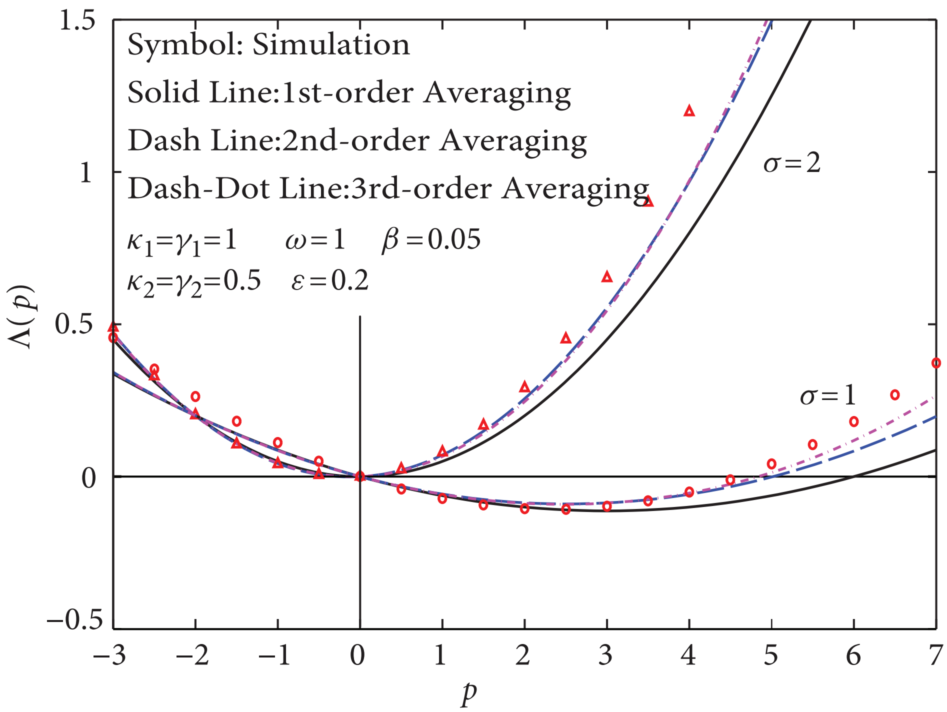

Figure 3.10 Moment Lyapunov exponents for SDOF systems of ordinary viscoelasticity with white noise

Case 2: The wide-band noise is taken as a real noise

Denoting

$$\begin{aligned} &x_1(t)=q(t), \quad x_2(t)=\dot{q}(t), \\ &x_{j+2}(t)=\int_0^t \gamma_j \mathrm{e}^{-\kappa_j(t-s)} q(s)\,\mathrm{d}s, \quad x_5(t)=\xi(t), \quad j=1,\,2, \end{aligned} \tag{3.3.88}$$

one can discretize equation (3.3.83) by using Euler scheme

$$\begin{aligned} x_1^{k+1} &= x_1^k + x_2^k \cdot h, \\ x_2^{k+1} &= x_2^k + \Big(-\omega^2 x_1^k - 2\varepsilon\beta x_2^k + \varepsilon\omega^2 \sum_{j=1}^{2} x_{j+2}^k - \varepsilon^{1/2}\omega^2 x_1^k x_5^k \Big) \cdot h, \\ x_{j+2}^{k+1} &= x_{j+2}^k + \big(\gamma_j x_1^k - \kappa_j x_{j+2}^k \big) \cdot h, \qquad j = 1,\ 2, \\ x_5^{k+1} &= x_5^k + \big(-\alpha x_5^k \big) \cdot h + \sigma \cdot \Delta W^k. \end{aligned} \tag{3.3.89}$$

x_1 and x_2 are related to the state variables of the original system and are used to calculate the pth norm $\|\mathbf{x}(t)\|^p = (x_1^2 + x_2^2)^{p/2}$.

Figures 3.11 and 3.12 show that the stronger the viscoelasticity (i.e., larger γ), the larger the relaxation (i.e., smaller κ), the more stable the system will be. Results from second-order averaging are almost the same as those of the third-order averaging, which agrees quite well with Monte-Carlo simulation results.

The effect of parameters of real noise process is also studied. Parameter σ plays a role of destabilization shown in Figure 3.13. However, from Figure 3.14, it is seen that α stabilizes the system. This can be explained from the power spectral density of real noise in equation (1.2.4), similar to Section 3.3.4.

3.4 Lyapunov Exponents of Fractional Viscoelastic Systems under Bounded Noise Excitation

In Section 3.3, fractional viscoelastic systems under wide-band noise excitation are studied. The ensuing two sections deal with fractional viscoelastic systems under bounded boise excitation: one is for Lyapunov exponents, the other is for moment Lyapunov exponents.

3.4.1 Lyapunov Exponents

To apply the averaging method, a transformation is made to the amplitude and phase variables a and φ by means of the relations

$$q(t) = a(t)\cos\Phi(t), \quad \dot{q}(t) = -\omega a(t)\sin\Phi(t), \quad \Phi(t) = \tfrac{1}{2}\nu t + \varphi(t). \tag{3.4.1}$$

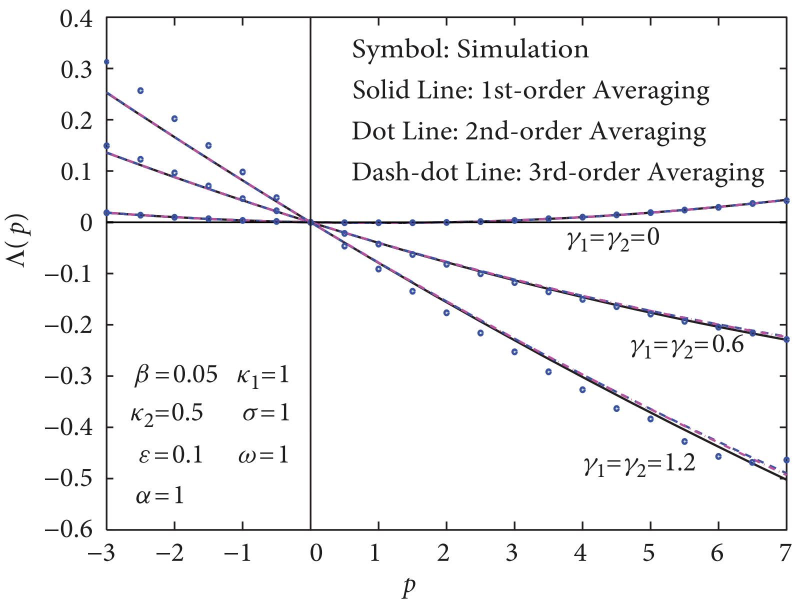

Figure 3.11 Moment Lyapunov exponents for ordinary viscoelasticity under real noise excitation

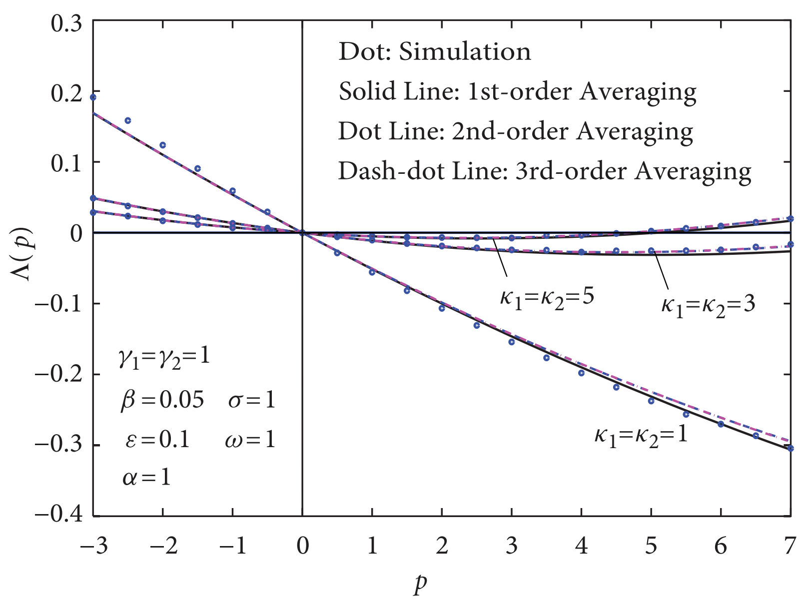

Figure 3.12 Moment Lyapunov exponents for ordinary viscoelasticity under real noise excitation

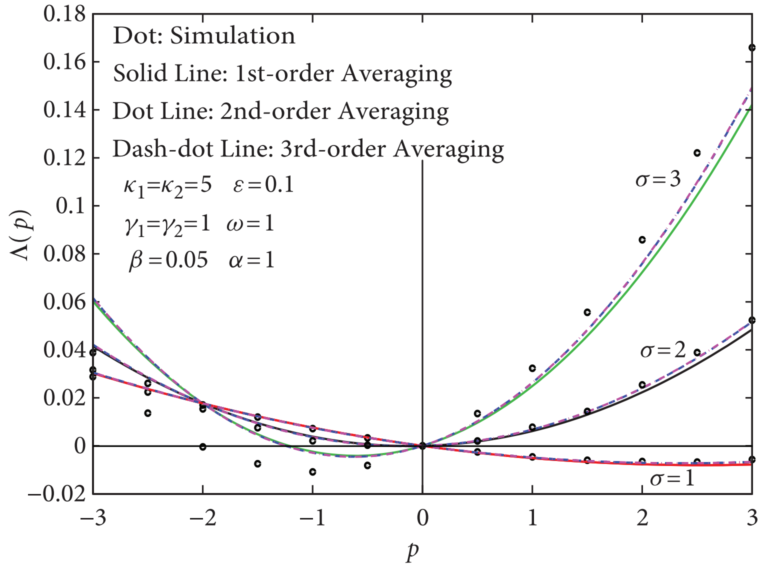

Figure 3.13 Moment Lyapunov exponents under real noise for various σ for ordinary viscoelasticity

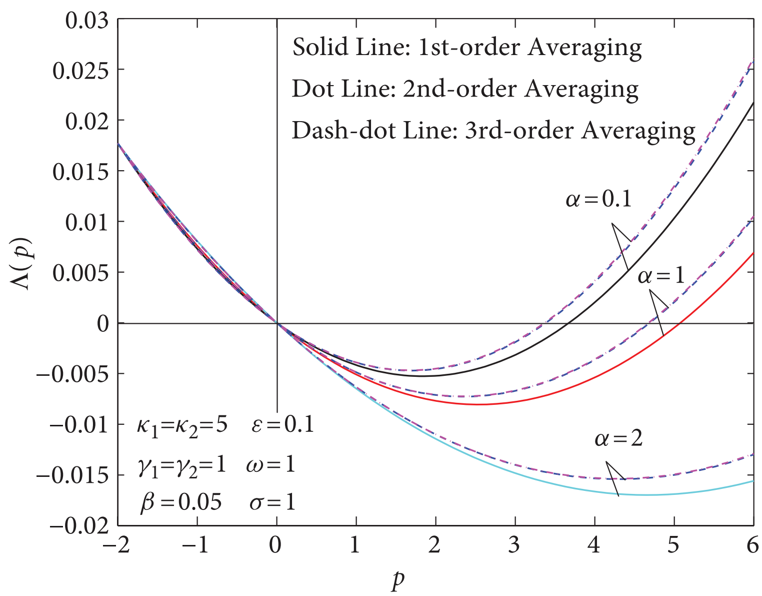

Figure 3.14 Moment Lyapunov exponents under real noise for various α for ordinary viscoelasticity

Substituting equation (3.4.1) into (3.1.8) yields

$$\begin{aligned}&\dot{a}\cos\Phi(t)-a\dot{\varphi}\sin\Phi(t)=-\varepsilon\Delta a\sin\Phi(t),\\&\dot{a}\sin\Phi(t)+a\dot{\varphi}\cos\Phi(t)=\varepsilon\Delta a\cos\Phi(t)-2\varepsilon a\beta\sin\Phi(t)\\&\qquad\qquad+\varepsilon\omega\xi(t)a\cos\Phi(t)+\varepsilon\omega\tau_\varepsilon\,{}^{\mathrm{RL}}_{0}\mathcal{D}^{\mu}_{t}q(s),\end{aligned}\tag{3.4.2}$$

where $\varepsilon\Delta=\omega-\frac{1}{2}\nu$. Solving equation (3.4.2) yields

$$\begin{aligned}\dot{a}(t)&=\varepsilon\Big\{-2\beta a(t)\sin^2\Phi(t)+\tfrac{1}{2}\omega\xi(t)a(t)\sin 2\Phi(t)+\omega\tau_\varepsilon\sin\Phi(t)\,{}^{\mathrm{RL}}_{0}\mathcal{D}^{\mu}_{t}\big[a(s)\cos\Phi(s)\big]\Big\},\\\dot{\varphi}(t)&=\varepsilon\Big\{\Delta-\beta\sin 2\Phi(t)+\omega\cos^2\Phi(t)\xi(t)+\frac{\omega}{a(t)}\tau_\varepsilon\cos\Phi(t)\,{}^{\mathrm{RL}}_{0}\mathcal{D}^{\mu}_{t}\big[a(s)\cos\Phi(s)\big]\Big\}.\end{aligned}\tag{3.4.3}$$

The bounded noise can be written as, by assuming that the magnitude is small and then introducing a small parameter $\varepsilon^{1/2}$,

$$\xi(t)=\zeta\cos\left[\nu t+\psi(t)\right],\qquad \psi(t)=\varepsilon^{1/2}\sigma W(t)+\theta.\tag{3.4.4}$$

Substituting $\xi(t)$ in equation (3.4.3) leads to

$$\begin{aligned}\dot{a}(t)&=\varepsilon\Big\{-\beta a[1-\cos 2\Phi]+\frac{\zeta\omega a}{2}\cos\left[\nu t+\psi(t)\right]\sin 2\Phi\\&\qquad+\omega\tau_\varepsilon\sin\Phi(t)\,{}^{\mathrm{RL}}_{0}\mathcal{D}^{\mu}_{t}\big[a(s)\cos\Phi(s)\big]\Big\},\\\dot{\varphi}(t)&=\varepsilon\Big\{\Delta-\beta\sin 2\Phi+\omega\zeta\cos\left[\nu t+\psi(t)\right]\cos^2\Phi+\frac{\omega}{a(t)}\tau_\varepsilon\cos\Phi(t)\,{}^{\mathrm{RL}}_{0}\mathcal{D}^{\mu}_{t}\big[a(s)\cos\Phi(s)\big]\Big\},\\\dot{\psi}(t)&=\varepsilon^{1/2}\sigma\dot{W}(t).\end{aligned}\tag{3.4.5}$$

Equations (3.4.5) are equivalent to (3.1.8) and cannot be solved exactly.

The averaging method can be applied to obtain the averaged equations as follows, without distinction between the averaged and the original non-averaged variables a and φ,

$$\begin{aligned}\dot{a}(t)&=\varepsilon\Big\{-\beta a+\frac{1}{4}\zeta\omega a\sin(2\varphi-\psi)+\omega\tau_\varepsilon\underset{t}{\mathscr{M}}\Big\{\sin\Phi(t)\,{}^{\mathrm{RL}}_{0}\mathcal{D}^{\mu}_{t}\big[a(s)\cos\Phi(s)\big]\Big\}\Big\},\\\dot{\varphi}(t)&=\varepsilon\Big\{\Delta+\frac{1}{4}\zeta\omega\cos(2\varphi-\psi)+\frac{\omega}{a}\tau_\varepsilon\underset{t}{\mathscr{M}}\Big\{\cos\Phi(t)\,{}^{\mathrm{RL}}_{0}\mathcal{D}^{\mu}_{t}\big[a(s)\cos\Phi(s)\big]\Big\}\Big\},\end{aligned}\tag{3.4.6}$$

where some averaged identities have been used

$$\begin{aligned}
&\underset{t}{\mathscr{M}}\{\cos 2\Phi\}=\underset{t}{\mathscr{M}}\{\sin 2\Phi\}=0,\\
&\underset{t}{\mathscr{M}}\Big\{\cos\big[\nu t+\psi(t)\big]\sin 2\Phi\Big\}=\tfrac{1}{2}\sin(2\varphi-\psi),\\
&\underset{t}{\mathscr{M}}\Big\{\cos\big[\nu t+\psi(t)\big]\cos^2\Phi\Big\}=\tfrac{1}{4}\cos(2\varphi-\psi).
\end{aligned}\tag{3.4.7}$$

By using equations (3.3.16) and (3.3.18), (3.4.6) becomes

$$\dot a(t)=\varepsilon\Big[-\hat\beta+\tfrac{1}{4}\zeta\omega\sin(2\varphi-\psi)\Big]a(t),\quad \dot\varphi(t)=\varepsilon\Big[\hat\Delta+\tfrac{1}{4}\zeta\omega\cos(2\varphi-\psi)\Big],\tag{3.4.8}$$

where

$$\hat\beta=\beta+\tfrac{1}{2}\omega^2\tau_\varepsilon\mathcal{H}^c\big(\tfrac{\nu}{2}\big),\quad \hat\Delta=\Delta+\tfrac{1}{2}\omega^2\tau_\varepsilon\mathcal{H}^s\big(\tfrac{\nu}{2}\big),\tag{3.4.9}$$

and

$$\begin{aligned}
\mathcal{H}^c\big(\tfrac{\nu}{2}\big)&=\frac{1}{\Gamma(1-\mu)}\int_0^\infty \tau^{-\mu}\cos\frac{\nu\tau}{2}\,\mathrm{d}\tau=\big(\tfrac{\nu}{2}\big)^{\mu-1}\sin\frac{\mu\pi}{2},\\
\mathcal{H}^s\big(\tfrac{\nu}{2}\big)&=\frac{1}{\Gamma(1-\mu)}\int_0^\infty \tau^{-\mu}\sin\frac{\nu\tau}{2}\,\mathrm{d}\tau=\big(\tfrac{\nu}{2}\big)^{\mu-1}\cos\frac{\mu\pi}{2}.
\end{aligned}\tag{3.4.10}$$

Upon the transformation $\rho=\log a$ and $\Theta=\varphi-\frac{1}{2}\psi$ and using $\dot\psi(t)=\varepsilon^{1/2}\sigma\dot W(t)$, equation (3.4.8) results in two Itô stochastic differential equations

$$\mathrm{d}\rho(t)=\varepsilon\Big[-\hat\beta+\tfrac{1}{4}\zeta\omega\sin 2\Theta(t)\Big]\mathrm{d}t,\tag{3.4.11}$$

$$\mathrm{d}\Theta(t)=\varepsilon\Big[\hat\Delta+\tfrac{1}{4}\zeta\omega\cos(2\varphi-\psi)\Big]\mathrm{d}t-\varepsilon^{1/2}\tfrac{1}{2}\sigma\dot W(t).\tag{3.4.12}$$

From equation (1.1.6), the Lyapunov exponents of system (3.1.8) is given by

$$\lambda=\lim_{t\to\infty}\frac{1}{t}\log\Big[q^2(t)+\frac{1}{\omega^2}\dot q^2(t)\Big]^{1/2}.\tag{3.4.13}$$

Substituting equation (3.4.1) into (3.4.13) yields the Lyapunov exponent

$$\lambda=\lim_{t\to\infty}\frac{1}{t}\log\Big[q^2(t)+\frac{1}{\omega^2}\dot q^2(t)\Big]=\lim_{t\to\infty}\frac{1}{t}\rho(t).\tag{3.4.14}$$

Integrating equation (3.4.11)

$$\rho(t)-\rho(0)=\tfrac{1}{4}\varepsilon\zeta\omega\int_0^t\sin 2\Theta(t)\mathrm{d}t-\varepsilon\hat\beta t,\tag{3.4.15}$$

and substituting into equation (3.4.14) yield

$$\lambda = \lim_{t\to\infty} \frac{1}{t}\rho(t) = \tfrac{1}{4}\varepsilon\zeta\omega \lim_{t\to\infty}\frac{1}{t}\int_0^t \sin 2\Theta(t)\mathrm{d}t - \varepsilon\hat{\beta}. \tag{3.4.16}$$

The stochastic process $\Theta(t)$ defined by equation (3.4.12) can be shown to be ergodic, in which case one can write

$$\lim_{t\to\infty}\frac{1}{t}\int_0^t \sin 2\Theta(t)\mathrm{d}t = \mathsf{E}\big[\sin 2\Theta(t)\big], \quad \text{w.p.1}, \tag{3.4.17}$$

where $\mathsf{E}[\cdot]$ denotes the expectation operator. Thus, with probability 1,

$$\lambda = \tfrac{1}{4}\varepsilon\zeta\omega\mathsf{E}\big[\sin 2\Theta(t)\big] - \varepsilon\hat{\beta}. \tag{3.4.18}$$

The remaining task is to evaluate $\mathsf{E}\big[\sin 2\Theta(t)\big]$ in order to obtain λ. For this purpose, the Fokker-Plank equation governing the stationary probability density function $p(\Theta)$ is set up

$$\tfrac{1}{2}\big(\varepsilon^{1/2}\frac{\sigma}{2}\big)^2\frac{\mathrm{d}^2 p(\Theta)}{\mathrm{d}\Theta^2} - \frac{\mathrm{d}}{\mathrm{d}\Theta}\Big[\varepsilon\big(\hat{\Delta} + \frac{1}{4}\zeta\omega\cos 2\Theta\big)p(\Theta)\Big] = 0. \tag{3.4.19}$$

Because the coefficients of the Fokker-Plank equation are periodic functions in Θ of period π, $p(\Theta)$ satisfies the periodicity condition $p(\Theta) = p(\Theta+\pi)$. Solving equation (3.4.19) yields

$$p(\Theta) = C^{-1}\mathrm{e}^{f(\Theta)}\int_\Theta^{\Theta+\pi}\mathrm{e}^{-f(\theta)}\mathrm{d}\theta, \quad 0 \leqslant \Theta \leqslant \pi, \tag{3.4.20}$$

where

$$f(\Theta) = 2\gamma\Theta + r\sin 2\Theta, \quad \gamma = \frac{2\hat{\Delta}}{\sigma^2}, \quad r = \frac{\zeta\omega}{\sigma^2}, \tag{3.4.21}$$

and the normalization constant C is given by

$$C = \pi^2\mathrm{e}^{-\gamma\pi}I_{\mathrm{i}\gamma}(r)I_{-\mathrm{i}\gamma}(r), \tag{3.4.22}$$

$I_{\mathrm{i}\gamma}(r)$ being the Bessel function of imaginary argument and imaginary order. Using equation (3.4.20), the expected value $\mathsf{E}\big[\sin 2\Theta(t)\big]$ is given by

$$\mathsf{E}\big[\sin 2\Theta(t)\big] = F_I(\gamma, r), \tag{3.4.23}$$

where

$$F_I(\gamma, r) = \frac{1}{2}\frac{\mathrm{d}}{\mathrm{d}r}\big[\log I_{\mathrm{i}\gamma}(r) + \log I_{-\mathrm{i}\gamma}(r)\big],$$

which can be written as, by making use of the property of the Bessel function,

$$F_I(\gamma, r) = \frac{1}{2}\left[\frac{I_{1+\mathrm{i}\gamma}(r)}{I_{\mathrm{i}\gamma}(r)} + \frac{I_{1-\mathrm{i}\gamma}(r)}{I_{-\mathrm{i}\gamma}(r)}\right].$$

Hence the Lyapunov exponent given by equation (3.4.18) becomes

$$\lambda = \frac{1}{4}\varepsilon\zeta\omega F_I(\gamma, r) - \varepsilon\hat{\beta}. \tag{3.4.24}$$

The stability boundary, which corresponds to $\lambda = 0$, is given by

$$\frac{1}{4}\varepsilon\zeta\omega F_I(\gamma, r) = \varepsilon\hat{\beta}. \tag{3.4.25}$$

Depending on the relations among the parameters γ, r, and unity, various asymptotic expansions of the Bessel functions involved in $F_I(\gamma, r)$ can be employed to simplify equation (3.4.24). For example, when the noise amplitude $\varepsilon^{1/2}\sigma \ll 1$ is so small that $\gamma \gg 1$ and $r > \gamma$, one can obtain

$$\lambda = \frac{1}{4}\varepsilon\zeta\omega\sqrt{1 - \left(\frac{4\hat{\Delta}}{\zeta\omega}\right)^2} - \frac{\varepsilon\sigma^2}{8\left[1 - \left(\frac{4\hat{\Delta}}{\zeta\omega}\right)^2\right]} - \varepsilon\hat{\beta}. \tag{3.4.26}$$

When $\sigma = 0$, i.e., the excitation is purely harmonic, the Lyapunov exponent is

$$\lambda = \frac{1}{4}\varepsilon\zeta\omega\sqrt{1 - \left(\frac{4\hat{\Delta}}{\zeta\omega}\right)^2} - \varepsilon\hat{\beta}. \tag{3.4.27}$$

When $\hat{\Delta} = 0$, i.e., the excitation frequency $\nu = 2\omega - \varepsilon\omega\mathcal{H}^c(\frac{\nu}{2})$, the asymptotic result is

$$\lambda = \frac{1}{4}\varepsilon\zeta\omega - \frac{\varepsilon\sigma^2}{8} - \varepsilon\hat{\beta}. \tag{3.4.28}$$

3.4.2 Numerical Determination of Lyapunov Exponents

In order to assess the accuracy of the approximate analytical result of (3.4.24) of the Lyapunov exponent, numerical determination of the Lyapunov exponent of the original fractional viscoelastic system (3.1.8) is performed, by using the method in Section 2.2.

Letting

$$q_1(t) = q(t), \quad q_2(t) = \dot{q}(t), \quad q_3(t) = \nu t + \varepsilon^{1/2}\sigma W(t) + \theta, \quad Q(t) = {}^{\mathrm{RL}}_{\ 0}\mathcal{D}^{\mu}_{t}[q(t)], \tag{3.4.29}$$

the equation of motion (3.1.8) can be written as a three-dimensional system

$$\dot{q}_1(t)=q_2,\quad \dot{q}_2(t)=-2\varepsilon\beta q_2-\omega^2\big[\big(1+\varepsilon\zeta\,\cos q_3\big)q_1+\varepsilon\tau_\varepsilon Q\big],\quad \dot{q}_3(t)=\nu+\varepsilon^{1/2}\sigma\,\dot{W}(t). \tag{3.4.30}$$

These equations can be discretized using the Euler scheme:

$$\begin{aligned} q_1^{k+1}&=q_1^k+q_2^k\cdot\Delta t,\\ q_2^{k+1}&=q_2^k-\Big\{2\varepsilon\beta q_2^k+\omega^2\big[\big(1+\varepsilon\zeta\,\cos q_s^k\big)q_1^k+\varepsilon\tau_\varepsilon Q^k\big]\Big\}\cdot\Delta t,\\ q_3^{k+1}&=q_3^k+\nu\cdot\Delta t+\varepsilon^{1/2}\sigma\cdot\Delta W^k,\\ Q^k&=\frac{1}{h^\mu}\sum_{j=1}^{n+1}\omega_j q_1^j. \end{aligned} \tag{3.4.31}$$

After the discretization, a time series of the response variable $q(t)$ can be obtained.

3.4.3 Results and Discussion

Consider two special cases first. From the equation of motion (3.1.8), suppose $\tau_\varepsilon=0$ and $\sigma=0$, it becomes the damped Mathieu equation. If further $\beta=0$ is assumed, the equation of motion reduces to undamped Mathieu equation.

From equation (3.4.27), the boundary for the case of $\sigma=0$, $\beta=0$, $\tau_\varepsilon=0$ is

$$\varepsilon\,\frac{\zeta}{2}=\left|1-\frac{\nu}{2\omega}\right|, \tag{3.4.32}$$

which is the same as the first-order approximation of the boundary for the undamped Mathieu equation obtained in equation (2.4.11) of Xie (2006). However, if damping is considered, the equation of motion in equation (3.1.8) becomes the damped Mathieu equation. Substituting equation (3.4.9) and $\Delta=\frac{1}{\varepsilon}\big[\omega-\frac{1}{2}\nu\big]$ into (3.4.27) leads to the stability boundaries

$$\left(1-\frac{\nu}{2\omega}\right)^2=\varepsilon^2\left(\frac{\zeta^2}{16}-\frac{\beta^2}{\omega^2}\right), \tag{3.4.33}$$

which is similar to the first-order approximation of the boundary for the damped Mathieu equation in the vicinity of $\nu=2\omega$ (Xie, 2006). This is due to that when the intensity σ approaches 0, the bounded noise becomes a sinusoidal function.

Consider the effect of bounded noises on system stability. From equation (3.4.28), it is found that, by introducing noise ($\sigma \neq 0$) in the system, stability of the viscoelastic system is improved in the vicinity of $\hat{\Delta} = 0$, because the term containing σ is negative. This result is also confirmed by Figure 3.15, where in the resonant region, with the increase of noise intensity $\varepsilon^{1/2}\sigma$, the unstable area of the system dwindles down and so becomes more stable. One probable explanation is that, from the power spectrum density function of bounded noise, the larger the value of σ, the wider the frequency band of the power spectrum of the bounded noise, as shown in Figure 1.4. When σ approaches infinite, the bounded noise becomes a white noise. As a result, the power of the noise is not concentrated in the neighborhood of the central frequency ν, which reduces the effect of the primary parametric resonance.

The effect of noise amplitude ζ on Lyapunov exponents is shown in Figure 3.16. The results of two noise intensities, $\varepsilon^{1/2}\sigma = 0.8$ and 0.2, are compared for various values of ζ. It is seen that, in the resonant region, increasing the noise amplitude ζ destabilizes the system. The maximum resonant point is not exactly at $\nu = 2\omega$, but in the neighborhood of $\nu = 2\omega$. This may be partly due to the viscoelasticity, partly due to the noise.

In the numerical simulation of Lyapunov exponents, the embedding dimension is $m = 50$, the reconstruction delay $J = 30$, the number of data points is $N = 20000$, and the time step is $\Delta t = 0.01$, which yields the total time period $T = N\Delta t = 200$. Typical results are shown in Figure 3.17 along with the approximate analytical results. It is found that the approximate analytical result in equation (3.4.24) agrees with the numerical result very well.

Finally, consider the effect of viscosity and damping on system stability. The fractional order μ of the system has a stabilizing effect, which is illustrated in Figure 3.18. This is due to the fact that when μ changes from 0 to 1, the property of the material moves from totally elasticity to viscosity, as shown in Figure 1.6. The same stabilizing effect of damping on stability is shown in Figure 3.19.

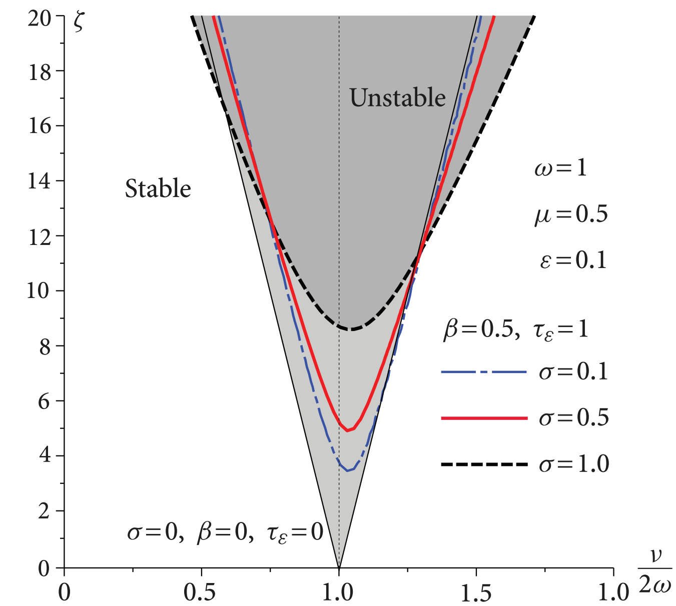

Figure 3.15 Stability boundaries of the viscoelastic system under bounded noise

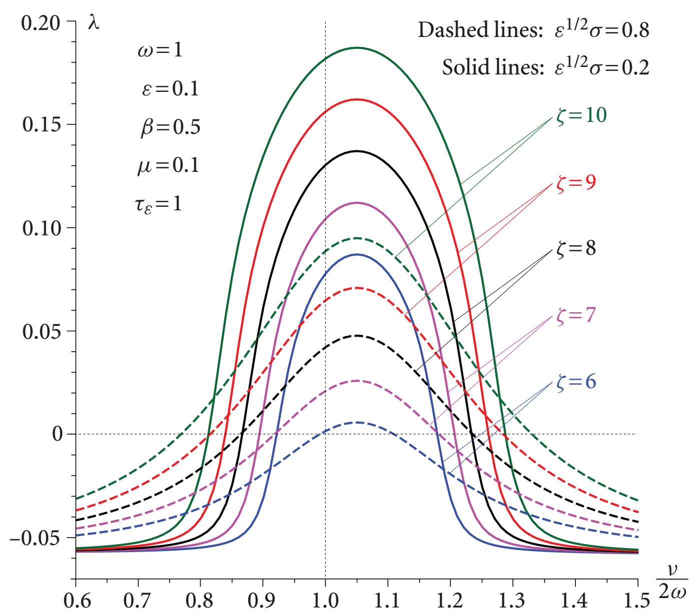

Figure 3.16 Lyapunov exponents of a viscoelastic system under bounded noise

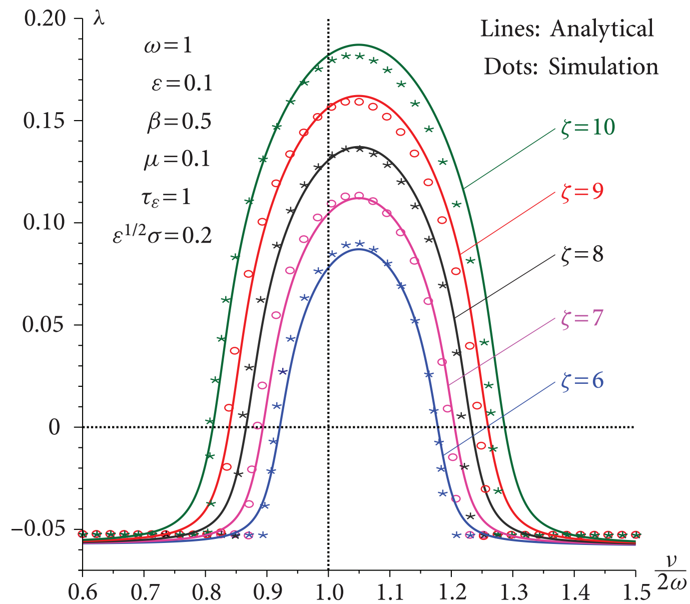

Figure 3.17 Lyapunov exponents of SDOF viscoelastic system

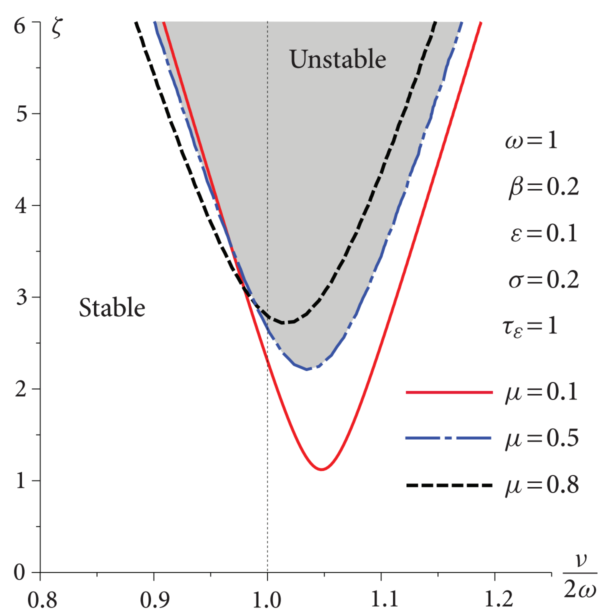

Figure 3.18 Effect of fractional order μ on system stability under bounded noise

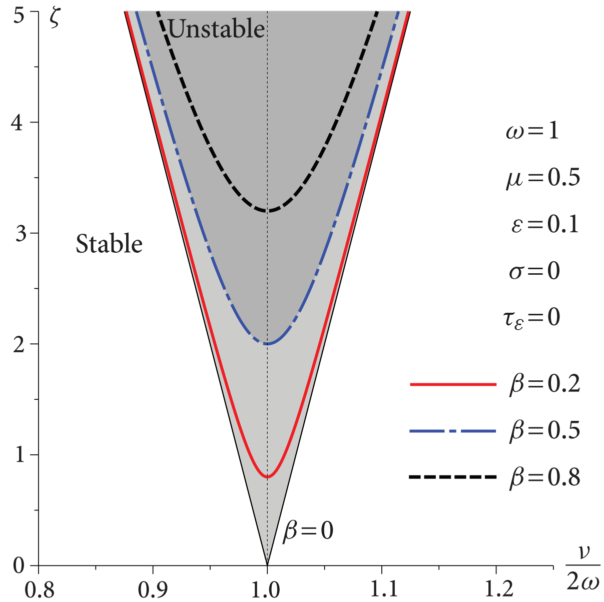

Figure 3.19 Effect of damping on stability boundaries under bounded noise

3.5 Moment Lyapunov Exponents of Fractional Systems under Bounded Noise Excitation

In Section 3.4, analytical Lyapunov exponents are obtained for fractional systems under bounded noise excitation. This section is devoted to determine moment Lyapunov exponents of the same systems under bounded noise excitation.

3.5.1 First-Order Stochastic Averaging

Substituting $P = a^p$, i.e., the pth norm of system (3.1.8), into equation (3.4.8) yields

$$\begin{aligned} \dot{P}(t) &= \varepsilon p P\Big[-\hat{\beta} + \frac{1}{4}\zeta\omega\sin(2\varphi-\psi)\Big], \\ \dot{\varphi}(t) &= \varepsilon\Big[\hat{\Delta} + \frac{1}{4}\zeta\omega\cos(2\varphi-\psi)\Big], \end{aligned} \tag{3.5.1}$$

where $\hat{\beta}$ and $\hat{\Delta}$ are given in equations (3.4.9).

Applying the transformation

$$\Theta(t) = \varphi(t) - \frac{1}{2}\psi(t), \quad \psi(t) = \varepsilon^{1/2}\sigma W(t) + \theta, \tag{3.5.2}$$

and using the Itô's Lemma, one can obtain three Itô stochastic differential equations

$$\mathrm{d}P(t)=m_pP\mathrm{d}t,\quad \mathrm{d}\Theta(t)=m_\Theta\,\mathrm{d}t-\varepsilon^{1/2}\frac{\sigma}{2}\mathrm{d}W(t),\quad \mathrm{d}\psi(t)=\varepsilon^{1/2}\sigma\,\mathrm{d}W(t),\tag{3.5.3}$$

where

$$m_p=\varepsilon p\Big(-\hat{\beta}+\frac{1}{4}\zeta\omega\sin 2\Theta\Big),\quad m_\Theta=\varepsilon\Big(\hat{\Delta}+\frac{1}{4}\zeta\omega\cos 2\Theta\Big).\tag{3.5.4}$$

It is observed that equations (3.5.3) are coupled, so directly solving these SDEs are very difficult. The eigenvalue problem governing the pth moment Lyapunov exponent can be formulated from these SDEs. To this purpose, applying a linear stochastic transformation

$$S=T(\Theta)P,\quad P=T^{-1}(\Theta)S,\qquad 0\leqslant\Theta\leqslant\pi,\tag{3.5.5}$$

the Itô equation for the transformed pth norm process S is given by, again using Itô Lemma in the vector case,

$$\begin{aligned}\mathrm{d}S&=\Big(m_pT+m_\Theta T'+\frac{\varepsilon\sigma^2}{8}T''\Big)P\mathrm{d}t-\frac{\varepsilon^{1/2}\sigma}{2}T'P\mathrm{d}W(t)\\&=\frac{1}{T}\Big(m_pT+m_\Theta T'+\frac{\varepsilon\sigma^2}{8}T''\Big)S\mathrm{d}t-\frac{\varepsilon^{1/2}\sigma}{2}\frac{T'}{T}S\mathrm{d}W(t),\end{aligned}\tag{3.5.6}$$

where T' and T'' are the first-order and second-order derivatives of $T(\Theta)$ with respect to Θ, respectively. For bounded and non-singular transformation $T(\Theta)$, both processes P and S are expected to have the same stability behaviour, as equation (3.5.5) is a linear transformation. Therefore, $T(\Theta)$ is chosen so that the drift term of the Itô equation (3.5.6) is independent of Θ, i.e.,

$$\frac{1}{T}\Big(m_pT+m_\Theta T'+\frac{\varepsilon\sigma^2}{8}T''\Big)=\Lambda,$$

so that

$$\mathrm{d}S=\Lambda S\mathrm{d}t+\sigma_S\mathrm{d}W(t).\tag{3.5.7}$$

Comparing the drift terms in equations (3.5.6) and (3.5.7), such a transformation $T(\Theta)$ is given by the following differential equation

$$\frac{\sigma^2}{8}T''+m_{\Theta1}T'+m_{p1}T=\hat{\Lambda}T,\tag{3.5.8}$$

where

$$m_{\Theta1}=\frac{m_{\Theta1}}{\varepsilon}=\hat{\Delta}+\frac{1}{4}\zeta\omega\cos 2\Theta,\quad m_{p1}=\frac{m_{p1}}{\varepsilon}=p\Big(-\hat{\beta}+\frac{1}{4}\zeta\omega\sin 2\Theta\Big).\tag{3.5.9}$$

$T(\Theta)$ is a periodic function in Θ of period π, and $\Lambda_{q(t)}(p) = \Lambda(p) = \varepsilon\hat{\Lambda}(p)$. Equation (3.5.8) defines an eigenvalue problem for a second-order differential operator with $\hat{\Lambda}(p)$ being the eigenvalue and $T(\Theta)$ the associated eigenfunction.

Taking the expected value of equation (3.5.7) leads to $\mathrm{dE}[S] = \Lambda \mathrm{E}[S]\,\mathrm{d}t$, from which it can be seen that Λ is the Lyapunov exponent of the transformed pth moment $\mathrm{E}[S]$ of equation (3.5.3) or (3.1.8). Since both processes P and S have the same stability behaviour, Λ is the Lyapunov exponent of pth moment $\mathrm{E}[P]$. The remaining task for determining the moment Lyapunov exponents is to solve the eigenvalue problem.

Determination of Moment Lyapunov Exponents

Even though the original problem in equation (3.1.8) has been transformed to an eigenvalue problem, it is difficult, if not possible, to analytically solve the eigenvalue problem. To make things worse, although the small term ε appears in system equation (3.4.6), it does not appear in the eigenvalue problem (3.5.8). Hence, the method of perturbation cannot be applied and the difficulty in solving equation (3.5.8) analytically is increased significantly.

Since the coefficients in (3.5.8) are periodic with period π, it is reasonable to consider a Fourier series expansion of the eigenfunction $T(\Theta)$ in the form

$$T(\Theta) = C_0 + \sum_{k=1}^{K} (C_k \cos 2k\Theta + S_k \sin 2k\Theta). \tag{3.5.10}$$

To solve equation (3.5.8), substituting the expansion into eigenvalue problem (3.5.8) and equating the coefficients of like trigonometric terms $\sin 2k\Theta$ and $\cos 2k\Theta$, $k = 0, 1, \cdots, K$ yield a set of homogeneous linear algebraic equations with infinitely many equations for the unknown coefficients C_0, C_k and S_k,

$$\begin{aligned}
\text{Constant}: &\quad -(c_0 + \hat{\Lambda})C_0 + b_0 S_1 = 0,\\
\cos 2\Theta: &\quad -(c_1 + \hat{\Lambda})C_1 + d_1 S_1 + b_1 S_2 = 0,\\
\sin 2\Theta: &\quad 2a_1 C_0 + d_1 C_1 + b_1 C_2 + (c_1 + \hat{\Lambda})S_1 = 0,\\
\cos 2k\Theta: &\quad a_k S_{k-1} + d_k S_k + b_k S_{k+1} - (c_k + \hat{\Lambda})C_k = 0,\\
\sin 2k\Theta: &\quad a_k C_{k-1} + d_k C_k + b_k C_{k+1} + (c_k + \hat{\Lambda})S_k = 0,
\end{aligned}$$

$$\begin{aligned} \cos 2K\Theta: &\quad a_K S_{K-1} + d_K S_K - (c_K + \hat{\Lambda}) C_K = 0, \\ \sin 2K\Theta: &\quad a_K C_{K-1} + d_K C_K + (c_K + \hat{\Lambda}) S_K = 0, \end{aligned} \tag{3.5.11}$$

where

$$\begin{aligned} &k = 2,\, 3, \cdots,\, K-1, \\ &a_n = \frac{1}{8}\zeta\omega(2n-2-p), \quad b_n = \frac{1}{8}\zeta\omega(2n+2+p), \\ &c_n = \frac{1}{2}\sigma^2 n^2 + p\hat{\beta}, \quad d_n = 2n\hat{\Delta}, \quad n = 0,\, 1,\, 2, \cdots,\, K. \end{aligned}$$

To have a non-trivial solution of the C_0, C_k and S_k, it is required that the determinant of the coefficient matrix of equation (3.5.11) equal zero to yield a polynomial equation of degree $2K+1$ for $\hat{\Lambda}^{(K)}(p)$,

$$e_{2K+1}^{(K)}[\hat{\Lambda}^{(K)}]^{2K+1} + e_{2K}^{(K)}[\hat{\Lambda}^{(K)}]^{2K} + \cdots + e_1^{(K)}\hat{\Lambda}^{(K)} + e_0^{(K)} = 0, \tag{3.5.12}$$

where $\hat{\Lambda}^{(K)}$ denotes the approximate moment Lyapunov exponent. Then, one may approximate the moment Lyapunov exponent of the system by

$$\Lambda_{q(t)}(p) \approx \varepsilon \hat{\Lambda}^{(K)}(p). \tag{3.5.13}$$

For $K=1$, equation (3.5.12) reduces to a cubic equation with

$$\begin{aligned} &e_3^{(1)} = 1, \quad e_2^{(1)} = \sigma^2 + 3p\hat{\beta}, \\ &e_1^{(1)} = 4\hat{\Delta}^2 + \frac{\sigma^4}{4} - \frac{1}{32}\zeta^2\omega^2 p(p+2) + 3\hat{\beta}^2 p^2 + 2\sigma^2\hat{\beta}p, \\ &e_0^{(1)} = \hat{\beta}^3 p^3 + \sigma^2\hat{\beta}^2 p^2 + p\hat{\beta}\Big[4\hat{\Delta}^2 + \frac{\sigma^4}{4} - \frac{1}{32}\zeta^2\omega^2 p(p+2)\Big] - \frac{1}{64}\zeta^2\omega^2\sigma^2 p(p+2), \end{aligned}$$

and an approximate expression of the moment Lyapunov exponent is given by

$$\begin{aligned} &\hat{\Lambda}^{(1)}(p) = \frac{A_2}{6} - \frac{2\left(3e_1 - e_2^2\right)}{3A_2} - \frac{e_2}{3}, \\ &A_2 = \left(12A_1 - 108e_0 + 36e_1e_2 - 8e_2^3\right)^{1/3}, \\ &A_1 = \left(81e_0^2 + 12e_1^3 - 54e_0e_1e_2 + 12e_0e_2^3 - 3e_1^2e_2^2\right)^{1/2}, \end{aligned} \tag{3.5.14}$$

in which the superscript "(1)" in the coefficients e's is dropped for clarity of presentation. When $K>1$, there are no analytical solutions for the polynomial equation (3.5.12) and numerical approaches must be applied to solve it.

3.5.2 Second-Order Stochastic Averaging

Substituting $P=a^p$, i.e., the pth norm of system (3.1.8),into the transformed equation of motion in Eq. (3.4.5) yields

$$\dot{P}(t) = \varepsilon f_1(P,\varphi,t), \quad \dot{\varphi}(t) = \varepsilon f_2(P,\varphi,t), \quad \dot{\psi}(t) = \varepsilon^{1/2}\sigma \dot{W}(t), \tag{3.5.15}$$

where

$$\begin{aligned} f_1(P,\varphi,t) &= -pP\Big\{\beta\big[1-\cos 2\Phi(t)\big] - \frac{\zeta\omega}{2}\cos\big[\nu t+\psi(t)\big]\sin 2\Phi + \omega\tau_\varepsilon I^{sc}\Big\}, \\ f_2(P,\varphi,t) &= \Delta - \beta\sin 2\Phi + \omega\zeta\cos\big[\nu t+\psi(t)\big]\cos^2\Phi + \omega\tau_\varepsilon I^{cc}. \end{aligned} \tag{3.5.16}$$

To formulate a second-order stochastic averaging, the near-identity transformation in equation (3.3.29) is introduced and the same steps in Section 3.3.2 is followed. Then three Itô stochastic differential equations can be obtained

$$\begin{aligned} \mathrm{d}P(t) &= \big(\varepsilon m_{p1} + \varepsilon^2 m_{p2}\big)P\mathrm{d}t, \\ \mathrm{d}\Theta(t) &= \big(\varepsilon m_{\Theta 1} + \varepsilon^2 m_{\Theta 2}\big)\mathrm{d}t - \varepsilon^{1/2}\frac{\sigma}{2}\mathrm{d}W(t), \\ \mathrm{d}\psi(t) &= \varepsilon^{1/2}\sigma\,\mathrm{d}W(t), \end{aligned} \tag{3.5.17}$$

where

$$\begin{aligned} m_{p2} &= -\frac{p\zeta\omega}{2\nu}\big(\hat{\beta}\cos 2\Theta - \hat{\alpha}\sin 2\Theta\big), \quad m_{\Theta 2} = \frac{1}{2\nu}\big(\zeta\omega\hat{\alpha}\cos 2\Theta + \hat{\beta}\omega\zeta\sin 2\Theta + \hat{\delta}\big), \\ \hat{\alpha} &= -\frac{1}{2}\omega\tau_\varepsilon \mathcal{H}^s\big(\frac{\nu}{2}\big), \\ \hat{\delta} &= -\Big\{\frac{1}{16}\omega^2\zeta^2 + \frac{1}{2}\omega^2\big[\mathcal{H}^c\big(\frac{\nu}{2}\big)\big]^2 + \frac{1}{2}\omega^2\big[\mathcal{H}^s\big(\frac{\nu}{2}\big)\big]^2 + 2\omega\beta\mathcal{H}^s\big(\frac{\nu}{2}\big) + 2\beta^2\Big\}. \end{aligned} \tag{3.5.18}$$

It is observed that Eq. (3.5.17) are coupled. Introducing a linear stochastic transformation in (3.5.5), the Itô equation for the transformed pth norm process S is given by

$$\begin{aligned} \mathrm{d}S &= \Big[\big(\varepsilon m_{p1} + \varepsilon^2 m_{p2}\big)T + \big(\varepsilon m_{\Theta 1} + \varepsilon^2 m_{\Theta 2}\big)T_\Theta + \frac{\varepsilon\sigma^2}{8}T_{\Theta\Theta}\Big]P\mathrm{d}t - \frac{\varepsilon^{1/2}\sigma}{2}T_\Theta P\mathrm{d}W(t) \\ &= \frac{1}{T}\Big[\big(\varepsilon m_{p1} + \varepsilon^2 m_{p2}\big)T + \big(\varepsilon m_{\Theta 1} + \varepsilon^2 m_{\Theta 2}\big)T_\Theta + \frac{\varepsilon\sigma^2}{8}T_{\Theta\Theta}\Big]S\mathrm{d}t - \frac{\varepsilon^{1/2}\sigma}{2}\frac{T_\Theta}{T}S\mathrm{d}W(t). \end{aligned} \tag{3.5.19}$$

The eigenvalue problem governing the pth moment Lyapunov exponent can be obtained as

$$\frac{\sigma^2}{8}T''+\left(m_{\Theta 1}+\boxed{\varepsilon m_{\Theta 2}}\right)T'+\left(m_{p1}+\boxed{\varepsilon m_{p2}}\right)T=\hat{\Lambda}T, \tag{3.5.20}$$

and $T(\Theta)$ is a periodic function in Θ of period π, and $\Lambda_{q(t)}(p)=\Lambda(p)\approx\varepsilon\hat{\Lambda}(p)$. Similarly, the eigenvalue problem can be solved by Fourier series expansion.

3.5.3 Higher-Order Stochastic Averaging

Following the same procedure in Section 3.3.3, one can obtained three Itô stochastic differential equations

$$\begin{aligned}
\mathrm{d}P(t) &= \left(\varepsilon m_{p1}+\varepsilon^2 m_{p2}+\varepsilon^3 m_{p3}\right)P\,\mathrm{d}t,\\
\mathrm{d}\Theta(t) &= \left(\varepsilon m_{\Theta 1}+\varepsilon^2 m_{\Theta 2}+\varepsilon^3 m_{\Theta 3}\right)\mathrm{d}t-\varepsilon^{1/2}\frac{\sigma}{2}\,\mathrm{d}W(t),\\
\mathrm{d}\psi(t) &= \varepsilon^{1/2}\sigma\,\mathrm{d}W(t),
\end{aligned} \tag{3.5.21}$$

where

$$\begin{aligned}
m_{p3} &= \frac{p\zeta\omega}{256\nu^2}\left(\hat{\gamma}\sin 2\Theta-128\hat{\alpha}\hat{\beta}\cos 2\Theta\right),\\
m_{\Theta 3} &= \frac{-\zeta\omega}{256\nu^2}\left(\hat{\gamma}\cos 2\Theta+128\hat{\alpha}\hat{\beta}\sin 2\Theta-\hat{\lambda}\right),\\
\hat{\gamma} &= 7\omega^2\zeta^2-128\hat{\alpha}^2,\\
\hat{\lambda} &= 128\omega\tau_\varepsilon\hat{\Delta}\left\{\omega\tau_\varepsilon\left[\mathcal{H}^c\left(\frac{\nu}{2}\right)\right]^2+4\beta\mathcal{H}^c\left(\frac{\nu}{2}\right)+\omega\tau_\varepsilon\left[\mathcal{H}^s\left(\frac{\nu}{2}\right)\right]^2\right\}\\
&\quad -8\hat{\alpha}\left(64\beta^2-3\omega^2\zeta^2\right)+8\Delta\left(64\beta^2+\omega^2\zeta^2\right).
\end{aligned} \tag{3.5.22}$$

The eigenvalue problem governing the pth moment Lyapunov exponent is

$$\frac{\sigma^2}{8}T''+\left(m_{\Theta 1}+\boxed{\varepsilon m_{\Theta 2}}+\varepsilon^2 m_{\Theta 3}\right)T'+\left(m_{p1}+\boxed{\varepsilon m_{p2}}+\varepsilon^2 m_{p3}\right)T=\hat{\Lambda}T. \tag{3.5.23}$$

Similarly, the eigenvalue problem can be solved by Fourier series expansion.

3.5.4 Results and Discussion

The moment Lyapunov exponent is the nontrivial solution of the equations (3.5.12), where the Fourier series expansion for $T(\Theta)$ is truncated to 4th order ($K=4$). The approximate moment Lyapunov exponents are compared in Figure 3.20 with the numerical results by using the method of Section 2.2. It shows that the two results agree well, although discrepancy is found when p is large. In the numerical calculation of the moment Lyapunov exponents, the embedding dimension is $m=50$, the reconstruction delay $J=40$, the number of data points is $N=5000$, the sample size for simulation is $S=1000$, and the time step is $\Delta t=0.01$, which yields the total time period $T=N\Delta t=50$.

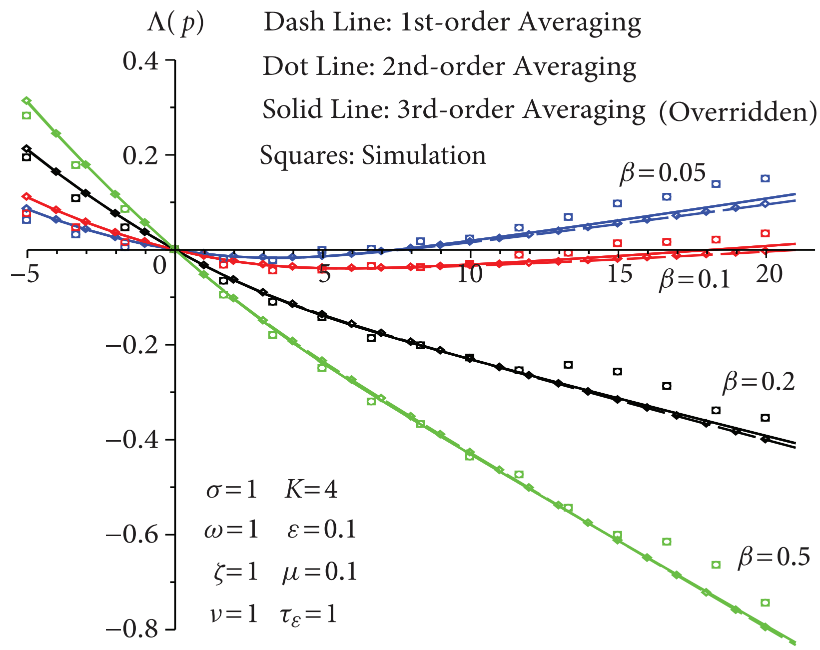

Figure 3.20 Comparison of simulation and approximation results for SDOF system under bounded noises

Figures 3.20 and 3.21 illustrate that there is some difference between first-order and higher-order averaging. However, the third-order averaging is almost identical to the second-order averaging, which suggests that for viscoelastic structures, second-order averaging analysis is adequate.

Figure 3.21 shows that with the increase of the noise intensity parameter σ, the stability of the system increases. One probable explanation is that from the power spectrum density function of bounded noise in equation (1.2.8), the larger the value of σ, the wider the frequency band of power spectrum, which suggests that the power of the noise not be concentrated in the neighborhood of the central frequency ν, which reduces the effect of the primary parametric resonance. Three-dimensionally, Figures 3.22 and 3.23 show that the smaller the noise intensity σ, the more significant the parametric resonance. Parametric resonance in terms of Lyapunov exponents can be found in Figure 3.24 when the noise intensity σ is small. This numerical observation is also confirmed by analytical results in Figure 3.16.

Effect of noise amplitude (ζ) on moment Lyapunov exponents is shown in Figure 3.25, which indicates the de-stabilizing effect of noise amplitude on the system stability. Great effect of ζ on parametric resonance is observed in Figure 3.26. Larger amplitude would result in prominent parametric resonance. This result agrees with the analytical analysis in Figure 3.17, where stability is expressed by Lyapunov exponents.

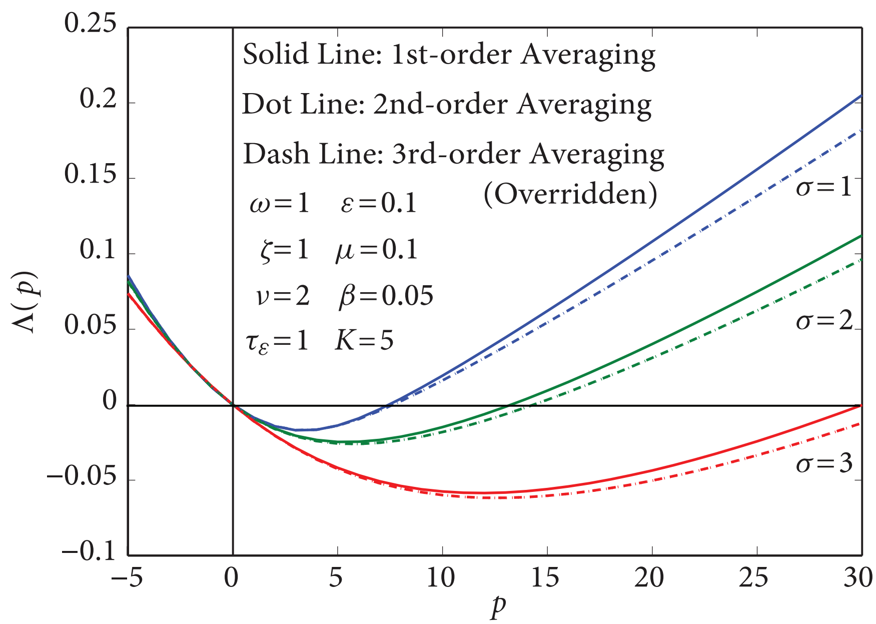

Figure 3.21 Effect of σ of bounded noises on moment Lyapunov exponents of SDOF systems

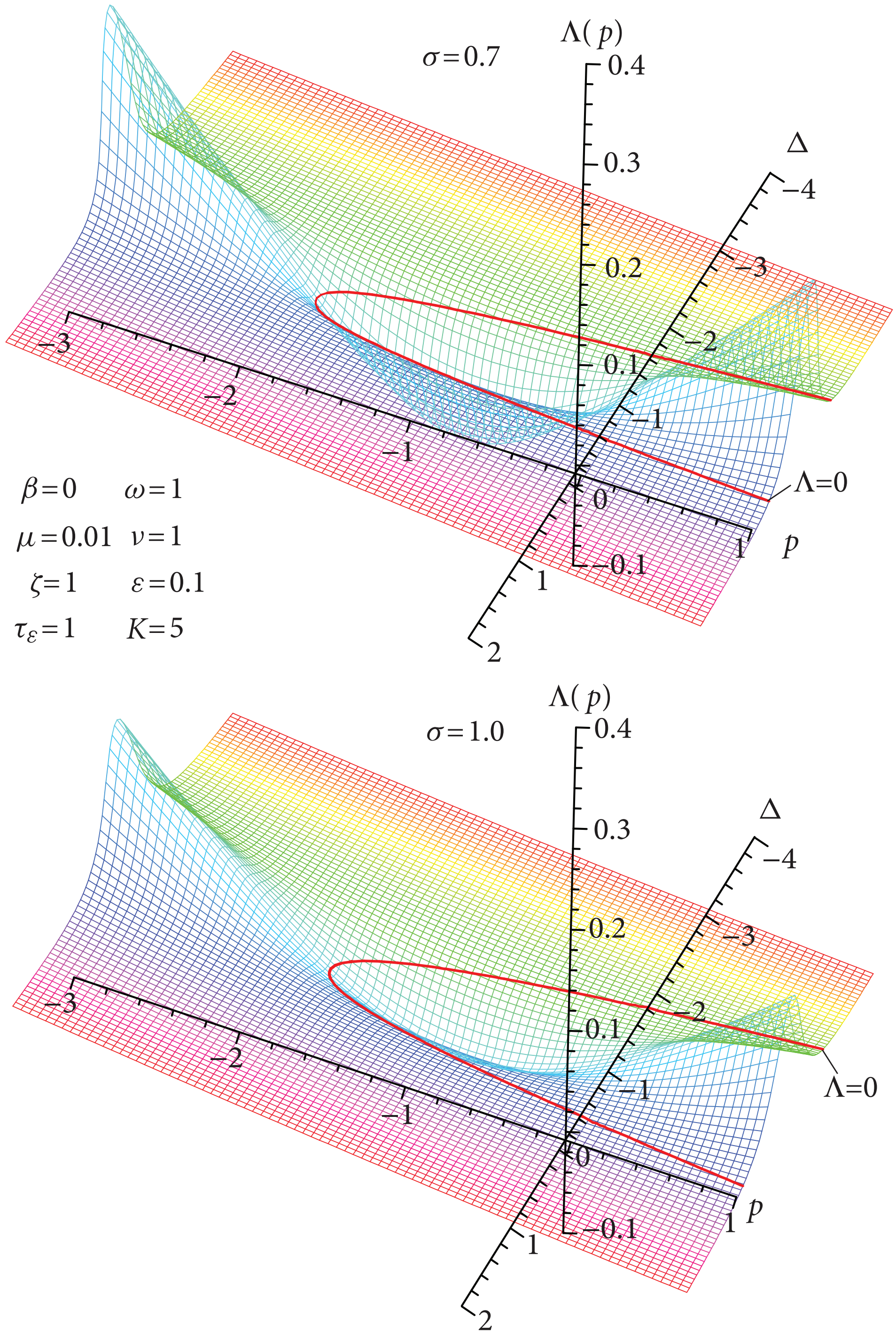

Figure 3.22 Parametric resonance of SDOF fractional viscoelastic system

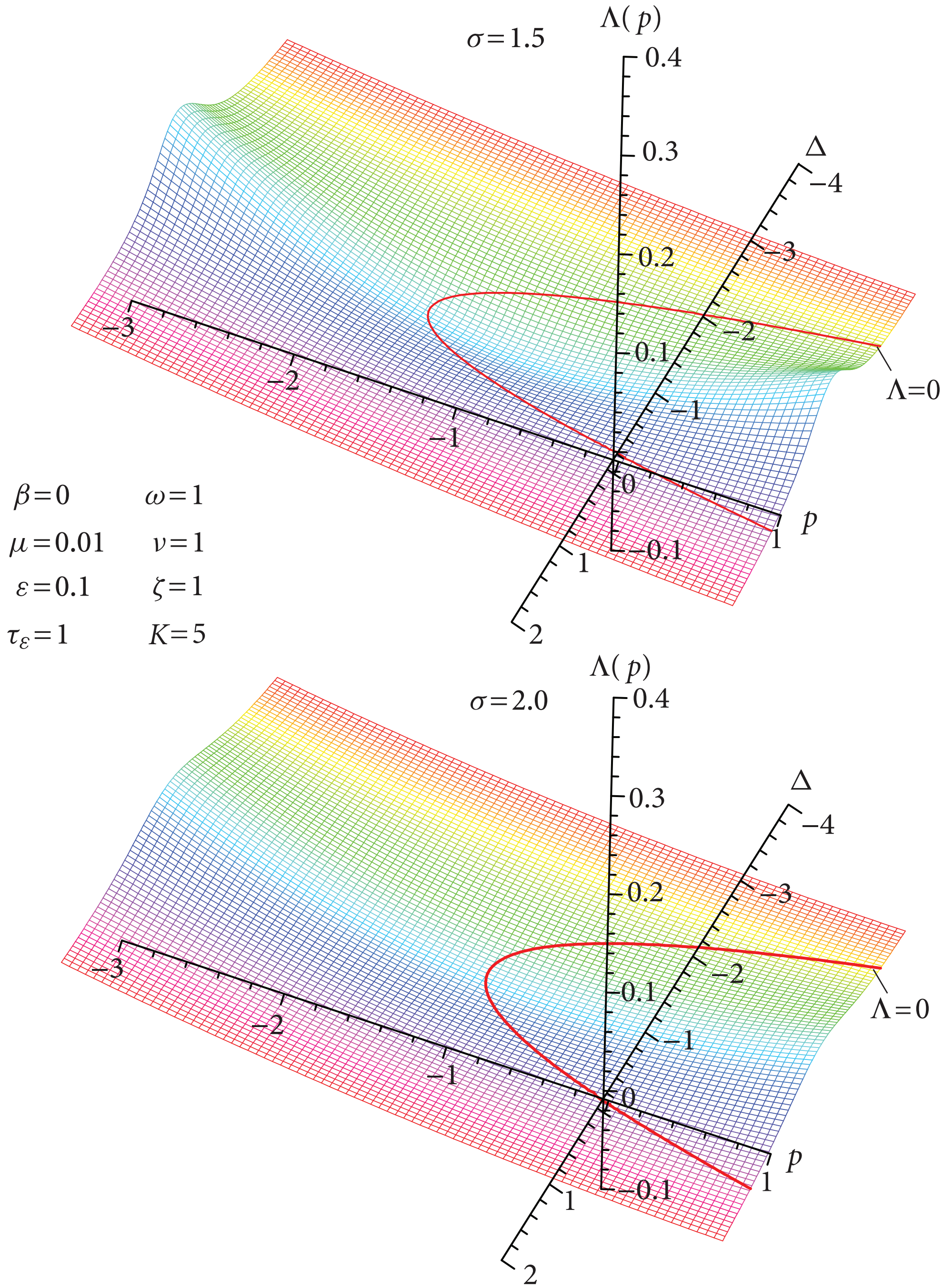

Figure 3.23 Parametric resonance of SDOF fractional viscoelastic system

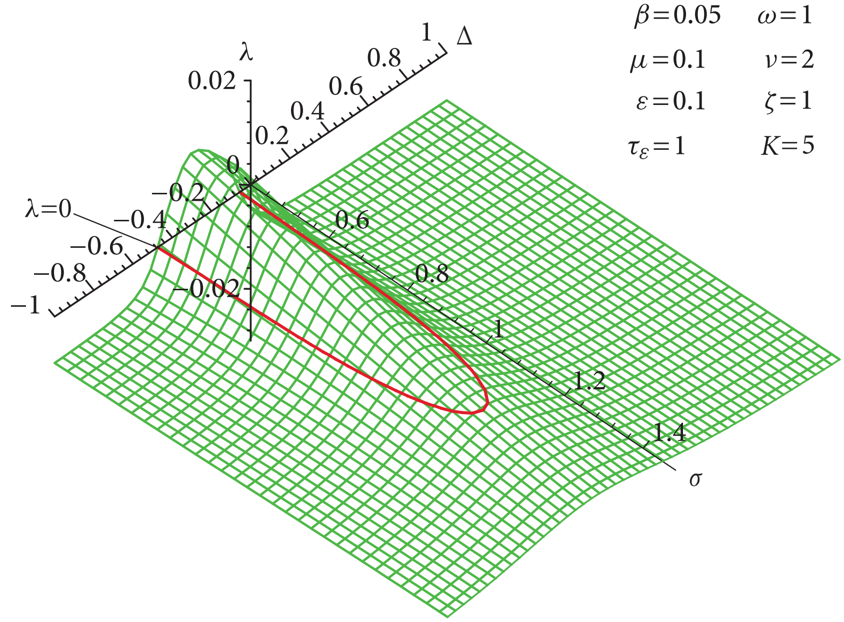

Figure 3.24 Largest Lyapunov exponents of SDOF fractional systems

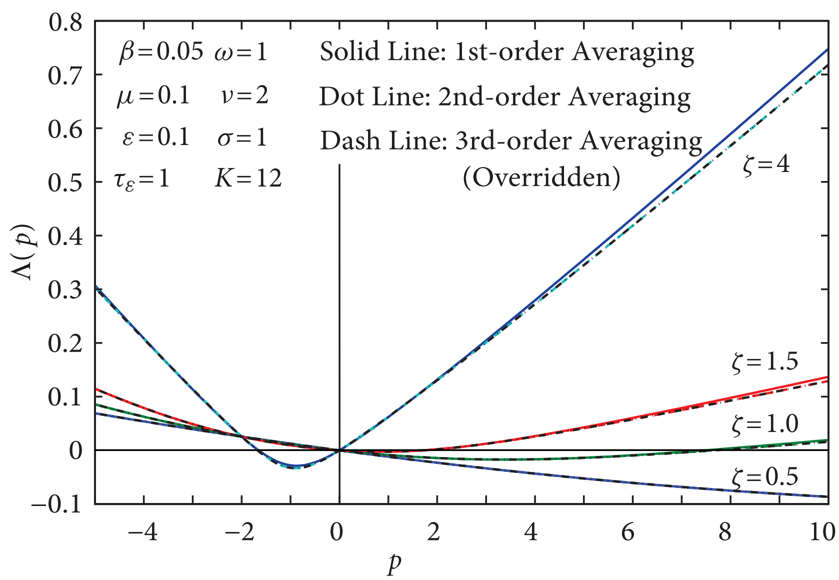

Figure 3.25 Effect of noise amplitude ζ of bounded noises on moment Lyapunov exponents of SDOF systems

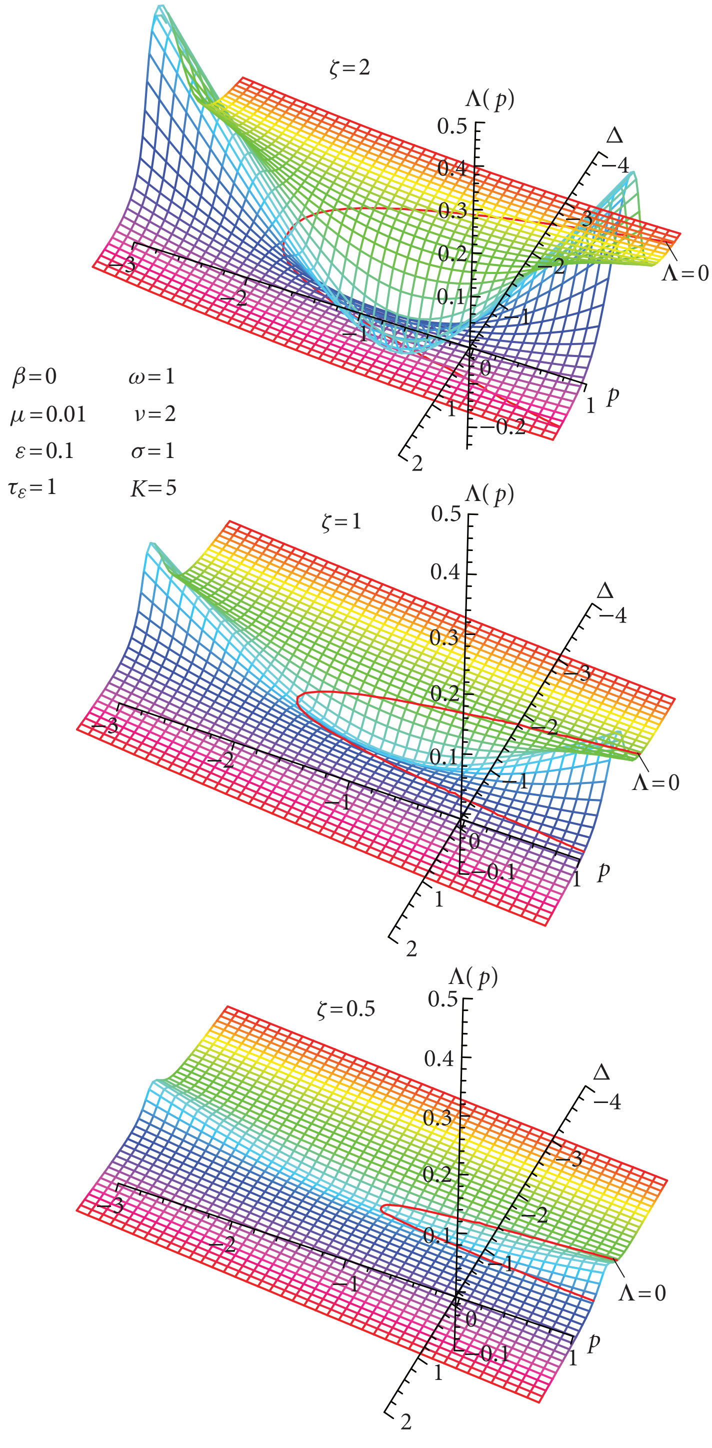

Figure 3.26 Parametric resonance of SDOF fractional viscoelastic system

3.6 Summary

The stochastic stability of a single-degree-of-freedom linear viscoelastic system under the excitation of a wide-band noise and bounded noise is investigated by using the method of higher-order stochastic averaging. The viscoelastic material is assumed to follow the fractional Kelvin-Voigt constitutive relation, which is capable of modelling hereditary property with long memory. A practical example of such a system is the transverse vibration of a viscoelastic column under the excitation of stochastic axial compressive load.

Higher-order stochastic averaging is able to capture the influence of such weak nonlinearities as integral stiffness nonlinearities, cubic inertia and stiffness nonlinearities, which were lost in the first-order averaging procedure. The first-order stochastic averaging distinguishes the slow and the fast motion in ε-terms; the second-order averaging allows separation of ε and ε^2-terms, which is highlighted in frame boxes; while the third-order averaging accommodates the ε^3-terms highlighted in grey boxes, together with ε and ε^2-terms.

Since a Riemann-Liouville fractional derivative is involved in the viscoelastic term, the method of stochastic averaging due to Larionov is extended to deal with equations of motion involving Riemann-Liouville fractional derivatives. Then the method of stochastic averaging is used to obtain the averaged equation of motion, from which the approximate Lyapunov exponents are obtained by solving the Fokker-Planck equation. In addition, the Lyapunov exponent can also be determined by Fourier series expansion of an eigenvalue problem, by making use of the relation between moment Lyapunov exponents and Lyapunov exponents.

To obtain a complete picture of the dynamic stability, asymptotic analytical expressions are derived for both the moment Lyapunov exponent and Lyapunov exponent of systems excited by wide-band noises. It is found that, under wide-band noise excitation, the parameters of damping β, the parameter of retardation τ_ε, real noise parameter α, and the model fractional order μ have stabilizing effects on the moment stability. However, the white and real noise intensity factor σ and the elastic modulus E destabilizes the system.

Moment Lyapunov exponent and Lyapunov exponent of systems under bounded noises must be obtained by solving an eigenvalue problem. It is seen that, under bounded noise excitation, the parameters of damping β, the noise intensity σ, and the fractional order μ have stabilizing effects on the almost-sure stability. The effects of σ and ζ on parametric resonance are discussed in detail. These results are useful in engineering applications.

In addition to studying system stability, higher-order stochastic averaging should have applications in stochastic response investigation and first passage failure analysis of systems.

C H A P T E R 4

Stochastic Stability of Coupled Non-Gyroscopic Viscoelastic Systems

Section 4.1 deals with coupled non-gyroscopic viscoelastic systems excited by wide-band noises. Moment Lyapunov exponents, stability boundaries, and stability index are determined. Section 4.2 is concerned with coupled non-gyroscopic viscoelastic systems excited by bounded noises. Parametric resonances are studied in detail. Both ordinary viscoelasticity and fractional viscoelasticity are considered, for few literature can be found on moment Lyapunov exponents of coupled viscoelastic systems.

4.1 Coupled Systems Excited by Wide-Band Noises

4.1.1 Formulation

Consider the following coupled system of two-degree-of-freedom

$$\ddot{q}_1+2\varepsilon\beta_1\dot{q}_1+\omega_1^2[1-\varepsilon\mathscr{H}]q_1+\varepsilon^{1/2}\omega_1(k_{11}q_1+k_{12}q_2)\xi(t)=0, \tag{4.1.1a}$$

$$\ddot{q}_2+2\varepsilon\beta_2\dot{q}_2+\omega_2^2[1-\varepsilon\mathscr{H}]q_2+\varepsilon^{1/2}\omega_2(k_{21}q_1+k_{22}q_2)\xi(t)=0, \tag{4.1.1b}$$

where q_1 and q_2 are state coordinates, β_1 and β_2 are damping coefficients, ω_1 and ω_2 are distinct natural frequencies, k_{ij}, i, $j=1$, 2, are constants, in which k_{12} and k_{21} are the so-called coupling parameters. The cases for $k_{12}=k_{21}=k$ and $k_{12}=-k_{21}=k$ are called symmetric coupling and skew-symmetric coupling, respectively. Specifically, a system with

$k=0$ is decoupled. ε is a small parameter showing that the effects of damping, viscoelasticity, and excitation are small. $\mathscr{H}$ is a linear viscoelastic operator given by

$$\mathscr{H}[q(t)]=\int_0^t \mathcal{H}(t-\tau)q(\tau)\mathrm{d}\tau, \quad 0\leqslant\int_0^\infty \mathcal{H}(t)\mathrm{d}t<1, \tag{4.1.2}$$

where $\mathcal{H}(t)$ is the relaxation kernel, of which the simplest form is from ordinary Maxwell model in equation (1.3.18) and is given by $\mathcal{H}(t)=\gamma \mathrm{e}^{-\kappa t}$, where γ and κ are material constants. If fractional Kelvin-Voigt viscoelastic model is considered, equations (4.1.1) becomes

$$\ddot{q}_1+2\varepsilon\beta_1\dot{q}_1+\omega_1^2[1+\varepsilon\, {}^{\mathrm{RL}}_{\;0}\mathcal{D}_t^{\mu}]q_1+\varepsilon^{1/2}\omega_1(k_{11}q_1+k_{12}q_2)\xi(t)=0, \tag{4.1.3a}$$

$$\ddot{q}_2+2\varepsilon\beta_2\dot{q}_2+\omega_2^2[1+\varepsilon\, {}^{\mathrm{RL}}_{\;0}\mathcal{D}_t^{\mu}]q_2+\varepsilon^{1/2}\omega_2(k_{21}q_1+k_{22}q_2)\xi(t)=0. \tag{4.1.3b}$$

From equation (1.3.12), the viscoelastic operator is taken as

$$\mathscr{H}[q(t)]=-\,{}^{\mathrm{RL}}_{\;0}\mathcal{D}_t^{\mu}[q(t)]=\frac{-1}{\Gamma(1-\mu)}\int_0^t \frac{q'(\tau)}{(t-\tau)^{\mu}}\mathrm{d}\tau=\int_0^t \mathcal{H}(t-\tau)q'(\tau)\mathrm{d}\tau, \tag{4.1.4}$$

where the relaxation kernel of fractional Kelvin-Voigt viscoelastic model is given by

$$\mathcal{H}(t)=-\frac{1}{\Gamma(1-\mu)}\frac{1}{t^{\mu}}. \tag{4.1.5}$$

Hence, the fractional equations (4.1.3) are identical to (4.1.1).

It is noted that this chapter only considers coupled viscoelastic oscillators with non-commensurable frequencies perturbed by a small intensity parametric noise process. It may be extended for coupled viscoelastic oscillators with commensurable frequencies. Stochastic stability of two coupled oscillators in resonance has been studied by Namachchivaya *et al.* (2003).

Equations (4.1.1) admit the trivial solution $q_1=q_2=0$. However, they are not the Lagrange standard form given in equation (1.2.27) or (1.2.40). Hence, to apply the averaging method, one should first consider the unperturbed system, i.e., $\varepsilon=0$ and $\xi(t)=0$, which reduces to: $\ddot{q}_i+\omega_i^2 q_i=0$, $i=1, 2$. The solutions for this unperturbed system are found to be

$$q_i=a_i\cos\Phi_i, \quad \dot{q}_i=-\omega_i a_i\sin\Phi_i, \quad \Phi_i=\omega_i t+\phi_i, \quad i=1, 2. \tag{4.1.6}$$

Then the method of variation of parameters is used. Differentiating the first equation of (4.1.6) and comparing with the second equation lead to

$$\dot{a}_i \cos\Phi_i - a_i\dot{\phi}_i \sin\Phi_i = 0. \tag{4.1.7}$$

Substituting equations (4.1.6) into (4.1.1) results in

$$\dot{a}_i\omega_i \sin\Phi_i + a_i\dot{\phi}_i \cos\Phi_i = G_i, \tag{4.1.8}$$

where

$$G_i = -\varepsilon\left\{2\beta_i\omega_i a_i \sin\Phi_i - \omega_i^2\mathscr{H}\left[a_i\cos\Phi_i\right]\right\} + \varepsilon^{1/2}\xi(t)\omega_i\left(k_{ii}a_i\cos\Phi_i + k_{ij}a_j\cos\Phi_j\right).$$

By solving equations (4.1.7) and (4.1.8), equations (4.1.1) can be written in amplitudes a_i and phase ϕ_i

$$\dot{a}_i = \varepsilon F_{a,i}^{(1)} + \varepsilon^{1/2}F_{a,i}^{(0)}, \quad \dot{\phi}_i = \varepsilon F_{\phi,i}^{(1)} + \varepsilon^{1/2}F_{\phi,i}^{(0)}, \tag{4.1.9}$$

where

$$\begin{aligned}
F_{a,i}^{(0)} &= \xi(t)\left[\frac{1}{2}k_{ii}a_i\sin 2\Phi_i + \frac{1}{2}k_{ij}a_j\cos\Phi_j\sin\Phi_i\right],\\
F_{a,i}^{(1)} &= -\beta_i a_i + \beta_i a_i\cos 2\Phi_i - \sin\Phi_i\omega_i\tau_\varepsilon\mathscr{H}\left[a_i\cos\Phi_i\right],\\
F_{\phi,i}^{(0)} &= \xi(t)\left[k_{ii}\cos^2\Phi_i + \frac{a_j}{a_i}k_{ij}\cos\Phi_i\cos\Phi_j\right],\\
F_{\phi,i}^{(1)} &= -\beta_i\sin 2\Phi_i - \frac{1}{a_i(t)}\cos\Phi_i\omega_i\tau_\varepsilon\mathscr{H}\left[a_i(s)\cos\Phi_i\right].
\end{aligned} \tag{4.1.10}$$

If the correlation function $R(\tau)$ of the noise $\xi(t)$ decays sufficiently quickly to zero as τ increases, then the processes a_i and ϕ_i converge weakly on a time interval of order $1/\varepsilon$ to an Itô stochastic differential equation for the averaged amplitudes $\bar{a}_i$ and phase angles $\bar{\phi}_i$, whose solutions provide a uniformly valid first-order approximation to the exact values

$$\mathrm{d}a_i = \varepsilon m_i^a \mathrm{d}t + \varepsilon^{1/2}\sum_{j=1}^{2}\sigma_{ij}^a \mathrm{d}W_j, \tag{4.1.11}$$

$$\mathrm{d}\phi_i = \varepsilon m_i^\phi \mathrm{d}t + \varepsilon^{1/2}\sum_{j=1}^{2}\sigma_{ij}^\phi \mathrm{d}W_j, \quad i = 1,\ 2, \tag{4.1.12}$$

where the overbar is dropped for simplicity of presentation and $\mathbf{W}=\{W_1, W_2\}^T$ are independent standard Wiener processes. The drift coefficients εm_i^a, εm_i^ϕ, and the 2×2 diffusion matrices $\varepsilon \mathbf{b}^a=\varepsilon \boldsymbol{\sigma}^a(\boldsymbol{\sigma}^a)^T$, $\varepsilon \mathbf{b}^\phi=\varepsilon \boldsymbol{\sigma}^\phi(\boldsymbol{\sigma}^\phi)^T$, in which $\boldsymbol{\sigma}^a=[\sigma_{ij}^a]$, $\boldsymbol{\sigma}^\phi=[\sigma_{ij}^\phi]$, $\mathbf{b}^a=[b_{ij}^a]$, $\mathbf{b}^\phi=[b_{ij}^\phi]$, are given by

$$m_i^a = \mathop{\mathscr{M}}_t\left\{F_{a,i}^{(1)}+\int_{-\infty}^0 \mathsf{E}\left[\sum_{j=1}^2\left(\frac{\partial F_{a,i}^{(0)}}{\partial a_j}F_{a,j\tau}^{(0)}+\frac{\partial F_{a,i}^{(0)}}{\partial \phi_j}F_{\phi,j\tau}^{(0)}\right)\right]\mathrm{d}\tau\right\}$$

$$= a_i\Big[-\beta_i-\omega_i\tau_\varepsilon \mathop{\mathscr{M}}_t\{I_i^{sc}\}+\frac{3}{16}k_{ii}^2 S(2\omega_i)+\frac{1}{8}k_{ij}k_{ji}S^-\Big]+\frac{1}{16}\frac{a_j^2}{a_i}k_{ij}^2 S^+,$$

$$m_i^\phi = \mathop{\mathscr{M}}_t\left\{F_{\phi,i}^{(1)}+\int_{-\infty}^0 \mathsf{E}\left[\sum_{j=1}^2\left(\frac{\partial F_{\phi,i}^{(0)}}{\partial a_j}F_{\phi,j\tau}^{(0)}+\frac{\partial F_{\phi,i}^{(0)}}{\partial \phi_j}F_{\phi,j\tau}^{(0)}\right)\right]\mathrm{d}\tau\right\}$$

$$= -\omega_i\tau_\varepsilon \mathop{\mathscr{M}}_t\{I_i^{cc}\}+\frac{1}{8}\Big\{-k_{ii}^2\Psi(2\omega_i)+k_{ij}k_{ji}\big[\Psi(\omega^+)+(-1)^i\Psi(\omega^-)\big]\Big\},$$

$$b_{ii}^a = \mathop{\mathscr{M}}_t\left\{\int_{-\infty}^\infty \mathsf{E}\big[F_{a,i}^{(0)}F_{a,i\tau}^{(0)}\big]\mathrm{d}\tau\right\}=\frac{1}{8}[k_{ii}^2a_i^2S(2\omega_i)+k_{ij}^2a_j^2S^+],$$

$$b_{ij}^a = \mathop{\mathscr{M}}_t\left\{\int_{-\infty}^\infty \mathsf{E}\big[F_{a,i}^{(0)}F_{a,j\tau}^{(0)}\big]\mathrm{d}\tau\right\}=\frac{1}{8}a_ia_jk_{ij}k_{ji}S^-,$$

$$b_{ii}^\phi = \mathop{\mathscr{M}}_t\left\{\int_{-\infty}^\infty \mathsf{E}\big[F_{\phi,i}^{(0)}F_{\phi,i\tau}^{(0)}\big]\mathrm{d}\tau\right\}=\frac{1}{8}k_{ii}^2[2S(0)+S(2\omega_i)]+\frac{1}{8}\frac{a_j^2}{a_i^2}k_{ij}^2S^+,$$

$$b_{ij}^\phi = \mathop{\mathscr{M}}_t\left\{\int_{-\infty}^\infty \mathsf{E}\big[F_{\phi,i}^{(0)}F_{\phi,j\tau}^{(0)}\big]\mathrm{d}\tau\right\}=\frac{1}{4}k_{ii}k_{jj}S(0)+\frac{1}{8}k_{ij}k_{ji}S^+$$

$$F_{j\tau}^{(0)}=F_j^{(0)}\big(a,\phi,\xi(t+\tau),t+\tau\big),\quad i,j=1,\ 2,$$

$$S^\pm=S(\omega_1+\omega_2)\pm S(\omega_1-\omega_2),$$

where it is assumed that $\omega_1\neq\omega_2$. $\mathop{\mathscr{M}}_t\{\cdot\}$ is the averaging operator defined in equation (1.2.32). For ordinary viscoelasticity, applying the transformation $s=t-\tau$ and changing the order of integration lead to

$$\mathop{\mathscr{M}}_t\{I_i^{sc}\}=\lim_{T\to\infty}\frac{1}{T}\int_{t=0}^T\int_{s=0}^t \mathcal{H}(t-s)\cos\Phi_i(s)\sin\Phi_i(t)\,\mathrm{d}s\,\mathrm{d}t$$

$$
\begin{aligned}
&= \lim_{T\to\infty} \frac{1}{T} \int_{t=0}^{T} \int_{\tau=0}^{t} \mathcal{H}(\tau) \sin \Phi_i(t) \cos \Phi_i(t-\tau)\, \mathrm{d}\tau\, \mathrm{d}t \\
&= \lim_{T\to\infty} \frac{1}{2T} \int_{\tau=0}^{T} \int_{t=\tau}^{T} \mathcal{H}(\tau) \big[\sin(2\omega_i t - \omega_i \tau + 2\bar{\varphi}) + \sin \omega_i \tau \big]\, \mathrm{d}t\, \mathrm{d}\tau \\
&= \frac{1}{2} \int_{0}^{\infty} \mathcal{H}(\tau) \sin \omega_i \tau\, \mathrm{d}\tau = \frac{1}{2} \mathcal{H}^s(\omega_i).
\end{aligned} \tag{4.1.13}
$$

Similarly, it is found that

$$
\underset{t}{\mathscr{M}} \{I_i^{cc}\} = \underset{t}{\mathscr{M}} \Big\{ \cos \Phi_i(t) \int_0^t \mathcal{H}(t-s) \cos \Phi_i(s)\, \mathrm{d}s \Big\} = \frac{1}{2} \mathcal{H}^c(\omega_i), \tag{4.1.14}
$$

where

$$
\mathcal{H}^s(\omega) = \int_0^\infty \mathcal{H}(\tau) \sin \omega\tau\, \mathrm{d}\tau, \qquad \mathcal{H}^c(\omega) = \int_0^\infty \mathcal{H}(\tau) \cos \omega\tau\, \mathrm{d}\tau \tag{4.1.15}
$$

are the sine and cosine transformations in equations (3.3.85) for ordinary viscoelasticity. Thus, from equations (3.3.16) and (3.3.19), one has

$$
\underset{t}{\mathscr{M}} \{I_i^{sc}\} = \begin{cases} \dfrac{1}{2} \omega_i \tau_\varepsilon \dfrac{\omega_i \gamma}{\kappa^2 + \omega_i^2}, & \text{For ordinary viscoelasticity;} \\[2ex] -\dfrac{\tau_\varepsilon}{2} \omega_i^{\mu+1} \sin \dfrac{\mu\pi}{2}, & \text{For fractional viscoelasticity,} \end{cases} \tag{4.1.16}
$$

and from equations (3.3.18) and (3.3.19),

$$
\underset{t}{\mathscr{M}} \{I_i^{cc}\} = \begin{cases} \dfrac{1}{2} \omega_i \tau_\varepsilon \dfrac{\gamma \kappa}{\kappa^2 + \omega_i^2}, & \text{For ordinary viscoelasticity;} \\[2ex] \dfrac{\tau_\varepsilon}{2} \omega_i^{\mu+1} \cos \dfrac{\mu\pi}{2}, & \text{For fractional viscoelasticity.} \end{cases} \tag{4.1.17}
$$

The term $E_i,\ i = 1, 2$

$$
E_i = \begin{cases} \beta_i + \omega_i \tau_\varepsilon \underset{t}{\mathscr{M}} \{I_i^{sc}\}, & \text{For ordinary viscoelasticity;} \\[2ex] \beta_i - \omega_i \tau_\varepsilon \underset{t}{\mathscr{M}} \{I_i^{sc}\}, & \text{For fractional viscoelasticity.} \end{cases} \tag{4.1.18}
$$

may be called pseudo-damping, as it plays the role of damping and includes viscoelasticity as well. The sign before $\underset{t}{\mathscr{M}} \{I_i^{sc}\}$ is opposite for ordinary and fractional viscoelasticity due to the difference in equations of motion between (4.1.1) and (4.1.3).

It is of importance to note that both the averaged amplitude a_i and phase angle ϕ_i equations do not involve the phase angles and the amplitude equations are decoupled from the phase angle equations. Hence, the averaged amplitude vector (a_1, a_2) is a two dimensional diffusion process.

4.1.2 Moment Lyapunov Exponents of 4-D Systems

This section presents an approach for determining moment Lyapunov exponents from Itô stochastic differential equations of systems with four dimensions (4-D). The eigenvalue problem is first derived by using Khasminskii's transformation, moment Lyapunov exponents are then determined from Fourier series expansion. In practice, Itô stochastic differential equations can be derived from direct transformation of Stratonovich stochastic differential equations or from stochastic averaging method.

Eigenvalue Problems from 4-D Itô Homogeneous Systems

As can be seen later, by applying the method of stochastic averaging, certain coupled non-gyroscopic stochastic engineering systems or gyroscopic stochastic engineering systems can usually be approximated by a four-dimensional system in terms of linear Itô stochastic differential equations, or nonlinear Itô equations but homogeneous of degree one in state variables a_1 and a_2:

$$\mathrm{d}a_1 = \varepsilon m_1^a \mathrm{d}t + \varepsilon^{1/2}\big(\sigma_{11}^a \mathrm{d}W_1 + \sigma_{12}^a \mathrm{d}W_2\big), \tag{4.1.19a}$$

$$\mathrm{d}a_2 = \varepsilon m_2^a \mathrm{d}t + \varepsilon^{1/2}\big(\sigma_{21}^a \mathrm{d}W_1 + \sigma_{22}^a \mathrm{d}W_2\big), \tag{4.1.19b}$$

$$\mathrm{d}\phi_1 = \varepsilon m_1^\phi \mathrm{d}t + \varepsilon^{1/2}\big(\sigma_{11}^\phi \mathrm{d}W_1 + \sigma_{12}^\phi \mathrm{d}W_2\big), \tag{4.1.19c}$$

$$\mathrm{d}\phi_2 = \varepsilon m_2^\phi \mathrm{d}t + \varepsilon^{1/2}\big(\sigma_{21}^\phi \mathrm{d}W_1 + \sigma_{22}^\phi \mathrm{d}W_2\big), \tag{4.1.19d}$$

where $\mathbf{W} = \{W_1, W_2\}^T$ are independent standard Wiener processes. εm_i^a and εm_i^ϕ are drift terms. The matrices $\boldsymbol{\sigma}^a = [\sigma_{ij}^a]$ and $\boldsymbol{\sigma}^\phi = [\sigma_{ij}^\phi]$ cannot be uniquely determined. However, they are governed by the 2×2 diffusion matrices as

$$\varepsilon \mathbf{b}^a = \varepsilon \boldsymbol{\sigma}^a (\boldsymbol{\sigma}^a)^T, \quad \varepsilon \mathbf{b}^\phi = \varepsilon \boldsymbol{\sigma}^\phi (\boldsymbol{\sigma}^\phi)^T, \quad \mathbf{b}^a = [b_{ij}^a], \quad \mathbf{b}^\phi = [b_{ij}^\phi], \; i, j = 1, 2, \tag{4.1.20}$$

or in the matrix form

$$\begin{bmatrix} b_{11}^a & b_{12}^a \\ b_{21}^a & b_{22}^a \end{bmatrix} = \begin{bmatrix} \sigma_{11}^a & \sigma_{12}^a \\ \sigma_{21}^a & \sigma_{22}^a \end{bmatrix} \begin{bmatrix} \sigma_{11}^a & \sigma_{21}^a \\ \sigma_{12}^a & \sigma_{22}^a \end{bmatrix} = \begin{bmatrix} (\sigma_{11}^a)^2 + (\sigma_{12}^a)^2 & \sigma_{11}^a\sigma_{21}^a + \sigma_{12}^a\sigma_{22}^a \\ \sigma_{11}^a\sigma_{21}^a + \sigma_{12}^a\sigma_{22}^a & (\sigma_{21}^a)^2 + (\sigma_{22}^a)^2 \end{bmatrix}. \tag{4.1.21}$$

The amplitude equations in equations (4.1.19a) and (4.1.19b) are usually decoupled from the phase angle equations (4.1.19c) and (4.1.19d). The coefficients of the amplitude equations are nonlinear but homogeneous of degree one in a_1 and a_2, which results in an important fact that Khasminskii's method (Khasminskii, 1967) can be extended to such nonlinear and homogeneous systems (Ariaratnam, 1977).

To this end, one may transform the Itô stochastic differential equations for the amplitudes by using Khasminskii's transformation (Khasminskii, 1967)

$$r = (a_1^2 + a_2^2)^{1/2}, \quad \varphi = \tan^{-1}\frac{a_2}{a_1}, \quad a_1 = r\cos\varphi, \quad a_2 = r\sin\varphi, \quad P = r^p, \tag{4.1.22}$$

and then the moment Lyapunov exponent is given by

$$\Lambda = \lim_{t\to\infty} \frac{1}{t} \log \mathbf{E}[P]. \tag{4.1.23}$$

Since

$$\begin{aligned}
&\frac{\partial P}{\partial a_1} = \frac{pP\cos\varphi}{r}, \quad \frac{\partial P}{\partial a_2} = \frac{pP\sin\varphi}{r}, \quad \frac{\partial^2 P}{\partial a_1 \partial a_2} = \frac{p(p-2)P\sin\varphi\cos\varphi}{r^2}, \\
&\frac{\partial^2 P}{\partial a_1^2} = \frac{pP\big[(p-2)\cos^2\varphi + 1\big]}{r^2}, \quad \frac{\partial^2 P}{\partial a_2^2} = \frac{pP\big[(p-2)\sin^2\varphi + 1\big]}{r^2}, \\
&\frac{\partial \varphi}{\partial a_1} = -\frac{\sin\varphi}{r}, \quad \frac{\partial \varphi}{\partial a_2} = \frac{\cos\varphi}{r}, \quad \frac{\partial^2 \varphi}{\partial a_1 \partial a_2} = -\frac{2\cos^2\varphi - 1}{r^2}, \\
&\frac{\partial^2 \varphi}{\partial a_1^2} = \frac{2\cos\varphi\sin\varphi}{r^2}, \quad \frac{\partial^2 \varphi}{\partial a_2^2} = -\frac{2\sin\varphi\cos\varphi}{r^2},
\end{aligned} \tag{4.1.24}$$

the Itô equations for P and φ can be obtained using the Itô Lemma,

$$\mathrm{d}P = m_P(P,\varphi)\mathrm{d}t + \sigma_{P1}\mathrm{d}W_1 + \sigma_{P2}\mathrm{d}W_2, \tag{4.1.25}$$

where

$$\sigma_{P1} = \varepsilon^{1/2}\Big(\sigma_{11}^a \frac{\partial P}{\partial a_1} + \sigma_{21}^a \frac{\partial P}{\partial a_2}\Big), \quad \sigma_{P2} = \varepsilon^{1/2}\Big(\sigma_{12}^a \frac{\partial P}{\partial a_1} + \sigma_{22}^a \frac{\partial P}{\partial a_2}\Big), \tag{4.1.26}$$

and

$$m_P(P,\varphi)=\varepsilon\Big\{m_1^a\frac{\partial P}{\partial a_1}+m_2^a\frac{\partial P}{\partial a_2}+\frac{1}{2}\Big[b_{11}^a\frac{\partial^2 P}{\partial a_1^2}+(b_{12}^a+b_{21}^a)\frac{\partial^2 P}{\partial a_1\partial a_2}+b_{22}^a\frac{\partial^2 P}{\partial a_2^2}\Big]\Big\},$$

$$=\varepsilon pP\Big\{\frac{m_1^a}{(a_1^2+a_2^2)^{1/2}}\cos\varphi+\frac{m_2^a}{(a_1^2+a_2^2)^{1/2}}\sin\varphi+\frac{1}{2}\Big[\frac{b_{11}^a}{a_1^2+a_2^2}[(p-2)\cos^2\varphi+1]$$

$$+\frac{b_{12}^a+b_{21}^a}{2(a_1^2+a_2^2)}(p-2)\sin 2\varphi+\frac{b_{22}^a}{a_1^2+a_2^2}[(p-2)\sin^2\varphi+1]\Big]\Big\}. \tag{4.1.27}$$

To determine the diffusion terms, one may use the following replacement

$$\Sigma_P\mathrm{d}W=\sigma_{P1}\mathrm{d}W_1+\sigma_{P2}\mathrm{d}W_2,$$

which yields, by using equation (4.1.21),

$$\Sigma_P^2=\sigma_{P1}^2+\sigma_{P2}^2=\varepsilon\Big\{\sigma_{11}^a\frac{\partial P}{\partial a_1}+\sigma_{21}^a\frac{\partial P}{\partial a_2}\quad \sigma_{12}^a\frac{\partial P}{\partial a_1}+\sigma_{22}^a\frac{\partial P}{\partial a_2}\Big\}\begin{Bmatrix}\sigma_{11}^a\dfrac{\partial P}{\partial a_1}+\sigma_{21}^a\dfrac{\partial P}{\partial a_2}\\ \sigma_{12}^a\dfrac{\partial P}{\partial a_1}+\sigma_{22}^a\dfrac{\partial P}{\partial a_2}\end{Bmatrix}$$

$$=\varepsilon\Big\{[(\sigma_{11}^a)^2+(\sigma_{12}^a)^2]\Big(\frac{\partial P}{\partial a_1}\Big)^2+2\big(\sigma_{11}^a\sigma_{21}^a+\sigma_{12}^a\sigma_{22}^a\big)\frac{\partial P}{\partial a_1}\frac{\partial P}{\partial a_2}+[(\sigma_{21}^a)^2+(\sigma_{22}^a)^2]\Big(\frac{\partial P}{\partial a_2}\Big)^2\Big\}$$

$$=\varepsilon\Big[b_{11}^a\Big(\frac{\partial P}{\partial a_1}\Big)^2+(b_{12}^a+b_{21}^a)\frac{\partial P}{\partial a_1}\frac{\partial P}{\partial a_2}+b_{22}^a\Big(\frac{\partial P}{\partial a_2}\Big)^2\Big]. \tag{4.1.28}$$

Hence, the Itô SDE of P can be written as

$$\mathrm{d}P=m_P(P,\varphi)\mathrm{d}t+\sigma_{P1}\mathrm{d}W_1+\sigma_{P2}\mathrm{d}W_2=m_P(P,\varphi)\mathrm{d}t+\Sigma_P(P,\varphi)\mathrm{d}W. \tag{4.1.29}$$

Similarly, one may obtain the Itô SDE of φ,

$$\mathrm{d}\varphi=m_\varphi(\varphi)\mathrm{d}t+\sigma_{\varphi1}\mathrm{d}W_1+\sigma_{\varphi2}\mathrm{d}W_2=m_\varphi(\varphi)\mathrm{d}t+\Sigma_\varphi(\varphi)\mathrm{d}W, \tag{4.1.30}$$

where

$$\sigma_{\varphi1}=\varepsilon^{1/2}\Big(\sigma_{11}^a\frac{\partial\varphi}{\partial a_1}+\sigma_{21}^a\frac{\partial\varphi}{\partial a_2}\Big),\quad \sigma_{\varphi2}=\varepsilon^{1/2}\Big(\sigma_{12}^a\frac{\partial\varphi}{\partial a_1}+\sigma_{22}^a\frac{\partial\varphi}{\partial a_2}\Big), \tag{4.1.31}$$

$$m_\varphi(\varphi)=\varepsilon\Big\{m_1^a\frac{\partial\varphi}{\partial a_1}+m_2^a\frac{\partial\varphi}{\partial a_2}+\frac{1}{2}\Big[b_{11}^a\frac{\partial^2\varphi}{\partial a_1^2}+(b_{12}^a+b_{21}^a)\frac{\partial^2\varphi}{\partial a_1\partial a_2}+b_{22}^a\frac{\partial^2\varphi}{\partial a_2^2}\Big]\Big\}$$

$$=\varepsilon\Big\{-\frac{m_1^a}{(a_1^2+a_2^2)^{1/2}}\sin\varphi+\frac{m_2^a}{(a_1^2+a_2^2)^{1/2}}\cos\varphi+\frac{1}{2}\Big[\frac{b_{11}^a}{a_1^2+a_2^2}\sin 2\varphi$$

$$-\frac{b_{12}^a+b_{21}^a}{a_1^2+a_2^2}\big(2\cos^2\varphi-1\big)-\frac{b_{22}^a}{a_1^2+a_2^2}\sin 2\varphi\Big]\Big\}, \tag{4.1.32}$$

$$\Sigma_\varphi^2=\sigma_{\varphi1}^2+\sigma_{\varphi2}^2=\varepsilon\Big[b_{11}^a\Big(\frac{\partial\varphi}{\partial a_1}\Big)^2+(b_{12}^a+b_{21}^a)\frac{\partial\varphi}{\partial a_1}\frac{\partial\varphi}{\partial a_2}+b_{22}^a\Big(\frac{\partial\varphi}{\partial a_2}\Big)^2\Big]$$

$$=\varepsilon\Big(\frac{b_{11}^a}{a_1^2+a_2^2}\sin^2\varphi-\frac{b_{12}^a+b_{21}^a}{a_1^2+a_2^2}\sin\varphi\cos\varphi+\frac{b_{22}^a}{a_1^2+a_2^2}\cos^2\varphi\Big). \tag{4.1.33}$$

It is noted that the coefficients of the right hand side terms of amplitude equations in equations (4.1.19a) and (4.1.19b), such as $m_i^a, i=1,\ 2$, are homogeneous of degree one in a_1 and a_2, which results in that the diffusion term $\mathbf{b}$ in (4.1.21) are homogeneous of degree two in a_1 and a_2.

Hence, submitting $a_1=r\cos\varphi$ and $a_2=r\sin\varphi$ in equation (4.1.24) into (4.1.27), one finds that the drift $m_P(P,\varphi)$ and diffusion $\Sigma_P(P,\varphi)$ are functions of P of degree one and φ. However, the drift $m_\varphi(\varphi)$ in (4.1.32) and diffusion term $\Sigma_\varphi(\varphi)$ in (4.1.33) are functions of φ only, which shows $P(t)$ in equation (4.1.29) and $\varphi(t)$ in (4.1.30) are coupled, although $\varphi(t)$ is itself a diffusion process.

To obtain the moment Lyapunov exponent, a linear stochastic transformation is adopted

$$S=T(\varphi)P,\quad P=T^{-1}(\varphi)S,\quad 0\leqslant\varphi<\pi,$$

from which one obtains

$$\frac{\partial S}{\partial P}=T(\varphi),\quad \frac{\partial S}{\partial\varphi}=T'P,\quad \frac{\partial^2 S}{\partial P^2}=0,\quad \frac{\partial^2 S}{\partial P\partial\varphi}=T',\quad \frac{\partial^2 S}{\partial^2\varphi}=PT'', \tag{4.1.34}$$

where T' and T'' denote the first-order and second-order derivatives of $T(\varphi)$ with respect to φ, respectively.

The Itô equation for the transformed pth norm process S can be derived using Itô's Lemma again

$$\mathrm{d}S=m_S\mathrm{d}t+\Big(\sigma_{P1}\frac{\partial S}{\partial P}\mathrm{d}W_1+\sigma_{P2}\frac{\partial S}{\partial P}\mathrm{d}W_2+\sigma_{\varphi1}\frac{\partial S}{\partial\varphi}\mathrm{d}W_1+\sigma_{\varphi2}\frac{\partial S}{\partial\varphi}\mathrm{d}W_2\Big). \tag{4.1.35}$$

The drift coefficient is given by

$$m_S=m_P\frac{\partial S}{\partial P}+m_\varphi\frac{\partial S}{\partial\varphi}+\frac{1}{2}\Big[b_{11}^S\frac{\partial^2 S}{\partial P^2}+(b_{12}^S+b_{21}^S)\frac{\partial^2 S}{\partial P\partial\varphi}+b_{22}^S\frac{\partial^2 S}{\partial\varphi^2}\Big]$$

$$=\frac{1}{2}P\big(\sigma_{\varphi 1}^2+\sigma_{\varphi 2}^2\big)T''+\big(m_\varphi P+\sigma_{P1}\sigma_{\varphi 1}+\sigma_{P2}\sigma_{\varphi 2}\big)T'+m_P T, \tag{4.1.36}$$

and the diffusion terms have the relation

$$\mathbf{b}^S=\sigma^S\big(\boldsymbol{\sigma}^S\big)^T,\quad \boldsymbol{\sigma}^S=\begin{bmatrix}\sigma_{P1} & \sigma_{P2}\\ \sigma_{\varphi 1} & \sigma_{\varphi 2}\end{bmatrix}. \tag{4.1.37}$$

Substituting σ_{P1} and σ_{P2} in equations (4.1.26), $\sigma_{\varphi 1}$ and $\sigma_{\varphi 2}$ in (4.1.31) into (4.1.37) and considering the relations in (4.1.21) lead to

$$\begin{aligned}
&b_{11}^S=\sigma_{P1}^2+\sigma_{P2}^2=\Sigma_P^2,\quad b_{22}^S=\sigma_{\varphi 1}^2+\sigma_{\varphi 2}^2=\Sigma_\varphi^2,\\
&b_{12}^S=b_{21}^S=\sigma_{P1}\sigma_{\varphi 1}+\sigma_{P2}\sigma_{\varphi 2}\\
&\quad=\varepsilon\big[(\sigma_{11}^a)^2+(\sigma_{12}^a)^2\big]\frac{\partial P}{\partial a_1}\frac{\partial \varphi}{\partial a_1}+\varepsilon\big(\sigma_{11}^a\sigma_{21}^a+\sigma_{12}^a\sigma_{22}^a\big)\Big[\frac{\partial P}{\partial a_1}\frac{\partial \varphi}{\partial a_2}+\frac{\partial P}{\partial a_2}\frac{\partial \varphi}{\partial a_1}\Big]\\
&\qquad+\varepsilon\big[(\sigma_{21}^a)^2+(\sigma_{22}^a)^2\big]\frac{\partial P}{\partial a_2}\frac{\partial \varphi}{\partial a_2}\\
&\quad=\varepsilon\bigg\{b_{11}^a\frac{\partial P}{\partial a_1}\frac{\partial \varphi}{\partial a_1}+b_{12}^a\Big[\frac{\partial P}{\partial a_1}\frac{\partial \varphi}{\partial a_2}+\frac{\partial P}{\partial a_2}\frac{\partial \varphi}{\partial a_1}\Big]+b_{22}^a\frac{\partial P}{\partial a_2}\frac{\partial \varphi}{\partial a_2}\bigg\}\\
&\quad=\varepsilon pP\bigg[-\frac{b_{11}^a}{a_1^2+a_2^2}\cos\varphi\sin\varphi+\frac{b_{12}^a}{a_1^2+a_2^2}\big(\cos^2\varphi-\sin^2\varphi\big)+\frac{b_{22}^a}{a_1^2+a_2^2}\cos\varphi\sin\varphi\bigg].
\end{aligned} \tag{4.1.38}$$

For bounded and non-singular transformation $T(\varphi)$, both processes P and S are expected to have the same stability behaviour. Therefore, $T(\varphi)$ is chosen so that the drift term of the Itô differential equation (4.1.35) is independent of the phase process φ so that

$$\mathrm{d}S=\varepsilon\Lambda S\mathrm{d}t+\varepsilon^{1/2}\big(\sigma_{S1}\mathrm{d}W_1+\sigma_{S2}\mathrm{d}W_2\big). \tag{4.1.39}$$

Comparing the drift terms of equations (4.1.35) and (4.1.39), one can find that such a transformation $T(\varphi)$ is given by the following equation

$$\frac{1}{2}P\big(\sigma_{\varphi 1}^2+\sigma_{\varphi 2}^2\big)T''+\big(m_\varphi P+\sigma_{P1}\sigma_{\varphi 1}+\sigma_{P2}\sigma_{\varphi 2}\big)T'+m_P T=\varepsilon\Lambda S,\quad 0\leqslant\varphi<\pi, \tag{4.1.40}$$

in which $T(\varphi)$ is a periodic function in φ of period π. Equation (4.1.40) defines an eigenvalue problem of a second-order differential operator with , Λ being the eigenvalue and $T(\varphi)$ the associated eigenfunction. Taking the expected value of both sides of equation (4.1.39), one can find that $\mathsf{E}[\sigma_{S1}\,\mathrm{d}W_1+\sigma_{S2}\,\mathrm{d}W_2]=0$ (Xie, 2006). Hence, one obtains $\mathsf{E}[S]=\varepsilon\Lambda\mathsf{E}[S]\mathrm{d}t$, from which the eigenvalue Λ is seen to be the Lyapunov exponent of the pth moment of system (4.1.19a), i.e., $\Lambda=\Lambda_{y(t)}(p)$. It is noted that both processes P and S have the same stability behaviour.

Substituting equations (4.1.38) into (4.1.40) yields

$$\mathcal{L}(p)[T]=\frac{1}{P}\left\{\frac{1}{2}\Sigma_{\varphi}^2 PT''+\left[m_{\varphi}P+b_{12}^S\right]T'+m_P T\right\}=\varepsilon\Lambda T,\quad 0\leqslant\varphi<\pi, \tag{4.1.41}$$

where Σ_{φ}^2, m_{φ}, b_{12}^S, and m_P are given in (4.1.33), (4.1.32), (4.1.38), and (4.1.27), respectively. Substituting these equations into (4.1.41) yields

$$\mathcal{L}(p)[T]=c_2T''+c_1T'+c_0T=\Lambda T,\quad 0\leqslant\varphi<\pi, \tag{4.1.42}$$

where

$$\begin{aligned}
c_2&=\frac{1}{2}\left[\frac{b_{11}^a}{a_1^2+a_2^2}\sin^2\varphi-\frac{b_{12}^a+b_{21}^a}{a_1^2+a_2^2}\sin\varphi\cos\varphi+\frac{b_{22}^a}{a_1^2+a_2^2}\cos^2\varphi\right],\\
c_1&=\left\{\left[\frac{m_2^a\cos\varphi}{(a_1^2+a_2^2)^{1/2}}-\frac{m_1^a\sin\varphi}{(a_1^2+a_2^2)^{1/2}}+\frac{b_{11}^a\sin 2\varphi}{2(a_1^2+a_2^2)}-\frac{(b_{12}^a+b_{21}^a)\left(2\cos^2\varphi-1\right)}{2(a_1^2+a_2^2)}-\frac{b_{22}^a\sin 2\varphi}{2(a_1^2+a_2^2)}\right]\right.\\
&\quad\left.+p\left[-\frac{b_{11}^a}{a_1^2+a_2^2}\cos\varphi\sin\varphi+\frac{b_{12}^a}{a_1^2+a_2^2}\left(\cos^2\varphi-\sin^2\varphi\right)+\frac{b_{22}^a}{a_1^2+a_2^2}\cos\varphi\sin\varphi\right]\right\},\\
c_0&=p\left\{\frac{m_1^a}{(a_1^2+a_2^2)^{1/2}}\cos\varphi+\frac{m_2^a}{(a_1^2+a_2^2)^{1/2}}\sin\varphi+\frac{1}{2}\left[\frac{b_{11}^a}{a_1^2+a_2^2}[(p-2)\cos^2\varphi+1]\right.\right.\\
&\quad\left.\left.+\frac{b_{12}^a+b_{21}^a}{2(a_1^2+a_2^2)}(p-2)\sin 2\varphi+\frac{b_{22}^a}{a_1^2+a_2^2}[(p-2)\sin^2\varphi+1]\right]\right\}.
\end{aligned} \tag{4.1.43}$$

Substituting $a_1=r\cos\varphi$, $a_2=r\sin\varphi$ into (4.1.43), one may find that the coefficients c_0, c_1, and c_2 are function of φ and p only.

This approach was first applied by Wedig (1988) to derive the eigenvalue problem for the moment Lyapunov exponent of a two-dimensional linear Itô stochastic system. It can be seen that the eigenvalue problem (4.1.42) derived from Wedig's approach is the same as that obtained from the general theory of moment Lyapunov exponents (Xie, 2006).

Determination of Moment Lyapunov Exponents

Since the coefficients in (4.1.42) are periodic with period π, it is reasonable to consider a Fourier cosine series expansion of the eigenfunction $T(\varphi)$ in the form

$$T(\varphi)=\sum_{i=0}^{K} C_i \cos 2i\varphi, \tag{4.1.44}$$

where K is Fourier series expansion order. Here only cosine functions are adopted because sometimes the eigenvalue problem in equation (4.1.42) contains $1/\sin(2\varphi)$. This Fourier expansion method is actually a method for solving partial differential equations and has been used by Wedig (1988), Bolotin (1964), Namachchivaya and Roessel (2001), and others.

Substituting this expansion and $a_1=r\cos\varphi$, $a_2=r\sin\varphi$ into eigenvalue problem (4.1.42), multiplying both sides by $\cos(2j\varphi)$, $j=0,\ 1,\cdots,K$, and performing integration with respect to φ from 0 to $\pi/2$ yield a set of equations for the unknown coefficients C_i, $i=0,\ 1,\cdots,K$:

$$\sum_{i=0}^{K} a_{ij}C_i=\hat{\Lambda}C_j, \quad j=0,\ 1,\ 2,\cdots, \tag{4.1.45}$$

where

$$a_{ij}=\frac{4}{\pi}\int_0^{\pi/2}\mathcal{L}(p)[\cos(2i\varphi)]\cos(2j\varphi)\mathrm{d}\varphi, \quad j=0,1,\cdots,K,$$

and

$$\int_0^{\pi/2}\cos(2i\varphi)\cos(2j\varphi)\mathrm{d}\varphi=\begin{cases}\frac{\pi}{4}, & i=j,\\ 0, & i\neq j.\end{cases}$$

The eigenvalue can be obtained by solution of a polynomial equation as follows. Rearranging equation (4.1.45) leads to

$$\begin{bmatrix} a_{00}-\hat{\Lambda} & a_{01} & a_{02} & a_{03} & \cdots \\ a_{10} & a_{11}-\hat{\Lambda} & a_{12} & a_{13} & \cdots \\ a_{20} & a_{21} & a_{22}-\hat{\Lambda} & a_{23} & \cdots \\ a_{30} & a_{31} & a_{32} & a_{33}-\hat{\Lambda} & \cdots \\ \cdots & \cdots & \cdots & \cdots & \ddots \end{bmatrix}\begin{Bmatrix} C_0 \\ C_1 \\ C_2 \\ C_3 \\ \cdots \end{Bmatrix}=0. \tag{4.1.46}$$

The elements of the first 3×3 submatrix are listed here. For convenience of presentation, $\hat{\Lambda}$ is inserted in a_{ii}.

$$
\begin{aligned}
a_{00} = & \frac{1}{128}\left[3k_{11}^2 S(2\omega_1) + 3k_{22}^2 S(2\omega_2) + 4k^2 S(\omega^{\pm})\right] p^2 \\
& + \frac{1}{64}\left[5k_{11}^2 S(2\omega_1) + 5k_{22}^2 S(2\omega_2) + 12k^2 S(\omega^{\pm}) - 32(E_1 + E_2)\right] p - \hat{\Lambda}, \\
a_{01} = & \frac{1}{64}\left[k_{11}^2 S(2\omega_1) - k_{22}^2 S(2\omega_2)\right] p^2 + \frac{1}{32}\left[k_{11}^2 S(2\omega_1) - k_{22}^2 S(2\omega_2) - 8(E_1 - E_2)\right] p, \\
a_{02} = & \frac{1}{256}\left[k_{11}^2 S(2\omega_1) + k_{22}^2 S(2\omega_2) - 4k^2 S(\omega^{\pm})\right] p^2 \\
& - \frac{1}{128}\left[k_{11}^2 S(2\omega_1) + k_{22}^2 S(2\omega_2) - 8k^2 S(\omega^{\pm})\right] p, \\
a_{10} = & \frac{1}{64}\left[k_{11}^2 S(2\omega_1) - k_{22}^2 S(2\omega_2)\right] p^2 + \frac{1}{16}\left[k_{11}^2 S(2\omega_1) - k_{22}^2 S(2\omega_2) - 4(E_1 - E_2)\right] p \\
& + \frac{1}{16}\left[k_{11}^2 S(2\omega_1) - k_{22}^2 S(2\omega_2) - 8(E_1 - E_2)\right], \\
a_{11} = & \frac{1}{512}\left[7k_{11}^2 S(2\omega_1) + 7k_{22}^2 S(2\omega_2) + 4k^2 S(\omega^{\pm})\right] p^2 \\
& + \frac{1}{256}\left[11k_{11}^2 S(2\omega_1) + 11k_{22}^2 S(2\omega_2) + 20k^2 S(\omega^{\pm}) - 64(E_1 + E_2)\right] p \\
& - \frac{1}{64}\left[k_{11}^2 S(2\omega_1) + k_{22}^2 S(2\omega_2) + 12k^2 S(\omega^{\pm}) + 16k^2 S(\omega^{\mp})\right] - \frac{\hat{\Lambda}}{2}, \\
a_{12} = & \frac{1}{128}\left[k_{11}^2 S(2\omega_1) - k_{22}^2 S(2\omega_2)\right] p^2 - \frac{1}{8}(E_1 - E_2) p \\
& - \frac{1}{32}\left[k_{11}^2 S(2\omega_1) - k_{22}^2 S(2\omega_2) - 8(E_1 - E_2)\right], \\
a_{20} = & \frac{1}{256}\left[k_{11}^2 S(2\omega_1) + k_{22}^2 S(2\omega_2) - 4k^2 S(\omega^{\pm})\right] p^2 \\
& + \frac{3}{128}\left[k_{11}^2 S(2\omega_1) + k_{22}^2 S(2\omega_2) - 4k^2 S(\omega^{\pm})\right] p \\
& + \frac{1}{32}\left[k_{11}^2 S(2\omega_1) + k_{22}^2 S(2\omega_2) - 20k^2 S(\omega^{\pm}) - 16k^2 S(\omega^{\mp})\right], \\
a_{21} = & \frac{1}{128}\left[k_{11}^2 S(2\omega_1) - k_{22}^2 S(2\omega_2)\right] p^2 + \frac{1}{64}\left[3k_{11}^2 S(2\omega_1) - 3k_{22}^2 S(2\omega_2) - 8(E_1 - E_2)\right] p
\end{aligned}
$$

$$
\begin{aligned}
&+\frac{1}{16}\left[k_{11}^2 S(2\omega_1)-k_{22}^2 S(2\omega_2)-8(E_1-E_2)\right],\\
a_{22}=&\frac{1}{256}\left[3k_{11}^2 S(2\omega_1)+3k_{22}^2 S(2\omega_2)+4k^2 S(\omega^{\pm})\right]p^2\\
&+\frac{1}{128}\left[5k_{11}^2 S(2\omega_1)+5k_{22}^2 S(2\omega_2)+12k^2 S(\omega^{\pm})-32(E_1+E_2)\right]p\\
&-\frac{1}{16}\left[k_{11}^2 S(2\omega_1)+k_{22}^2 S(2\omega_2)+8k^2 S(\omega^{\pm})+12k^2 S(\omega^{\mp})\right]-\frac{\hat{\Lambda}}{2},
\end{aligned}
\tag{4.1.47}
$$

where E_i is the pseudo-damping defined in equation (4.1.18), and the upper sign is taken when $k_{12}=k_{21}=k$ and the lower sign when $k_{12}=-k_{21}=k$.

To have a non-trial solution of the C_k, it is required that the determinant of the coefficient matrix of equation (4.1.46) equal zero, from which the eigenvalue $\hat{\Lambda}(p)$ can be obtained,

$$
e_{K+1}^{(K)}\left[\hat{\Lambda}^{(K)}\right]^{K+1}+e_K^{(K)}\left[\hat{\Lambda}^{(K)}\right]^{K}+\cdots+e_1^{(K)}\hat{\Lambda}^{(K)}+e_0^{(K)}=0, \tag{4.1.48}
$$

where $\hat{\Lambda}^{(K)}$ denotes the approximate moment Lyapunov exponent under the assumption that the expansion of eigenfunction $T(\varphi)$ is up to Kth order Fourier cosine series. The set of approximate eigenvalues obtained by this procedure converge to the corresponding true eigenvalues as $K\to\infty$. However, as shown in Figure 4.1, the approximate eigenvalues converge so quickly that the approximations almost coincide when the order $K\geqslant 3$.

One may approximate the moment Lyapunov exponent of the system by

$$
\Lambda_{q(t)}(p)\approx\hat{\Lambda}^{(K)}(p). \tag{4.1.49}
$$

Determination of Lyapunov Exponents

The pth moment Lyapunov exponent $\Lambda_{q(t)}(p)$ is a convex analytic function in p that passes through the origin and the slope at the origin is equal to the largest Lyapunov exponent $\lambda_{q(t)}$, i.e.,

$$
\lambda_{q(t)}(p)=\lim_{p\to 0}\frac{\hat{\Lambda}^{(K)}(p)}{p}=-\lim_{p\to 0}\frac{e_0^{(K)}}{p e_1^{(K)}}, \tag{4.1.50}
$$

which is obtained directly from equation (4.1.48).

For comparison, the largest Lyapunov exponent for system (4.1.11) can be directly derived from the invariant probability density by solving a Fokker-Plank equation (Xie, 2006, equations (8.6.14))

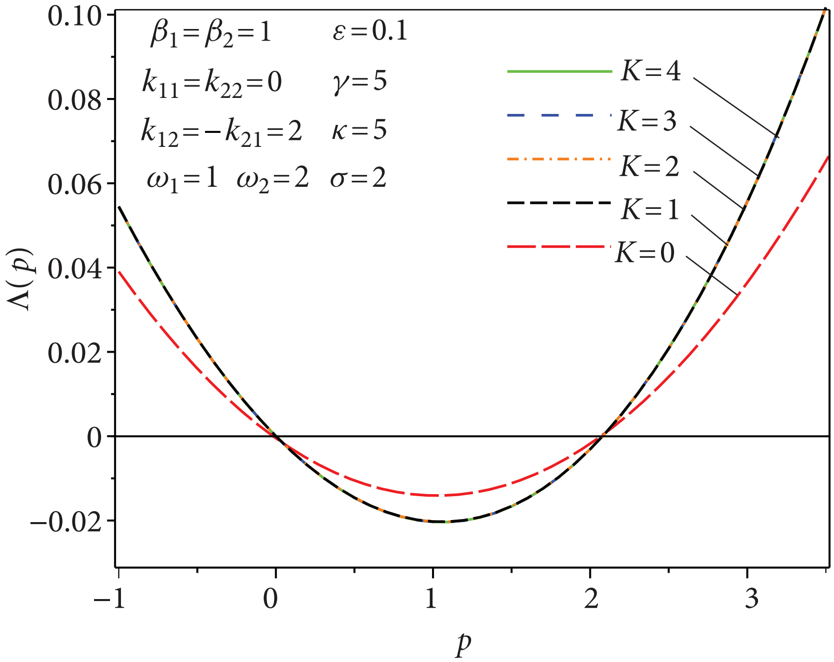

Figure 4.1 Moment Lyapunov exponents of coupled system for κth order Fourier expansion

(1) If $k_{11}^2 S(2\omega_1)+k_{22}^2 S(2\omega_2) > 4\,|k_{12}k_{21}|\,S(\omega_1 \pm \omega_2)$, i.e., $\Delta_0 > 0$

$$\lambda = \frac{1}{2}\left[(\lambda_1+\lambda_2)+(\lambda_1-\lambda_2)\coth\left(\frac{\lambda_1-\lambda_2}{\sqrt{\Delta_0}}\alpha\right)\right]+\frac{1}{8}k_{12}k_{21}S^-, \tag{4.1.51}$$

where $\alpha = \cosh^{-1}[Q/(2\,|k_{12}k_{21}|\,S^+)]$.

(2) If $k_{11}^2 S(2\omega_1)+k_{22}^2 S(2\omega_2) < 4\,|k_{12}k_{21}|\,S(\omega_1 \pm \omega_2)$, i.e., $\Delta_0 < 0$

$$\lambda = \frac{1}{2}\left[(\lambda_1+\lambda_2)+(\lambda_1-\lambda_2)\coth\left(\frac{\lambda_1-\lambda_2}{\sqrt{-\Delta_0}}\alpha\right)\right]+\frac{1}{8}k_{12}k_{21}S^-, \tag{4.1.52}$$

where $\alpha = \cos^{-1}[Q/(2\,|k_{12}k_{21}|\,S^+)]$.

(3) If $k_{11}^2 S(2\omega_1)+k_{22}^2 S(2\omega_2) = 4\,|k_{12}k_{21}|\,S(\omega_1 \pm \omega_2)$, i.e., $\Delta_0 = 0$

$$\lambda = \frac{1}{2}\left\{(\lambda_1+\lambda_2)+(\lambda_1-\lambda_2)\coth\left[\frac{4(\lambda_1-\lambda_2)}{|k_{12}k_{21}|\,S^+}\right]\right\}+\frac{1}{8}k_{12}k_{21}S^-. \tag{4.1.53}$$

The constants Q and Δ_0 are given as

$$Q = k_{11}^2 S(2\omega_1)+k_{22}^2 S(2\omega_2)-2k_{12}k_{21}S^+, \quad \Delta_0 = \frac{1}{64}[Q^2-4k_{12}^2k_{21}^2(S^+)^2],$$

$$\lambda_1 = -\beta_1 - \omega_1 \tau_\varepsilon \underset{t}{\mathscr{M}}\{I_1^{sc}\} + \frac{1}{8}k_{11}^2 S(2\omega_1), \quad \lambda_2 = -\beta_2 - \omega_2 \tau_\varepsilon \underset{t}{\mathscr{M}}\{I_2^{sc}\} + \frac{1}{8}k_{22}^2 S(2\omega_2). \tag{4.1.54}$$

4.1.3 Stability Boundary

Moment Lyapunov exponents can be numerically determined from equation (4.1.48). To obtain the stability boundary, some cases with smaller values of Fourier series expansion order K in equation (4.1.44) are discussed.

Case 1: Fourier cosine series expansion order $K=1$

When $K=1$, the eigenfunction in equation (4.1.44) is $T(\varphi)=C_0+C_1\cos 2\varphi$, the moment Lyapunov exponent can be solved from

$$\begin{vmatrix} a_{00}-\hat{\Lambda}^{(1)} & a_{01} \\ a_{10} & a_{11}-\hat{\Lambda}^{(1)} \end{vmatrix} = 0, \quad \text{or} \quad \left(\hat{\Lambda}^{(1)}\right)^2 + e_1^{(1)}\hat{\Lambda}^{(1)} + e_0^{(1)} = 0. \tag{4.1.55}$$

This is a quadratic equation, of which the solution obtained analytically is moment Lyapunov exponent. The coefficients for the viscoelastic coupled non-gyroscopic systems with white noise ($S(\omega)=S_0$) are given by

$$e_1^{(1)} = -\frac{1}{256}\left(13p^2+42p-8\right)S_0(k_{11}^2+k_{22}^2) - \frac{1}{64}\left(3p^2+22P-56\right)S_0 k^2 + p(E_1+E_2),$$

$$\begin{aligned}
e_0^{(1)} = {} & S_0^2(k_{11}^4+k_{22}^4)\Big(\frac{5}{32768}p^4+\frac{5}{4096}p^3+\frac{1}{8192}p^2-\frac{13}{2048}p\Big) \\
& + S_0^2 k_{11}^2 k_{22}^2\Big(\frac{37}{16384}p^4+\frac{29}{2048}p^3+\frac{97}{4096}p^2+\frac{3}{1024}p\Big) \\
& + S_0^2 k^4\Big(\frac{1}{2048}p^4+\frac{1}{128}p^3+\frac{1}{512}p^2-\frac{21}{128}p\Big) \\
& + S_0^2(k_{11}^2+k_{22}^2)k^2\Big(\frac{5}{4096}p^4+\frac{13}{1024}p^3+\frac{7}{1024}p^2-\frac{19}{256}p\Big) \\
& + S_0 k_{11}^2\Big[-\Big(\frac{5}{512}E_1+\frac{21}{512}E_2\Big)p^3-\Big(\frac{5}{256}E_1+\frac{37}{256}E_2\Big)p^2+\Big(\frac{5}{64}E_1-\frac{3}{64}E_2\Big)p\Big] \\
& + S_0 k_{22}^2\Big[-\Big(\frac{5}{512}E_2+\frac{21}{512}E_1\Big)p^3-\Big(\frac{5}{256}E_2+\frac{37}{256}E_1\Big)p^2+\Big(\frac{5}{64}E_2-\frac{3}{64}E_1\Big)p\Big]
\end{aligned}$$

$$+S_0k^2(E_1+E_2)\Big(-\frac{3}{128}p^3-\frac{11}{64}p^2+\frac{7}{16}p\Big)+\frac{p^2}{8}\big(E_1^2+E_2^2+6E_1E_2\big)-\frac{p}{4}\big(E_1-E_2\big)^2. \tag{4.1.56}$$

It can be found that, for the case of white noise, equation (4.1.56) reduces to the results in Appendix 4 of Janevski *et al.* (2012).

The Lyapunov exponent is given by

$$\lambda^{(1)}=-\lim_{p\to 0}\frac{e_0^{(K)}}{pe_1^{(K)}}=\frac{1}{64}\frac{A^{(1)}}{2k_{12}k_{21}S^- - k_{11}^2S(2\omega_1)-k_{22}^2S(2\omega_2)-7(k_{12}^2+k_{21}^2)S^+}, \tag{4.1.57}$$

where

$$\begin{aligned}A^{(1)}=&-\big[5(k_{12}^4+k_{21}^4)+74k_{12}^2k_{21}^2\big](S^+)^2+\big[-36k_{12}k_{21}(k_{12}^2+k_{21}^2)S^-\\&-(46k_{12}^2+30k_{21}^2)k_{11}^2S(2\omega_1)-(30k_{12}^2+46k_{21}^2)k_{22}^2S(2\omega_2)\\&+(288E_1+160E_2)k_{12}^2+(160E_1+288E_2)k_{21}^2\big]S^+\\&+12k_{12}^2k_{21}^2(S^-)^2+\big[4k_{11}^2k_{12}k_{21}S(2\omega_1)+4k_{22}^2k_{12}k_{21}S(2\omega_2)-64(E_1+E_2)k_{12}k_{21}\big]S^-\\&-13k_{11}^4S(2\omega_1)^2-13k_{22}^4S(2\omega_2)^2+\big[6k_{11}^2k_{22}^2S(2\omega_2)+(160E_1-96E_2)k_{11}^2\big]S(2\omega_1)\\&-(96E_1-160E_2)k_{22}^2S(2\omega_2)-512(E_1-E_2)^2.\end{aligned}$$

It is noted that only those values of the excitation spectrum at frequencies $2\omega_1$, $2\omega_2$, and $\omega_1\pm\omega_2$ have an effect on the stability condition. Substituting the power spectral density of white noises $S(\omega)=S_0$ and $k_{11}=k_{22}=0$ into equation (4.1.56) and solving equation (4.1.55) give the moment Lyapunov exponent for white noises

$$\begin{aligned}\Lambda^{(1)+}(p)=\Lambda^{(1)-}(p)=&\Big(\frac{3}{128}p^2+\frac{11}{64}p-\frac{7}{16}\Big)k^2S_0-\frac{p}{2}\big(E_1+E_2\big)\\&+\frac{1}{128}\Big[\big(3136+224p+116p^2+4p^3+p^4\big)k^4S_0^2+2048p(p+2)(E_1-E_2)^2\Big]^{1/2}.\end{aligned} \tag{4.1.58}$$

The moment stability boundary is then obtained as

$$\begin{aligned}&\Big(\frac{3}{128}p^2+\frac{11}{64}p-\frac{7}{16}\Big)k^2S_0-\frac{p}{2}\big(E_1+E_2\big)\\&+\frac{1}{128}\Big[\big(3136+224p+116p^2+4p^3+p^4\big)k^4S_0^2+2048p(p+2)(E_1-E_2)^2\Big]^{1/2}=0.\end{aligned} \tag{4.1.59}$$

From this boundary, one can establish the relation betweenship E_1 and E_2, and the critical excitation S_0.

The corresponding largest Lyapunov exponents are

$$\lambda^{(1)+}(p)=\lambda^{(1)-}(p)=\frac{1}{112}\frac{21k^4S_0^2-56k^2S_0(E_1+E_2)+32(E_1-E_2)^2}{k^2S_0}, \tag{4.1.60}$$

where $\Lambda^{(1)+}$ and $\lambda^{(1)+}$ correspond to symmetric coupling with first-order expansion, while $\Lambda^{(1)-}$ and $\lambda^{(1)-}$ correspond to skew-symmetric coupling with first-order expansion.

The almost-sure stability region is found to be

$$21k^4S_0^2-56k^2S_0(E_1+E_2)+32(E_1-E_2)^2<0. \tag{4.1.61}$$

Case 2: Fourier cosine series expansion order $K=2$

When $K=2$, the eigenfunction is $T(\varphi)=C_0+C_1\cos 2\varphi+C_2\cos 4\varphi$, the moment Lyapunov exponent can be solved from

$$\begin{vmatrix} a_{00}-\hat{\Lambda}^{(2)} & a_{01} & a_{02} \\ a_{10} & a_{11}-\hat{\Lambda}^{(2)} & a_{12} \\ a_{20} & a_{21} & a_{22}-\hat{\Lambda}^{(2)} \end{vmatrix}=0. \tag{4.1.62}$$

This is a cubic equation, which is $\left(\hat{\Lambda}^{(2)}\right)^3+e_2^{(2)}\left(\hat{\Lambda}^{(2)}\right)^2+e_1^{(2)}\hat{\Lambda}^{(2)}+e_0^{(2)}=0.$ The coefficients for symmetric coupled systems with white noise ($S(\omega)=S_0$, $k12=k21=k$,and $k11=k22=0$) are given by

$$e_2^{(2)}=-\frac{1}{256}\left(13p^2+\frac{17}{32}p-\frac{27}{8}\right)S_0k^2+\frac{3}{2}p(E_1+E_2),$$

$$e_1^{(2)}=S_0^2k^4\left(\frac{3}{2048}p^4+\frac{13}{512}p^3-\frac{55}{512}p^2-\frac{143}{128}p+\frac{35}{16}\right)-S_0k^2(E_1+E_2\left(\frac{5}{64}p^3+\frac{17}{32}p^2-\frac{27}{8}p\right)$$
$$+\left(\frac{9}{16}E_1^2+\frac{9}{16}E_2^2+\frac{15}{8}E_1E_1\right)p^2+(E_1-E_2)^2\left(\frac{1}{2}-\frac{3}{8}p\right),$$

$$e_0^{(2)}=-S_0^3k^6\left(\frac{1}{131072}p^6+\frac{15}{65536}p^5-\frac{1}{32768}p^4-\frac{427}{16384}p^3+\frac{1}{1024}p^2+\frac{357}{1024}p\right)$$
$$+S_0^2k^4(E_1+E_2)\left(\frac{3}{4096}p^5+\frac{13}{1024}p^4-\frac{55}{1024}p^3-\frac{143}{256}p^2+\frac{35}{32}p\right)$$

$$+S_0k^2\Big[-\big(\frac{5}{512}E_1^2+\frac{5}{512}E_2^2+\frac{15}{256}E_1E_2\big)p^4-\big(\frac{9}{128}E_1^2+\frac{9}{128}E_2^2+\frac{25}{64}E_1E_2\big)p^3$$
$$+\big(\frac{89}{128}E_1^2+\frac{89}{128}E_2^2+\frac{127}{64}E_1E_2\big)p^2-\big(\frac{33}{32}E_1^2+\frac{33}{32}E_2^2-\frac{33}{16}E_1E_2\big)p\Big]$$
$$+\big(\frac{1}{32}E_1^3+\frac{1}{32}E_2^3+\frac{15}{32}E_1^2E_2+\frac{15}{32}E_1E_2^2\big)p^3+(E_1^3+E_2^3-E_1^2E_2-E_1E_2^2)\big(\frac{1}{4}p-\frac{3}{16}p^2\big). \tag{4.1.63}$$

The analytical expression for moment Lyapunov exponent can then be obtained by solving this cubic equation. However, for $K\geqslant 3$, no explicit expressions can be presented, as quartic equation is involved.

The Lyapunov exponent for $K=2$ is given by

$$\lambda^{(2)}=-\lim_{p\to 0}\frac{e_0^{(2)}}{pe_1^{(2)}}=\frac{1}{256}\frac{A^{(2)}}{B^{(2)}}, \tag{4.1.64}$$

where

$$\begin{aligned}A^{(2)}=&\,22848S_0^3k^6+\big[14480\big(k_{11}^2+k_{22}^2\big)S_0-71680(E_1+E_2)\big]S_0^2k^4\\&+\Big\{\big(2076k_{11}^4+2076k_{22}^4-72k_{11}^2k_{22}^2\big)S_0^2\\&+\big[(10752k_{11}^2-23040k_{22}^2)E_2+(10752k_{22}^2-23040k_{11}^2)E_1\big]S_0\\&+67584(E_1-E_2)^2\Big\}S_0k^2+\big(k_{11}^4k_{22}^2+k_{11}^2k_{22}^4+75k_{11}^6+75k_{22}^6\big)S_0^3\\&+\Big[(512k_{22}^4+256k_{22}^2k_{22}^2-1280k_{11}^4)E_1+(512k_{11}^4+256k_{22}^2k_{22}^2-1280k_{22}^4)E_2\Big]S_0^2\\&+\Big[(7680k_{11}^2-512k_{22}^2)E_1^2-7168(k_{11}^2+k_{22}^2)E_1E_2+(7680k_{22}^2-512k_{11}^2)E_2^2\Big]S_0\\&-16384\big(E_1^3+E_2^3-E_1^2E_2-E_1E_2^2\big),\\B^{(2)}=&\,560S_0^2k^4+48\big(k_{11}^2+k_{22}^2\big)S_0^2k^2+\big(3k_{11}^4+3k_{22}^4-2k_{22}^2k_{22}^2\big)S_0^2\\&+32\Big[\big(k_{22}^2-k_{11}^2\big)E_1+\big(k_{11}^2-k_{22}^2\big)E_2\Big]S_0+128(E_1-E_2)^2.\end{aligned}$$

The second-order expansion $K=1$ is almost as accurate as other higher-order expansions, as shown in Figures 4.1 for moment Lyapunov exponents and 4.2 for Lyapunov exponents.

Figure 4.2 illustrates that Lyapunov moments converge so quickly with the increase of expansion order K that results of $K=1$ are accurate enough.

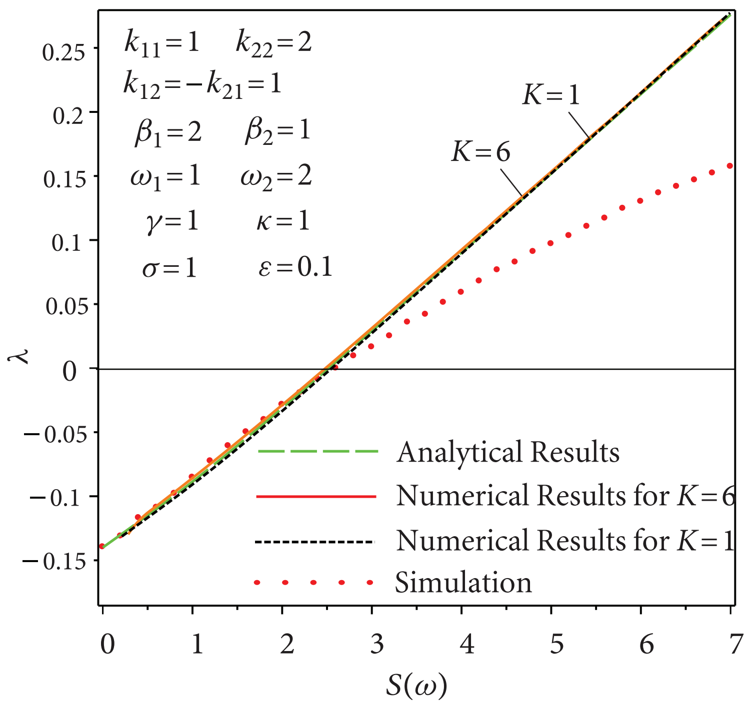

Figure 4.2 Comparison of Lyapunov exponents of coupled system under white noise

4.1.4 Simulation

Monte Carlo simulation is applied to determine the pth moment Lyapunov exponents and to check the accuracy of the approximate results from the stochastic averaging.

Case 1: The wide-band noise is taken as Gaussian white noise

Suppose the excitation is approximated by a Gaussian white noise with spectral density $S(\omega)=\sigma^2=constant$ for all ω, and then $\xi(t)\mathrm{d}t=\sigma\,\mathrm{d}W(t)$. Let

$$\begin{aligned} &x_1(t)=q_1(t), \quad x_2(t)=\dot{q}_1(t), \quad x_3(t)=q_2(t), \quad x_4(t)=\dot{q}_2(t), \\ &x_5(t)=\int_0^t \gamma\,\mathrm{e}^{-\kappa(t-s)}q_1(s)\,\mathrm{d}s, \quad x_6(t)=\int_0^t \gamma\,\mathrm{e}^{-\kappa(t-s)}q_2(s)\,\mathrm{d}s. \end{aligned} \tag{4.1.65}$$

Equation (4.1.1) can be written as an 6 dimensional system of Itô differential equations

$$\mathrm{d}\mathbf{x} = \mathbf{A}\mathbf{x}\mathrm{d}t + \mathbf{B}\mathbf{x}\sigma\,\mathrm{d}W, \tag{4.1.66}$$

where $\mathbf{x} = \{x_1, x_2, x_3, x_4, x_5, x_6\}^T$, and

$$\mathbf{A} = \begin{bmatrix} 0 & 1 & 0 & 0 & 0 & 0 \\ -\omega_1^2 & -2\varepsilon\beta_1 & 0 & 0 & -\varepsilon\omega_1^2 & 0 \\ 0 & 0 & 0 & 1 & 0 & 0 \\ 0 & 0 & -\omega_2^2 & -2\varepsilon\beta_2 & 0 & -\varepsilon\omega_2^2 \\ \gamma & 0 & 0 & 0 & -\kappa & 0 \\ 0 & 0 & \gamma & 0 & 0 & -\kappa \end{bmatrix},$$

$$\mathbf{B} = \begin{bmatrix} 0 & 0 & 0 & 0 & 0 & 0 \\ -\varepsilon^{1/2}\omega_1 k_{11} & 0 & -\varepsilon^{1/2}\omega_1 k_{12} & 0 & 0 & 0 \\ 0 & 0 & 0 & 0 & 0 & 0 \\ -\varepsilon^{1/2}\omega_2 k_{21} & 0 & -\varepsilon^{1/2}\omega_2 k_{22} & 0 & 0 & 0 \\ 0 & 0 & 0 & 0 & 0 & 0 \\ 0 & 0 & 0 & 0 & 0 & 0 \end{bmatrix}. \tag{4.1.67}$$

Equation (4.1.66) is linear homogeneous. The algorithm proposed by Xie (2006) and Wolf *et al.* (1985) are applied to simulate the moment Lyapunov exponents and Lyapunov exponents, respectively. The norm for simulations is $\|\mathbf{x}(t)\| = \sqrt{\sum_{i=1}^{6} x_i^2}$. The iteration equations are given by, using the explicit Euler scheme,

$$\begin{aligned} x_1^{k+1} &= x_1^k + x_2^k \cdot \Delta t, \\ x_2^{k+1} &= x_2^k + \left(-\omega_1^2 x_1^k - 2\varepsilon\beta_1 x_2^k + \varepsilon\omega_1^2 x_5^k\right)\Delta t - \varepsilon^{1/2}\omega_1 (k_{11}x_1^k + k_{12}x_3^k)\sigma \cdot \Delta W^k, \\ x_3^{k+1} &= x_3^k + x_4^k \cdot \Delta t, \\ x_4^{k+1} &= x_4^k + \left(-\omega_2^2 x_3^k - 2\varepsilon\beta_2 x_4^k + \varepsilon\omega_2^2 x_6^k\right)\Delta t - \varepsilon^{1/2}\omega_2 (k_{21}x_1^k + k_{22}x_3^k)\sigma \cdot \Delta W^k, \\ x_5^{k+1} &= x_5^k + \left(\gamma x_1^k - \kappa x_5^k\right)\Delta t, \\ x_6^{k+1} &= x_6^k + \left(\gamma x_3^k - \kappa x_6^k\right)\Delta t, \end{aligned} \tag{4.1.68}$$

with Δt being the time step and k denoting the kth iteration.

Case 2: The wide-band noise is taken as a real noise

Denoting

$$\begin{aligned} &x_1(t)=q_1(t), \quad x_2(t)=\dot{q}_1(t), x_3(t)=q_2(t), \quad x_4(t)=\dot{q}_2(t),\\ &x_5(t)=\int_0^t \gamma\, \mathrm{e}^{-\kappa(t-s)} q_1(s)\,\mathrm{d}s, \quad x_6(t)=\int_0^t \gamma\, \mathrm{e}^{-\kappa(t-s)} q_2(s)\,\mathrm{d}s, \\ &x_7(t)=\xi(t), \end{aligned} \tag{4.1.69}$$

equation (4.1.1) can be converted to the Itô differential equations

$$\mathrm{d}\mathbf{x}=\mathbf{A}\,\mathbf{x}\mathrm{d}t+\mathbf{B}\mathrm{d}W, \tag{4.1.70}$$

where $\mathbf{x}=\{x_1,x_2,x_3,x_4,x_5,x_6,x_7\}^T$, and

$$\mathbf{A}=\begin{bmatrix} 0 & 1 & 0 & 0 & 0 & 0 & 0\\ -\omega_1^2 & -2\varepsilon\beta_1 & 0 & 0 & -\varepsilon\omega_1^2 & 0 & -\varepsilon^{1/2}\omega_1(k_{11}x_1+k_{12}x_3)\\ 0 & 0 & 0 & 1 & 0 & 0 & 0\\ -\omega_2^2 & -2\varepsilon\beta_2 & 0 & 0 & 0 & -\varepsilon\omega_2^2 & -\varepsilon^{1/2}\omega_2(k_{21}x_1+k_{22}x_3)\\ \gamma & 0 & 0 & 0 & -\kappa & 0 & 0\\ 0 & 0 & \gamma & 0 & 0 & -\kappa & 0\\ 0 & 0 & 0 & 0 & 0 & 0 & -\alpha \end{bmatrix}, \quad \mathbf{B}=\begin{bmatrix}0\\0\\0\\0\\0\\0\\\sigma\end{bmatrix}. \tag{4.1.71}$$

Thus the discretized equations using explicit Euler scheme are

$$\begin{aligned} x_1^{k+1}&=x_1^k+x_2^k\cdot\Delta t,\\ x_2^{k+1}&=x_2^k+\left[-\omega_1^2x_1^k-2\varepsilon\beta_1x_2^k+\varepsilon\omega_1^2x_5^k-\varepsilon^{1/2}\omega_1(k_{11}x_1^k+k_{12}x_3^k)x_7^k\right]\Delta t,\\ x_3^{k+1}&=x_3^k+x_4^k\cdot\Delta t,\\ x_4^{k+1}&=x_4^k+\left[-\omega_2^2x_3^k-2\varepsilon\beta_2x_4^k+\varepsilon\omega_2^2x_6^k-\varepsilon^{1/2}\omega_2(k_{21}x_1^k+k_{22}x_3^k)x_7^k\right]\Delta t,\\ x_5^{k+1}&=x_5^k+\left(\gamma x_1^k-\kappa x_5^k\right)\Delta t,\\ x_6^{k+1}&=x_6^k+\left(\gamma x_3^k-\kappa x_6^k\right)\Delta t,\\ x_7^{k+1}&=x_7^k+\left(-\alpha x_7^k\right)\cdot\Delta t+\sigma\cdot\Delta W^k, \end{aligned} \tag{4.1.72}$$

with Δt being the time step and k denoting the kth iteration.

Results and discussion

In Figure 4.3, the analytical results of Lyapunov exponents from equation (4.1.51) and numerical results from (4.1.50) are compared so well that they are almost overlapped, which show that the long and tedious derivations in Sections 4.1.1 and 4.1.2 are correct.

Figure 4.3 also shows that for small values of $S(\omega)$, the numerical results are consistent with simulation results. The analytical and numerical Lyapunov exponents in Figures 4.3 and 4.2 are tangent lines of results from Monte-Carlo simulation, which confirms the method of stochastic averaging is a valid first-order approximation method. In the Monte Carlo simulation, the sample size for estimating the expected value is $N=5000$, time step is $\Delta t=0.0005$, and the number of iteration is 10^8.

Care should be taken that for $S(\omega)\rightarrow 0$, the numerical results may become unstable due to roundoff errors. It is noted that although the numerical and analytical results in Figure 4.3 are almost overlapped, the analytical expressions from equation (4.1.51) to (4.1.53) seem not to agree with the expression given in equation (4.1.57). This can be explained by the discrepancy between exact solutions and a sequence of approximations.

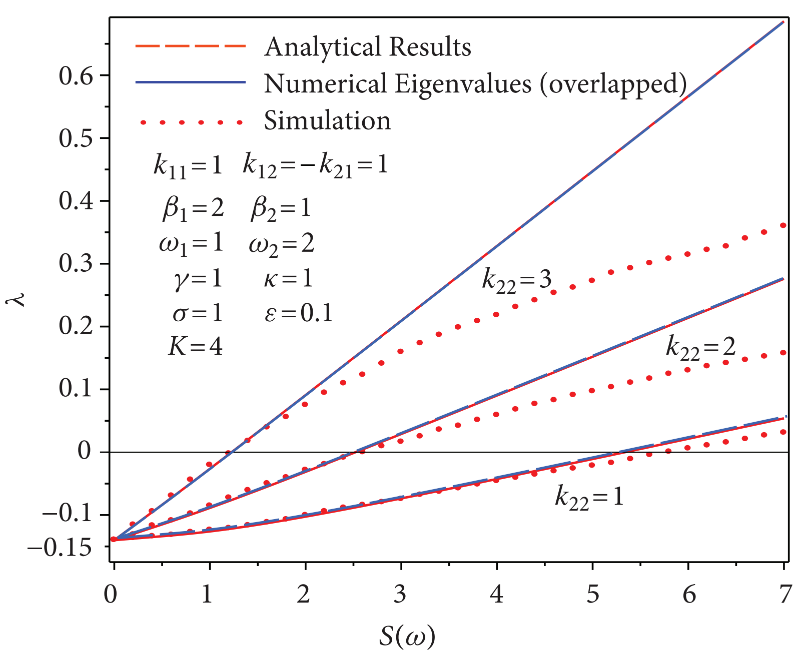

Figure 4.3 Lyapunov exponents of couple system excited by white noise

4.1.5 Stability Index

The stability index is the non-trivial zero of the moment Lyapunov exponent. Hence, it can be determined as a root-finding problem such that $\Lambda_{q(t)}(\delta_{q(t)})=0$. Here we consider the case for white noises. When $K=1$, the stability index is the non-trivial solution of equation (4.1.59). Typical results of the stability index are shown in Figure 4.4. It is seen that the stability index decreases from positive to negative values with the increase of the amplitude of power spectrum, which suggests that the noise destabilize the system. It is also found that the larger the pseudo-damping coefficient E_1, the larger the stability index, and then the more stable the system.

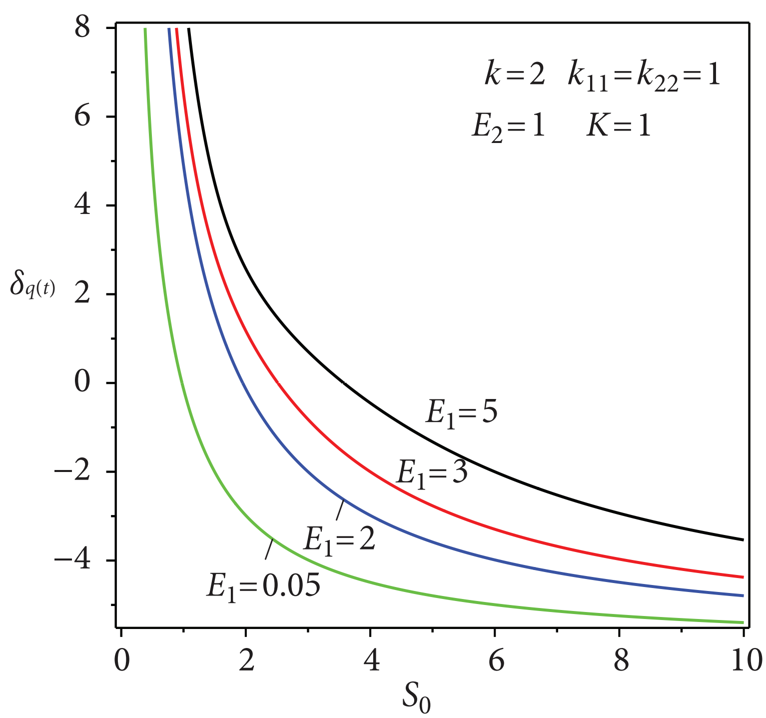

Figure 4.4 Stability index of coupled system under white noise

4.1.6 Application: Flexural-Torsional Stability of a Rectangular Beam

As an application, the flexural-torsional stability of a simply supported, uniform, narrow, rectangular, viscoelastic beam of length L subjected to a stochastically varying concentrated load $P(t)$ acting at the center of the beam cross-section as shown in Figure 4.5 is considered. Both non-follower and follower loading cases are studied.

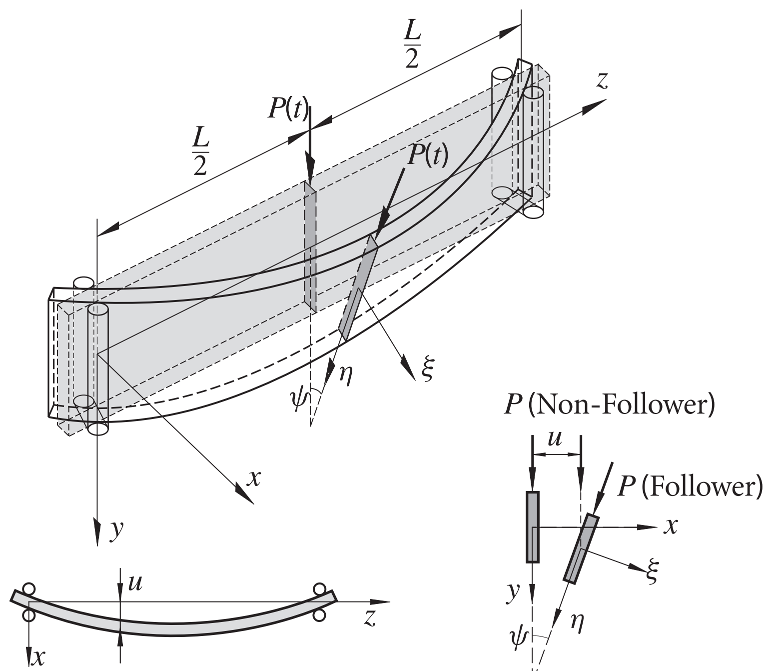

Figure 4.5 Flexural-torsional vibration of a rectangular beam

For the elastic beam under dynamic loading, the flexural and torsional equations of motion are given by (Xie, 2006)

$$\begin{aligned} &EI_y\frac{\partial^4 u}{\partial z^4}+\frac{\partial^2(M_x\psi)}{\partial z^2}-\frac{\partial^2 M_y}{\partial z^2}+m\frac{\partial^2 u}{\partial t^2}+D_u\frac{\partial u}{\partial t}=0,\\ &-GJ\frac{\partial^2\psi}{\partial z^2}+\frac{\partial M_x}{\partial z}\frac{\partial u}{\partial t}+M_x\frac{\partial^2 u}{\partial z^2}+\frac{\partial M_z}{\partial z}+mr^2\frac{\partial^2\psi}{\partial t^2}+D_\psi\frac{\partial\psi}{\partial t}=0,\end{aligned} \tag{4.1.73}$$

with boundary conditions

$$u(0,t)=u(L,t)=\frac{\partial^2 u(0,t)}{\partial z^2}=\frac{\partial^2 u(L,t)}{\partial z^2}=0,$$
$$\psi(0,t)=\psi(L,t)=0, \tag{4.1.74}$$

where M_x, M_y, and M_z are the bending moments in the x, y, and z direction, respectively. $u(t)$ is the lateral deflection and $\psi(t)$ is the angle of twist. E is Young's modulus of elasticity G is the shear modulus. I_y is the moment of inertia in the y direction. J is Saint-Venant's torsional constant. EI_y is the flexural rigidity, GJ is the torsional rigidity, m is the mass per unit length of the beam, r is the polar radius of gyration of the cross-section, D_ψ and D_u are the viscous damping coefficients in the ψ and u directions,respectively, t is time and z is the axial coordinate.

For problems with viscoelastic materials, one may replace the elastic moduli E and G in elastic problems by the Voltera operators $E(1-\mathscr{H})$ and $G(1-\mathscr{H})$, respectively (Abdelrahman, 2002). The governing equation for a viscoelastic deep beam can be obtained from equation (4.1.73) as

$$EI_y(1-\mathscr{H})\frac{\partial^4 u}{\partial z^4}+\frac{\partial^2(M_x\psi)}{\partial z^2}-\frac{\partial^2 M_y}{\partial z^2}+m\frac{\partial^2 u}{\partial t^2}+D_u\frac{\partial u}{\partial t}=0,$$
$$-GJ(1-\mathscr{H})\frac{\partial^2\psi}{\partial z^2}+\frac{\partial M_x}{\partial z}\frac{\partial u}{\partial z}+M_x\frac{\partial^2 u}{\partial z^2}+\frac{\partial M_z}{\partial z}+mr^2\frac{\partial^2\psi}{\partial t^2}+D_\psi\frac{\partial\psi}{\partial t}=0. \tag{4.1.75}$$

These equations are partial stochastic differential equations and are difficult to analyze. An approximate solution can be used such as the Galerkin method. Seek solutions of the form

$$u(z,t)=q_1\sin\frac{\pi z}{L},\qquad \psi(z,t)=q_2\sin\frac{\pi z}{L}, \tag{4.1.76}$$

in which $q_1=u_m=u\left(\frac{1}{2}L,t\right), q_2=\psi_m=\psi\left(\frac{1}{2}L,t\right)$. Substituting into equation (4.1.75), multiplying by $\sin(\pi z/L)$, and integrating with respect to z from 0 to L yield (Xie, 2006)

$$\ddot{Q}_1+2\beta_1\dot{Q}_1+\omega_1^2(1-\mathscr{H})Q_1+\omega_1 k_{12}\xi(t)Q_2=0,$$
$$\ddot{Q}_2+2\beta_2\dot{Q}_2+\omega_2^2(1-\mathscr{H})Q_2+\omega_2 k_{21}\xi(t)Q_1=0, \tag{4.1.77}$$

where

$$K=\sqrt{\frac{\omega_2(12-\pi^2)}{\omega_1(4+\pi^2)}},\quad \beta_1=\frac{D_u}{2m},\quad \beta_2=\frac{D_\psi}{2mr^2},\quad \omega_1^2=\left(\frac{\pi}{L}\right)^4\frac{EI_y}{m},\quad \omega_2^2=\left(\frac{\pi}{L}\right)^2\frac{GJ}{mr^2},$$

$$\xi(t)=\frac{P(t)}{P_{cr}},\quad P_{cr}=\frac{4mrL|\omega_1^2-\omega_2^2|}{\left[(12-\pi^2)(4+\pi^2)\right]^{1/2}},\quad k_{12}=-k_{21}=\frac{|\omega_1^2-\omega_2^2|}{2\sqrt{\omega_1\omega_2}}=k_F,\tag{4.1.78}$$

where β_1 and β_2 are reduced viscous damping coefficients, P_{cr} is the critical force for the simply supported narrow rectangular beam.

For the non-follower force case, the only difference is that $M_y=0$ in equation (4.1.75). The equations of motion are of the same form of (4.1.77), but the parameters are different,

$$\begin{aligned}&K=-\sqrt{\frac{\omega_2}{\omega_1}},\quad 2\beta_1=\frac{D_u}{m},\quad 2\beta_2=\frac{D_\psi}{mr^2},\quad \omega_1^2=\left(\frac{\pi}{L}\right)^4\frac{EI_y}{m},\quad \omega_2^2=\left(\frac{\pi}{L}\right)^2\frac{GJ}{mr^2},\\&\xi(t)=\frac{P(t)}{P_{cr}},\quad P_{cr}=\frac{8mrL\omega_1\omega_2}{4+\pi^2},\quad k_{12}=k_{21}=\sqrt{\omega_1\omega_2}=k_N.\end{aligned}\tag{4.1.79}$$

It is seen that equation (4.1.77) has the same form of (4.1.1), except that $k_{11}=k_{22}=0$. By introducing the polar transformation and using the method of stochastic averaging, equation (4.1.77) can be approximated in amplitude by Itô stochastic differential equations in (4.1.11), where the drift and diffusion terms are given by

$$\begin{aligned}&m_i^a=a_i\left[-\beta_i-\tau_\varepsilon\underset{t}{\mathscr{M}}\{I_i^{sc}\}+\frac{1}{8}k_{ij}k_{ji}S^-\right]+\frac{1}{16}\frac{a_j^2}{a_i}k_{ij}^2S^+,\\&b_{ii}^a=\frac{1}{8}k_{ij}^2a_j^2S^+,\quad b_{ij}^a=\frac{1}{8}a_ia_jk_{ij}k_{ji}S^-,\quad S^\pm=S(\omega_1+\omega_2)\pm S(\omega_1-\omega_2).\end{aligned}\tag{4.1.80}$$

Substituting equation (4.1.80) and $a_1=r\cos\varphi$, $a_2=r\sin\varphi$ into (4.1.42) yields the eigenvalue problem, from which moment Lyapunov exponents can be determined by solving equation (4.1.48).

Some analytical stability boundaries are discussed here. For non-follower symmetric coupled systems under white noise excitations, the moment stability boundaries can be obtained from equation (4.1.59), and the almost-sure stability boundaries are from (4.1.61), which are shown in Figure 4.6. It is found that the moment stability boundaries are more conservative than the almost-sure boundary. With p increase, these moment boundaries become more and more conservative.

One can also obtain the critical amplitude of power spectrum excitation of white noise from equation (4.1.59) and (4.1.61), which is illustrated in Figure 4.7. It is found that the critical excitation increases with the pseudo-damping coefficient, which confirms that damping and viscoelasticity would consume some energy of motion during vibration. A small amplitude of excitation would destabilize the system with respect to higher-order moment stability, which suggests that stability region with higher-order moment is more conservative than that with lower-order moment stability. The almost-sure stability is the least conservative. Some numerical values for discrete points already shown in Figure 4.7 are listed in Table 4.1 for reference.

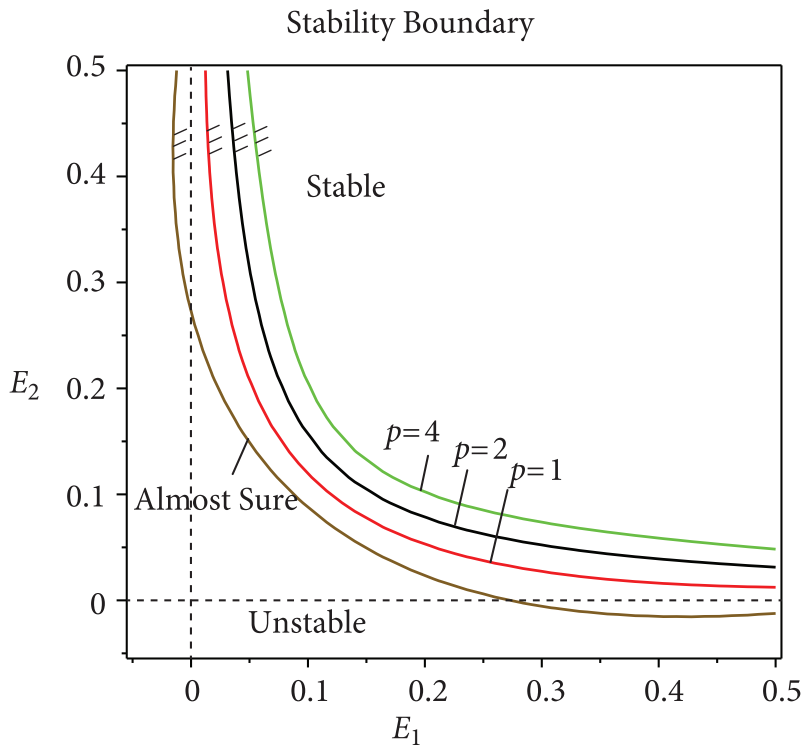

Figure 4.6 Almost-sure and pth moment stability boundaries of coupled system under white noise

4.1.7 Results and Discussion

As expected, both fractional order μ and damping β play a stabilizing role in flexural-torsional analysis of the beam under white noise excitation. Figures 4.8 and 4.9 show that with the increase of μ or β, the slope of the moment curves at the original point change from negative to positive, which suggests the beam's status changes from instability to stability.

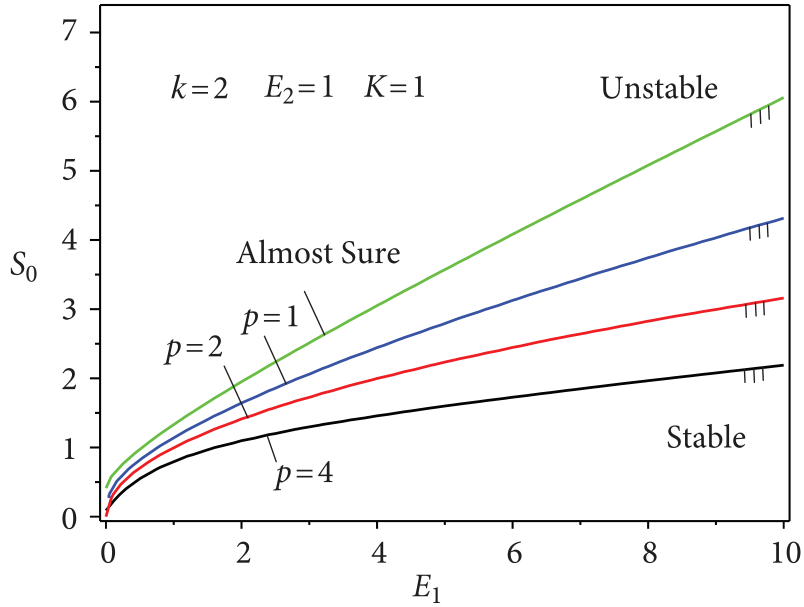

Figure 4.7 Critical excitation and pseudo-damping of coupled system under white noise

Table 4.1 Critical excitations s_0 for case $K=1$ under white noise

E_1	$p=0$	$p=1$	$p=2$	$p=4$
0	0.4593	0.2500	0	0.1000
2	1.9512	1.6443	1.4142	1.1000
4	3.0526	2.4459	2.0000	1.4600
6	4.0836	3.1290	2.4495	1.7286
8	5.0816	3.7463	2.8284	1.9667
10	6.0605	4.3184	3.1623	2.1909

As discussed in Figure 3.5, the retardation (τ_ε) stabilizes the SDOF system. This is conformed in Figure 4.10 for fractional coupled system.

The two ordinary viscosity parameters are studied in Figures 4.11 and 4.12, which shows that the viscoelastic intensity γ has a stabilizing effect but κ plays a destabilizing effect on systems under white noise. With the increase of of γ, the stability region for $p>0$ becomes wider such that the viscoelasticity help stabilization. However, the decrease of κ means the relaxation time increases, the stability region for $p > 0$ also becomes wider, which shows larger relaxation time helps to stabilize the system. The effect of destabilization is prominent only when κ is small. As κ exceeds 10, large increase of κ produces very small effect on stabilization. These results can be extended to systems under real noises.

Figures 4.13 and 4.14 illustrate the variation of moment Lyapunov exponents with respect to the parameters of real noises. The larger the noise parameter σ, the narrower the stability region for $p > 0$, the more unstable the system. On the contrary, the parameter α plays a stabilizing role, i.e., with the increase of α, the stability region of the pth moment (for $p > 0$) increase and the system is more stable. This can be explained from equation (1.2.4), which suggests that smaller σ or larger α reduces the power cosine spectral density. Then the power of noise would spread over a wider frequency band, which in turn reduces the power of the noise in the neighborhood of resonance and stabilizes the system.

As seen from Figures 4.11 to 4.15, the simulation results are compared well with the numerical approximation results, which shows that the method based upon stochastic averaging can be used for stability analysis of coupled non-gyroscopic systems.

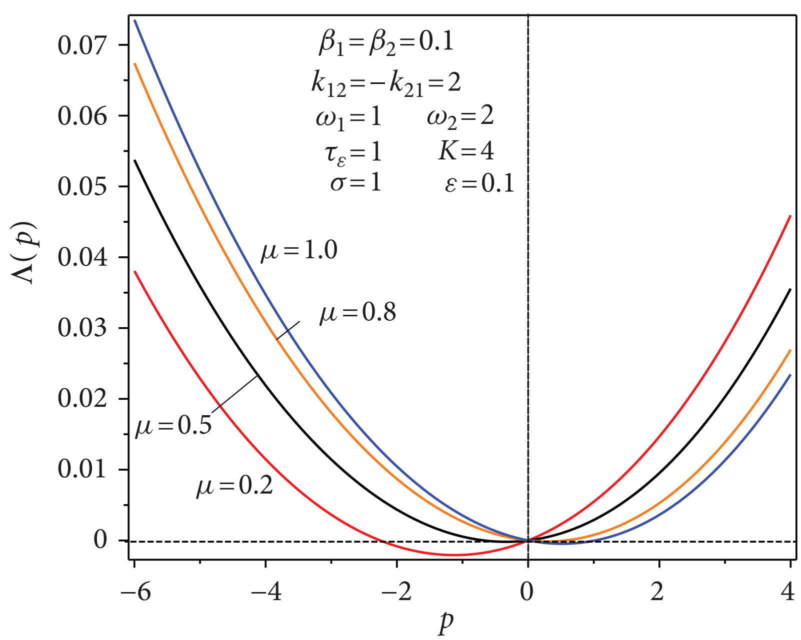

Figure 4.8 Effect of fractional order on fractional coupled system under white noise excitation

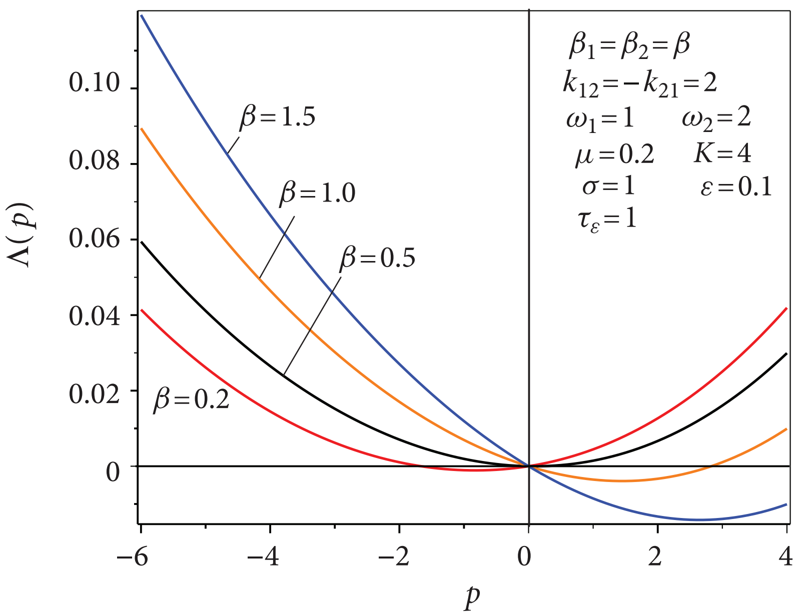

Figure 4.9 Effect of damping on fractional coupled system under white noise excitation

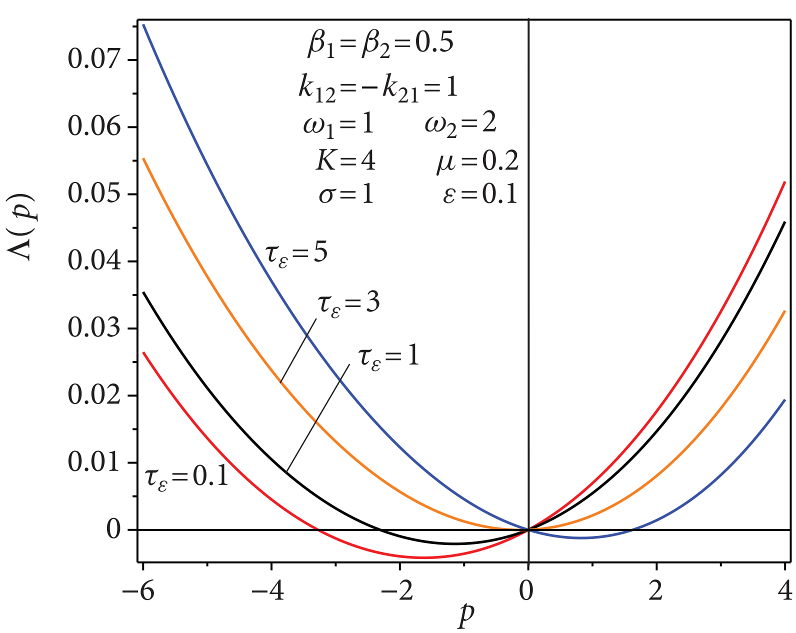

Figure 4.10 Effect of τ_ε on fractional coupled system under white noise excitation

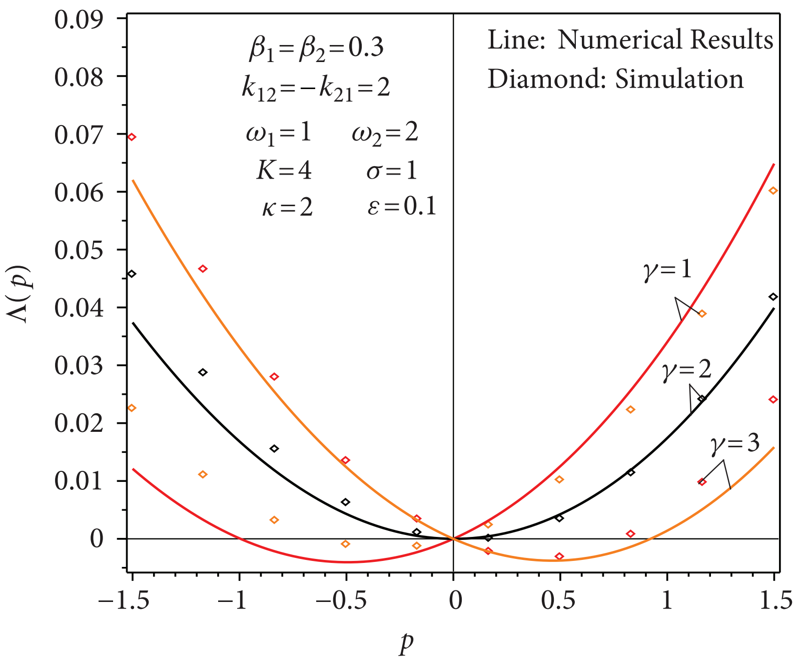

Figure 4.11 Effect of viscosity γ on coupled system under white noise excitation

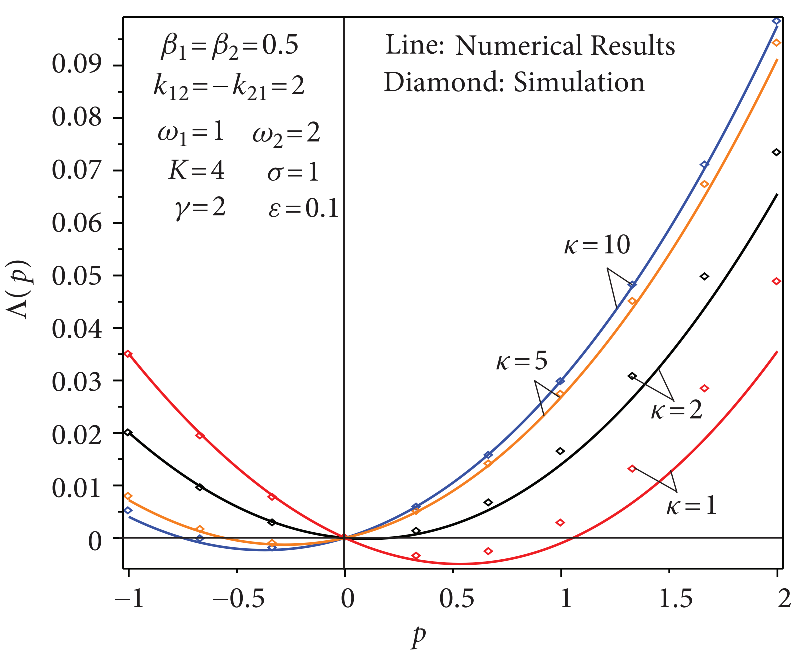

Figure 4.12 Effect of viscosity κ on coupled system under white noise excitation

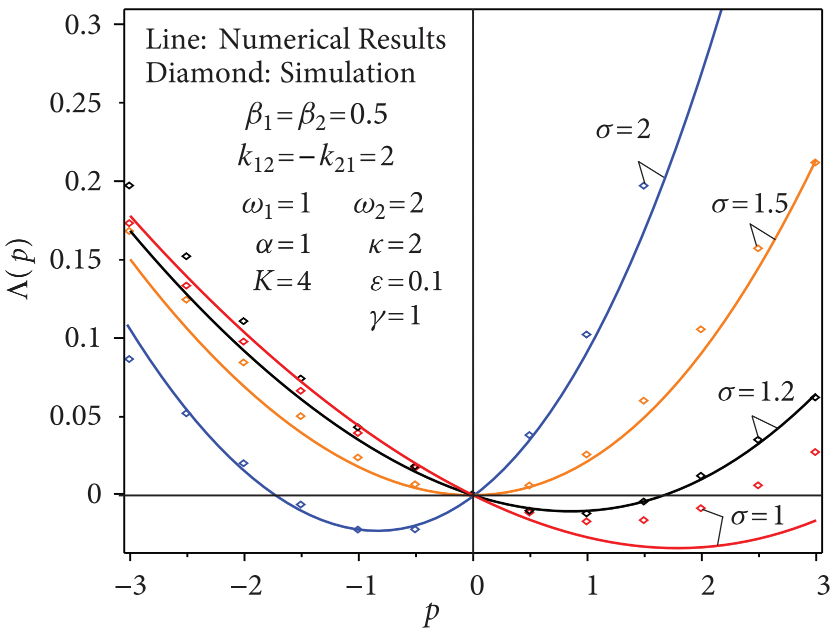

Figure 4.13 Effect of σ on coupled system under real noise excitation

4.2 Coupled Systems Excited by Bounded Noise

4.2.1 Formulation

Consider the following coupled system excited by bounded noise, which is similar to equation (4.1.1),

$$q_1'' + 2\varepsilon\zeta_1\omega_1 q_1' + \omega_1^2[1 - 2\varepsilon\mathscr{H}]q_1 + 2\varepsilon\omega_1^2(k_{11}q_1 + k_{12}q_2)\bar{\zeta}(\tau) = 0, \tag{4.2.1a}$$

$$q_2'' + 2\varepsilon\zeta_2\omega_2 q_2' + \omega_2^2[1 - 2\varepsilon\mathscr{H}]q_2 + 2\varepsilon\omega_2^2(k_{21}q_1 + k_{22}q_2)\bar{\zeta}(\tau) = 0, \tag{4.2.1b}$$

$$\bar{\zeta}(\tau) = \zeta\cos[\nu\tau + \sigma_0 W(\tau) + \theta], \tag{4.2.1c}$$

where the prime denotes differentiation with respect to time τ, $\bar{\zeta}(\tau)$ is a bounded noise.

To simplify the system, one may apply the time scaling $t = \nu\tau$. To investigate the cases of combination resonances when $\nu = \omega_0(1 - \varepsilon\Delta)$, where Δ is the detuning parameter and the small parameter ε shows that the excitation frequency ν vary around the reference frequency ω_0. The parameter ω_0 is assumed to be the following cases: $\omega_0 \neq 2\omega_i$, $\omega_0 = 2\omega_i$, and $\omega_0 = |\omega_1 \pm \omega_2|$.

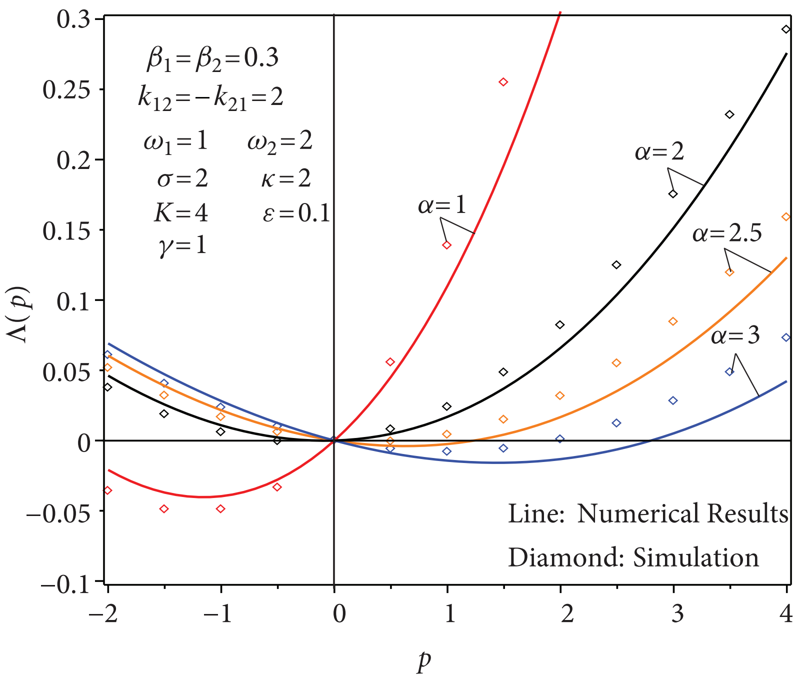

Figure 4.14 Effect of α on coupled system under real noise excitation

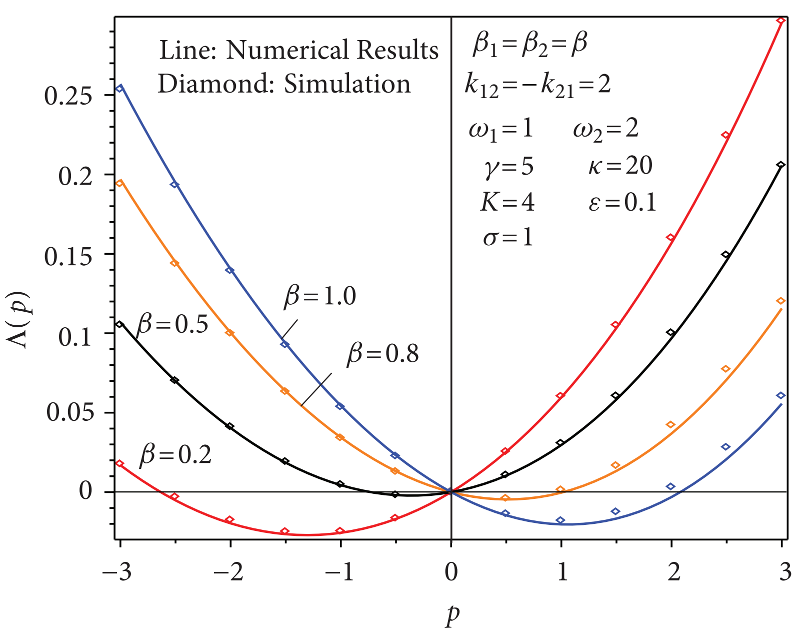

Figure 4.15 Effect of damping on coupled system under white noise excitation

Using $\kappa_i = \omega_i/\omega_0 \neq 0, i=1, 2$, and $(1-\varepsilon\Delta)^{-2} \approx 1+2\varepsilon\Delta$, equation (4.2.1) becomes, after dropping terms of order $o(\varepsilon)$,

$$\begin{aligned}
&\ddot{q}_1(t)+\kappa_1^2 q_1(t)\\
&=2\varepsilon\kappa_1\Big\{-\zeta_1\dot{q}_1(t)-\kappa_1\Delta q_1(t)+\kappa_1\mathscr{H}\, q_1(t)-\kappa_1\big[k_{11}q_1(t)+k_{12}q_2(t)\big]\zeta\cos\eta(t)\Big\},\\
&\ddot{q}_2(t)+\kappa_2^2 q_2(t)\\
&=2\varepsilon\kappa_2\Big\{-\zeta_2\dot{q}_2(t)-\kappa_2\Delta q_2(t)+\kappa_2\mathscr{H}\, q_2(t)-\kappa_2\big[k_{21}q_1(t)+k_{22}q_2(t)\big]\zeta\cos\eta(t)\Big\},
\end{aligned} \tag{4.2.2}$$

where the dot denotes differentiation with respect to time t and

$$\eta(t)=t+\psi(t), \quad \psi(t)=\varepsilon^{1/2}\sigma W(t)+\theta, \quad \sigma=\sigma_0/\sqrt{\nu}. \tag{4.2.3}$$

Equations (4.2.2) admit the trivial solution $q_1(t)=q_2(t)=0$. However, they are not the Lagrange standard form given in equation (1.2.27) or (1.2.40). Hence, to apply the averaging method, one should first consider the unperturbed system, i.e., $\varepsilon=0$ and $\xi(t)=0$, which is of the form: $\ddot{q}_i+\kappa_i^2 q_i=0$, $i=1, 2$. The stable solutions for the unperturbed system are found to be in equation (4.1.6). Then the method of variation of parameters is used. Differentiating the first equation of (4.1.6) and comparing with the second equation lead to

$$\dot{a}_i\cos\Phi_i - a_i\dot{\phi}_i\sin\Phi_i=0. \tag{4.2.4}$$

Substituting equations (4.1.6) into (4.2.2) results in

$$\dot{a}_i\sin\Phi_i + a_i\dot{\phi}_i\cos\Phi_i=G_i, \tag{4.2.5}$$

where

$$\begin{aligned}
G_i=2\varepsilon\kappa_i\Big\{&-\zeta_i a_i\sin\Phi_i+\Delta a_i\cos\Phi_i-\mathscr{H}\,[a_i\cos\Phi_i]\\
&+\big[k_{ii}a_i\cos\Phi_i+k_{ij}a_j\cos\Phi_j\big]\zeta\cos\eta(t)\Big\}.
\end{aligned}$$

By solving equations (4.2.4) and (4.2.5), equations (4.2.2) can be written in amplitudes a_i and phase ϕ_i

$$\dot{a}_i=\varepsilon\kappa_i\Big\{a_i\Big[\zeta_i\big(\underline{\cos(2\kappa_i t+2\phi_i)}-1\big)+\Delta\underline{\sin(2\kappa_i t+2\phi_i)}-2I_i^{sc}\Big]$$

$$+\frac{1}{2}\zeta k_{ii}a_i\Big[\underline{\sin\Big((2\kappa_i+1)t+2\phi_i+\psi\Big)}+\sin\Big((2\kappa_i-1)t+2\phi_i-\psi\Big)\Big]$$

$$+\frac{1}{2}\zeta k_{ij}a_j\Big[\underline{\sin\Big((\kappa_i+\kappa_j+1)t+\phi_i+\phi_j+\psi\Big)}+\sin\Big((\kappa_i+\kappa_j-1)t+\phi_i+\phi_j-\psi\Big)$$

$$+\sin\Big((\kappa_i-\kappa_j+1)t+\phi_i-\phi_j+\psi\Big)+\sin\Big((\kappa_i-\kappa_j-1)t+\phi_i-\phi_j-\psi\Big)\Big]\Big\},$$

$$a_i\dot{\phi}_i=\varepsilon\kappa_i\Big\{a_i\Big[-\zeta_i\underline{\sin(2\kappa_i t+2\phi_i)}+\big(\underline{\cos(2\kappa_i t+2\phi_i)}+1\big)\Delta-2I_i^{cc}\Big]$$

$$+\frac{1}{2}\zeta k_{ii}a_i\Big[\underline{\cos\big((2\kappa_i+1)t+2\phi_i+\psi\big)}+\cos\big((2\kappa_i-1)t+2\phi_i-\psi\big)+2\underline{\cos(\psi+t)}\Big]$$

$$+\frac{1}{2}\zeta k_{ij}a_j\Big[\underline{\cos\big((\kappa_i+\kappa_j+1)t+\phi_i+\phi_j+\psi\big)}+\cos\big((\kappa_i+\kappa_j-1)t+\phi_i+\phi_j-\psi\big)$$

$$+\cos\big((\kappa_i-\kappa_j-1)t+\phi_i-\phi_j-\psi\big)+\cos\big((\kappa_i-\kappa_j+1)t+\phi_i-\phi_j+\psi\big)\Big]\Big\},$$

$$\dot{\psi}(t)=\varepsilon^{1/2}\sigma\dot{W}(t),\quad i=1,\,2,\quad i\neq j. \tag{4.2.6}$$

Because of the small parameter ε appearing on the right sides of equation (4.2.6), the stochastic averaging method can be applied to obtain the averaged equations. The underlined terms would vanish when the averaging operator is applied and the values of other sinusoidal terms depend on the κ_i and κ_j.

$$\dot{a}_i=\varepsilon\kappa_i a_i\big(-\zeta_i-2\bar{I}_i^{sc}\big)+\frac{1}{2}\varepsilon\kappa_i\zeta\underset{t}{\mathscr{M}}\Big\{k_{ii}a_i\underline{\sin\big((2\kappa_i-1)t+2\phi_i-\psi\big)}$$

$$+k_{ij}a_j\Big[\sin\big((\kappa_i+\kappa_j-1)t+\phi_i+\phi_j-\psi\big)+\boxed{\sin\big((\kappa_i-\kappa_j+1)t+\phi_i-\phi_j+\psi\big)}$$

$$+\sin\big((\kappa_i-\kappa_j-1)t+\phi_i-\phi_j-\psi\big)\Big]\Big\},$$

$$a_i\dot{\phi}_i=\varepsilon\kappa_i a_i\big(\Delta-2\bar{I}_i^{cc}\big)+\frac{1}{2}\varepsilon\kappa_i\zeta\underset{t}{\mathscr{M}}\Big\{k_{ii}a_i\underline{\cos\big((2\kappa_i-1)t+2\phi_i-\psi\big)}$$

$$+k_{ij}a_j\Big[\cos\big((\kappa_i+\kappa_j-1)t+\phi_i+\phi_j-\psi\big)+\boxed{\cos\big((\kappa_i-\kappa_j-1)t+\phi_i-\phi_j-\psi\big)}$$

$$+\cos\left((\kappa_i-\kappa_j+1)t+\phi_i-\phi_j+\psi\right)\Big]\Big\},$$

$$\bar{I}_i^{sc}=\underset{t}{\mathscr{M}}\{I_i^{sc}\},\quad \bar{I}_i^{cc}=\underset{t}{\mathscr{M}}\{I_i^{cc}\},\quad i=1,\,2,\quad i\neq j. \tag{4.2.7}$$

4.2.2 Parametric Resonances

Case 1: No Resonance: $\kappa_i \neq \frac{1}{2}$ and $|\kappa_1 \pm \kappa_2| \neq 1$

This case implies that $\omega_0 \neq 2\omega_i$ and $\omega_0 \neq |\omega_1 \pm \omega_2|$, or the excitation frequency ν is not approximately $2\omega_i$ or $|\omega_1 \pm \omega_2|$. Hence, all sinusoidal terms in equation (4.2.7) vanish when averaged. The averaged equations reduce to

$$\dot{a}_i=\varepsilon\kappa_i a_i\left(-\zeta_i-2\bar{I}_i^{sc}\right),\quad \dot{\phi}_i=\varepsilon\kappa_i\left(\Delta-2\bar{I}_i^{cc}\right),\quad i=1,\,2. \tag{4.2.8}$$

Solving equation (4.2.8) gives

$$a_i(\tau)=a_{i0}\mathrm{e}^{\varepsilon\kappa_i\left(-\zeta_i-2\bar{I}_i^{sc}\right)\tau},\quad \phi_i=\varepsilon\kappa_i\left(\Delta-2\bar{I}_i^{cc}\right)\tau+\phi_{i0},\quad i=1,\,2, \tag{4.2.9}$$

and the solutions of system (4.2.1) are

$$q_i(\tau)\approx a_i(\tau)\cos(\kappa_i\tau+\phi_i)=a_{i0}\mathrm{e}^{\varepsilon\kappa_i\left(-\zeta_i-2\bar{I}_i^{sc}\right)\tau}\cos\left\{\kappa_i\left[1+\varepsilon\left(\Delta-2\bar{I}_i^{cc}\right)\right]\tau+\phi_{i0}\right\}. \tag{4.2.10}$$

It is noting that $\kappa_i\tau=\omega_i/\omega_0\cdot\nu t=\omega_i(1-\varepsilon\Delta)t$, the solution can be given by, after neglecting terms of order $o(\varepsilon)$

$$q_i(\tau)\approx a_{i0}\mathrm{e}^{\varepsilon\kappa_i\left(-\zeta_i-2\bar{I}_i^{sc}\right)\tau}\cos\left\{\omega_i\left(1-2\varepsilon\bar{I}_i^{cc}\right)t+\phi_{i0}\right\}, \tag{4.2.11}$$

which represents the free vibrations of 2 uncoupled damped viscoelastic single-degree-of-freedom systems, which approach zero when $t\to\infty$. Hence, when the excitation frequency ν is not in the vicinity of $2\omega_i$ or $|\omega_1 \pm \omega_2|$, the parametric random excitation has no effect on the system's stability.

Case 2: Subharmonic Resonance: $\kappa_i=\frac{1}{2}$, $\kappa_j\neq\frac{1}{2}$, $i, j=1,\,2$, and $i\neq j$

When $\kappa_i=\frac{1}{2}$, $\omega_0=2\omega_i$, or $\nu=\omega_0(1-\varepsilon\Delta)\approx 2\omega_i$. For $j\neq i$, all sinusoidal terms in equation (4.2.7) vanish when averaged and the averaged equations are the same as equation (4.2.8); hence $q_j(t)\to 0$ as $t\to\infty$ for $j\neq i$.

For the ith mode, when averaged only the underlined sinusoidal terms in equation (4.2.7) survive, hence the averaged equations are given by (take $i=1$ as an example)

$$\begin{aligned}
\dot{a}_1 &= \frac{1}{2}\varepsilon a_1\big[-\zeta_1 - 2\bar{I}_1^{sc} + \frac{1}{2}\zeta k_{11}\sin(2\phi_1-\psi)\big],\\
\dot{\phi}_1 &= \frac{1}{2}\varepsilon\big[\Delta - 2\bar{I}_1^{cc} + \frac{1}{2}\zeta k_{11}\cos(2\phi_1-\psi)\big],\\
\dot{a}_2 &= \varepsilon\kappa_2 a_2\big(-\zeta_2 - 2\bar{I}_2^{sc}\big), \quad \dot{\phi}_2 = \varepsilon\kappa_2\big(\Delta - 2\bar{I}_2^{cc}\big),\\
\dot{\psi}(t) &= \varepsilon^{1/2}\sigma\dot{W}(t).
\end{aligned} \tag{4.2.12}$$

It is found that a_2 and ϕ_2 are independent from other processes a_1, ϕ_1, and ψ. One doesn't have to consider a_2 to obtain moment Lyapunov exponents. If the random noise is not considered, $\psi(t)=0$, the system becomes deterministic, then equations (4.2.12) reduces to the deterministic cases (see Xie, 2006, equation (3.3.9)).

By defining the pth norm $P=a_1^p$ and a new process $\chi=2\phi_1-\psi$, the Itô equation for P and χ can be obtained using Itô's Lemma

$$\begin{aligned}
\mathrm{d}P &= \frac{1}{2}\varepsilon pP\big[\big(-\zeta_1 - 2\bar{I}_1^{sc}\big) + \frac{1}{2}\zeta k_{11}\sin\chi\big]\mathrm{d}t,\\
\mathrm{d}\chi &= \varepsilon\big(\Delta - 2\bar{I}_1^{cc} + \frac{1}{2}\zeta k_{11}\cos\chi\big)\mathrm{d}t - \varepsilon^{1/2}\sigma\dot{W}(t).
\end{aligned} \tag{4.2.13}$$

Applying a linear stochastic transformation

$$S=T(\chi)P, \quad P=T^{-1}(\chi)S, \quad 0\leqslant\chi\leqslant 2\pi, \tag{4.2.14}$$

and Itô's Lemma, one finds the Itô equation for S is

$$\begin{aligned}
\mathrm{d}S = \frac{1}{2}\varepsilon P\Big\{&\sigma^2 T'' + \big[2\big(\Delta - 2\bar{I}_1^{cc}\big) + \zeta k_{11}\cos\chi\big]T'\\
&+ p\big[\big(-\zeta_1 - 2\bar{I}_1^{sc}\big) + \frac{1}{2}\zeta k_{11}\sin\chi\big]T\Big\}\mathrm{d}t - \sqrt{\varepsilon}P\sigma T'\mathrm{d}W,
\end{aligned} \tag{4.2.15}$$

where T' and T'' are the first-order and second-order derivative of $T(\chi)$ with respect to χ, respectively. The eigenvalue problem can be obtained from equation (4.2.15)

$$\frac{1}{2}\varepsilon\sigma^2 T'' + \varepsilon\big[\big(\Delta - 2\bar{I}_1^{cc}\big) + \frac{1}{2}\zeta k_{11}\cos\chi\big]T' + p\varepsilon\big[\frac{1}{2}\big(-\zeta_1 - 2\bar{I}_1^{sc}\big) + \frac{1}{4}\zeta k_{11}\sin\chi\big]T = \hat{\Lambda}T, \tag{4.2.16}$$

which is a second-order differential operator with $\hat{\Lambda}$ being the eigenvalue and $T(\chi)$ the associated eigenfunctions. It can be shown that after a minor modification, this eigenvalue problem reduces to that of a single-degree-of-freedom viscoelastic problem discussed by Huang (2008, equation (3.3.14)). Since the coefficients are periodic with period 2π, equation (4.2.16) can be solved using a Fourier series expansion of the eigenfunction in the form

$$T(\chi)=C_0+\sum_{k=1}^{K}\left(C_k\cos k\chi+S_k\sin k\chi\right), \tag{4.2.17}$$

where C_0, C_k, S_k, $k=1,2,\cdots,K$, are constant coefficients to be determined. Substituting the expansion into eigenvalue problem (4.2.16) and equating the coefficients of like trigonometric terms $\sin k\chi$ and $\cos k\chi$, $k=0,1,\cdots,K$ yield a set of homogeneous linear algebraic equations for the unknown coefficients C_0, C_k and S_k. Similar to Section 3.5.1, the moment Lyapunov exponents can be determined by the method Fourier series expansion.

Monte Carlo simulation is applied to determine the maximum Lyapunov exponents and to check the accuracy of the approximate results from the stochastic averaging. Denoting

$$\begin{gathered}x_1(t)=q_1(t),\quad x_2(t)=\dot{q}_1(t),\quad x_3(t)=q_2(t),\quad x_4(t)=\dot{q}_2(t),\\ x_5(t)=\int_0^t\gamma\,\mathrm{e}^{-\kappa(t-s)}q_1(s)\,\mathrm{d}s,\quad x_6(t)=\int_0^t\gamma\,\mathrm{e}^{-\kappa(t-s)}q_2(s)\,\mathrm{d}s,\end{gathered} \tag{4.2.18}$$

equation (4.2.2) can be converted discretized equations using explicit Euler scheme

$$\begin{aligned}
x_1^{k+1}&=x_1^k+x_2^k\cdot h,\\
x_2^{k+1}&=x_2^k+\Big\{-\kappa_1^2x_1^k+2\varepsilon\kappa_1\big[-\zeta_1x_2^k-\kappa_1\Delta x_1^k+\kappa_1x_5^k-\kappa_1\big(k_{11}x_1^k+k_{12}x_3^k\big)\zeta\cos\varphi^k\big]\Big\}h,\\
x_3^{k+1}&=x_3^k+x_4^k\cdot h,\\
x_4^{k+1}&=x_4^k+\Big\{-\kappa_2^2x_4^k+2\varepsilon\kappa_2\big[-\zeta_2x_4^k-\kappa_2\Delta x_3^k+\kappa_2x_6^k-\kappa_2\big(k_{21}x_1^k+k_{22}x_3^k\big)\zeta\cos\varphi^k\big]\Big\}h,\\
x_5^{k+1}&=x_5^k+\big(\gamma x_1^k-\kappa x_5^k\big)h,\\
x_6^{k+1}&=x_6^k+\big(\gamma x_3^k-\kappa x_6^k\big)h,\\
\varphi^{k+1}&=\varphi^k+h+\varepsilon^{1/2}\sigma\cdot\Delta W^k,
\end{aligned} \tag{4.2.19}$$

with h being the time step and k denoting the kth iteration.

The numerical algorithm for determining the Lyapunov exponents proposed by Wolf *et al.* (1985) is used to evaluate $\lambda_{x(t)}$. By comparison, Figure 4.16 shows that there is an good agreement between Monte Carlo simulation and approximation results. The simulation time step is chosen as $\Delta t = 10^{-5}$ and the number of iterations is 10^9.

It is seen that the maximum resonance does not exactly lie at $\Delta = 0$, which is due to the effect of viscoelasticity. The significant effect of the parametric resonance for small σ can be clearly found in a three-dimensional plot in Figure 4.17. Figure 4.18 illustrates with the increase of the material relaxation γ, the deviation of maximum resonance from $\Delta = 0$ increases accordingly, and the system becomes more stable, as the maximum value of Lyapunov exponents decreases.

For fractional coupled system, the stabilizing effect of fractional order μ is shown in Figure 4.19.

The stability boundaries are shown in Figures 4.20 and three-dimensionally in 4.21, which depict that the parametric resonance around $\Delta = 0$ and the effect of σ. The moment Lyapunov exponents are shown in Figure 4.22 and compared very well with simulation results from Xie's algorithm (Xie, 2006).

Case 3: Combination Additive Resonance: $\kappa_1 + \kappa_2 = 1$ **or** $\omega_0 = \omega_1 + \omega_2$, $\kappa_1 \neq \frac{1}{2}$

When $\kappa_1 + \kappa_2 = 1$, one has $\nu = \omega_0(1 - \varepsilon\Delta) \approx \omega_1 + \omega_2$. When averaged only the grey-background sinusoidal terms in equation (4.2.7) survive, so the averaged equations are

$$\dot{a}_1 = \varepsilon\kappa_1\big[-a_1E_1 + \frac{1}{2}\zeta k_{12}a_2 \sin\big(\phi_1 + \phi_2 - \psi\big)\big],$$

$$\dot{\phi}_1 = \varepsilon\kappa_1\big[G_1 + \frac{1}{2}\zeta k_{12}\frac{a_2}{a_1} \cos\big(\phi_1 + \phi_2 - \psi\big)\big],$$

$$\dot{a}_2 = \varepsilon\kappa_2\big[-a_2E_2 + \frac{1}{2}\zeta k_{21}a_1 \sin\big(\phi_2 + \phi_1 - \psi\big)\big],$$

$$\dot{\phi}_2 = \varepsilon\kappa_2\big[G_2 + \frac{1}{2}\zeta k_{21}\frac{a_1}{a_2} \cos\big(\phi_2 + \phi_1 - \psi\big)\big],$$

$$\dot{\psi}(t) = \varepsilon^{1/2}\sigma\dot{W}(t), \tag{4.2.20}$$

where $E_1 = \zeta_1 + 2\bar{I}_1^{sc}$, $E_2 = \zeta_2 + 2\bar{I}_2^{sc}$ and $G_1 = \Delta - 2\bar{I}_1^{cc}$, $G_2 = \Delta - 2\bar{I}_2^{cc}$.

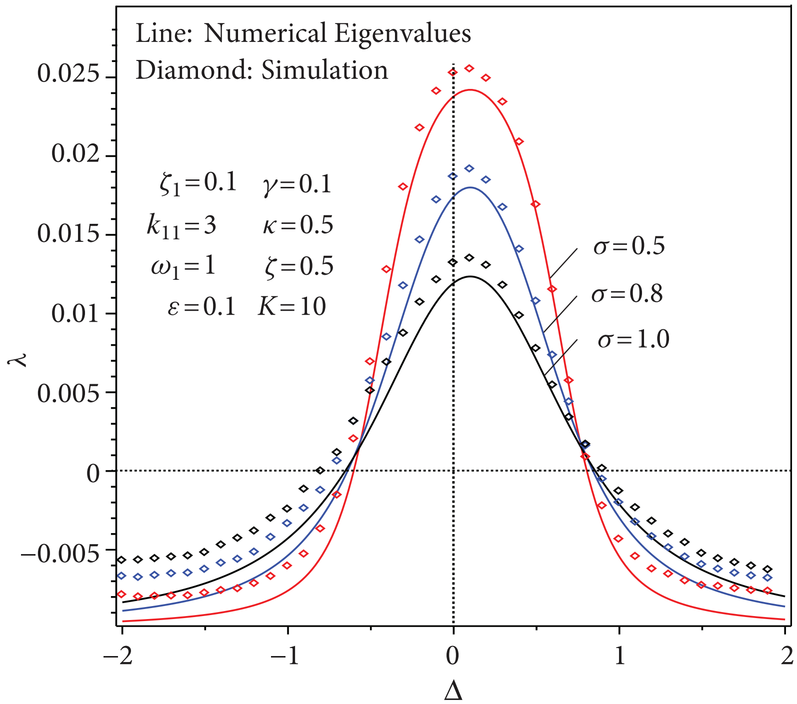

Figure 4.16 Largest Lyapunov exponents of coupled system for subharmonic resonance

By applying the Khasminskii transformation and defining the pth norm,

$$P = a^p, \quad a = \sqrt{a_1^2 + a_2^2}, \quad \cos\varphi = \frac{a_1}{a}, \quad \sin\varphi = \frac{a_2}{a}, \tag{4.2.21}$$

and a new process $\chi = \phi_1 + \phi_2 - \psi$, the Itô equation for P, φ, and χ can be obtained by using Itô's Lemma

$$\begin{aligned}
\mathrm{d}P &= m_P \mathrm{d}t = \frac{1}{2}\varepsilon pP\Big[-2\kappa_2 E_2 \sin^2\varphi - 2\kappa_1 E_1 \cos^2\varphi + \zeta \sin\varphi\cos\varphi\sin\chi\left(\kappa_1 k_{12} + \kappa_2 k_{21}\right)\Big]\mathrm{d}t,\\
\mathrm{d}\chi &= \varepsilon\Big[\kappa_1 G_1 + \frac{1}{2}\zeta\kappa_1 k_{12}\tan\varphi\cos\chi + \kappa_2 G_2 + \frac{1}{2}\zeta\kappa_2 k_{21}\cot\varphi\cos\chi\Big]\mathrm{d}t - \varepsilon^{1/2}\sigma\,\mathrm{d}W,\\
\mathrm{d}\varphi &= m_\varphi \mathrm{d}t = \frac{1}{2}\varepsilon\Big[\left(\kappa_1 E_1 - \kappa_2 E_2\right)\sin(2\varphi) + \zeta\left(-\kappa_1 k_{12}\sin^2\varphi + \kappa_2 k_{21}\cos^2\varphi\right)\sin\chi\Big]\mathrm{d}t.
\end{aligned} \tag{4.2.22}$$

Applying a linear stochastic transformation

$$S = T(\varphi, \chi)P, \quad P = T^{-1}(\varphi, \chi)S, \tag{4.2.23}$$

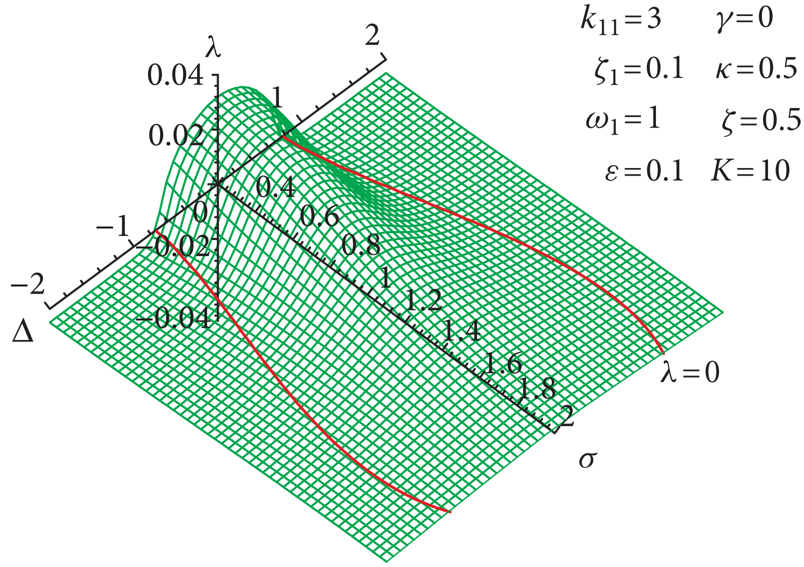

Figure 4.17 Parametric subharmonic resonance of Lyapunov exponents for coupled system

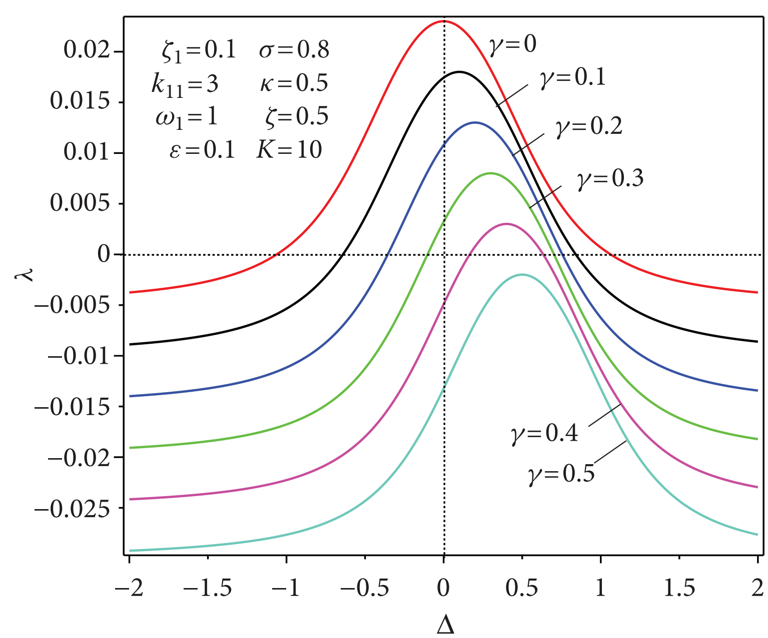

Figure 4.18 Effects of viscosity γ on coupled system for subharmonic resonance

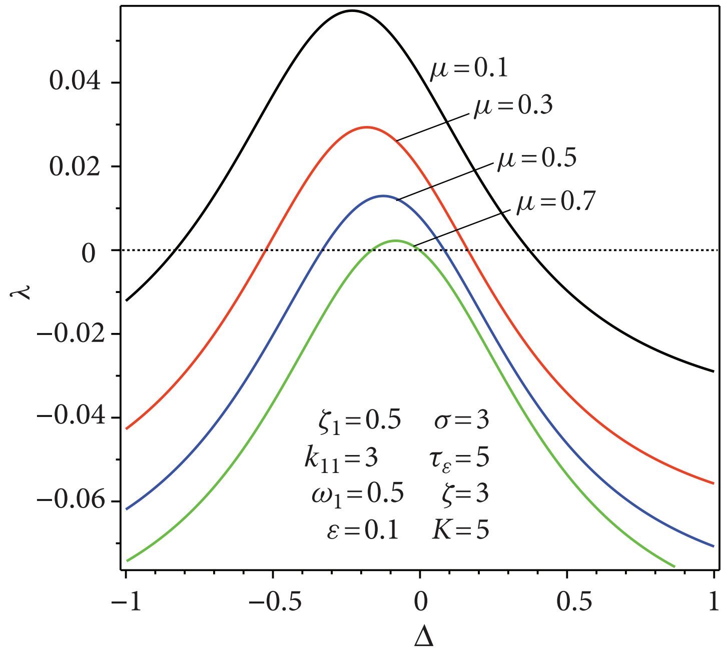

Figure 4.19 Effects of fractional order μ on coupled system for subharmonic resonance

and Itô's Lemma, one finds the Itô equation for S is

$$
\begin{aligned}
\mathrm{d}S &= \frac{1}{2}\varepsilon P\left(\sigma^2 T'' + m_{1\varphi}T^{\text{‘}} + m_{1\chi}T' + m_0 T\right)\mathrm{d}t - \varepsilon^{1/2}P\sigma T'\mathrm{d}W,\\
m_{1\varphi} &= (\kappa_1 E_1 - \kappa_2 E_2)\sin(2\varphi) + \zeta\sin\chi\left(-\kappa_1 k_{12}\sin^2\varphi + \kappa_2 k_{21}\cos^2\varphi\right),\\
m_{1\chi} &= 2\kappa_1 G_1 + 2\kappa_2 G_2 + \zeta\cos\chi\left(\kappa_1 k_{12}\tan\varphi + \kappa_2 k_{21}\cot\varphi\right),\\
m_0 &= p\left[-2\kappa_2 E_2\sin^2\varphi - 2\kappa_1 E_1\cos^2\varphi + \zeta\sin\varphi\cos\varphi\sin\chi\left(\kappa_1 k_{12} + \kappa_2 k_{21}\right)\right],
\end{aligned}
\tag{4.2.24}
$$

where $T^{\text{‘}}$ and T' are the first-order partial derivatives of $T(\varphi, \chi)$ with respect to φ and χ, respectively. T'' is the second-order partial derivatives with respect to χ.

The eigenvalue problem can be obtained from equation (4.2.24),

$$
\bar{\mathcal{L}}(p)T = \frac{1}{2}\left(\sigma^2 T'' + m_{1\varphi}T^{\text{‘}} + m_{1\chi}T' + m_0 T\right) = \hat{\Lambda}T, \tag{4.2.25}
$$

which is a two-dimensional second-order partial differential operator with $\hat{\Lambda}$ being the eigenvalue and $T(\varphi, \chi)$ the associated eigenfunctions. It is found that the coefficient $m_{1\chi}$ is singular at $\varphi = \pm\pi/2$ because of the $\tan\varphi$ terms by which the density $T(\varphi, \chi)$ is limited in

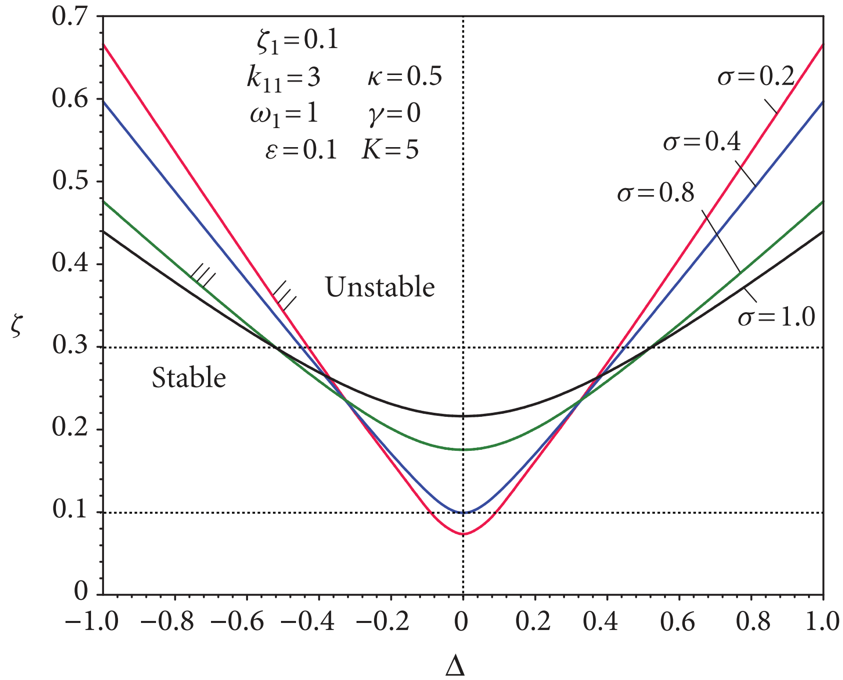

Figure 4.20 Stability boundaries of coupled system for subharmonic resonance

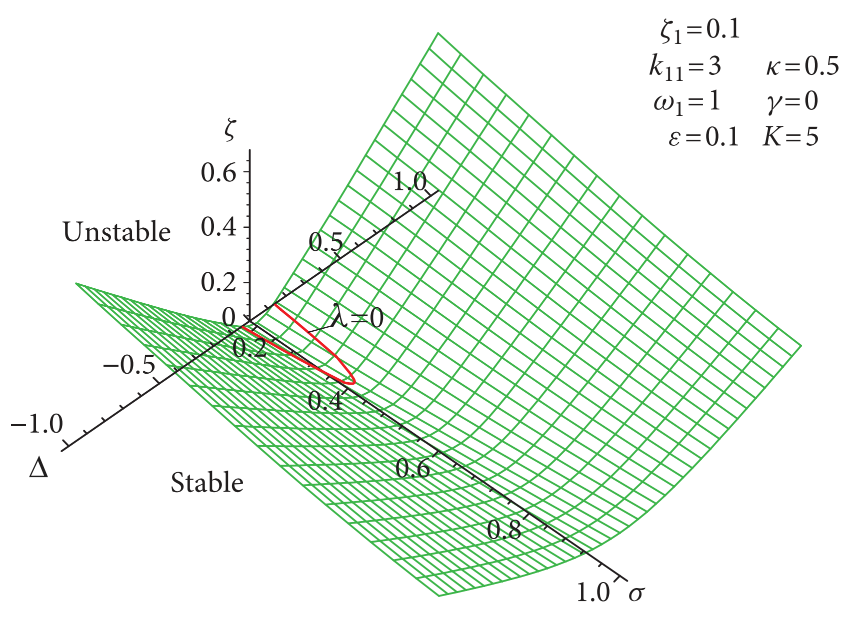

Figure 4.21 Stability boundaries of coupled system for subharmonic resonance

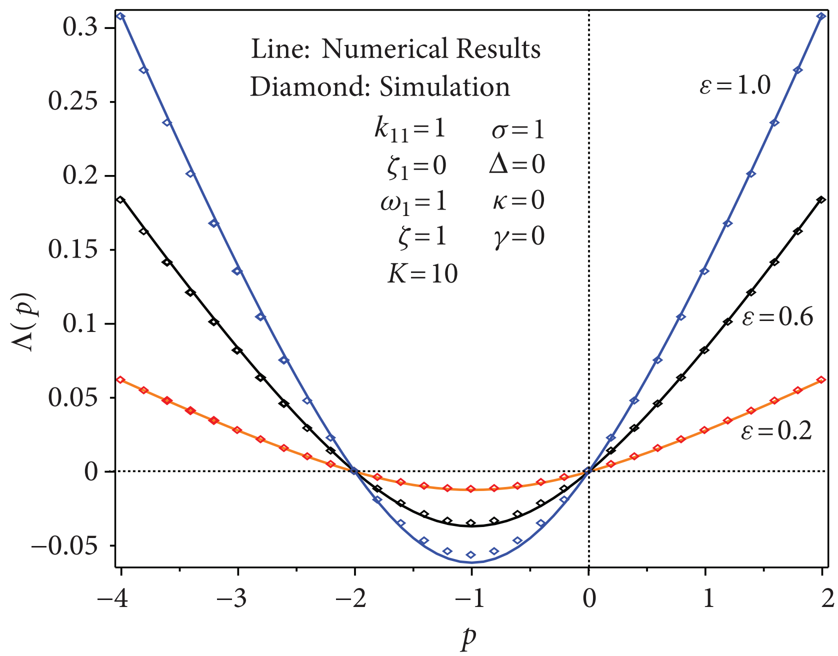

Figure 4.22 Moment Lyapunov exponents of coupled system for subharmonic resonance

the angle range $\varphi \leqslant \pi/2$. It is also singular at $\varphi=0$ because of the $\cot\varphi$ term. To eliminate the singularities at $\varphi=0$ or $\pi/2$, multiplying equation (4.2.25) by $\sin 2\varphi$ leads to

$$\begin{aligned}
&\frac{1}{2}\sin(2\varphi)\sigma^2 T'' + \big[\sin(2\varphi)\big(\kappa_1 G_1+\kappa_2 G_2\big)+\zeta\cos\chi\big(\kappa_1 k_{12}\sin^2\varphi+\kappa_2 k_{21}\cos^2\varphi\big)\big]T' \\
&+\frac{1}{2}\big[(\kappa_1 E_1-\kappa_2 E_2)\sin^2(2\varphi)+\zeta\sin\chi\sin(2\varphi)\big(-\kappa_1 k_{12}\sin^2\varphi+\kappa_2 k_{21}\cos^2\varphi\big)\big]T^{\text{‘}} \\
&+\frac{1}{2}p\sin(2\varphi)\big[-2\kappa_2 E_2\sin^2\varphi-2\kappa_1 E_1\cos^2\varphi+\zeta\sin\varphi\cos\varphi\sin\chi\big(\kappa_1 k_{12}+\kappa_2 k_{21}\big)\big]T \\
&=\hat{\Lambda}\sin(2\varphi)T. \qquad (4.2.26)
\end{aligned}$$

The eigenvalue problem becomes

$$\mathcal{L}(p)T=\frac{1}{2}\big(\sigma^2\sin(2\varphi)T''+n_{1\varphi}T^{\text{‘}}+n_{1\chi}T'+n_0 T\big)=\Lambda\sin(2\varphi)T, \qquad (4.2.27)$$

where $n_{1\varphi}=m_{1\varphi}\sin(2\varphi)$, $n_{1\chi}=m_{1\chi}\sin(2\varphi)$, and $n_0=m_0\sin(2\varphi)$.

Since the coefficients of the eigenvalue problem are periodic functions in χ of period 2π and in φ of period $\pi/2$, the eigenfunction $T(\varphi,\chi)$ can be expanded in double Fourier series in the complex form

$$T(\varphi,\chi)=\sum_{l=-\infty}^{\infty}\sum_{k=-\infty}^{\infty}C_{l,k}\,\mathrm{e}^{\mathrm{i}\,(l\chi+4k\varphi)}, \tag{4.2.28}$$

where the coefficients $C_{l,k}$ are complex numbers.

Substituting equation (4.2.28) into equation (4.2.25), multiplying the resulting equation by $\mathrm{e}^{-\mathrm{i}\,(r\chi+4s\varphi)}$, integrating with respect to χ from 0 to 2π and with respect to φ from 0 to $\pi/2$ yields, for $r,s=0,\pm1,\pm2,\ldots$,

$$\begin{aligned}&\sum_{l=-\infty}^{\infty}\sum_{k=-\infty}^{\infty}\int_{\chi=0}^{2\pi}\int_{\varphi=0}^{\pi/2}C_{l,k}\mathcal{L}(p)[\mathrm{e}^{\mathrm{i}(l\chi+4k\varphi)}]\mathrm{e}^{-\mathrm{i}(r\chi+4s\varphi)}\mathrm{d}\varphi\mathrm{d}\chi\\&=\Lambda\sum_{l=-\infty}^{\infty}\sum_{k=-\infty}^{\infty}\int_{\chi=0}^{2\pi}\int_{\varphi=0}^{\pi/2}C_{l,k}\mathrm{e}^{\mathrm{i}(l\chi+4k\varphi)}\mathrm{e}^{-\mathrm{i}(r\chi+4s\varphi)}\Big[-\mathrm{i}\frac{\mathrm{e}^{i2\varphi}-\mathrm{e}^{-\mathrm{i}2\varphi}}{2}\Big]\mathrm{d}\varphi\mathrm{d}\chi,\end{aligned} \tag{4.2.29}$$

where

$$\begin{aligned}&\mathcal{L}(p)[\mathrm{e}^{\mathrm{i}(l\chi+4k\varphi)}]\\&=\Big\{\frac{\varepsilon}{2}\sin(2\varphi)\sigma^2(-l^2)+\varepsilon\big[\sin(2\varphi)\big(\kappa_1G_1+2\kappa_2G_2\big)\\&+\zeta\cos\chi\left(\kappa_1k_{12}\sin^2\varphi+\kappa_2k_{21}\cos^2\varphi\right)\big](\mathrm{i}l)\\&+\frac{\varepsilon}{2}\big[(\kappa_1E_1-\kappa_2E_2)\sin^2(2\varphi)+\zeta\sin\chi\sin(2\varphi)\big(-\kappa_1k_{12}\sin^2\varphi+\kappa_2k_{21}\cos^2\varphi\big)\big](\mathrm{i}4k)\\&+\frac{\varepsilon}{2}p\sin(2\varphi)\big[-2\kappa_2E_2\sin^2\varphi-2\kappa_1E_1\cos^2\varphi\\&+\zeta\sin\varphi\cos\varphi\sin\chi\left(\kappa_1k_{12}+\kappa_2k_{21}\right)\big]\Big\}\mathrm{e}^{\mathrm{i}(l\chi+4k\varphi)},\end{aligned} \tag{4.2.30}$$

and

$$\sin\phi=-\mathrm{i}\frac{\mathrm{e}^{\mathrm{i}\phi}-\mathrm{e}^{-\mathrm{i}\phi}}{2},\quad \cos\phi=\frac{\mathrm{e}^{\mathrm{i}\phi}+\mathrm{e}^{-\mathrm{i}\phi}}{2},\quad \phi=\varphi,\chi,2\varphi,2\chi. \tag{4.2.31}$$

For ease of numerical computation of the eigenvalues, truncate the double Fourier series (4.2.28) for $l,r=-L,-L+1,\cdots,L$ and $k,s=-K,-K+1,\cdots,K$. Transform the rectangular array for the coefficients $C_{l,k}$ to a vector Z of length $(2L+1)(2K+1)$, with the jth element Z_j, $j=(2K+1)(L+l)+(K+k)+1$, corresponding to $C_{l,k}$. Equation (4.2.29) can be further cast into a generalized linear algebraic eigenvalue problem

$$\mathbf{AZ}=\Lambda\mathbf{BZ}, \tag{4.2.32}$$

where both **A** and **B** are matrix with dimension $(2L+1)(2K+1)\times(2L+1)(2K+1)$. For the element of Ith row and jth column of **A** and **B** are given by, respectively,

$$\begin{aligned}
A_{Ij} &= \int_{\chi=0}^{2\pi}\int_{\varphi=0}^{\pi/2}\mathcal{L}(p)\Big[\mathrm{e}^{\mathrm{i}(l\chi+4k\varphi)}\Big]\mathrm{e}^{-\mathrm{i}(r\chi+4s\varphi)}\mathrm{d}\varphi\mathrm{d}\chi,\\
B_{Ij} &= \int_{\chi=0}^{2\pi}\int_{\varphi=0}^{\pi/2}\mathrm{e}^{\mathrm{i}(l\chi+4k\varphi)}\mathrm{e}^{-\mathrm{i}(r\chi+4s\varphi)}\Big[-\mathrm{i}\frac{\mathrm{e}^{\mathrm{i}2\varphi}-\mathrm{e}^{-\mathrm{i}2\varphi}}{2}\Big]\mathrm{d}\varphi\mathrm{d}\chi,\\
I &= (2K+1)(L+r)+(K+s)+1,\quad j=(2K+1)(L+l)+(K+k)+1,\\
r &= -L,\cdots,-1,0,1,\cdots,L,\quad s=-K,\cdots,-1,0,1,\cdots,K.
\end{aligned}\tag{4.2.33}$$

To have nontrivial solutions for system (4.2.32), the determinant of the coefficient matrix must be zero, i.e., $|\mathbf{A}-\Lambda\mathbf{B}|=0$. By solving this generalized eigenvalue problem, the moment Lyapunov exponent can be determined.

The Lyapunov exponents can be obtained from the relation with moment Lyapunov exponents in equation (1.1.7), which is shown in Figure 4.23. With the increase of σ, the bandwidth of bounded noises also increases, in the limit as σ approaches infinite, the bounded noise becomes a white noise of constant spectral density. The effect of combination additive resonance is reduced, with the decrease of the Lyapunov exponents in Figure 4.24. It is expected that as σ approaches infinite, there is no any resonance at all. When Lyapunov exponents $\lambda>0$, the system is unstable. The effect of σ on the stability boundaries is shown in Figure 4.25. The stabilizing effect of σ and the parametric resonance around $\Delta=0$ can be clearly seen. The stabilizing effect of σ on moment Lyapunov exponents is shown in Figure 4.26.

As in Figure 4.16, the parametric resonance is around the corner of $\Delta=0$. The combination resonance is reduced with the increase of the detuning parameter Δ. This is also found from the moment Lyapunov exponents in Figure 4.27.

As expected, the fractional order μ plays a stabilized role in Figure 4.28 on moment Lyapunov exponents of fractional coupled system for combination additive resonance.

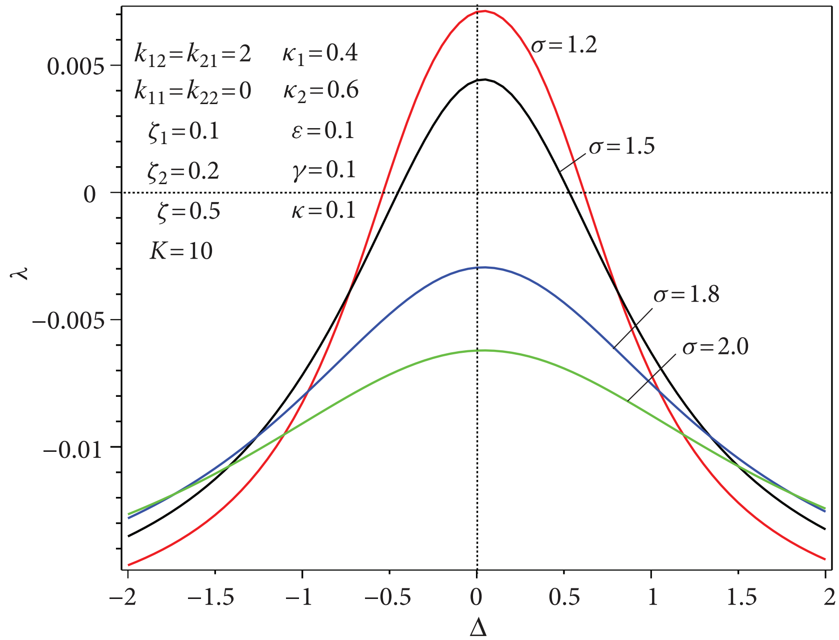

Figure 4.23 Lyapunov exponents of coupled system for combination additive resonance

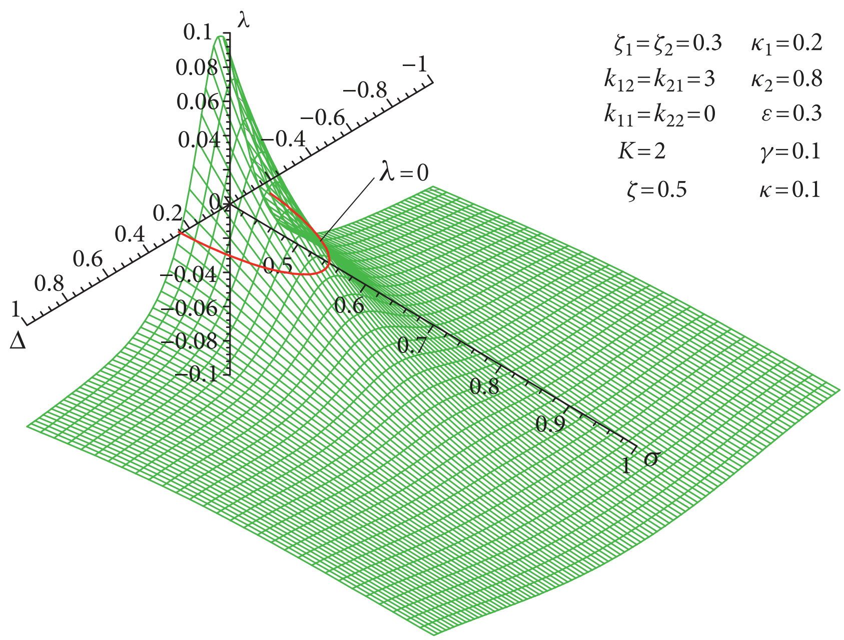

Figure 4.24 Lyapunov exponents of coupled system for combination additive resonance

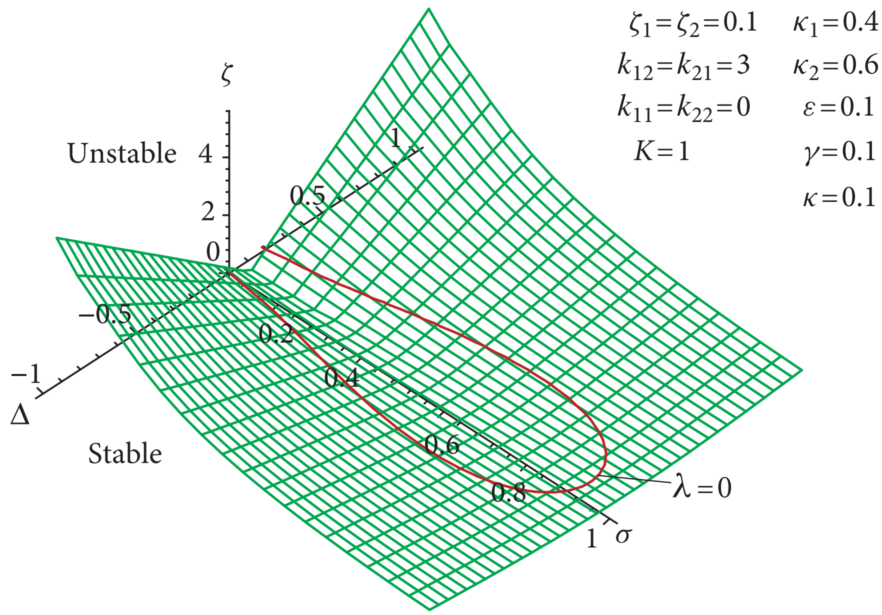

Figure 4.25 Stability boundaries of coupled system for combination additive resonance

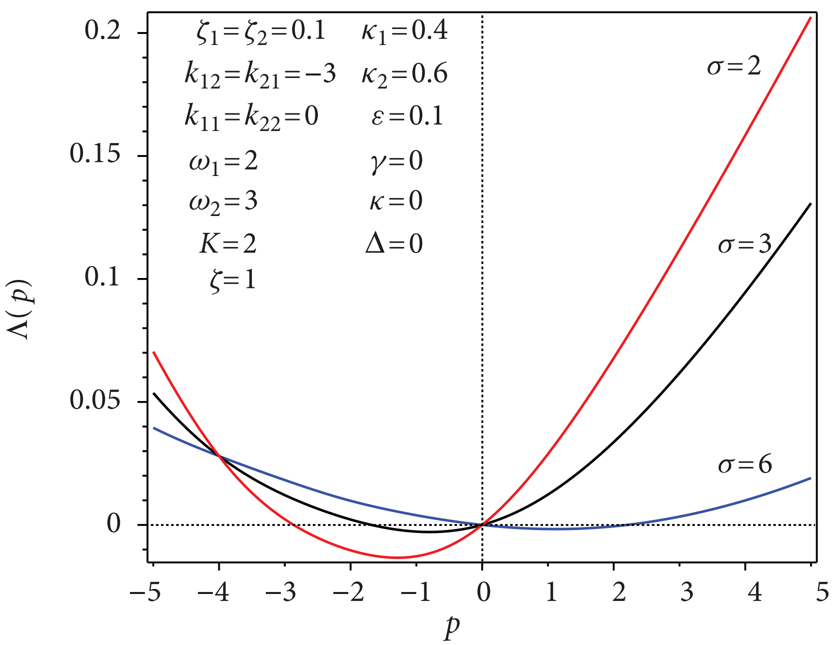

Figure 4.26 Moment Lyapunov exponents of coupled system for combination additive resonance

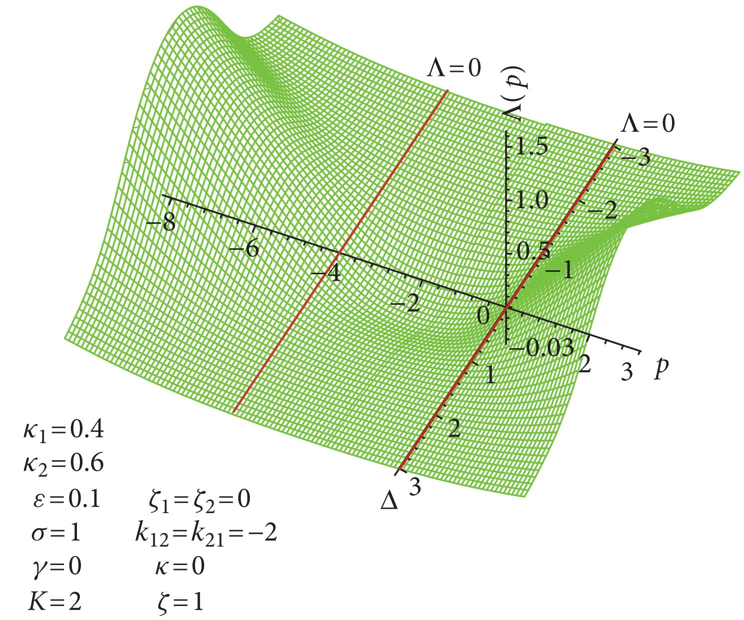

Figure 4.27 Moment Lyapunov exponents of coupled system for combination additive resonance

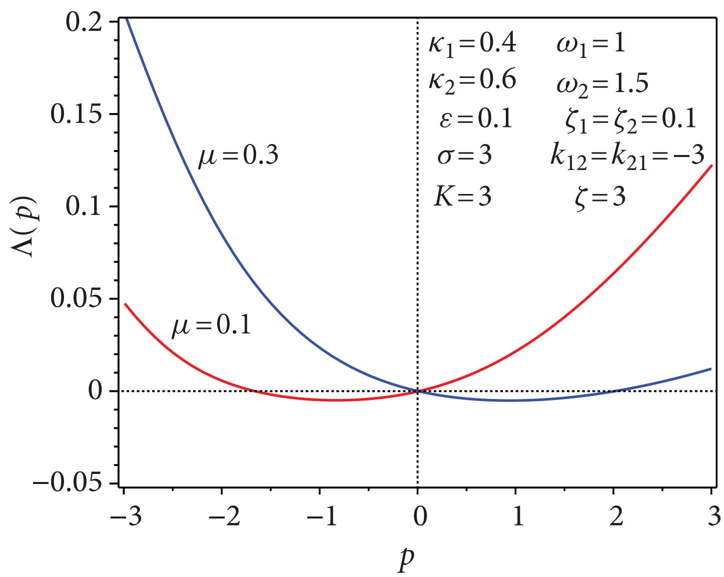

Figure 4.28 Moment Lyapunov exponents of fractional coupled system for combination additive resonance

Case 4: Combination Differential Resonance: $|\kappa_1-\kappa_2|=1$ **or** $\omega_0=|\omega_1-\omega_2|,\ \kappa_1\neq\frac{1}{2}$

When $|\kappa_1-\kappa_2|=1$, one has $\nu=\omega_0(1-\varepsilon\Delta)\approx|\omega_1-\omega_2|$. When averaged only the boxed sinusoidal terms in equation (4.2.7) survive, so the averaged equations are

$$\begin{aligned}
\dot{a}_1&=-\varepsilon\kappa_1 a_1 E_1+\frac{1}{2}\varepsilon\kappa_1\zeta k_{12}a_2\sin(\phi_1-\phi_2+\psi),\\
\dot{\phi}_1&=\varepsilon\kappa_1 G_1+\frac{1}{2}\varepsilon\kappa_1\zeta k_{12}\frac{a_2}{a_1}\cos(\phi_1-\phi_2+\psi),\\
\dot{a}_2&=-\varepsilon\kappa_2 a_2 E_2+\frac{1}{2}\varepsilon\kappa_2\zeta k_{21}a_1\sin(\phi_1-\phi_2+\psi),\\
\dot{\phi}_2&=\varepsilon\kappa_2 G_2+\frac{1}{2}\varepsilon\kappa_2\zeta k_{21}\frac{a_1}{a_2}\cos(\phi_1-\phi_2+\psi),\\
\dot{\psi}(t)&=\varepsilon^{1/2}\sigma\dot{W}(t),
\end{aligned}\tag{4.2.34}$$

where $E_1=\zeta_1+2\bar{I}_1^{sc}$, $E_2=\zeta_2+2\bar{I}_2^{sc}$ and $G_1=\Delta-2\bar{I}_1^{cc}$, $G_2=\Delta-2\bar{I}_2^{cc}$.

By applying the Khasminskii transformation and defining the pth norm, as in (4.2.21), and a new process $\chi=\phi_1-\phi_2+\psi$, the Itô equation for P,φ, and χ can be obtained by using Itô's Lemma

$$\begin{aligned}
\mathrm{d}P&=m_P\mathrm{d}t=\frac{1}{2}\varepsilon pP\left[-2\kappa_2E_2\sin^2\varphi-2\kappa_1E_1\cos^2\varphi+\zeta\sin\varphi\cos\varphi\sin\chi(\kappa_1k_{12}+\kappa_2k_{21})\right]\mathrm{d}t,\\
\mathrm{d}\chi&=\varepsilon\Big(\kappa_1G_1+\frac{1}{2}\zeta\kappa_1k_{12}\tan\varphi\cos\chi-\kappa_2G_2-\frac{1}{2}\zeta\kappa_2k_{21}\cot\varphi\cos\chi\Big)\mathrm{d}t+\varepsilon^{1/2}\sigma\,\mathrm{d}W,\\
\mathrm{d}\varphi&=m_\varphi\mathrm{d}t=\frac{1}{2}\varepsilon\left[(\kappa_1E_1-\kappa_2E_2)\sin(2\varphi)+\zeta(-\kappa_1k_{12}\sin^2\varphi+\kappa_2k_{21}\cos^2\varphi)\sin\chi\right]\mathrm{d}t.
\end{aligned}\tag{4.2.35}$$

Following the same procedure in the preceding section, one can obtain the eigenvalue problem

$$\begin{aligned}
&\frac{\varepsilon}{2}\sin(2\varphi)\sigma^2T''+\varepsilon\left[\sin(2\varphi)\big(\kappa_1G_1-\kappa_2G_2\big)+\zeta\cos\chi(\kappa_1k_{12}\sin^2\varphi-\kappa_2k_{21}\cos^2\varphi)\right]T'\\
&+\frac{\varepsilon}{2}\left[(\kappa_1E_1-\kappa_2E_2)\sin^2(2\varphi)+\zeta\sin\chi\sin(2\varphi)(-\kappa_1k_{12}\sin^2\varphi+\kappa_2k_{21}\cos^2\varphi)\right]T`\\
&+\frac{\varepsilon}{2}p\sin(2\varphi)\left[-2\kappa_2E_2\sin^2\varphi-2\kappa_1E_1\cos^2\varphi+\zeta\sin\varphi\cos\varphi\sin\chi(\kappa_1k_{12}+\kappa_2k_{21})\right]T\\
&=\Lambda\sin(2\varphi)T.
\end{aligned}\tag{4.2.36}$$

Comparing with equation (4.2.26), one can find that the eigenvalue problems for combinational additive resonance and combination differential resonance have the same form, which leads to the fact that moment Lyapunov exponents for combination differential resonance can be similarly obtained.

4.3 Summary

The stochastic stability of coupled viscoelastic systems described by Stratonovich stochastic fractional equations of two-degree-of-freedom was investigated. The system was parametrically excited by wide-band noises of small intensity and small damping was assumed. The Stratonovich equations of motion were first decoupled into four-dimensional Itô stochastic differential equations, by making use of the method of stochastic averaging for the non-viscoelastic terms and the method of Larionov for viscoelastic terms. An elegant scheme for determining the moment Lyapunov exponents is presented by only using Khasminskii and Wedig's mathematical transformations from the decoupled Itô equations. The moment Lyapunov exponents and Lyapunov exponents obtained compare well with the Monte Carlo simulation results and other analytical expressions.

As an application, the flexural-torsional stability of a simply supported rectangular viscoelastic beam of length subjected to a stochastically varying concentrated load acting at the center of the beam cross-section is considered. It is found that, under wide noise excitation, the parameters of damping β, the noise intensity σ, and the viscosity γ have stabilizing effects on the moment and almost-sure stability. However, viscosity parameter η and real noise parameter α play destabilizing role. These results are useful in engineering applications.

In the second part of this chapter, coupled non-gyroscopic viscoelastic systems excited by bounded noises are studied. Parametric resonance is discussed in detail, which includes subharmonic resonance, combination additive resonance and combination differential resonance. Moment Lyapunov exponents are obtained from the eigenvalue problem which is solved by Fourier series expansion. The Lyapunov exponents can be obtained from the relation with moment Lyapunov exponents. It is seen that the parametric resonance occurs around the detuning parameter $\Delta = 0$.

CHAPTER 5

Stochastic Stability of Gyroscopic Viscoelastic Systems

By taking the vibration of a rotating shaft as an example, the equations of motion of a gyroscopic system are derived in Section 5.1. Lyapunov exponents and moment Lyapunov exponents of gyroscopic systems excited by wide-band noises and by bounded noises are investigated in Sections 5.2 and 5.3, respectively. Both ordinary viscoelasticity and fractional viscoelasticity are considered, for few literature can be found on moment Lyapunov exponents of gyroscopic viscoelastic systems.

5.1 Vibration of a Rotating Shaft

Consider a rotor-bearing system as shown in Figure 5.1. The rotor, which is subjected to a dynamic axial compressive load $P(t)$, is mounted in a rigid, axially symmetric bearing at each end and rotates about the centreline Oz of the bearing with a constant angular velocity W. The non-rotating Cartesian coordinates xyz and the rotating coordinates uvz are used to describe the motion of the system, which rotate with the shaft about the z-axis with angular velocity W. Some parameters of the shaft are: length L, mass per unit length m, coefficient of external damping D_e, flexural rigidities EI_u and EI_w, respectively, in directions parallel to Ou and Ow. The torsional rigidities of the shaft are negligible.

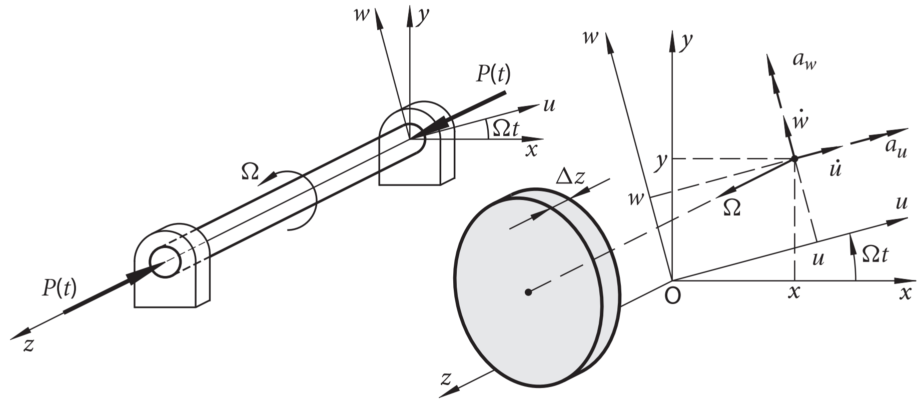

Figure 5.1 Vibration of a rotating shaft

For this elastic shaft under dynamic loading, the transverse flexural equations of motion are given by (Dimentberg, 1961)

$$\begin{aligned} &EI_u \frac{\partial^4 u}{\partial z^4} + P(t) \frac{\partial^2 u}{\partial z^2} + m\left(\frac{\partial^2 u}{\partial t^2} - 2W \frac{\partial w}{\partial t} - W^2 u\right) + D_e\left(\frac{\partial u}{\partial t} - Ww\right) = 0, \\ &EI_w \frac{\partial^4 w}{\partial z^4} + P(t) \frac{\partial^2 w}{\partial z^2} + m\left(\frac{\partial^2 w}{\partial t^2} + 2W \frac{\partial u}{\partial t} - W^2 w\right) + D_e\left(\frac{\partial w}{\partial t} + Wu\right) = 0, \end{aligned} \tag{5.1.1}$$

with boundary conditions

$$\begin{aligned} u(0,t) = u(L,t) = \frac{\partial^2 u(0,t)}{\partial z^2} = \frac{\partial^2 u(L,t)}{\partial z^2} = 0, \\ w(0,t) = w(L,t) = \frac{\partial^2 w(0,t)}{\partial z^2} = \frac{\partial^2 w(L,t)}{\partial z^2} = 0, \end{aligned} \tag{5.1.2}$$

for the case of simply supported ends for small bearings.

For problems with viscoelastic materials, one may simply replace the elastic modulus E in elastic problems by the Voltera operators $E(1-\mathscr{H})$, where $\mathscr{H}$ is the relaxation operator defined in equation (4.1.4) for fractional viscoelastic materials, or equation (4.1.2) for ordinary viscoelastic materials. The governing equation for a viscoelastic rotating shaft can be obtained from equation (5.1.1) in the rotating coordinate system as

$$\begin{aligned} &E(1-\mathscr{H})I_u \frac{\partial^4 u}{\partial z^4} + P(t) \frac{\partial^2 u}{\partial z^2} + m\left(\frac{\partial^2 u}{\partial t^2} - 2W \frac{\partial w}{\partial t} - W^2 u\right) + D_e\left(\frac{\partial u}{\partial t} - Ww\right) = 0, \\ &E(1-\mathscr{H})I_w \frac{\partial^4 w}{\partial z^4} + P(t) \frac{\partial^2 w}{\partial z^2} + m\left(\frac{\partial^2 w}{\partial t^2} + 2W \frac{\partial u}{\partial t} - W^2 w\right) + D_e\left(\frac{\partial w}{\partial t} + Wu\right) = 0. \end{aligned} \tag{5.1.3}$$

These are partial differential equations. Apply Galerkin's method and take

$$u(z,t)=q_1(t)\sin\frac{\pi z}{L},\qquad w(z,t)=q_2(t)\sin\frac{\pi z}{L}. \tag{5.1.4}$$

The partial differential equations in (5.1.3) can then be converted into two ordinary differential equations by using equation (5.1.4), i.e., multiplying (5.1.3) by $\sin\frac{\pi z}{L}$ and integrating from 0 to L,

$$\begin{aligned} &q_1''+\frac{D_e}{m}q_1'-2Wq_2'+\left\{\frac{\pi^2}{mL^2}\left[\frac{\pi^2 EI_u}{L^2}(1-\mathscr{H})-P(t)\right]-W^2\right\}q_1-W\frac{D_e}{m}q_2=0,\\ &q_2''+\frac{D_e}{m}q_2'+2Wq_1'+\left\{\frac{\pi^2}{mL^2}\left[\frac{\pi^2 EI_w}{L^2}(1-\mathscr{H})-P(t)\right]-W^2\right\}q_2+W\frac{D_e}{m}q_1=0. \end{aligned} \tag{5.1.5}$$

The axial thrust $P(t)$ is assumed to be a stationary stochastic process having a mean value P_0 and a fluctuation part $\xi(t)$

$$P(t)=P_0+\xi(t),\qquad \mathrm{E}[\xi(t)]=0. \tag{5.1.6}$$

When the nondimensional time t_1 is introduced by

$$t_1=\varpi_1 t=\frac{\pi^2}{L^2}\sqrt{\frac{EI_u}{m}}\;t, \tag{5.1.7}$$

and the dot is used to denote differentiation with respect to the new time t_1, Eq. (5.1.5) becomes

$$\begin{aligned} &\ddot{q}_1+2\beta\dot{q}_1-2\Omega\dot{q}_2+[\bar{\omega}_1^2-\Omega^2-\mathscr{H}-p(t)]q_1-2\beta\Omega q_2=0,\\ &\ddot{q}_2+2\beta\dot{q}_2+2\Omega\dot{q}_1+[\bar{\omega}_2^2-\Omega^2-e_2\mathscr{H}-p(t)]q_2+2\beta\Omega q_1=0, \end{aligned} \tag{5.1.8}$$

or in the matrix form

$$\ddot{\mathbf{q}}+2\beta\dot{\mathbf{q}}+2\Omega\begin{bmatrix}0 & -1\\ 1 & 0\end{bmatrix}\dot{\mathbf{q}}+\begin{bmatrix}\bar{\omega}_1^2-\Omega^2-\mathscr{H} & -2\beta\Omega\\ 2\beta\Omega & \bar{\omega}_2^2-\Omega^2-e_2\mathscr{H}\end{bmatrix}\mathbf{q}-p(t)\mathbf{q}=0, \tag{5.1.9}$$

where $\mathbf{q}=\{q_1,q_2\}^T$ and

$$\varpi_1=\frac{\pi^2}{mL^2}\frac{\pi^2 EI_u}{L^2},\qquad \varpi_2=\frac{\pi^2}{mL^2}\frac{\pi^2 EI_w}{L^2},$$

$$\beta=\frac{D_e}{2m\varpi_1},\qquad p(t)=\frac{\pi^2}{mL^2\varpi_1^2}\xi(t),\qquad \Omega=\frac{W}{\varpi_1},\qquad e_2=\frac{\varpi_2}{\varpi_1},$$

$$\bar{\omega}_1^2 = 1 - \frac{\pi^2}{mL^2\varpi_1^2}P_0, \quad \bar{\omega}_2^2 = e_2 - \frac{\pi^2}{mL^2\varpi_1^2}P_0. \tag{5.1.10}$$

It is gyroscopic because of the third term which arises from the Coriolis forces. This is a two-degree-of-freedom gyroscopic system under stochastic parametric excitation $p(t)$.

5.2 Gyroscopic Systems Excited by Wide-band Noise

5.2.1 Formulation

By introducing a small parameter $0 < \varepsilon \ll 1$ to show that damping, viscoelasticity, and parametric excitation are small, the gyroscopic system in equation (5.1.9) becomes

$$\ddot{\mathbf{q}} + 2\varepsilon\beta\dot{\mathbf{q}} + 2\Omega\begin{bmatrix} 0 & -1 \\ 1 & 0 \end{bmatrix}\dot{\mathbf{q}} + \begin{bmatrix} \bar{\omega}_1^2 - \Omega^2 - \varepsilon\mathscr{H} & -2\varepsilon\beta\Omega \\ 2\varepsilon\beta\Omega & \bar{\omega}_2^2 - \Omega^2 - \varepsilon e_2\mathscr{H} \end{bmatrix}\mathbf{q} - \varepsilon^{1/2}\xi(t)\mathbf{q} = 0, \tag{5.2.1}$$

where $\mathbf{q} = \{q_1, q_2\}^T$ are state coordinates, β is the damping coefficient, Ω is the axial angular velocity. $\bar{\omega}_{1,2}$ are the natural frequencies with $\bar{\omega}_1 < \bar{\omega}_2$. $\mathscr{H}$ is a linear viscoelastic operator.

Equations (5.2.1) admit the trivial solution $q_1 = q_2 = 0$. However, they are not the Lagrange standard form given in equation (1.2.27) or (1.2.40). Hence, to apply the averaging method, one should consider first the unperturbed system, i.e., $\varepsilon = 0$ and $\xi(t) = 0$, which reduces to

$$\ddot{q}_1 + (\bar{\omega}_1^2 - \Omega^2)q_1 - 2\Omega\dot{q}_2 = 0, \quad \ddot{q}_2 + (\bar{\omega}_2^2 - \Omega^2)q_2 + 2\Omega\dot{q}_1 = 0. \tag{5.2.2}$$

This is a system of two linear second-order ordinary differential equations, which can be solved by the method of operator (Xie, 2010). Using the D-operator, $D(\cdot) \equiv \mathrm{d}(\cdot)/\mathrm{d}t$, the differential equations become

$$\left[D^2 + (\bar{\omega}_1^2 - \Omega^2)\right]q_1 - 2\Omega D q_2 = 0, \quad 2\Omega D q_1 + \left[D^2 + (\bar{\omega}_2^2 - \Omega^2)\right]q_2 = 0. \tag{5.2.3}$$

The determinant of the coefficient matrix is

$$\begin{aligned}\phi(D) &= \begin{vmatrix} D^2 + (\bar{\omega}_1^2 - \Omega^2) & -2\Omega D \\ 2\Omega D & D^2 + (\bar{\omega}_2^2 - \Omega^2) \end{vmatrix} \\ &= D^4 + (\bar{\omega}_1^2 + \bar{\omega}_2^2 + 2\Omega^2)D^2 + (\bar{\omega}_1^2 - \Omega^2)(\bar{\omega}_2^2 - \Omega^2). \end{aligned} \tag{5.2.4}$$

Hence, the characteristic equation is

$$\phi(\lambda)=\lambda^4+(\bar{\omega}_1^2+\bar{\omega}_2^2+2\Omega^2)\lambda^2+(\bar{\omega}_1^2-\Omega^2)(\bar{\omega}_2^2-\Omega^2)=0,$$

and its solutions are

$$\lambda_{1,2}^2=\frac{-(\bar{\omega}_1^2+\bar{\omega}_2^2+2\Omega^2)\pm\sqrt{(\bar{\omega}_1^2+\bar{\omega}_2^2+2\Omega^2)^2-4(\bar{\omega}_1^2-\Omega^2)(\bar{\omega}_2^2-\Omega^2)}}{2}=-\omega_{1,2}^2, \quad (5.2.5)$$

where $\omega_{1,2}^2$ can be rewritten as

$$\omega_{1,2}^2=\frac{1}{2}\left[(\bar{\omega}_1^2+\bar{\omega}_2^2+2\Omega^2)\mp\sqrt{(\bar{\omega}_1^2-\bar{\omega}_2^2)^2+8\Omega^2(\bar{\omega}_1^2+\bar{\omega}_2^2)}\right]. \quad (5.2.6)$$

To ensure the undamped and unperturbed system to be stable, the eigenfrequencies $\lambda_{1,2}$ must be pure imaginary numbers, which means that $\omega_{1,2}$ must be real numbers. This is possible if $(\bar{\omega}_1^2-\Omega^2)(\bar{\omega}_2^2-\Omega^2)>0$, i.e., $\Omega<\bar{\omega}_1, \Omega>\bar{\omega}_2$, implying that the stability regions are $0\leqslant\Omega\leqslant\bar{\omega}_1$ and $\Omega\geqslant\bar{\omega}_2$. The system is unstable when $\bar{\omega}_1\leqslant\Omega\leqslant\bar{\omega}_2$. Hence, $\bar{\omega}_1$ and $\bar{\omega}_2$ are the two critical angular velocities of the system.

The complementary solutions of q_1 and q_2 in (5.2.2) have the same form and are given by

$$\begin{aligned} q_1&=A_{11}\cos\omega_1 t+A_{12}\sin\omega_1 t+A_{13}\cos\omega_2 t+A_{14}\sin\omega_2 t,\\ q_2&=A_{21}\cos\omega_1 t+A_{22}\sin\omega_1 t+A_{23}\cos\omega_2 t+A_{24}\sin\omega_2 t, \end{aligned} \quad (5.2.7)$$

which contain eight arbitrary constants. However, since $\phi(D)$ is a polynomial of degree 4 in D, the complementary solutions should contain only four arbitrary constants. Substituting equations (5.2.7) into the first equation of (5.2.2) to eliminate the four extra constants gives

$$\begin{aligned} &\frac{A_{22}}{A_{11}}=-\frac{\omega_1^2-(\bar{\omega}_1^2-\Omega^2)}{2\omega\omega_1}, \quad \frac{A_{21}}{A_{12}}=\frac{\omega_1^2-(\bar{\omega}_1^2-\Omega^2)}{2\Omega\omega_1},\\ &\frac{A_{24}}{A_{13}}=-\frac{\omega_2^2-(\bar{\omega}_1^2-\Omega^2)}{2\Omega\omega_2}, \quad \frac{A_{23}}{A_{14}}=\frac{\kappa_2^2-(\bar{\omega}_1^2-\Omega^2)}{2\Omega\omega_2}. \end{aligned} \quad (5.2.8)$$

Similarly, substituting equations (5.2.7) into the second equation of (5.2.2) yields

$$\begin{aligned} &\frac{A_{22}}{A_{11}}=-\frac{2\Omega\omega_1}{\omega_1^2-(\bar{\omega}_2^2-\Omega^2)}, \quad \frac{A_{21}}{A_{12}}=\frac{2\Omega\omega_1}{\omega_1^2-(\bar{\omega}_2^2-\Omega^2)},\\ &\frac{A_{24}}{A_{13}}=-\frac{2\Omega\omega_2}{\omega_2^2-(\bar{\omega}_2^2-\Omega^2)}, \quad \frac{A_{23}}{A_{14}}=\frac{2\Omega\omega_2}{\omega_2^2-(\bar{\omega}_2^2-\Omega^2)}. \end{aligned} \quad (5.2.9)$$

Comparing equations (5.2.8) and (5.2.9) yields

$$\frac{\omega_i^2-(\bar{\omega}_1^2-\Omega^2)}{2\Omega\omega_i}=\frac{2\Omega\omega_i}{\omega_i^2-(\bar{\omega}_2^2-\Omega^2)}=\alpha_i, \quad i=1,\ 2. \tag{5.2.10}$$

Substituting equations (5.2.10) into (5.2.8) and then into (5.2.7) gives the solutions of equations (5.2.2)

$$q_1=\alpha_{11}a_1\sin\Phi_1+\alpha_{22}a_2\sin\Phi_2, \quad q_2=\alpha_{11}a_1\alpha_1\cos\Phi_1+\alpha_{22}a_2\alpha_2\cos\Phi_2, \tag{5.2.11}$$

where $\Phi_1=\omega_1 t+\phi_1$ and $\Phi_2=\omega_2 t+\phi_2$. The four constants are a_1, a_2, ϕ_1, and ϕ_2. α_{11} and α_{22} are suitable coordinates scaling parameters to make the evaluation of the moment Lyapunov exponent somewhat simpler.

The method of variation of parameters is applied to determine the solutions of the original perturbed system in equations (5.2.1). Varying the parameters a_1, a_2, ϕ_1, and ϕ_2 in equations (5.2.11) to make them functions of t lead to solutions of the form

$$\begin{aligned}q_1&=\alpha_{11}a_1(t)\sin\Phi_1+\alpha_{22}a_2(t)\sin\Phi_2,\\ q_2&=\alpha_{11}a_1(t)\alpha_1\cos\Phi_1+\alpha_{22}a_2(t)\alpha_2\cos\Phi_2,\end{aligned} \tag{5.2.12}$$

where a_r and ϕ_r, $r=1,\ 2$, are solutions of the following four first-order equations

$$\begin{aligned}\dot{a}_1&=\frac{A}{\alpha_{11}}\big(+B_1F\cos\Phi_1-G\sin\Phi_1\big), \quad a_1\dot{\phi}_1=\frac{A}{\alpha_{11}}\big(-B_1F\sin\Phi_1-G\cos\Phi_1\big),\\ \dot{a}_2&=\frac{A}{\alpha_{22}}\big(-B_2F\cos\Phi_2+G\sin\Phi_2\big), \quad a_2\dot{\phi}_2=\frac{A}{\alpha_{22}}\big(+B_2F\sin\Phi_2+G\cos\Phi_2\big),\end{aligned} \tag{5.2.13}$$

where

$$A=\frac{1}{\alpha_1\omega_1-\alpha_2\omega_2}=\frac{2\Omega}{\omega_1^2-\omega_2^2},$$

$$B_1=-\frac{\alpha_2\big(\alpha_1\omega_1-\alpha_2\omega_2\big)}{\alpha_1\omega_2-\alpha_2\omega_1}=-\frac{\alpha_2\omega_1\omega_2}{\bar{\omega}_1^2-\Omega^2}$$

$$=-\frac{\omega_1}{\bar{\omega}_1^2-\Omega^2}\frac{\omega_2^2-(\bar{\omega}_1^2-\Omega^2)}{2\Omega}=-\frac{\omega_1}{\bar{\omega}_1^2-\Omega^2}\frac{\frac{(\bar{\omega}_1^2-\Omega^2)(\bar{\omega}_2^2-\Omega^2)}{\omega_1^2}-(\bar{\omega}_1^2-\Omega^2)}{2\Omega}=\frac{1}{\alpha_1},$$

$$B_2=-\frac{\alpha_1\big(\alpha_1\omega_1-\alpha_2\omega_2\big)}{\alpha_1\omega_2-\alpha_2\omega_1}==-\frac{\alpha_1\omega_1\omega_2}{\bar{\omega}_1^2-\Omega^2}$$

$$=-\frac{\omega_1}{\bar{\omega}_1^2-\Omega^2}\frac{\omega_1^2-(\bar{\omega}_1^2-\Omega^2)}{2\Omega}=-\frac{\omega_1}{(\bar{\omega}_1^2-\Omega^2)}\frac{\frac{(\bar{\omega}_1^2-\Omega^2)(\bar{\omega}_2^2-\Omega^2)}{\omega_2^2}-(\bar{\omega}_1^2-\Omega^2)}{2\Omega}=\frac{1}{\alpha_2},$$

$$F=-\varepsilon\{-\mathscr{H}[q_1]+2\beta\dot{q}_1-2\beta\Omega q_2\}+\varepsilon^{1/2}\xi(t)q_1,$$

$$G=-\varepsilon\{-e_2\mathscr{H}[q_2]+2\beta\dot{q}_2+2\beta\Omega q_1\}+\varepsilon^{1/2}\xi(t)q_2.$$

On deriving (5.2.13), equation (5.2.5) and the relations $\omega_1^2+\omega_2^2=\bar{\omega}_1^2+\bar{\omega}_2^2-2\Omega^2$ and $\omega_1^2\omega_2^2=(\bar{\omega}_1^2-\Omega^2)(\bar{\omega}_2^2-\Omega^2)$ are used. Equation (5.2.13) can then be expanded as

$$\dot{a}_r=\varepsilon^{1/2}F_{a,r}^{(0)}+\varepsilon F_{a,r}^{(1)},\quad \dot{\phi}_r=\varepsilon^{1/2}F_{\phi,r}^{(0)}+\varepsilon F_{\phi,r}^{(1)},\quad r=1,\ 2,\tag{5.2.14}$$

where

$$F_{a,r}^{(0)}=\frac{(-1)^r2\Omega\xi(t)}{\alpha_r\alpha_{rr}(\omega_1^2-\omega_2^2)}\left\{-\cos\Phi_r\sum_{i=1}^{2}\alpha_{ii}a_i\sin\Phi_i+\alpha_r\sin\Phi_r\sum_{i=1}^{2}\alpha_{ii}\alpha_ia_i\cos\Phi_i\right\},$$

$$\begin{aligned}F_{a,r}^{(1)}=\frac{(-1)^r2\Omega}{\alpha_r\alpha_{rr}(\omega_1^2-\omega_2^2)}&\left\{-\cos\Phi_r\left[2\beta\sum_{i=1}^{2}\alpha_{ii}a_i\omega_i\cos\Phi_i-2\beta\Omega\sum_{i=1}^{2}\alpha_{ii}\alpha_ia_i\cos\Phi_i\right.\right.\\&\left.-\sum_{i=1}^{2}\alpha_{ii}a_i\mathscr{H}[\sin\Phi_i]\right]-\alpha_r\sin\Phi_r\left[2\beta\sum_{i=1}^{2}\alpha_{ii}\alpha_ia_i\omega_i\sin\Phi_i\right.\\&\left.\left.-2\beta\Omega\sum_{i=1}^{2}\alpha_{ii}a_i\sin\Phi_i+\sum_{i=1}^{2}\alpha_i\alpha_{ii}a_ie_i\mathscr{H}[\cos\Phi_i]\right]\right\},\end{aligned}$$

$$F_{\phi,r}^{(0)}=\frac{(-1)^r2\Omega\xi(t)}{a_r\alpha_r\alpha_{rr}(\omega_1^2-\omega_2^2)}\left\{\sin\Phi_r\sum_{i=1}^{2}\alpha_{ii}a_i\sin\Phi_i+\alpha_r\cos\Phi_r\sum_{i=1}^{2}\alpha_{ii}\alpha_ia_i\cos\Phi_i\right\},$$

$$\begin{aligned}F_{\phi,r}^{(1)}=\frac{(-1)^r2\Omega}{a_r\alpha_r\alpha_{rr}(\omega_1^2-\omega_2^2)}&\left\{-\sin\Phi_r\left[-2\beta\sum_{i=1}^{2}\alpha_{ii}a_i\omega_i\cos\Phi_i+2\beta\Omega\sum_{i=1}^{2}\alpha_{ii}\alpha_ia_i\cos\Phi_i\right.\right.\\&\left.+\sum_{i=1}^{2}\alpha_{ii}a_i\mathscr{H}[\sin\Phi_i]\right]+\alpha_r\cos\Phi_r\left[-2\beta\sum_{i=1}^{2}\alpha_{ii}\alpha_ia_i\omega_i\sin\Phi_i\right.\\&\left.\left.+2\beta\sum_{i=1}^{2}\alpha_{ii}a_i\sin\Phi_i-\sum_{i=1}^{2}\alpha_i\alpha_{ii}a_ie_i\mathscr{H}[\cos\Phi_i]\right]\right\}.\end{aligned}\tag{5.2.15}$$

Under certain conditions, the method of stochastic averaging may be applied to equation (5.2.14) to yield diffusive processes for the averaged amplitudes a_r and phase angles ϕ_r

$$\mathrm{d}a_r = \varepsilon m_r^a \mathrm{d}t + \varepsilon^{1/2} \sum_{s=1}^{2} \sigma_{rs}^a \mathrm{d}W_s^a, \tag{5.2.16a}$$

$$\mathrm{d}\phi_r = \varepsilon m_r^\phi \mathrm{d}t + \varepsilon^{1/2} \sum_{s=1}^{2} \sigma_{rs}^\phi \mathrm{d}W_s^\phi, \quad r=1,\ 2, \tag{5.2.16b}$$

where $\mathbf{W}^a = \{W_1^a, W_2^a\}^T$ and $\mathbf{W}^\phi = \{W_1^\phi, W_2^\phi\}^T$ are 2-dimensional vectors of independent standard Wiener processes, the drift coefficients $\varepsilon m_r^a, \varepsilon m_r^\phi$, and the 2×2 diffusion matrices $\mathbf{b}^a = \boldsymbol{\sigma}^a(\boldsymbol{\sigma}^a)^T, \mathbf{b}^\phi = \boldsymbol{\sigma}^\phi(\boldsymbol{\sigma}^\phi)^T$, in which $\boldsymbol{\sigma}^a = [\sigma_{rs}^a], \boldsymbol{\sigma}^\phi = [\sigma_{rs}^\phi], \mathbf{b}^a = [b_{rs}^a]$, and $\mathbf{b}^\phi = [b_{rs}^\phi]$. The drift and diffusion coefficients of amplitude are given by

$$\begin{aligned}
m_1^a &= \mathop{\mathscr{M}}_t \left\{ F_{a,1}^{(1)} + \int_{-\infty}^{0} \mathsf{E}\left[\sum_{j=1}^{2} \left(\frac{\partial F_{a,1}^{(0)}}{\partial a_j} F_{a,j\tau}^{(0)} + \frac{\partial F_{a,1}^{(0)}}{\partial \phi_j} F_{\phi,j\tau}^{(0)} \right) \right] \mathrm{d}\tau \right\} \\
&= a_1 E_1 + V_0 \left[(3V_1 + 2V_3) a_1 + \frac{\alpha_{21}^2 D_2 a_2^2}{a_1} \right], \\
m_2^a &= \mathop{\mathscr{M}}_t \left\{ F_{a,2}^{(1)} + \int_{-\infty}^{0} \mathsf{E}\left[\sum_{j=1}^{2} \left(\frac{\partial F_{a,2}^{(0)}}{\partial a_j} F_{a,j\tau}^{(0)} + \frac{\partial F_{\phi,2}^{(0)}}{\partial \phi_j} F_{\phi,j\tau}^{(0)} \right) \right] \mathrm{d}\tau \right\} \\
&= a_2 E_2 + V_0 \left[(3V_2 + 2V_3) a_2 + \frac{\alpha_{12}^2 D_1 a_1^2}{a_2} \right], \\
b_{11}^a &= \mathop{\mathscr{M}}_t \left\{ \int_{-\infty}^{\infty} \mathsf{E}\left[F_{a,1}^{(0)} F_{a,1\tau}^{(0)} \right] \mathrm{d}\tau \right\} = 2V_0 \left(V_1 a_1^2 + \alpha_{21}^2 D_2 a_2^2 \right), \\
b_{12}^a &= \mathop{\mathscr{M}}_t \left\{ \int_{-\infty}^{\infty} \mathsf{E}\left[F_{a,1}^{(0)} F_{a,2\tau}^{(0)} \right] \mathrm{d}\tau \right\} = 2V_0 V_3 a_1 a_2, \\
b_{22}^a &= \mathop{\mathscr{M}}_t \left\{ \int_{-\infty}^{\infty} \mathsf{E}\left[F_{a,2}^{(0)} F_{a,2\tau}^{(0)} \right] \mathrm{d}\tau \right\} = 2V_0 \left(V_2 a_2^2 + \alpha_{12}^2 D_1 a_1^2 \right),
\end{aligned} \tag{5.2.17}$$

where the constants are given by

$$\alpha_{12} = \frac{\alpha_{11}}{\alpha_{22}}, \quad \alpha_{21} = \frac{\alpha_{22}}{\alpha_{11}}, \quad V_0 = \frac{\Omega^2}{4\left(\omega_1^2 - \omega_2^2\right)^2}, \quad V_1 = \left(\alpha_1 - \frac{1}{\alpha_1}\right)^2 S(2\omega_1),$$

$$
\begin{aligned}
&V_2=\left(\alpha_2-\frac{1}{\alpha_2}\right)^2 S(2\omega_2), \quad V_3=2S^+-\left(\alpha_1\alpha_2+\frac{1}{\alpha_1\alpha_2}\right)S^-,\\
&D_1=\left(\alpha_1^2+\frac{1}{\alpha_2^2}\right)S^+-2\frac{\alpha_1}{\alpha_2}S^-, \quad D_2=\left(\alpha_2^2+\frac{1}{\alpha_1^2}\right)S^+-2\frac{\alpha_2}{\alpha_1}S^-,\\
&S^{\pm}=S(\omega_1+\omega_2)\pm S(\omega_1-\omega_2),
\end{aligned}
\tag{5.2.18}
$$

$$
\begin{aligned}
E_1&=-\beta+\frac{2\Omega}{\alpha_{11}(\omega_1^2-\omega_2^2)}\left[\frac{\mathscr{M}_t\left\{\cos\Phi_1\mathscr{H}[q_1]\right\}}{\alpha_1}-e_2\mathscr{M}_t\left\{\sin\Phi_1\mathscr{H}[q_2]\right\}\right],\\
E_2&=-\beta+\frac{2\Omega}{\alpha_{22}(\omega_1^2-\omega_2^2)}\left[-\frac{\mathscr{M}_t\left\{\cos\Phi_2\mathscr{H}[q_1]\right\}}{\alpha_2}+e_2\mathscr{M}_t\left\{\sin\Phi_2\mathscr{H}[q_2]\right\}\right],
\end{aligned}
\tag{5.2.19}
$$

where $S(\omega)$ is the cosine power spectral densities of the process $\xi(t)$. When applying the averaging operator, the integration is performed over explicitly appearing τ only.

Similar to equation (4.1.13), applying the transformation $s=t-\tau$ and changing the order of integration lead to

$$
\begin{aligned}
&\mathscr{M}_t\left\{I_r^{cs}\right\}=\mathscr{M}_t\left\{\cos\Phi_r\mathscr{H}[\sin\Phi_r]\right\}=-\frac{1}{2}\mathcal{H}^s(\omega_r), \quad r=1,\,2,\\
&\mathscr{M}_t\left\{\cos\Phi_r\mathscr{H}[\sin\Phi_i]\right\}=0, \quad r\neq i,\\
&\mathscr{M}_t\left\{I_r^{cc}\right\}=\mathscr{M}_t\left\{\cos\Phi_r\mathscr{H}[\cos\Phi_r]\right\}=\frac{1}{2}\mathcal{H}^c(\omega_r), \quad \mathscr{M}_t\left\{\cos\Phi_r\mathscr{H}[\cos\Phi_i]\right\}=0,\\
&\mathscr{M}_t\left\{I_r^{sc}\right\}=\mathscr{M}_t\left\{\sin\Phi_r\mathscr{H}[\cos\Phi_r]\right\}=\frac{1}{2}\mathcal{H}^s(\omega_1), \quad \mathscr{M}_t\left\{\sin\Phi_r\mathscr{H}[\cos\Phi_i]\right\}=0,\\
&\mathscr{M}_t\left\{I_r^{ss}\right\}=\mathscr{M}_t\left\{\sin\Phi_r\mathscr{H}[\sin\Phi_r]\right\}=\frac{1}{2}\mathcal{H}^c(\omega_1), \quad \mathscr{M}_t\left\{\sin\Phi_r\mathscr{H}[\sin\Phi_i]\right\}=0,
\end{aligned}
\tag{5.2.20}
$$

where $\mathcal{H}^s(\omega)$ and $\mathcal{H}^c(\omega)$ are the sine and cosine transformations of the viscoelastic kernel function $\mathcal{H}(t)$. Combining equations (5.2.12) and (5.2.20) results in

$$
\mathscr{M}_t\left\{\cos\Phi_r\mathscr{H}[q_1]\right\}=-\frac{1}{2}\alpha_{rr}a_r\mathcal{H}^s(\omega_r), \quad \mathscr{M}_t\left\{\sin\Phi_r\mathscr{H}[q_1]\right\}=\frac{1}{2}\alpha_{rr}a_r\mathcal{H}^c(\omega_r),
$$

$$\underset{t}{\mathscr{M}}\left\{\sin\Phi_r\mathscr{H}[q_2]\right\}=\frac{1}{2}\alpha_{rr}\alpha_r a_r H^s(\omega_r),\quad \underset{t}{\mathscr{M}}\left\{\cos\Phi_r\mathscr{H}[q_2]\right\}=\frac{1}{2}\alpha_{rr}\alpha_r a_r H^c(\omega_r). \tag{5.2.21}$$

Substituting equation (5.2.21) into (5.2.19) yields

$$\begin{aligned} E_1&=-\beta-\frac{\Omega H^s(\omega_1)}{\omega_1^2-\omega_2^2}\Big(\frac{1}{\alpha_1}+\alpha_1\Big),\\ E_2&=-\beta+\frac{\Omega H^s(\omega_2)}{\omega_1^2-\omega_2^2}\Big(\frac{1}{\alpha_2}+e_2\alpha_2\Big), \end{aligned} \tag{5.2.22}$$

which may be called pseudo-damping coefficients.

It is of importance to note that both the averaged amplitude a_i in (5.2.16a) and phase angle equations ϕ_i in (5.2.16b) do not involve the phase angles and the amplitude equations are decoupled from the phase angle equations. Hence, the averaged amplitude vector (a_1,a_2) is a two dimensional diffusion process.

5.2.2 Moment Lyapunov Exponents

For a two dimensional amplitude system such as equation (5.2.16a) , the eigenvalue problem for moment Lyapunov exponents is given in equation (4.1.42).

To simplify the eigenvalue problem, the parameters α_{11} and α_{22} are deliberately chosen such that

$$\alpha_{21}^2=\frac{\alpha_{22}^2}{\alpha_{11}^2}=\begin{cases}1, & \text{if}\quad D_1D_2=0,\\ \sqrt{\frac{D_1}{D_2}}, & \text{if}\quad D_1D_2\neq 0.\end{cases} \tag{5.2.23}$$

From equation (5.2.18), it is seen that D_1 and D_2 can be rewritten as

$$\begin{aligned} D_1&=\big(\alpha_1-\frac{1}{\alpha_2}\big)^2S(\omega_1+\omega_2)+\big(\alpha_1+\frac{1}{\alpha_2}\big)^2S(\omega_1-\omega_2),\\ D_2&=\big(\alpha_2-\frac{1}{\alpha_1}\big)^2S(\omega_1+\omega_2)+\big(\alpha_2+\frac{1}{\alpha_1}\big)^2S(\omega_1-\omega_2), \end{aligned}$$

which show that D_1 and D_2 are non-negative and D_1 is zero if and only if D_2 equals zero.

Employing the notations

$$D=\alpha_{21}^2 D_2=\alpha_{12}^2 D_1=\sqrt{D_1 D_2}=\left|\left(\alpha_1\alpha_2+\frac{1}{\alpha_1\alpha_2}\right)S^+ -8S^-\right|,$$

$$\tilde{a}=\frac{V_0}{4}(V_1+V_2-2V_3+2D), \quad \tilde{b}=\frac{V_0}{4}(V_1+V_2-2V_3-2D), \tag{5.2.24}$$

$$\Delta_1=E_1+2V_0(V_1+V_3), \quad \Delta_2=E_2+2V_0(V_2+V_3),$$

and substituting equation (5.2.17) and $a_1=r\cos\varphi$, $a_2=r\sin\varphi$ into (4.1.42) yield the eigenvalue problem

$$\begin{aligned}\mathcal{L}(p)=&(D-\tilde{b}\cos^2 2\varphi)T''+\Big\{p\big[\frac{1}{2}V_0(V_2-V_1)\sin 2\varphi-\tilde{b}\sin 4\varphi\big]\\&+\frac{1}{\sin 2\varphi}\big[\frac{1}{2}(\Delta_2-\Delta_1)\sin^2(2\varphi)+2\cos 2\varphi(\tilde{a}-\tilde{b}\cos^2 2\varphi)\big]\Big\}T'\\&+p\Big\{\frac{1}{2}(\Delta_1+\Delta_2)+\frac{1}{2}(\Delta_1-\Delta_2)\cos 2\varphi+2(D-\tilde{b}\cos^2 2\varphi)\\&+p(V_1\cos^2\varphi+V_2\sin^2\varphi+\tilde{b}\cos^2 2\varphi)\Big\}T=\Lambda T, \quad 0\leqslant\varphi<\pi,\end{aligned} \tag{5.2.25}$$

where T' and T'' are the first-order and second-order derivatives of $T(\varphi)$ with respect to φ, respectively. The coefficients are periodic with period π; hence one can use a Fourier cosine series expansion in equation (4.1.44) to obtain the moment Lyapunov exponents from (5.2.25) and Lyapunov exponents from (4.1.50).

For comparison, the largest Lyapunov exponent for system (5.2.16a) can be directly derived from invariant probability density by solving a Fokker-Plank equation (Yin, 1991, equation (3.19)), for the case of $\hat{a}_1\neq\hat{a}_2$ and $\hat{a}_1\neq 0$:

(1) If $\hat{a}_2>0$,

$$\lambda=\frac{\varepsilon}{2}\Big[(\hat{\lambda}_1+\hat{\lambda}_2)+(\hat{\lambda}_1-\hat{\lambda}_2)\coth\Big(\frac{\hat{\lambda}_1-\hat{\lambda}_2}{\sqrt{\Delta_0}}\alpha\Big)\Big], \tag{5.2.26}$$

where $\alpha=\cosh^{-1}(\frac{K}{D})$.

(2) If $\hat{a}_2<0$,

$$\lambda=\frac{\varepsilon}{2}\Big[(\hat{\lambda}_1+\hat{\lambda}_2)+(\hat{\lambda}_1-\hat{\lambda}_2)\coth\Big(\frac{\hat{\lambda}_1-\hat{\lambda}_2}{\sqrt{-\Delta_0}}\alpha\Big)\Big], \tag{5.2.27}$$

where $\alpha=\cos^{-1}(\frac{K}{D})$.

(3) If $\hat{a}_2=0$,

$$\lambda=\frac{\varepsilon}{2}\left[\left(\hat{\lambda}_1+\hat{\lambda}_2\right)+\left(\hat{\lambda}_1-\hat{\lambda}_2\right)\coth\left(\frac{\hat{\lambda}_1-\hat{\lambda}_2}{2\hat{a}_1}\right)\right]. \tag{5.2.28}$$

The constants K and Δ_0 are given as

$$\begin{aligned}
\hat{a}_r&=\frac{V_0}{2}[V_1+V_2-2V_3-(-1)^r 2D]\\
&=\frac{\Omega^2}{32\left(\omega_1^2-\omega_2^2\right)^2}\left[\left(\alpha_1-\frac{1}{\alpha_1}\right)^2 S(2\omega_1)+\left(\alpha_2-\frac{1}{\alpha_2}\right)^2 S(2\omega_2)-4S^+\right.\\
&\quad\left.+2\left(\alpha_1\alpha_2+\frac{1}{\alpha_1\alpha_2}\right)S^- -(-1)^r 2\left|\left(\alpha_1\alpha_2+\frac{1}{\alpha_1\alpha_2}\right)S^+ -8S^-\right|\right],\\
K&=\frac{\hat{a}_1+\hat{a}_2}{2V_0},\quad \Delta_0=16\hat{a}_1\hat{a}_2,\\
\hat{\lambda}_r&=-E_r+2V_0(V_r+V_3)\\
&=\frac{\Omega^2}{2\left(\omega_1^2-\omega_2^2\right)^2}\left[(\alpha_r-\frac{1}{\alpha_r})^2 S(2\omega_r)+2S^+ -\left(\alpha_1\alpha_2+\frac{1}{\alpha_1\alpha_2}\right)S^-\right]\\
&\quad-\beta+(-1)^r\frac{\Omega\, H^s(\omega_r)}{\omega_1^2-\omega_2^2}\left(\frac{1}{\alpha_r}+\alpha_r\right),\quad r=1,\ 2.
\end{aligned}$$

5.2.3 Stability Boundary

Although moment Lyapunov exponents can be numerically determined from equation (5.2.25), sometimes analytical expressions are needed, which can be obtained by setting Fourier series order $K=1,\ 2$ in (4.1.44) as follows.

Case 1: Fourier cosine series expansion order $K=1$

When $K=1$, the eigenfunction is $T(\varphi)=C_0+C_1\cos 2\varphi$, the moment Lyapunov exponent can be solved from

$$\begin{vmatrix} a_{00}-\hat{\Lambda}^{(1)} & a_{01}\\ a_{10} & a_{11}-\hat{\Lambda}^{(1)}\end{vmatrix}=0,\quad \text{or}\quad \left(\hat{\Lambda}^{(1)}\right)^2+e_1^{(1)}\hat{\Lambda}^{(1)}+e_0^{(1)}=0. \tag{5.2.29}$$

This is a quadratic equation, of which the solution obtained analytically is moment Lyapunov exponent. The coefficients for this quadratic equation are given by

$$
\begin{aligned}
e_1^{(1)} =& -\frac{1}{8}\big(13V_1+13V_2+6V_3+6D\big)V_0 p^2 \\
& -\Big[\frac{1}{4}\big(21V_1+21V_2+22V_3+22D\big)V_0+2(E_1+E_2)\Big]p+\big(V_1+V_2-2V_3+14D\big)V_0, \\
e_0^{(1)} =& \Big[\frac{5}{64}(V_1^2+V_2^2)+\frac{37}{32}V_1V_2+\frac{5}{16}\big(V_3+D\big)\big(V_1+V_2\big)+\frac{1}{16}\big(V_3+D\big)^2\Big]V_0^2 p^4 \\
& +\Big\{\Big[\frac{5}{8}(V_1^2+V_2^2)+\frac{29}{4}V_1V_2+\frac{13}{4}\big(V_3+D\big)\big(V_1+V_2\big)+\big(V_3+D\big)^2\Big]V_0 \\
& -\frac{3}{8}(E_1+E_2)(D+V_3)-\big(\frac{5}{16}E_1+\frac{21}{16}E_2\big)V_1-\big(\frac{5}{16}E_2+\frac{21}{16}E_1\big)V_2\Big\}V_0 p^3 \\
& +\Big\{\Big[\frac{1}{16}(V_1^2+V_2^2)+\frac{97}{8}V_1V_2+\big(\frac{31}{4}V_3+\frac{7}{4}D\big)\big(V_1+V_2\big)+\frac{1}{4}\big(17V_3+D\big)\big(V_3+D\big)\Big]V_0^2 \\
& -\Big[\frac{11}{4}(E_1+E_2)(D+V_3)+\big(\frac{5}{8}E_1+\frac{37}{8}E_2\big)V_1+\big(\frac{5}{8}E_2+\frac{37}{8}E_1\big)V_2\Big]V_0 \\
& +\frac{1}{4}E_1^2+\frac{1}{4}E_2^2+\frac{3}{2}E_1E_2\Big\}p^2+\Big\{\Big[-\frac{13}{4}(V_1^2+V_2^2)+V_1V_3+\big(\frac{3}{2}V_2-19D\big)V_1 \\
& +\big(V_3-19D\big)V_2-18DV_3-21D^2+V_3^2\Big]V_0^2 \\
& +\Big[7\big(E_1+E_2\big)D+\big(\frac{5}{2}E_1-\frac{3}{2}E_2\big)V_1+\big(\frac{5}{2}E_2-\frac{3}{2}E_1\big)V_2-\big(E_1+E_2\big)V_3\Big]V_0\Big\}p. \qquad (5.2.30)
\end{aligned}
$$

The Lyapunov exponent is given by

$$
\lambda^{(1)} = -\lim_{p\to 0}\frac{e_0^{(K)}}{p e_1^{(K)}} = \frac{1}{4}\frac{A^{(1)}}{V_1+V_2-2V_3+14D}, \qquad (5.2.31)
$$

where

$$
\begin{aligned}
A^{(1)} =& \Big[13(V_1^2+V_2^2)-6V_1V_2+\big(76D-4V_3\big)\big(V_1+V_2\big)+\big(84D-12V_3\big)\big(D+V_3\big)\Big]V_0 \\
& +(E_1+E_2)(4V_3-28D)-\big(10E_1-6E_2\big)V_1-\big(10E_2-6E_1\big)V_2+2\big(E_1+E_2\big)^2.
\end{aligned}
$$

For white noise, there exists $S^+ = 2S_0$, $S^- = 0$, and

$$V_1 = \left(\alpha_1 - \frac{1}{\alpha_1}\right)^2 S_0, \quad V_2 = \left(\alpha_2 - \frac{1}{\alpha_2}\right)^2 S_0, \quad V_3 = 4S_0,$$
$$D_1 = \left(\alpha_1^2 + \frac{1}{\alpha_2^2}\right) 2S_0, \quad D_2 = \left(\alpha_2^2 + \frac{1}{\alpha_1^2}\right) 2S_0. \tag{5.2.32}$$

The moment Lyapunov exponent is obtained by solving the quadratic equation in (5.2.29) with coefficients in (5.2.30) and the corresponding largest Lyapunov exponents are given in (5.2.31).

Case 2: Fourier cosine series expansion order $K = 2$

When $K = 2$, the eigenfunction is $T(\varphi) = C_0 + C_1 \cos 2\varphi + C_2 \cos 4\varphi$, the moment Lyapunov exponent can be solved from

$$\begin{vmatrix} a_{00} - \hat{\Lambda}^{(2)} & a_{01} & a_{02} \\ a_{10} & a_{11} - \hat{\Lambda}^{(2)} & a_{12} \\ a_{20} & a_{21} & a_{22} - \hat{\Lambda}^{(2)} \end{vmatrix} = 0. \tag{5.2.33}$$

This is a cubic equation, which is $\left(\hat{\Lambda}^{(2)}\right)^3 + e_2^{(2)} \left(\hat{\Lambda}^{(2)}\right)^2 + e_1^{(2)} \hat{\Lambda}^{(2)} + e_0^{(2)} = 0$. The coefficients are too long to list here. For $K \geqslant 3$, no explicit expressions for moment Lyapunov moments can be presented.

5.2.4 Stability Index

The stability index is the non-trivial zero of the moment Lyapunov exponent. Hence, it can be determined as a root-finding problem such that $\Lambda_{q(t)}(\delta_{q(t)}) = 0$. When $K = 1$, the stability index is the non-trivial solution of equation (5.2.29). Typical results of the stability index are shown in Figure 5.2. It is seen that the stability index decreases from positive to negative values with the increase of the amplitude of power spectrum, which suggests that the noise destabilizes the system. It is also found that the larger the damping coefficient β, the larger the stability index, and then the more stable the system.

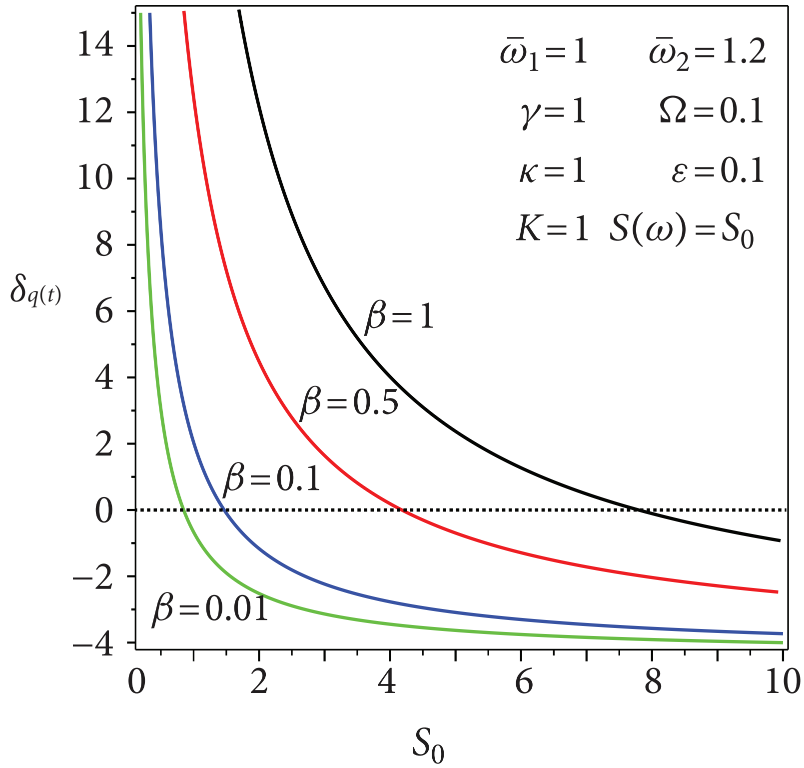

Figure 5.2 Stability index for gyroscopic system under white noises

5.2.5 Simulation

Consider the two-degree-of-freedom system with viscoelastic model in equation (5.2.1) and suppose the excitation is approximated by a Gaussian white noise with spectral density $S(\omega) = \sigma^2 = \text{constant}$ for all ω, then $\xi(t)\mathrm{d}t = \sigma\,\mathrm{d}W(t)$. Let

$$\begin{aligned} &x_1(t) = q_1(t), \quad x_2(t) = \dot{q}_1(t), \quad x_3(t) = q_2(t), \quad x_4(t) = \dot{q}_2(t), \\ &x_5(t) = \int_0^t \gamma\,\mathrm{e}^{-\kappa(t-s)} q_1(s)\,\mathrm{d}s, \quad x_6(t) = \int_0^t \gamma\,\mathrm{e}^{-\kappa(t-s)} q_2(s)\,\mathrm{d}s. \end{aligned} \tag{5.2.34}$$

Equation (5.2.1) can be written as a 6 dimensional system of Itô differential equations

$$\mathrm{d}\mathbf{x} = \mathbf{A}\mathbf{x}\mathrm{d}t + \mathbf{B}\mathbf{x}\mathrm{d}W, \tag{5.2.35}$$

where $\mathbf{x} = \{x_1, x_2, x_3, x_4, x_5, x_6\}^T$, and

$$\mathbf{A} = \begin{bmatrix} 0 & 1 & 0 & 0 & 0 & 0 \\ -(\bar{\omega}_1^2 - \Omega^2) & -\varepsilon 2\beta & \varepsilon 2\beta\Omega & 2\Omega & \varepsilon & 0 \\ 0 & 0 & 0 & 1 & 0 & 0 \\ -\varepsilon 2\beta\Omega & -2\Omega & -(\bar{\omega}_2^2 - \Omega^2) & -\varepsilon 2\beta & 0 & \varepsilon \\ \gamma & 0 & 0 & 0 & -\kappa & 0 \\ 0 & 0 & \gamma & 0 & 0 & -\kappa \end{bmatrix},$$

$$\mathbf{B} = \begin{bmatrix} 0 & 0 & 0 & 0 & 0 & 0 \\ -\varepsilon^{1/2} & 0 & 0 & 0 & 0 & 0 \\ 0 & 0 & 0 & 0 & 0 & 0 \\ 0 & 0 & -\varepsilon^{1/2} & 0 & 0 & 0 \\ 0 & 0 & 0 & 0 & 0 & 0 \\ 0 & 0 & 0 & 0 & 0 & 0 \end{bmatrix}. \tag{5.2.36}$$

Equation (5.2.35) is linear homogeneous. The algorithm introduced by Xie (2006) is applied to simulate the moment Lyapunov exponents. The norm for evaluating the moment Lyapunov exponents is $\|\mathbf{x}(t)\| = \sqrt{x_1^2 + x_2^2 + x_3^2 + x_4^2}$, for x_1, $x_2 x_3$ and x_4 are related to the state variables of the original system. The iteration equations are given by, using the explicit Euler scheme,

$$\begin{aligned}
x_1^{k+1} &= x_1^k + x_2^k \cdot \Delta t, \\
x_2^{k+1} &= x_2^k + \left[-(\bar{\omega}_1^2 - \Omega^2)x_1^k - \varepsilon 2\beta x_2^k + \varepsilon 2\beta\Omega x_3^k + 2\Omega x_4^k + \varepsilon x_5^k\right]\Delta t - \varepsilon^{1/2} x_1^k \sigma \cdot \Delta W^k, \\
x_3^{k+1} &= x_3^k + x_4^k \cdot \Delta t, \\
x_4^{k+1} &= x_4^k + \left[-\varepsilon 2\beta\Omega x_1^k - 2\Omega x_2^k - (\bar{\omega}_2^2 - \Omega^2)x_3^k - \varepsilon 2\beta x_4^k + \varepsilon x_6^k\right]\Delta t - \varepsilon^{1/2} x_3^k \sigma \cdot \Delta W^k, \\
x_5^{k+1} &= x_5^k + \left(\gamma x_1^k - \kappa x_5^k\right)\Delta t, \\
x_6^{k+1} &= x_6^k + \left(\gamma x_3^k - \kappa x_6^k\right)\Delta t,
\end{aligned}$$

with Δt being the time step and k denoting the kth iteration.

5.2.6 Results and Discussion

As expected, both fractional order μ and damping β play a stabilizing role in transverse flexural analysis of the rotating shaft under white noise excitation. Figures 5.3 and 5.4 show that with the increase of μ or β, the slope of the moment curves at the original point change from negative to positive, which suggests the rotating shaft's status changes from instability to stability.

The analytical results from equation (5.2.26) and Fourier series expansion numerical results from (5.2.25) are compared so well that they are nearly overlapped in Figure 5.5, which show that the long and tedious derivations in Sections 5.2.1 and 5.2.2 are correct. Simulations in this figure confirm the numerical and analytical results. Figure 5.5 shows that for small values of $S(\omega)$, the numerical results are consistent with simulation results. The analytical and numerical Lyapunov exponents are tangent lines of results from Monte-Carlo simulation, which confirms the method of stochastic averaging is a valid first-order approximation method. Care should be taken that for $S(\omega) \to 0$, the numerical results may become unstable due to roundoff errors. These results are similar to those in Section 4.1.4 for non-gyroscopic systems.

Figures 5.6 and 5.7 show that when $0 \leqslant \Omega \leqslant \bar{\omega}_1$ and near $\bar{\omega}_1$, the system becomes more and more unstable with the increase of Ω. When $\bar{\omega}_1 \leqslant \Omega \leqslant \bar{\omega}_2$, the system is already unstable. When $\Omega \geqslant \bar{\omega}_2$ and near $\bar{\omega}_2$, with the increase of parameter Ω, the instability area decreases. Furthermore, the boundary is "V"-shaped in Figure 5.7. The viscosity have a great influence on the boundaries when Ω is large.

Figures 5.6 and 5.7 show also show that the noise destabilizes the system, for the increase of $S(\omega)$, the stable region dwindles. This can be clearly seen three-dimensionally in Figures 5.8 and 5.9 for elastic and viscoelastic structures, respectively.

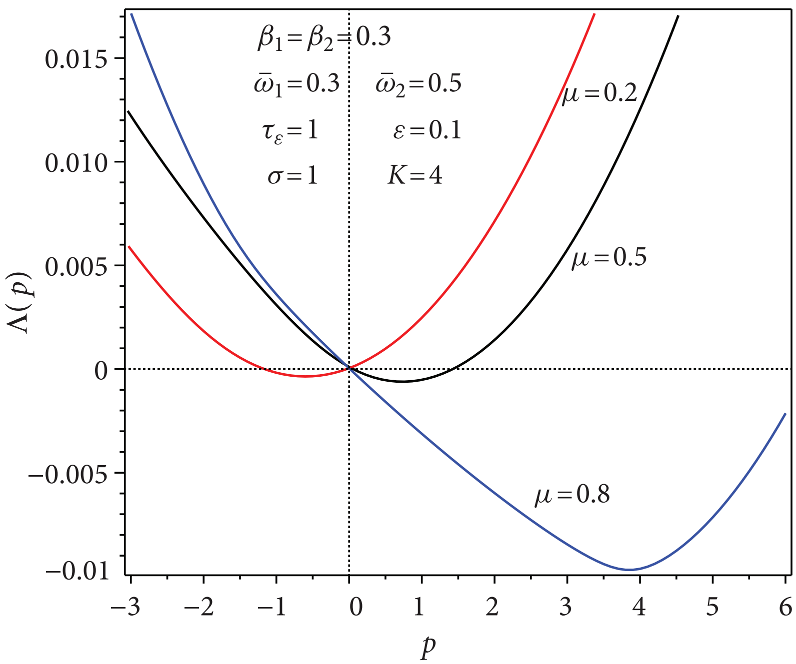

Figure 5.3 Effect of fractional order μ on Moment Lyapunov exponents of fractional gyroscopic systems under Gaussian white noise excitation

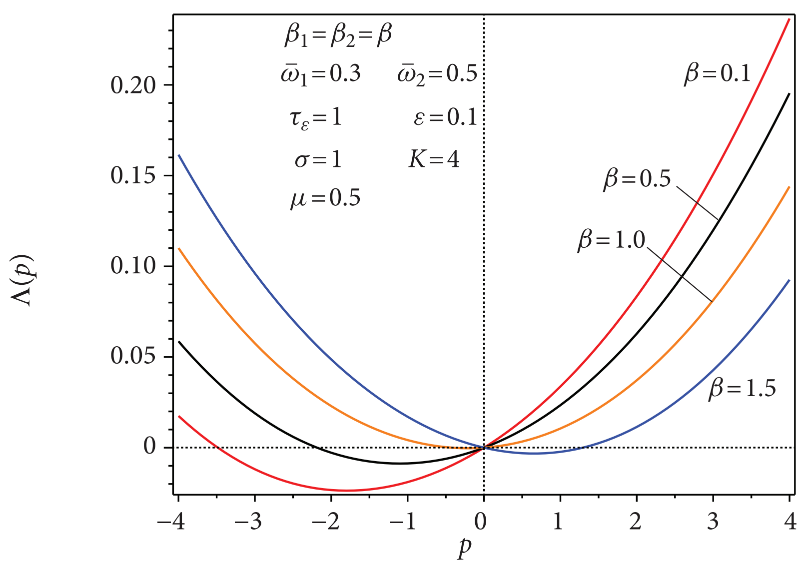

Figure 5.4 Effect of damping on Moment Lyapunov exponents of fractional gyroscopic systems under Gaussian white noise excitation

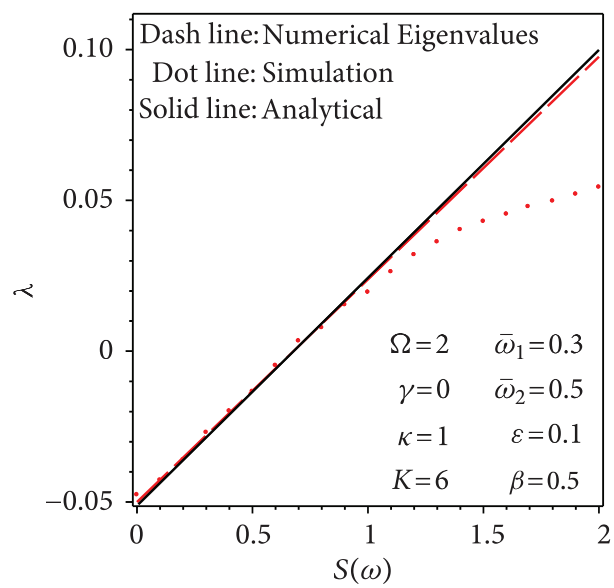

Figure 5.5 Largest Lyapunov exponents of gyroscopic system under white noise excitation

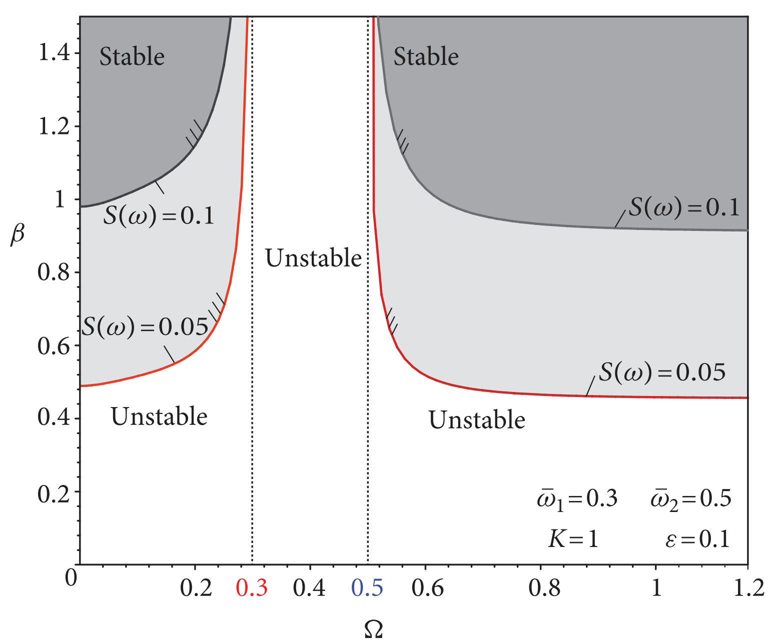

Figure 5.6 Stability boundaries of gyroscopic elastic system with white noise excitation

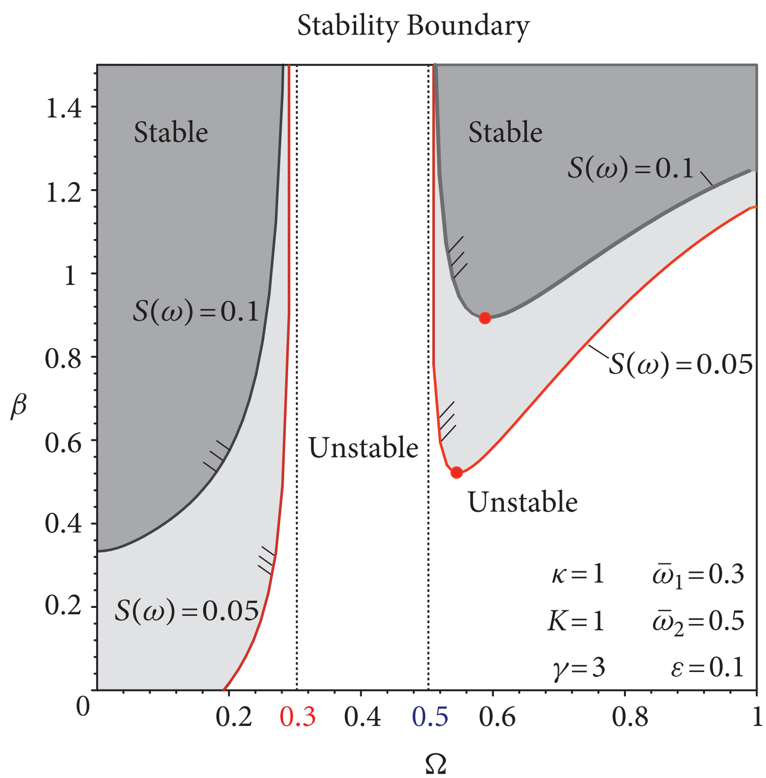

Figure 5.7 Stability boundaries of gyroscopic viscoelastic system with white noise excitation

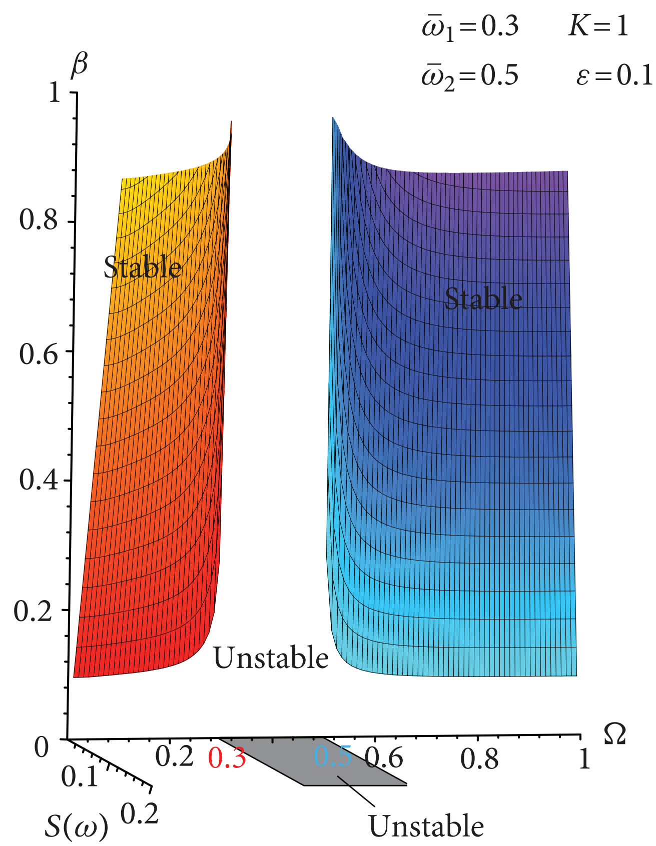

Figure 5.8 Stability boundaries of gyroscopic elastic system with white noise excitation (3D)

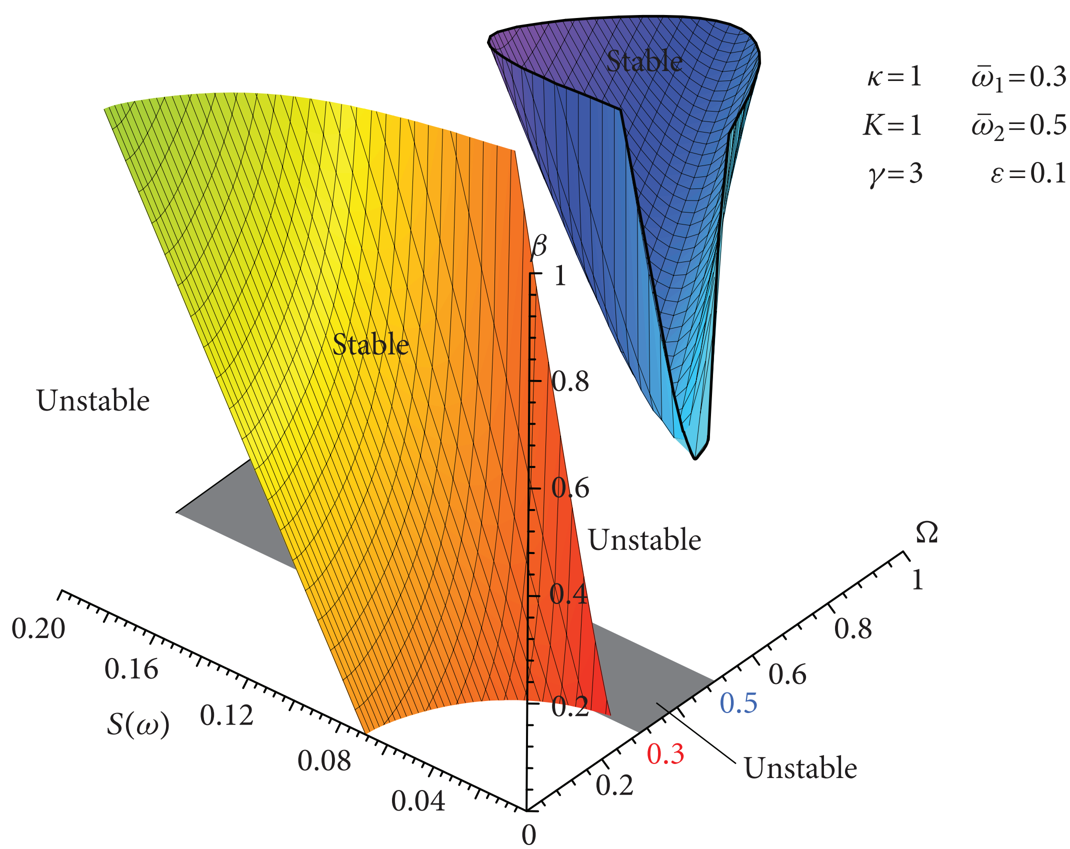

Figure 5.9 Stability boundaries of gyroscopic viscoelastic system with white noise excitation (3D)

5.3 Gyroscopic Systems Excited by Bounded Noise

Stochastic stability of gyroscopic systems under bounded noises has been studied through the property of Lyapunov exponents (Abdelrahman, 2002). Lyapunov exponents can characterize almost sure or sample stability or instability of stochastic systems. However, sample stability cannot assure moment stability which can be explained by the theory of large deviation (Baxendale and Stroock, 1988). It is noted that moment Lyapunov exponents give not only the moment stability but also the almost-sure stability. Although moment Lyapunov exponents play an important role in the dynamic stability analysis of stochastic systems, the actual determination of moment Lyapunov exponents is very difficult, even approximately.

The purpose of this section is to study the moment Lyapunov exponents and Lyapunov exponents of gyroscopic systems under the excitation of weak bounded stochastic parametric loadings. The study is motivated by problems in the dynamic stability of rotating shafts subjected to stochastically fluctuating loadings. The eigenvalue problems for various parametric resonances are formulated by using stochastic averaging method and mathematical transformations. Moment Lyapunov exponents are determined by solving the eigenvalue problems through Fourier series expansions. Stability boundaries are obtained and the effects of various parameters are discussed.

5.3.1 Stochastic Averaging

Consider the gyroscopic system in equation (5.1.9) excited by bounded noise

$$\mathbf{x}''+2\varepsilon_0\beta\mathbf{x}'+2\Omega\begin{bmatrix}0 & -1\\ 1 & 0\end{bmatrix}\mathbf{x}'+\begin{bmatrix}\tilde{\omega}_1^2-\Omega^2-\varepsilon_0\mathscr{H} & -2\varepsilon_0\beta\Omega\\ 2\varepsilon_0\beta\Omega & \tilde{\omega}_2^2-\Omega^2-e_2\varepsilon_0\mathscr{H}\end{bmatrix}\mathbf{x}-\varepsilon_0\tilde{B}(\tau)\mathbf{x}=0,$$
$$\tilde{B}(\tau)=\tilde{\zeta}\cos\left[\nu\tau+\sigma_0 W(\tau)+\theta\right], \tag{5.3.1}$$

where the prime denotes differentiation with respect to time τ. $\mathbf{x}=\{x_1,x_2\}^T$ is the vector of state variables, β is damping coefficient, and $\mathscr{H}$ is an operator for viscoelasticity. For ease of calculation, the damping terms are considered in this section and the viscoelastic terms are treated in next section.

The damping term can be removed by the transformation $x_i(\tau)=q_i(\tau)\mathrm{e}^{-\varepsilon_0\beta\tau}$, $i=1,\ 2$,

$$\mathbf{q}''+2\Omega\begin{bmatrix}0 & -1\\ 1 & 0\end{bmatrix}\mathbf{q}'+\begin{bmatrix}\bar{\omega}_1^2-\Omega^2 & 0\\ 0 & \bar{\omega}_2^2-\Omega^2\end{bmatrix}\mathbf{q}-\varepsilon_0\tilde{B}(\tau)\mathbf{q}=0,$$

$$\tilde{B}(\tau)=\tilde{\zeta}\cos\left[\nu\tau+\sigma_0 W(\tau)+\theta\right], \tag{5.3.2}$$

where $\bar{\omega}_i^2=\tilde{\omega}_i^2-\varepsilon_0^2\beta^2$. To simplify the system, apply the time scaling $t=\nu\tau$

$$\ddot{q}_1-2\frac{\Omega}{\nu}\dot{q}_2+\left(\frac{\bar{\omega}_1^2-\Omega^2}{\nu^2}-\frac{\varepsilon_0}{\nu^2}\tilde{\zeta}\cos\eta(t)\right)q_1=0,$$

$$\ddot{q}_2+2\frac{\Omega}{\nu}\dot{q}_1+\left(\frac{\bar{\omega}_2^2-\Omega^2}{\nu^2}-\frac{\varepsilon_0}{\nu^2}\tilde{\zeta}\cos\eta(t)\right)q_2=0, \tag{5.3.3}$$

$$\eta(t)=t+\psi(t),\quad \psi(t)=\varepsilon^{1/2}\sigma W(t)+\theta,\quad \sigma=\sigma_0/\sqrt{\nu}.$$

The Lyapunov exponents and the moment Lyapunov exponents of system (5.3.3) and (5.3.1) are related by

$$\lambda_{x(\tau)}=-\varepsilon_0\beta+\nu\lambda_{q(t)},\quad \Lambda_{x(\tau)}(p)=-p\varepsilon_0\beta+\nu\Lambda_{q(t)}, \tag{5.3.4}$$

and the Lyapunov exponent is equal to the slope of moment Lyapunov exponent at the origin (Xie, 2006)

$$\lambda_{q(t)}=\Lambda'_{q(t)}(0)=\lim_{p\to 0}\frac{\Lambda_{q(t)}(p)}{p}. \tag{5.3.5}$$

To investigate combination resonances when $\nu=\omega_0(1-\varepsilon\Delta)$, where Δ is the detuning parameter and the small parameter ε shows that the excitation frequency ν vary around the reference frequency ω_0. Equation (5.3.1) becomes

$$\ddot{q}_1-2\omega\dot{q}_2+\left(\bar{\kappa}_1^2-\omega^2\right)q_1=2\varepsilon\left[+\omega\Delta\dot{q}_2-(\bar{\kappa}_1^2-\omega^2)\Delta q_1+\zeta q_1\cos\eta\right],$$

$$\ddot{q}_2+2\omega\dot{q}_1+\left(\bar{\kappa}_2^2-\omega^2\right)q_2=2\varepsilon\left[-\omega\Delta\dot{q}_1-(\bar{\kappa}_2^2-\omega^2)\Delta q_2+\zeta q_2\cos\eta\right], \tag{5.3.6}$$

$$\eta(t)=t+\psi(t),\quad \psi(t)=\varepsilon^{1/2}\sigma W(t)+\theta,\quad \sigma=\sigma_0/\sqrt{\nu},$$

where

$$\bar{\kappa}_{1,2}=\frac{\bar{\omega}_{1,2}}{\omega_0},\quad \omega=\frac{\Omega}{\omega_0},\quad 2\varepsilon\zeta=\frac{\varepsilon_0\tilde{\zeta}}{\omega_0^2}, \tag{5.3.7}$$

with the natural frequencies $\bar{\omega}_1\leqslant\bar{\omega}_2$, then $\bar{\kappa}_1\leqslant\bar{\kappa}_2$.

Equations (5.3.6) admit the trivial solution $q_1=q_2=0$. However, they are not the Lagrange standard form given in equation (1.2.27) or (1.2.40). Hence, to apply the averaging method, one should consider first the unperturbed system, i.e., $\varepsilon=0$, which is of the form

$$\ddot{q}_1+(\bar{\kappa}_1^2-\omega^2)q_1-2\omega\dot{q}_2=0, \quad \ddot{q}_2+(\bar{\kappa}_2^2-\omega^2)q_2+2\omega\dot{q}_1=0. \tag{5.3.8}$$

This is a system of two linear second-order ordinary differential equations, which can be solved by the method of operator (Xie, 2010). Using the D-operator, $D(\cdot)\equiv \mathrm{d}(\cdot)/\mathrm{d}t$, the differential equations become

$$\left[D^2+(\bar{\kappa}_1^2-\omega^2)\right]q_1-2\omega D q_2=0, \quad 2\omega D q_1+\left[D^2+(\bar{\kappa}_2^2-\omega^2)\right]q_2=0. \tag{5.3.9}$$

The determinant of the coefficient matrix is

$$\begin{aligned}\phi(D)&=\begin{vmatrix} D^2+(\bar{\kappa}_1^2-\omega^2) & -2\omega D \\ 2\omega D & D^2+(\bar{\kappa}_2^2-\omega^2)\end{vmatrix}\\ &=D^4+(\bar{\kappa}_1^2+\bar{\kappa}_2^2+2\omega^2)D^2+(\bar{\kappa}_1^2-\omega^2)(\bar{\kappa}_2^2-\omega^2).\end{aligned} \tag{5.3.10}$$

Hence, the characteristic equation is $\phi(\lambda)=\lambda^4+(\bar{\kappa}_1^2+\bar{\kappa}_2^2+2\omega^2)\lambda^2+(\bar{\kappa}_1^2-\omega^2)(\bar{\kappa}_2^2-\omega^2)=0$, and its solutions are

$$\lambda_{1,2}^2=\frac{-(\bar{\kappa}_1^2+\bar{\kappa}_2^2+2\omega^2)\pm\sqrt{(\bar{\kappa}_1^2+\bar{\kappa}_2^2+2\omega^2)^2-4(\bar{\kappa}_1^2-\omega^2)(\bar{\kappa}_2^2-\omega^2)}}{2}=-\kappa_{1,2}^2, \tag{5.3.11}$$

where

$$\kappa_{1,2}^2=\frac{1}{2}\left[(\bar{\kappa}_1^2+\bar{\kappa}_2^2+2\omega^2)\mp\sqrt{(\bar{\kappa}_1^2-\bar{\kappa}_2^2)^2+8\omega^2(\bar{\kappa}_1^2+\bar{\kappa}_2^2)}\right], \tag{5.3.12}$$

or, denoting $\kappa_{1,2}=\omega_{1,2}/\omega_0$,

$$\omega_{1,2}^2=\frac{1}{2}\left[(\bar{\omega}_1^2+\bar{\omega}_2^2+2\Omega^2)\mp\sqrt{(\bar{\omega}_1^2-\bar{\omega}_2^2)^2+8\Omega^2(\bar{\omega}_1^2+\bar{\omega}_2^2)}\right]. \tag{5.3.13}$$

To ensure the undamped and unperturbed system to be stable, the eigenfrequencies $\lambda_{1,2}$ must be pure imaginary numbers, which means that $\kappa_{1,2}$ must be real numbers. This is possible if $(\bar{\kappa}_1^2-\omega^2)(\bar{\kappa}_2^2-\omega^2)>0$, i.e., $\omega<\bar{\kappa}_1, \omega>\bar{\kappa}_2$, implying that the stability regions are $0\leqslant\Omega<\bar{\omega}_1$ and $\Omega>\bar{\omega}_2$, where $\bar{\omega}_i=\bar{\kappa}_i\omega_0$, $i=1, 2$. The system is unstable when $\bar{\omega}_1\leqslant\Omega\leqslant\bar{\omega}_2$. Hence, $\bar{\omega}_1$ and $\bar{\omega}_2$ are the two critical angular velocities of the system.

The complementary solutions of q_1 and q_2 in (5.3.8) have the same form and are given by

$$\begin{aligned} q_1 &= A_{11}\cos\kappa_1 t + A_{12}\sin\kappa_1 t + A_{13}\cos\kappa_2 t + A_{14}\sin\kappa_2 t, \\ q_2 &= A_{21}\cos\kappa_1 t + A_{22}\sin\kappa_1 t + A_{23}\cos\kappa_2 t + A_{24}\sin\kappa_2 t, \end{aligned} \tag{5.3.14}$$

which contain eight arbitrary constants. However, since $\phi(D)$ is a polynomial of degree 4 in D, the complementary solutions should contain only four arbitrary constants. Substituting equations (5.3.14) into the first equation of (5.3.8) to eliminate the four extra constants gives

$$\begin{aligned} \frac{A_{22}}{A_{11}} &= -\frac{\kappa_1^2-(\bar{\kappa}_1^2-\omega^2)}{2\omega\kappa_1}, \quad \frac{A_{21}}{A_{12}} = \frac{\kappa_1^2-(\bar{\kappa}_1^2-\omega^2)}{2\omega\kappa_1}, \\ \frac{A_{24}}{A_{13}} &= -\frac{\kappa_2^2-(\bar{\kappa}_1^2-\omega^2)}{2\omega\kappa_2}, \quad \frac{A_{23}}{A_{14}} = \frac{\kappa_2^2-(\bar{\kappa}_1^2-\omega^2)}{2\omega\kappa_2}. \end{aligned} \tag{5.3.15}$$

Similarly, substituting equations (5.3.14) into the second equation of (5.3.8) yields

$$\begin{aligned} \frac{A_{22}}{A_{11}} &= -\frac{2\omega\kappa_1}{\kappa_1^2-(\bar{\kappa}_2^2-\omega^2)}, \quad \frac{A_{21}}{A_{12}} = \frac{2\omega\kappa_1}{\kappa_1^2-(\bar{\kappa}_2^2-\omega^2)}, \\ \frac{A_{24}}{A_{13}} &= -\frac{2\omega\kappa_2}{\kappa_2^2-(\bar{\kappa}_2^2-\omega^2)}, \quad \frac{A_{23}}{A_{14}} = \frac{2\omega\kappa_2}{\kappa_2^2-(\bar{\kappa}_2^2-\omega^2)}. \end{aligned} \tag{5.3.16}$$

Comparing equations (5.3.15) and (5.3.16) yields

$$\frac{\kappa_i^2-(\bar{\kappa}_1^2-\omega^2)}{2\omega\kappa_i} = \frac{2\omega\kappa_i}{\kappa_i^2-(\bar{\kappa}_2^2-\omega^2)} = \alpha_i, \quad i=1,\ 2. \tag{5.3.17}$$

Substituting equations (5.3.17) into (5.3.14), the solutions of equations (5.3.8) can be written as

$$q_1 = a_1\sin\Phi_1 + a_2\sin\Phi_2, \quad q_2 = a_1\alpha_1\cos\Phi_1 + a_2\alpha_2\cos\Phi_2, \tag{5.3.18}$$

where $\Phi_1 = \kappa_1 t + \phi_1$ and $\Phi_2 = \kappa_2 t + \phi_2$, and a_1, a_2, ϕ_1, and ϕ_2 are constants.

The method of variation of parameters is now applied to determine the solutions of the original perturbed system. Varying the parameters a_1, a_2, ϕ_1, and ϕ_2 in equations (5.3.18) to make them functions of t lead to solutions of the form

$$\begin{aligned} q_1 &= a_1(t)\sin\Phi_1 + a_2(t)\sin\Phi_2, \\ q_2 &= a_1(t)\alpha_1\cos\Phi_1 + a_2(t)\alpha_2\cos\Phi_2, \end{aligned} \tag{5.3.19}$$

where a_r and ϕ_r, $r=1,\ 2$ are solutions of the following four first-order equations

$$\begin{aligned} \dot{a}_1 &= A\big(+B_1 F\cos\Phi_1 - G\sin\Phi_1\big), \quad a_1\dot{\phi}_1 = A\big(-B_1 F\sin\Phi_1 - G\cos\Phi_1\big), \\ \dot{a}_2 &= A\big(-B_2 F\cos\Phi_2 + G\sin\Phi_2\big), \quad a_2\dot{\phi}_2 = A\big(+B_2 F\sin\Phi_2 + G\cos\Phi_2\big), \end{aligned} \tag{5.3.20}$$

where

$$\begin{aligned} A &= \frac{1}{\alpha_1\kappa_1 - \alpha_2\kappa_2} = \frac{2\omega}{\kappa_1^2 - \kappa_2^2}, \\ B_1 &= -\frac{\alpha_2\big(\alpha_1\kappa_1 - \alpha_2\kappa_2\big)}{\alpha_1\kappa_2 - \alpha_2\kappa_1} = -\frac{\alpha_2\kappa_1\kappa_2}{\bar{\kappa}_1^2 - \omega^2} = -\frac{\kappa_1}{\bar{\kappa}_1^2 - \omega^2}\,\frac{\kappa_2^2 - (\bar{\kappa}_1^2 - \omega^2)}{2\omega} \\ &= -\frac{\kappa_1}{\bar{\kappa}_1^2 - \omega^2}\,\frac{\frac{(\bar{\kappa}_1^2 - \omega^2)(\bar{\kappa}_2^2 - \omega^2)}{\kappa_1^2} - (\bar{\kappa}_1^2 - \omega^2)}{2\omega} = \frac{1}{\alpha_1}, \\ B_2 &= \frac{1}{\alpha_2}, \\ F &= 2\varepsilon\Big[+\omega\Delta\dot{q}_2 - (\bar{\kappa}_1^2 - \omega^2)\Delta q_1 + \zeta q_1\cos\eta\Big], \\ G &= 2\varepsilon\Big[-\omega\Delta\dot{q}_1 - (\bar{\kappa}_2^2 - \omega^2)\Delta q_2 + \zeta q_2\cos\eta\Big]. \end{aligned}$$

On deriving (5.3.20), equation (5.3.12) and the corresponding $\kappa_1^2\kappa_2^2 = (\bar{\kappa}_1^2 - \omega^2)(\bar{\kappa}_2^2 - \omega^2)$ and $\kappa_1^2 + \kappa_2^2 = \bar{\kappa}_1^2 + \bar{\kappa}_2^2 - 2\omega^2$ are used.

To obtain first-order approximate solutions of equation (5.3.20), the method of stochastic averaging is used.

$$\begin{aligned} \dot{a}_1 = -\varepsilon\bar{\zeta}\underset{t}{\mathscr{M}}\Big\{&\alpha_1^- a_1\underline{\sin(2\Phi_1 - t - \psi)} + \alpha_{21}^- a_2\sin(\Phi_1 + \Phi_2 - t - \psi) \\ &+ \alpha_{21}^+ a_2\Big[\boxed{\sin(\Phi_1 - \Phi_2 - t - \psi)} + \sin(\Phi_1 - \Phi_2 + t + \psi)\Big]\Big\}, \\ \dot{a}_2 = +\varepsilon\bar{\zeta}\underset{t}{\mathscr{M}}\Big\{&\alpha_2^- a_2\underline{\sin(2\Phi_2 - t - \psi)} + \alpha_{12}^- a_1\sin(\Phi_1 + \Phi_2 - t - \psi) \\ &- \alpha_{12}^+ a_1\Big[\boxed{\sin(\Phi_1 - \Phi_2 - t - \psi)} + \sin(\Phi_1 - \Phi_2 + t + \psi)\Big]\Big\}, \\ a_1\dot{\phi}_1 = \varepsilon\Delta\kappa_1 a_1 - \varepsilon\bar{\zeta}\underset{t}{\mathscr{M}}\Big\{&\alpha_1^- a_1\underline{\cos(2\Phi_1 - t - \psi)} + \alpha_{21}^- a_2\cos(\Phi_1 + \Phi_2 - t - \psi) \end{aligned}$$

$$+\alpha_{21}^{+}a_2\Big[\boxed{\cos(\Phi_1-\Phi_2-t-\psi)}+\cos(\Phi_1-\Phi_2+t+\psi)\Big]\Big\},$$

$$a_2\dot{\phi}_2=\varepsilon\Delta\kappa_2 a_2+\varepsilon\bar{\zeta}\underset{t}{\mathscr{M}}\Big\{\alpha_2^{-}a_2\underline{\cos(2\Phi_2-t-\psi)}+\alpha_{12}^{-}a_1\cos(\Phi_1+\Phi_2-t-\psi)$$

$$+\alpha_{12}^{+}a_1\Big[\boxed{\cos(\Phi_1-\Phi_2-t-\psi)}+\cos(\Phi_1-\Phi_2+t+\psi)\Big]\Big\},$$

$$\dot{\psi}(t)=\varepsilon^{1/2}\sigma\dot{W}(t), \tag{5.3.21}$$

where

$$\alpha_1^{-}=\alpha_1-\frac{1}{\alpha_1}=\frac{\kappa_1-(\bar{\kappa}_1^2-\omega^2)}{2\omega\kappa_1}-\frac{\kappa_1-(\bar{\kappa}_2^2-\omega^2)}{2\omega\kappa_1}=\frac{\bar{\kappa}_2^2-\bar{\kappa}_1^2}{\omega},$$

$$\alpha_1^{+}=\alpha_1+\frac{1}{\alpha_1},\quad \alpha_2^{\pm}=\alpha_2\pm\frac{1}{\alpha_2},$$

$$\alpha_{12}^{\pm}=\alpha_1\pm\frac{1}{\alpha_2},\quad \alpha_{21}^{\pm}=\alpha_2\pm\frac{1}{\alpha_1},\quad \bar{\zeta}=\frac{\zeta\omega}{\kappa_1^2-\kappa_2^2}. \tag{5.3.22}$$

On deriving equation (5.3.21), the following equations are used,

$$K_1=+\frac{2\omega}{\kappa_1^2-\kappa_2^2}\left[\frac{\bar{\kappa}_1^2-\omega^2}{\alpha_1}+\alpha_1(\bar{\kappa}_2^2-\omega^2)+2\omega\kappa_1\right]$$

$$=\frac{2\omega}{\kappa_1^2-\kappa_2^2}\left[(\bar{\kappa}_1^2-\omega^2)\frac{\kappa_1^2-(\bar{\kappa}_2^2-\omega^2)}{2\omega\kappa_1}+(\bar{\kappa}_2^2-\omega^2)\frac{\kappa_1^2-(\bar{\kappa}_1^2-\omega^2)}{2\omega\kappa_1}+2\omega\kappa_1\right]$$

$$=\frac{\kappa_1^2\left(\bar{\kappa}_1^2+\bar{\kappa}_2^2+2\omega^2\right)-2(\bar{\kappa}_1^2-\omega^2)(\bar{\kappa}_2^2-\omega^2)}{\kappa_1(\kappa_1^2-\kappa_2^2)}=\frac{\kappa_1^2(\kappa_1^2+\kappa_2^2)-2\kappa_1^2\kappa_2^2}{\kappa_1(\kappa_1^2-\kappa_2^2)}=\kappa_1,$$

$$K_2=-\frac{2\omega}{\kappa_1^2-\kappa_2^2}\left[\frac{\bar{\kappa}_1^2-\omega^2}{\alpha_2}+\alpha_2(\kappa_2^2-\omega^2)+2\omega\kappa_2\right]=\kappa_2.$$

The explicit averaged equations in equation (5.3.21) depend on the values of κ_1 and κ_2, which leads to the various types of parametric resonances.

5.3.2 Parametric Resonances

Case 1: No Resonance: $\kappa_i \neq \frac{1}{2}$ **and** $|\kappa_1 \pm \kappa_2| \neq 1$

This case implies that all sinusoidal terms in equation (5.3.21) vanish when averaged. The averaged equations are reduced to

$$\dot{a}_i = 0, \quad \dot{\phi}_i = \varepsilon \kappa_i \Delta, \quad i = 1,\ 2, \tag{5.3.23}$$

so that

$$a_i(t) = a_{i0}, \quad \phi_i(t) = \varepsilon \kappa_i \Delta t + \phi_{i0}.$$

The solutions of system equation (5.3.19) are given by

$$\begin{aligned} q_1(t) &= a_{10}(t) \sin\left[\kappa_1\left(1+\varepsilon\Delta\right)t+\phi_{10}\right] + a_{20}(t) \sin\left[\kappa_2\left(1+\varepsilon\Delta\right)t+\phi_{20}\right], \\ q_2(t) &= a_{10}(t)\alpha_1 \cos\left[\kappa_1\left(1+\varepsilon\Delta\right)t+\phi_{10}\right] + a_{20}(t)\alpha_2 \cos\left[\kappa_2\left(1+\varepsilon\Delta\right)t+\phi_{20}\right], \end{aligned} \tag{5.3.24}$$

which are bounded and periodic.

Case 2: Subharmonic Resonance: $\kappa_i = \frac{1}{2}$**,** $\kappa_j \neq \frac{1}{2}$, $i, j = 1,\ 2$**, and** $i \neq j$

When $\kappa_i = \frac{1}{2}$, $\omega_0 = 2\omega_i$, or $\nu = \omega_0(1-\varepsilon\Delta) \approx 2\omega_i$. For $j \neq i$, all sinusoidal terms in equation (5.3.21) vanish when averaged and the averaged equations are the same as equation (5.3.24); hence $q_j(t)$ is bounded and periodic for $j \neq i$.

For the ith mode, when averaged only the underlined sinusoidal terms in equation (5.3.21) survive, hence the averaged equations are given as (take $i = 1$ as an example)

$$\begin{aligned} &\dot{a}_1 = -\varepsilon\bar{\zeta}\alpha_1^- a_1 \sin(2\phi_1 - \psi), \quad \dot{\phi}_1 = \varepsilon\frac{1}{2}\Delta - \varepsilon\bar{\zeta}\alpha_1^- \cos(2\phi_1 - \psi), \\ &\dot{a}_2 = 0, \quad \dot{\phi}_2 = \varepsilon\kappa_2\Delta, \\ &\dot{\psi}(t) = \varepsilon^{1/2}\sigma\dot{W}(t). \end{aligned} \tag{5.3.25}$$

It is seen that a_2 and ϕ_2 are independent from other processes a_1, ϕ_1, and ψ. One doesn't have to consider a_2 to obtain moment Lyapunov exponents. If the random noise is not considered, $\psi(t) = 0$, the system becomes deterministic, then equation (5.3.25) is reduced to the cases in (Xie, 2006).

By defining the pth norm $P=a_1^p$ and a new process $\chi=2\phi_1-\psi$, the Itô equation for P and χ can be obtained using Itô's Lemma

$$\mathrm{d}P=-\varepsilon pP\bar{\zeta}\alpha_1^- \sin\chi\,\mathrm{d}t,\quad \mathrm{d}\chi=\varepsilon[\Delta-2\bar{\zeta}\alpha_1^- \cos\chi]\mathrm{d}t-\varepsilon^{1/2}\sigma\dot{W}(t). \tag{5.3.26}$$

Applying a linear stochastic transformation

$$S=T(\chi)P,\quad P=T^{-1}(\chi)S,\quad 0\leqslant\chi\leqslant 2\pi \tag{5.3.27}$$

and Itô's Lemma, one obtains the Itô equation for S

$$\mathrm{d}S=\frac{1}{2}\varepsilon P\Big\{\sigma^2T''+[2\Delta-4\bar{\zeta}\alpha_1^- \cos\chi]T'-2p\bar{\zeta}\alpha_1^- \sin\chi\, T\Big\}\mathrm{d}t-\sqrt{\varepsilon}P\sigma T'\mathrm{d}W, \tag{5.3.28}$$

where T' and T'' are the first-order and second-order derivatives of $T(\chi)$ with respect to χ, respectively. For bounded and non-singular transformation $T(\chi)$, both processes P and S are expected to have the same stability behaviour, as equation (5.3.27) is a linear transformation. Therefore, $T(\chi)$ is chosen so that the drift term of the Itô equation (5.3.28) is independent of χ, so that

$$\mathrm{d}S=\Lambda S\,\mathrm{d}t+\sigma_S\mathrm{d}W(t). \tag{5.3.29}$$

Comparing the drift terms in equations (5.3.28) and (5.3.29), such a transformation $T(\chi)$ is given by the following differential equation

$$\frac{1}{2}\varepsilon\sigma^2T''+\varepsilon[\Delta-2\bar{\zeta}\alpha_1^- \cos\chi]T''-\varepsilon p\bar{\zeta}\alpha_1^- \sin\chi\, T=\Lambda T. \tag{5.3.30}$$

Equation (5.3.30) defines an eigenvalue problem for a second-order differential operator with $\Lambda(p)$ being the eigenvalue and $T(\chi)$ the associated eigenfunction. Taking the expected value of equation (5.3.29) leads to $\mathrm{dE}[S]=\Lambda\mathrm{E}[S]\mathrm{d}t$, from which it can be seen that Λ is the Lyapunov exponent of the transformed pth moment $\mathrm{E}[S]$ of equation (5.3.26). Since both processes P and S have the same stability behaviour, Λ is the Lyapunov exponent of pth moment $\mathrm{E}[P]$. The remaining task for determining the moment Lyapunov exponents is to solve the eigenvalue problem.

Since the coefficients are periodic with period 2π, equation (5.3.30) can be solved using a Fourier series expansion of the eigenfunction.

$$T(\chi)=C_0+\sum_{k=1}^{N}[C_k\cos(k\chi)+S_k\sin(k\chi)], \tag{5.3.31}$$

where C_0, C_k, S_k, $k=1, 2, \cdots, N$ are constant coefficients to be determined.

Substituting the expansion into eigenvalue problem (5.3.30) and equating the coefficients of like trigonometric terms $\sin k\chi$ and $\cos k\chi$, $k=0, 1, \cdots, N$ yield a set of homogeneous linear algebraic equations with $2N+1$ equations for the unknown coefficients C_0, C_k and S_k. To have a non-trial solution of the C_0, C_k and S_k, it is required that the determinant of the coefficient matrix of the homogeneous equations equal zero to yield a polynomial equation of degree $2N+1$ for $\Lambda^{(N)}(p)$,

$$a_{2N+1}^{(N)}[\Lambda^{(N)}]^{2N+1}+a_{2N}^{(N)}[\Lambda^{(N)}]^{2N}+\cdots+a_1^{(N)}\Lambda^{(N)}+a_0^{(N)}=0, \tag{5.3.32}$$

where $\Lambda^{(N)}$ denotes the approximate moment Lyapunov exponent. Using the relation in equation (1.1.7) between the moment Lyapunov exponent and the Lyapunov exponent yields the approximate largest Lyapunov exponent. For small N, the analytical moment Lyapunov exponent and Lyapunov exponent can be obtained. For example, when $N=2$, the analytical Lyapunov exponent of the original system (5.3.1) can be obtained as follows, also considering the effect of damping

$$\lambda=E_i+\nu\frac{2\varepsilon^2\bar{\zeta}^2(\alpha_1^-)^2\sigma^2[\sigma^4+2\bar{\zeta}^2(\alpha_1^-)^2+\Delta^2]}{4\bar{\zeta}^2(\alpha_1^-)^2[\bar{\zeta}^2(\alpha_1^-)^2+\sigma^4-2\Delta^2]+4\Delta^4+\sigma^8+5\sigma^4\Delta^2}, \tag{5.3.33}$$

where E_i, $i=1, 2$, are given in equations (5.2.19) or (5.2.22).

The stability boundaries are shown three-dimensionally in Figures 5.10 and 5.11, which depict the parametric resonance around reference frequencies $2\omega_1$ and $2\omega_2$, respectively. The characteristics of parametric resonance around reference frequencies $2\omega_1$ and $2\omega_2$ are quite different. In parametric resonance around $2\omega_1$, when $\Omega<\bar{\omega}_1$, the angular velocity stabilizes the system, as the unstable areas diminish with the increase of Ω. On the contrary, when $\Omega>\bar{\omega}_2$, the unstable areas expand with the increase of Ω, which suggests the angular velocity destabilizes the system. However, in parametric resonance around $2\omega_2$, the unstable areas always decrease with the increase of Ω. Note that the unperturbed system is already unstable when $\bar{\omega}_1\leqslant\Omega\leqslant\bar{\omega}_2$. The unstable areas are always "V"-shaped. The frequency of parametric resonance varies with the parameter Ω. This is due to the fact that $\omega_{1,2}$ is a function of Ω from equation (5.3.13).

The effect of noise parameters ζ and σ on the Lyapunov exponents are shown in Figures 5.12 and 5.13, respectively. It is seen that noise amplitude ζ destabilizes the system but the noise intensity σ has the effect of stabilization. The reason comes from the spectral density function of bounded noise in equation (1.2.8). When ζ decreases or σ increases, the spectral density curve becomes flat, and the energy distributes more equally over the whole range of frequencies instead of concentrating around one single frequency; hence, the system becomes more stable.

Moment Lyapunov exponents are plotted in Figure 5.14. It is seen that for small noise σ, the excitation is a narrow-band process, the effect of parametric resonance is very significant. When σ is increased, the bandwidth of the bounded noise increases, and less prominent effect of the parametric resonance is observed.

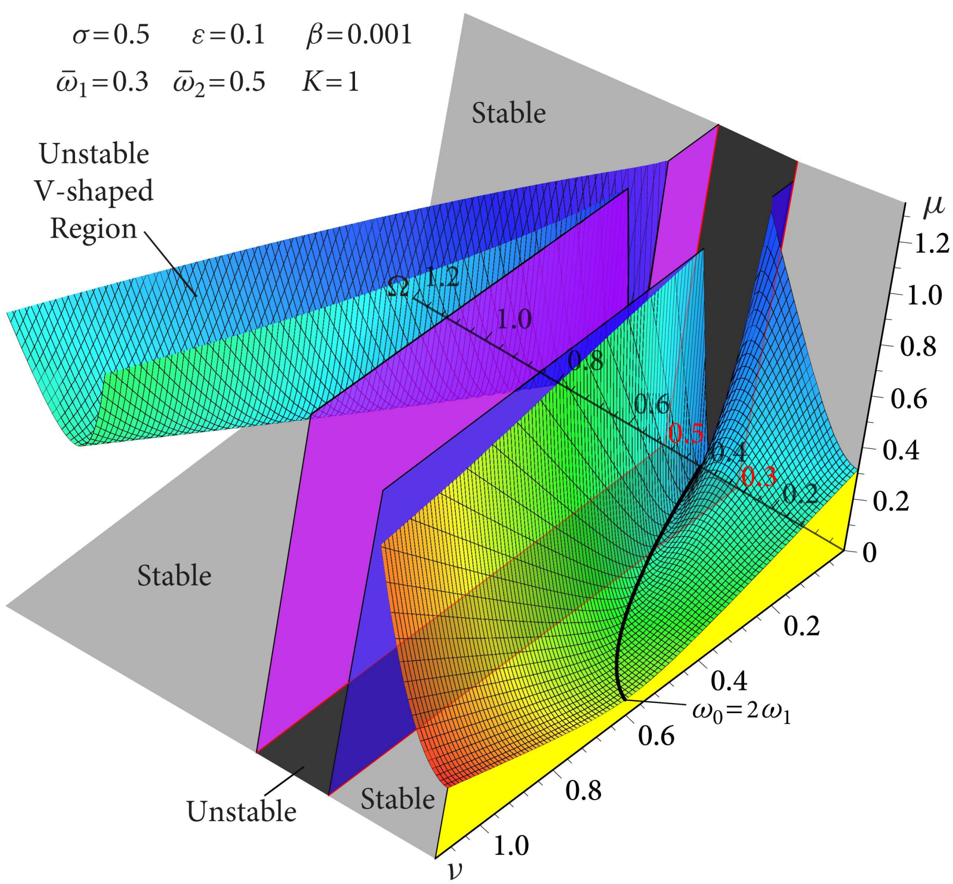

Figure 5.10 Instability regions for subharmonic resonance with $\omega_0 = 2\omega_1$

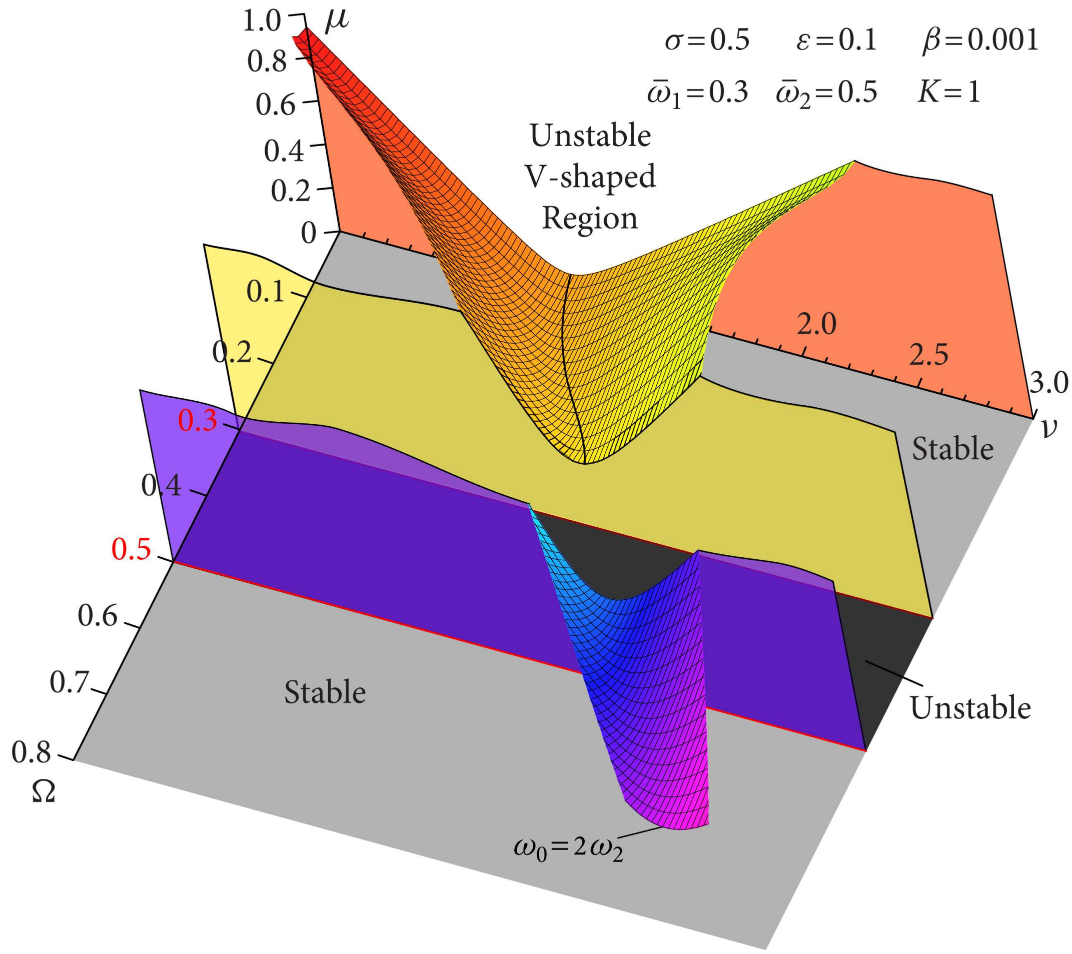

Figure 5.11 Instability regions for subharmonic resonance with $\omega_0 = 2\omega_2$

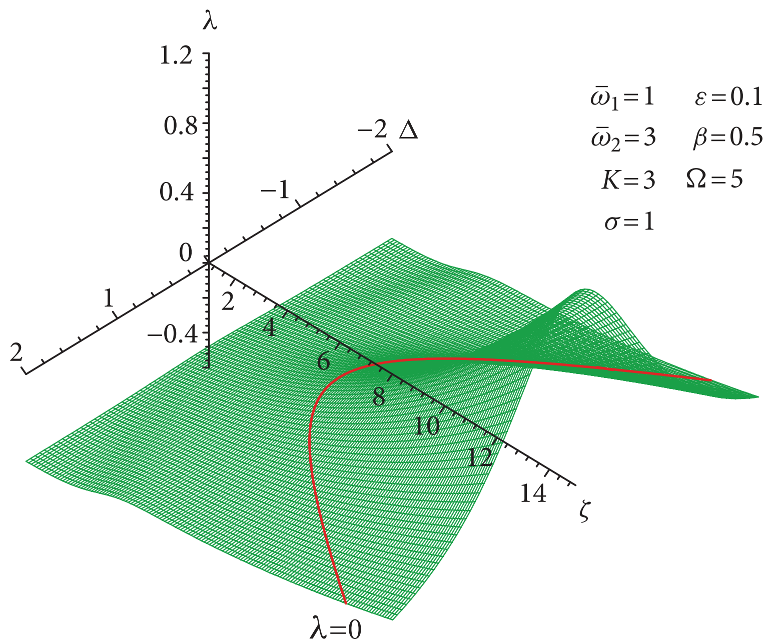

Figure 5.12 Effect of ζ on Lyapunov exponents for subharmonic resonance

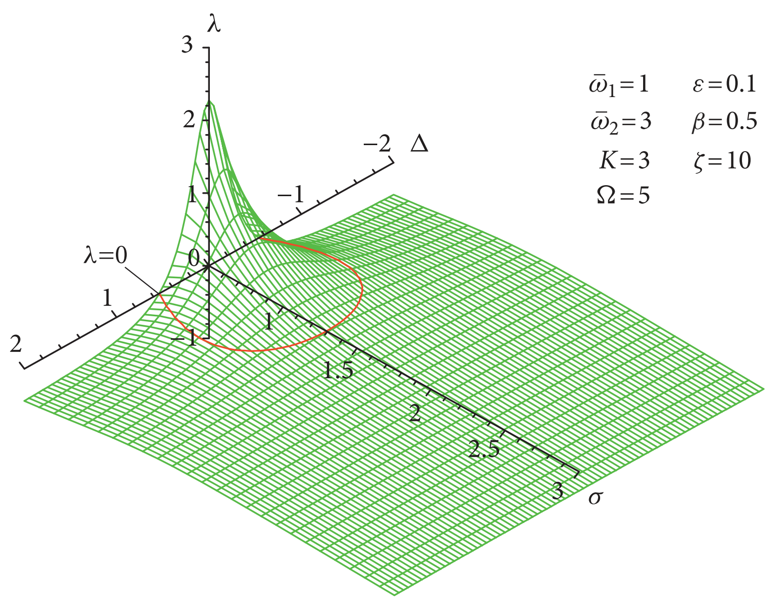

Figure 5.13 Effect of σ on Lyapunov exponents for subharmonic resonance

Case 3: Combination Additive Resonance: $\kappa_1+\kappa_2=1$ **or** $\omega_0=\omega_1+\omega_2$, $\kappa_1\neq\frac{1}{2}$

When $\kappa_1+\kappa_2=1$, one has $\nu=\omega_0(1-\varepsilon\Delta)\approx\omega_1+\omega_2$. When averaged, only the grey-background sinusoidal terms in equation (5.3.21) survive, so the averaged equations are

$$\begin{aligned}
&\dot{a}_1=-\varepsilon\bar{\zeta}\alpha_{21}^{-}a_2\sin(\phi_1+\phi_2-\psi),\quad \dot{a}_2=\varepsilon\bar{\zeta}\alpha_{12}^{-}a_1\sin(\phi_1+\phi_2-\psi),\\
&\dot{\phi}_1=\varepsilon\kappa_1\Delta-\varepsilon\bar{\zeta}\alpha_{21}^{-}\frac{a_2}{a_1}\cos(\phi_1+\phi_2-\psi),\\
&\dot{\phi}_2=\varepsilon\kappa_2\Delta+\varepsilon\bar{\zeta}\alpha_{12}^{-}\frac{a_1}{a_2}\cos(\phi_1+\phi_2-\psi),\\
&\dot{\psi}(t)=\varepsilon^{1/2}\sigma\dot{W}(t).
\end{aligned}\tag{5.3.34}$$

By applying the Khasminskii transformation and defining the pth norm,

$$P=a^p,\quad a=\sqrt{a_1^2+a_2^2},\quad \cos\varphi=\frac{a_1}{a},\quad \sin\varphi=\frac{a_2}{a},\tag{5.3.35}$$

and a new process $\chi=\phi_1+\phi_2-\psi$, the Itô equation for P,φ, and χ can be obtained by using Itô's Lemma

$$\begin{aligned}
&\mathrm{d}P=m_P\mathrm{d}t=\varepsilon pP\bar{\zeta}\sin\varphi\cos\varphi\sin\chi\left(\alpha_{12}^{-}-\alpha_{21}^{-}\right)\mathrm{d}t,\\
&\mathrm{d}\chi=\varepsilon\left[(\kappa_1+\kappa_2)\Delta-\bar{\zeta}\cos\chi\left(\alpha_{21}^{-}\frac{a_2}{a_1}-\alpha_{12}^{-}\frac{a_1}{a_2}\right)\right]\mathrm{d}t-\varepsilon^{1/2}\sigma\mathrm{d}W,\\
&\mathrm{d}\varphi=m_\varphi\mathrm{d}t=\varepsilon\bar{\zeta}\sin\chi\left(\alpha_{12}^{-}\cos^2\varphi+\alpha_{21}^{-}\sin^2\varphi\right)\mathrm{d}t.
\end{aligned}\tag{5.3.36}$$

Applying a linear stochastic transformation

$$S=T(\varphi,\chi)P,\quad P=T^{-1}(\varphi,\chi)S,\tag{5.3.37}$$

and Itô's Lemma, one finds the Itô equation for S is

$$\begin{aligned}
&\mathrm{d}S=\varepsilon P\left\{\frac{1}{2}\sigma^2T''+m_{1\varphi}T`+m_{1\chi}T'+m_0T\right\}\mathrm{d}t-\sqrt{\varepsilon}P\sigma T'\mathrm{d}W,\\
&m_{1\varphi}=\bar{\zeta}\sin\chi\left(\alpha_{12}^{-}\cos^2\varphi+\alpha_{21}^{-}\sin^2\varphi\right),\\
&m_{1\chi}=\Delta-\bar{\zeta}\cos\chi\left(\alpha_{21}^{-}\tan\varphi-\alpha_{12}^{-}\cot\varphi\right),\\
&m_0=p\bar{\zeta}\sin\varphi\cos\varphi\sin\chi\left(\alpha_{12}^{-}-\alpha_{21}^{-}\right),
\end{aligned}\tag{5.3.38}$$

where T' and $T`$ are the first-order partial derivatives of $T(\varphi, \chi)$ with respect to χ and φ, respectively. T'' is the second-order partial derivative with respect to χ.

The eigenvalue problem can be obtained from equation (5.3.38), similar to equation (5.3.30),

$$\varepsilon\left\{\frac{1}{2}\sigma^2 T''+m_{1\varphi}T`+m_{1\chi}T'+m_0 T\right\}=\Lambda T, \tag{5.3.39}$$

which is a two-dimensional second-order partial differential equation with Λ being the eigenvalue and $T(\varphi, \chi)$ the associated eigenfunctions. To eliminate the singularities at $\varphi=0$ or $\pi/2$ in $m_{1\chi}$, multiplying equation (5.3.39) by $\sin 2\varphi$ leads to

$$\begin{aligned}&\frac{\varepsilon}{2}\sigma^2\sin 2\varphi T''+\varepsilon\bar{\zeta}\sin\chi\left(\alpha_{12}^-\cos^2\varphi+\alpha_{21}^-\sin^2\varphi\right)\sin 2\varphi T`\\&+\varepsilon\Big[\Delta\sin 2\varphi-2\bar{\zeta}\cos\chi\left(\alpha_{21}^-\sin^2\varphi-\alpha_{12}^-\cos^2\varphi\right)\Big]T'\\&+\frac{\varepsilon}{2}p\bar{\zeta}\sin^2 2\varphi\sin\chi\left(\alpha_{12}^- -\alpha_{21}^-\right)T=\Lambda T\sin 2\varphi.\end{aligned} \tag{5.3.40}$$

This equation can be transformed into a generalized eigenvalue problem. Since the coefficients of the eigenvalue problem are periodic functions in χ of period 2π and in φ of period $\pi/2$, the eigenfunction $T(\varphi, \chi)$ can be expanded in double Fourier series in the complex form

$$T(\varphi,\chi)=\sum_{l=-\infty}^{\infty}\sum_{k=-\infty}^{\infty}C_{l,k}\,\mathrm{e}^{\mathrm{i}\,(l\chi+4k\varphi)}, \tag{5.3.41}$$

where the coefficients $C_{l,k}$ are complex numbers. Substituting equation (5.3.41) into equation (5.3.40), multiplying the resulting equation by $\mathrm{e}^{-\mathrm{i}\,(r\chi+4s\varphi)}$, integrating with respect to χ from 0 to 2π and with respect to φ from 0 to $\pi/2$ yields, for $r, s=0, \pm1, \pm2, \ldots,$

$$\begin{aligned}&\sum_{l=-\infty}^{\infty}\sum_{k=-\infty}^{\infty}\int_{\chi=0}^{2\pi}\int_{\varphi=0}^{\pi/2}C_{l,k}\mathcal{L}(p)[\mathrm{e}^{\mathrm{i}(l\chi+4k\varphi)}]\mathrm{e}^{-\mathrm{i}(r\chi+4s\varphi)}\mathrm{d}\varphi\mathrm{d}\chi\\&=\Lambda\sum_{l=-\infty}^{\infty}\sum_{k=-\infty}^{\infty}\int_{\chi=0}^{2\pi}\int_{\varphi=0}^{\pi/2}C_{l,k}\mathrm{e}^{\mathrm{i}(l\chi+4k\varphi)}\mathrm{e}^{-\mathrm{i}(r\chi+4s\varphi)}\left[-\mathrm{i}\cdot\frac{\mathrm{e}^{\mathrm{i}2\varphi}-\mathrm{e}^{-\mathrm{i}2\varphi}}{2}\right]\mathrm{d}\varphi\mathrm{d}\chi,\end{aligned} \tag{5.3.42}$$

where

$$\mathcal{L}(p)[\mathrm{e}^{\mathrm{i}(l\chi+4k\varphi)}]$$

$$
\begin{aligned}
&=\Big\{\frac{\varepsilon}{2}\sin(2\varphi)\sigma^2(-l^2)+\varepsilon\Big[\Delta\sin 2\varphi-2\bar{\zeta}\cos\chi\left(\alpha_{21}^-\sin^2\varphi-\alpha_{12}^-\cos^2\varphi\right)\Big](\mathrm{i}l)\\
&+\varepsilon\bar{\zeta}\sin\chi\left(\alpha_{12}^-\cos^2\varphi+\alpha_{21}^-\sin^2\varphi\right)\sin 2\varphi\cdot(\mathrm{i}4k)\\
&+\frac{\varepsilon}{2}p\bar{\zeta}\sin^2 2\varphi\sin\chi\left(\alpha_{12}^--\alpha_{21}^-\right)\Big\}\mathrm{e}^{\mathrm{i}(l\chi+4k\varphi)}. \qquad (5.3.43)
\end{aligned}
$$

For ease of numerical computation of the eigenvalues, truncate the double Fourier series (5.3.41) for $l,r=-L,-L+1,\cdots,L$, and $k,s=-K,-K+1,\cdots,K$. Transform the rectangular array for the coefficients $C_{l,k}$ to a vector Z of length $(2L+1)(2K+1)$, with the jth element Z_j, $j=(2K+1)(L+l)+(K+k)+1$, corresponding to $C_{l,k}$. Equation (5.3.42) can be further cast into a generalized linear algebraic eigenvalue problem

$$\mathbf{AZ}=\Lambda\mathbf{BZ}, \qquad (5.3.44)$$

where both $\mathbf{A}$ and $\mathbf{B}$ are matrices with dimension $(2L+1)(2K+1)\times(2L+1)(2K+1)$. For the element of Ith row and jth column of $\mathbf{A}$ and $\mathbf{B}$ are given by, respectively,

$$
\begin{aligned}
&A_{Ij}=\int_{\chi=0}^{2\pi}\int_{\varphi=0}^{\pi/2}\mathcal{L}(p)[\mathrm{e}^{\mathrm{i}(l\chi+4k\varphi)}]\mathrm{e}^{-\mathrm{i}(r\chi+4s\varphi)}\mathrm{d}\varphi\mathrm{d}\chi,\\
&B_{Ij}=\int_{\chi=0}^{2\pi}\int_{\varphi=0}^{\pi/2}\mathrm{e}^{\mathrm{i}(l\chi+4k\varphi)}\mathrm{e}^{-\mathrm{i}(r\chi+4s\varphi)}\left[-\mathrm{i}\frac{\mathrm{e}^{\mathrm{i}2\varphi}-\mathrm{e}^{-\mathrm{i}2\varphi}}{2}\right]\mathrm{d}\varphi\mathrm{d}\chi, \qquad (5.3.45)\\
&I=(2K+1)(L+r)+(K+s)+1,\quad j=(2K+1)(L+l)+(K+k)+1,\\
&r=-L,\cdots,-1,0,1,\cdots,L,\quad s=-K,\cdots,-1,0,1,\cdots,K.
\end{aligned}
$$

To have nontrivial solutions for system (5.3.44), the determinant of the coefficient matrix must be zero, i.e., $|\mathbf{A}-\Lambda\mathbf{B}|=0$. By solving this generalized eigenvalue problem, the moment Lyapunov exponent can be determined.

The effect of noise parameters of ζ and σ on Lyapunov exponents for combination additive resonance is the same as cases for subharmonic resonance, shown in Figures 5.15 and 5.16, respectively. The parametric resonance around $\Delta=0$ can be clearly seen.

Figure 5.17 shows that although the parametric resonance is significant when σ is small; with the increase of σ, the V-shaped unstable region becomes flat. The effect of σ on Lyapunov exponents for combination additive resonance is shown in Figure 5.18. The bounded noise is a sinusoidal function with noise superimposed. The larger the value of σ, the noisier the bounded noise $\eta(t)$, resulting in a smaller effect of the parametric resonance. This result is similar to the conclusion of McDonald and Namachchivaya (2002), which stated that the addition of forcing can extend the stability region of this system. Figure 5.20 confirms that the parametric resonance is around $\Delta=0$.

The stability boundaries are shown in Figure 5.19. When $\Omega \geqslant \bar{\omega}_2$, the system is stable. When $\bar{\omega}_1 \leqslant \Omega \leqslant \bar{\omega}_2$, the system is already unstable. When $\Omega \leqslant \bar{\omega}_1$, with the increase of Ω, the "V"-shaped instability area expands. This clearly shows that the parameter Ω destabilizes the system.

Case 4: Combination Differential Resonance: $|\kappa_1-\kappa_2|=1$ **or** $\omega_0=|\omega_1-\omega_2|$, $\kappa_1 \neq \frac{1}{2}$

When $|\kappa_1-\kappa_2|=1$, one has $\nu=\omega_0(1-\varepsilon\Delta) \approx |\omega_1-\omega_2|$. When averaged, only the boxed sinusoidal terms in equation (5.3.21) survive, and the averaged equations are

$$
\begin{aligned}
&\dot{a}_1=-\varepsilon\bar{\zeta}\,\alpha_{21}^{-}a_2\sin(\phi_1-\phi_2-\psi), \quad \dot{a}_2=-\varepsilon\bar{\zeta}\,\alpha_{12}^{-}a_1\sin(\phi_1-\phi_2-\psi),\\
&\dot{\phi}_1=\varepsilon\kappa_1\Delta-\varepsilon\bar{\zeta}\,\alpha_{21}^{-}\frac{a_2}{a_1}\cos(\phi_1-\phi_2-\psi),\\
&\dot{\phi}_2=\varepsilon\kappa_2\Delta+\varepsilon\bar{\zeta}\,\alpha_{12}^{-}\frac{a_1}{a_2}\cos(\phi_1-\phi_2-\psi),\\
&\dot{\psi}(t)=\varepsilon^{1/2}\sigma\dot{W}(t).
\end{aligned}
\tag{5.3.46}
$$

The eigenvalue problem can be obtained as

$$
\bar{\mathcal{L}}(p)T=\varepsilon\left\{\frac{1}{2}\sigma^2T''+m_{1\varphi}T^{`}+m_{1\chi}T'+m_0T\right\}=\Lambda T,
\tag{5.3.47}
$$

which is a two-dimensional second-order partial differential equation with Λ being the eigenvalue and $T(\varphi,\chi)$ the associated eigenfunctions. To eliminate the singularities at $\varphi=0$ or $\pi/2$ in $m_{1\chi}$, multiplying equation (5.3.47) by $\sin 2\varphi$ leads to

$$
\begin{aligned}
&\frac{1}{2}\sigma^2\sin 2\varphi T''+\bar{\zeta}\sin\chi\left(\alpha_{21}^{-}\sin^2\varphi-\alpha_{12}^{-}\cos^2\varphi\right)\sin 2\varphi T^{`}\\
&+\left[\Delta\sin 2\varphi-2\bar{\zeta}\cos\chi\left(\alpha_{21}^{-}\sin^2\varphi+\alpha_{12}^{-}\cos^2\varphi\right)\right]T'\\
&-\frac{1}{2}p\bar{\zeta}\sin^2 2\varphi\sin\chi\left(\alpha_{12}^{-}+\alpha_{21}^{-}\right)T=\Lambda T\sin 2\varphi.
\end{aligned}
\tag{5.3.48}
$$

This equation can be transformed into a generalized eigenvalue problem, from which the moment Lyapunov exponents Λ can be obtained by using double Fourier series expansion. The stability boundaries are shown in Figure 5.21. For differential resonances, when $0 \leqslant \Omega \leqslant \bar{\omega}_1$, the system is stable. When $\bar{\omega}_1 \leqslant \Omega \leqslant \bar{\omega}_2$, the system is already unstable. When $\Omega \geqslant \bar{\omega}_2$, the instability area is "V"-shaped. With the increase of parameter Ω, the instability area decreases, which shows Ω plays a role of stability.

5.3.3 Effect of Viscoelasticity

To investigate the effect of viscoelasticity and combination resonances when $\nu = \omega_0(1-\varepsilon\Delta)$, one may obtain the following equations from equations (5.1.5) or (5.3.1) , similar to (5.3.6),

$$\begin{aligned}
&\ddot{q}_1 - 2\omega\dot{q}_2 + \big(\bar{\kappa}_1^2 - \omega^2\big)q_1 = 2\varepsilon\Big[+\omega\Delta\dot{q}_2 - (\bar{\kappa}_1^2-\omega^2)\Delta q_1 + \bar{\kappa}_1^2\mathscr{H}\, q_1 + \zeta q_1 \cos\eta\Big],\\
&\ddot{q}_2 + 2\omega\dot{q}_1 + \big(\bar{\kappa}_2^2 - \omega^2\big)q_2 = 2\varepsilon\Big[-\omega\Delta\dot{q}_1 - (\bar{\kappa}_2^2-\omega^2)\Delta q_2 + \bar{\kappa}_2^2\mathscr{H}\, q_2 + \zeta q_2 \cos\eta\Big], \qquad (5.3.49)\\
&\eta(t) = t + \psi(t), \quad \psi(t) = \varepsilon^{1/2}\sigma W(t) + \theta, \quad \sigma = \sigma_0/\sqrt{\nu}.
\end{aligned}$$

In this case, F and G in equations (5.3.20) becomes,

$$\begin{aligned}
F &= 2\varepsilon\Big[+\omega\Delta\dot{q}_2 - (\bar{\kappa}_1^2-\omega^2)\Delta q_1 + \bar{\kappa}_1^2\mathscr{H}\, q_1 + \zeta q_1 \cos\eta\Big],\\
G &= 2\varepsilon\Big[-\omega\Delta\dot{q}_1 - (\bar{\kappa}_2^2-\omega^2)\Delta q_2 + \bar{\kappa}_2^2\mathscr{H}\, q_2 + \zeta q_2 \cos\eta\Big].
\end{aligned}$$

By following the same procedure of Section 5.3.1, the method of stochastic averaging is used to obtain first-order approximate solutions of equation (5.3.49),

$$\begin{aligned}
\dot{a}_1 &= \varepsilon a_1 E_1 - \varepsilon\bar{\zeta}\underset{t}{\mathscr{M}}\Big\{\alpha_1^- a_1 \underline{\sin(2\Phi_1 - t - \psi)} + \alpha_{21}^- a_2 \sin(\Phi_1 + \Phi_2 - t - \psi)\\
&\quad + \alpha_{21}^+ a_2\Big[\boxed{\sin(\Phi_1 - \Phi_2 - t - \psi)} + \sin(\Phi_1 - \Phi_2 + t + \psi)\Big]\Big\},\\
\dot{a}_2 &= \varepsilon a_2 E_2 + \varepsilon\bar{\zeta}\underset{t}{\mathscr{M}}\Big\{\alpha_2^- a_2 \underline{\sin(2\Phi_2 - t - \psi)} + \alpha_{12}^- a_1 \sin(\Phi_1 + \Phi_2 - t - \psi)\\
&\quad - \alpha_{12}^+ a_1\Big[\boxed{\sin(\Phi_1 - \Phi_2 - t - \psi)} + \sin(\Phi_1 - \Phi_2 + t + \psi)\Big]\Big\},\\
a_1\dot{\phi}_1 &= \varepsilon\Delta\kappa_1 a_1 - \varepsilon\bar{\zeta}\underset{t}{\mathscr{M}}\Big\{\alpha_1^- a_1 \underline{\cos(2\Phi_1 - t - \psi)} + \alpha_{21}^- a_2 \cos(\Phi_1 + \Phi_2 - t - \psi)
\end{aligned}$$

$$+\alpha_{21}^{+}a_2\Big[\boxed{\cos(\Phi_1-\Phi_2-t-\psi)}+\cos(\Phi_1-\Phi_2+t+\psi)\Big]\Big\},$$

$$a_2\dot{\phi}_2=\varepsilon\Delta\kappa_2 a_2+\varepsilon\bar{\zeta}\mathop{\mathscr{M}}_t\Big\{\alpha_2^{-}a_2\underline{\cos(2\Phi_2-t-\psi)}+\alpha_{12}^{-}a_1\cos(\Phi_1+\Phi_2-t-\psi)$$

$$+\alpha_{12}^{+}a_1\Big[\boxed{\cos(\Phi_1-\Phi_2-t-\psi)}+\cos(\Phi_1-\Phi_2+t+\psi)\Big]\Big\},$$

$$\dot{\psi}(t)=\varepsilon^{1/2}\sigma\dot{W}(t),\quad \Phi_1=\kappa_1 t+\phi_1,\quad \Phi_2=\kappa_2 t+\phi_2, \tag{5.3.50}$$

where $\alpha_1^{\pm}$, $\alpha_2^{\pm}$, $\alpha_{12}^{\pm}$, $\alpha_{21}^{\pm}$, $\bar{\zeta}$ are given in equations (5.3.22). For fractional viscoelasticity,

$$\begin{aligned}
E_1&=-\frac{2\Omega}{\kappa_1^2-\kappa_2^2}\left[\frac{\bar{\kappa}_1^2\mathop{\mathscr{M}}_t\{\cos\Phi_1\mathscr{H}[q_1]\}}{\alpha_1}-\bar{\kappa}_2^2\mathop{\mathscr{M}}_t\{\sin\Phi_1\mathscr{H}[q_2]\}\right],\\
E_2&=-\frac{2\Omega}{\kappa_1^2-\kappa_2^2}\left[-\frac{\bar{\kappa}_1^2\mathop{\mathscr{M}}_t\{\cos\Phi_2\mathscr{H}[q_1]\}}{\alpha_2}+\bar{\kappa}_2^2\mathop{\mathscr{M}}_t\{\sin\Phi_2\mathscr{H}[q_2]\}\right].
\end{aligned} \tag{5.3.51}$$

For $r=1,2,$, there exists

$$\begin{aligned}
&\mathop{\mathscr{M}}_t\{\cos\Phi_r\mathscr{H}[q_1]\}=a_r\mathop{\mathscr{M}}_t\{I_r^{cs}\}=\frac{1}{2}a_r H^c(\omega_r)=\frac{a_r\tau_\varepsilon}{2}\omega_r^\mu\sin\frac{\mu\pi}{2},\\
&\mathop{\mathscr{M}}_t\{\sin\Phi_r\mathscr{H}[q_1]\}=a_r\mathop{\mathscr{M}}_t\{I_r^{ss}\}=\frac{1}{2}a_r H^s(\omega_r)=\frac{a_r\tau_\varepsilon}{2}\omega_r^\mu\cos\frac{\mu\pi}{2},\\
&\mathop{\mathscr{M}}_t\{\sin\Phi_r\mathscr{H}[q_2]\}=a_r\alpha_r\mathop{\mathscr{M}}_t\{I_r^{sc}\}=-\frac{1}{2}a_r H^c(\omega_r)=-\frac{a_r\tau_\varepsilon}{2}\omega_r^\mu\sin\frac{\mu\pi}{2},\\
&\mathop{\mathscr{M}}_t\{\cos\Phi_r\mathscr{H}[q_2]\}=a_r\alpha_r\mathop{\mathscr{M}}_t\{I_r^{cc}\}=\frac{1}{2}a_r H^s(\omega_r)=\frac{a_r\tau_\varepsilon}{2}\omega_r^\mu\cos\frac{\mu\pi}{2}.
\end{aligned} \tag{5.3.52}$$

The explicit averaged equations in equation (5.3.50) depend on the values of κ_1 and κ_2, which leads to the various types of parametric resonances.

Subharmonic Resonance: $\kappa_i=\frac{1}{2}$, $\kappa_j\neq\frac{1}{2}$, $i,j=1,2$, and $i\neq j$

For the ith mode, the averaged equations are given as (take $i=1$ as an example)

$$\begin{aligned}
&\dot{a}_1=\varepsilon a_1E_1-\varepsilon\bar{\zeta}\alpha_1^{-}a_1\sin(2\phi_1-\psi),\quad \dot{\phi}_1=\varepsilon\frac{1}{2}\Delta-\varepsilon\bar{\zeta}\alpha_1^{-}\cos(2\phi_1-\psi),\\
&\dot{a}_2=\varepsilon a_2E_2,\quad \dot{\phi}_2=\varepsilon\kappa_2\Delta,\\
&\dot{\psi}(t)=\varepsilon^{1/2}\sigma\dot{W}(t).
\end{aligned} \tag{5.3.53}$$

Defining the pth norm $P=a_1^p$ and a new process $\chi=2\phi_1-\psi$, and applying a linear stochastic transformation in equation (5.3.27), one can obtain an eigenvalue problem for a second-order differential operator with $\Lambda(p)$ being the eigenvalue and $T(\chi)$ the associated eigenfunction,

$$\frac{1}{2}\varepsilon\sigma^2 T''+\varepsilon\big(\Delta-2\bar{\zeta}\alpha_1^-\cos\chi\big)T'+\varepsilon p\big(E_1-\bar{\zeta}\alpha_1^-\sin\chi\big)T=\Lambda T. \tag{5.3.54}$$

Since the coefficients are periodic with period 2π, equation (5.3.54) can be solved using a Fourier series expansion of the eigenfunction, similar to equation (5.3.30).

The stability boundaries are shown three-dimensionally in Figures 5.22 and 5.23, which illustrate the parametric resonance around reference frequencies $2\omega_1$ and $2\omega_2$, respectively. The characteristics of parametric resonance around reference frequencies $2\omega_1$ and $2\omega_2$ are quite different. In parametric resonance around $2\omega_1$, when $\Omega<\bar{\omega}_1$, the unstable areas diminish with the increase of Ω, which shows the angular velocity stabilizes the system. When $\Omega>\bar{\omega}_2$, however, the unstable areas expand with the increase of Ω, which suggests the angular velocity destabilizes the system. For parametric resonance around $2\omega_2$, the unstable areas always decrease with the increase of Ω. The unperturbed system is already unstable when $\bar{\omega}_1\leqslant\Omega\leqslant\bar{\omega}_2$. The unstable areas are always "V"-shaped. The frequency of parametric resonance varies with the parameter Ω. This is due to the fact that $\omega_{1,2}$ is a function of Ω from equation (5.3.13). These results have practical applications in engineering, for if the angular velocity Ω is given, not only the stability status of the system but also the effect of Ω can be accurately predicted.

The effect of fractional order μ on the Lyapunov exponents is shown in Figure 5.24. The fractional parameter μ stabilizes the system. The reason is that with the increase of μ, the system changes from elastic to viscous, then it becomes more stable.

Combination Additive Resonance: $\kappa_1+\kappa_2=1$ or $\omega_0=\omega_1+\omega_2$, $\kappa_1\neq\frac{1}{2}$

When averaged, only the grey-background sinusoidal terms in equation (5.3.50) survive, so the averaged equations are

$$\dot{a}_1=\varepsilon a_1E_1-\varepsilon\bar{\zeta}\alpha_{21}^-a_2\sin(\phi_1+\phi_2-\psi),\quad \dot{a}_2=\varepsilon a_2E_2+\varepsilon\bar{\zeta}\alpha_{12}^-a_1\sin(\phi_1+\phi_2-\psi),$$

$$\dot{\phi}_1=\varepsilon\kappa_1\Delta-\varepsilon\bar{\zeta}\alpha_{21}^-\frac{a_2}{a_1}\cos(\phi_1+\phi_2-\psi),\quad \dot{\phi}_2=\varepsilon\kappa_2\Delta+\varepsilon\bar{\zeta}\alpha_{12}^-\frac{a_1}{a_2}\cos(\phi_1+\phi_2-\psi),$$

$$\dot{\psi}(t) = \varepsilon^{1/2}\sigma\dot{W}(t). \tag{5.3.55}$$

By applying the Khasminskii transformation and defining the pth norm in equations (5.3.35) and $\chi = \phi_1 + \phi_2 - \psi$, the eigenvalue problem can be obtained, similar to equation (5.3.39),

$$\varepsilon\left\{\frac{1}{2}\sigma^2 T'' + m_{1\varphi}T` + m_{1\chi}T' + m_0 T\right\} = \Lambda T, \tag{5.3.56}$$

which is a two-dimensional second-order partial differential equation with Λ being the eigenvalue and $T(\varphi, \chi)$ the associated eigenfunctions. T' and $T`$ are the first-order partial derivatives of $T(\varphi, \chi)$ with respect to χ and φ, respectively. T'' is the second-order partial derivative with respect to χ. Other terms are given as

$$\begin{aligned}
m_{1\varphi} &= (E_2 - E_1)\sin\varphi\cos\varphi + \bar{\zeta}\sin\chi\left(\alpha_{12}^{-}\cos^2\varphi + \alpha_{21}^{-}\sin^2\varphi\right),\\
m_{1\chi} &= (\kappa_1 + \kappa_2)\Delta - \bar{\zeta}\cos\chi\left(\alpha_{21}^{-}\tan\varphi - \alpha_{12}^{-}\cot\varphi\right),\\
m_0 &= p\left[E_1\cos^2\varphi + E_2\sin^2\varphi + \bar{\zeta}\sin\varphi\cos\varphi\sin\chi\left(\alpha_{12}^{-} - \alpha_{21}^{-}\right)\right].
\end{aligned} \tag{5.3.57}$$

Since the coefficients of the eigenvalue problem are periodic functions in χ of period 2π and in φ of period $\pi/2$, the eigenfunction $T(\varphi, \chi)$ can be expanded in double Fourier series in the complex form (5.3.41). Consequently, this eigenvalue can be solved by double Fourier series expansion method, similar to the solution method for equation (5.3.39). The effect of fractional order μ on the Lyapunov exponents is shown in Figure 5.25, which shows that the fractional parameter μ stabilizes the system as expected. The stability boundaries are shown in Figure 5.26. When $\Omega \geqslant \bar{\omega}_2$, the system is stable. When $\bar{\omega}_1 \leqslant \Omega \leqslant \bar{\omega}_2$, the system is already unstable. When $\Omega \leqslant \bar{\omega}_1$, with the increase of Ω, the "V"-shaped instability area expands. This clearly shows that the parameter Ω destabilizes the system.

Combination Differential Resonance: $|\kappa_1 - \kappa_2| = 1$ or $\omega_0 = |\omega_1 - \omega_2|$, $\kappa_1 \neq \frac{1}{2}$

When averaged, only the boxed sinusoidal terms in equation (5.3.50) survive, and the averaged equations are

$$\dot{a}_1 = \varepsilon a_1 E_1 - \varepsilon\bar{\zeta}\alpha_{21}^{-}a_2\sin(\phi_1 - \phi_2 - \psi), \quad \dot{a}_2 = \varepsilon a_2 E_2 - \varepsilon\bar{\zeta}\alpha_{12}^{-}a_1\sin(\phi_1 - \phi_2 - \psi),$$

$$\dot{\phi}_1 = \varepsilon\kappa_1\Delta - \varepsilon\bar{\zeta}\alpha_{21}^{-}\frac{a_2}{a_1}\cos(\phi_1 - \phi_2 - \psi),$$

$$\dot{\phi}_2 = \varepsilon\kappa_2\Delta + \varepsilon\bar{\zeta}\,\alpha_{12}^- \frac{a_1}{a_2}\cos(\phi_1 - \phi_2 - \psi),$$

$$\dot{\psi}(t) = \varepsilon^{1/2}\sigma\,\dot{W}(t). \tag{5.3.58}$$

The eigenvalue problem can be obtained as

$$\bar{\mathcal{L}}(p)T = \varepsilon\left\{\frac{1}{2}\sigma^2 T'' + m_{1\varphi}T` + m_{1\chi}T' + m_0 T\right\} = \Lambda T, \tag{5.3.59}$$

$$m_{1\varphi} = (E_2 - E_1)\sin\varphi\cos\varphi + \bar{\zeta}\sin\chi\left(\alpha_{21}^-\sin^2\varphi - \alpha_{12}^-\cos^2\varphi\right),$$

$$m_{1\chi} = (\kappa_1 - \kappa_2)\Delta - \bar{\zeta}\cos\chi\left(\alpha_{21}^-\tan\varphi + \alpha_{12}^-\cot\varphi\right),$$

$$m_0 = p\left[E_1\cos^2\varphi + E_2\sin^2\varphi - \bar{\zeta}\sin\varphi\cos\varphi\sin\chi\left(\alpha_{12}^- + \alpha_{21}^-\right)\right],$$

which is a two-dimensional second-order partial differential equation with Λ being the eigenvalue and $T(\varphi,\chi)$ the associated eigenfunctions.

This eigenvalue can be solved by double Fourier series expansion method, similar to the solution method for equation (5.3.47). The stability boundaries are shown in Figure 5.27. When $0 \leqslant \Omega \leqslant \bar{\omega}_1$, the system is stable. When $\Omega \geqslant \bar{\omega}_2$, the instability area is "V"-shaped. The parameter Ω plays a role of stability, because with the increase of parameter Ω, the instability area decreases. When $\bar{\omega}_1 \leqslant \Omega \leqslant \bar{\omega}_2$, the system is already unstable. These results are very important in engineering, for if Ω is given, not only the stability status of the system can be obtained, but also the effect of Ω can be predicted. The effect of fractional order μ on the Lyapunov exponents is shown in Figure 5.28, which again shows the stabilization effect of fractional parameter μ.

5.4 Summary

In this chapter, parametric resonances of a parametrically excited two-degree-of-freedom gyroscopic system are investigated by determining the moment Lyapunov exponents and the Lyapunov exponents. A typical example of such gyroscopic system is the rotating shaft under the excitation of the fluctuating axial thrust. The influence of noise is modelled using wide-band noise process and a bounded noise process with a narrow-band characteristic.

5.4 SUMMARY

The partial differential eigenvalue problem governing the moment Lyapunov exponent is established using the method of stochastic averaging and mathematical transformations. Moment Lyapunov exponents are obtained from the solution of eigenvalue problems through Fourier series expansions. The Lyapunov exponent is then obtained using the relationship between the moment Lyapunov exponent and the Lyapunov exponent. The effects of noise and parameters on the parametric resonance are investigated.

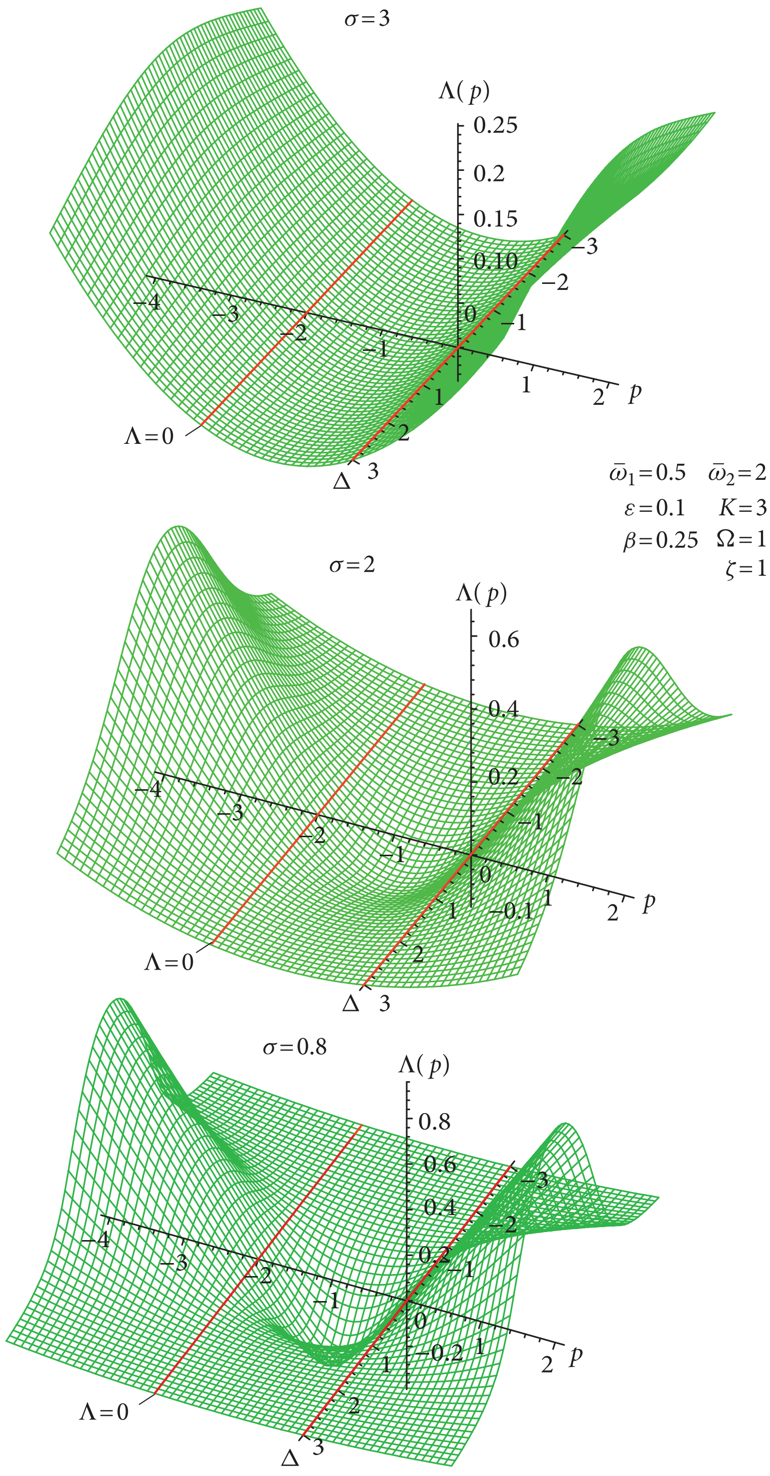

Figure 5.14 Moment Lyapunov exponents for subharmonic resonance

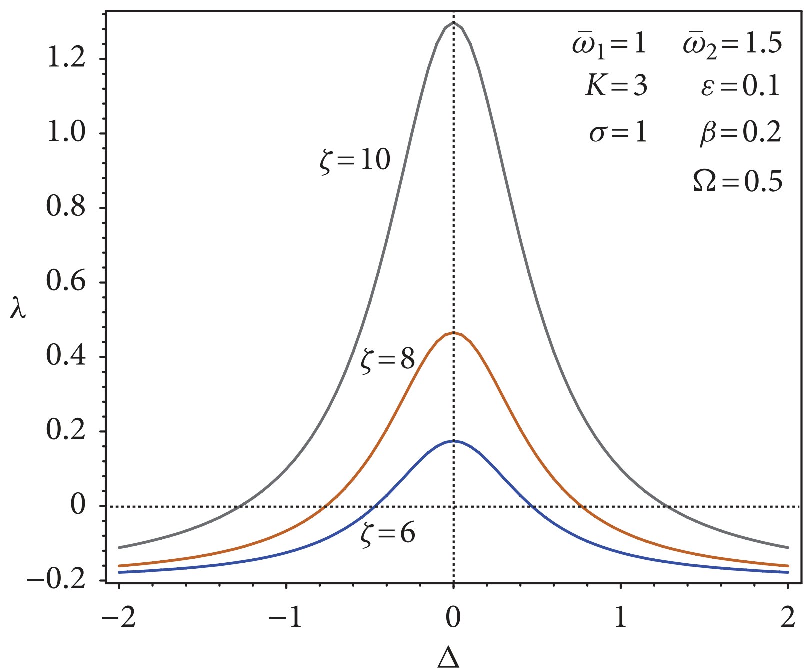

Figure 5.15 Effect of ζ on Lyapunov exponents for combination additive resonance

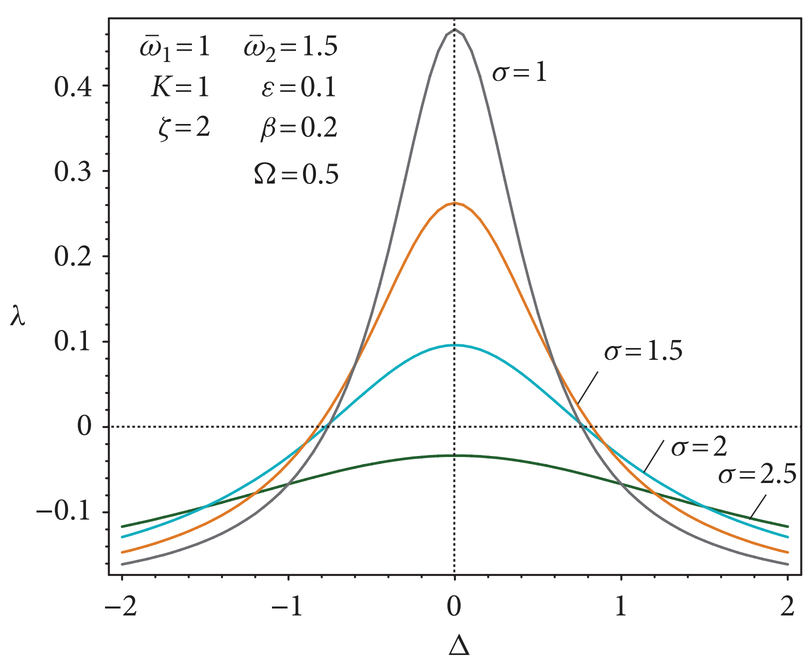

Figure 5.16 Effect of σ on Lyapunov exponents for combination additive resonance

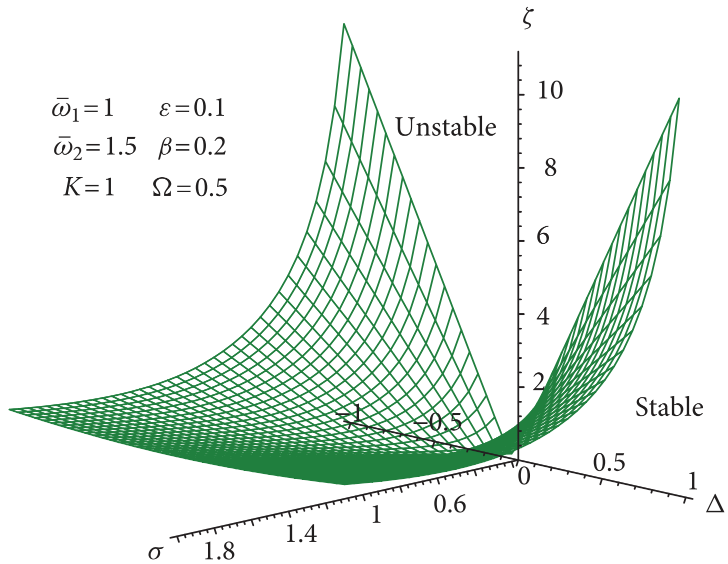

Figure 5.17 Stability boundaries for gyroscopic systems under bounded noises with combination additive resonance

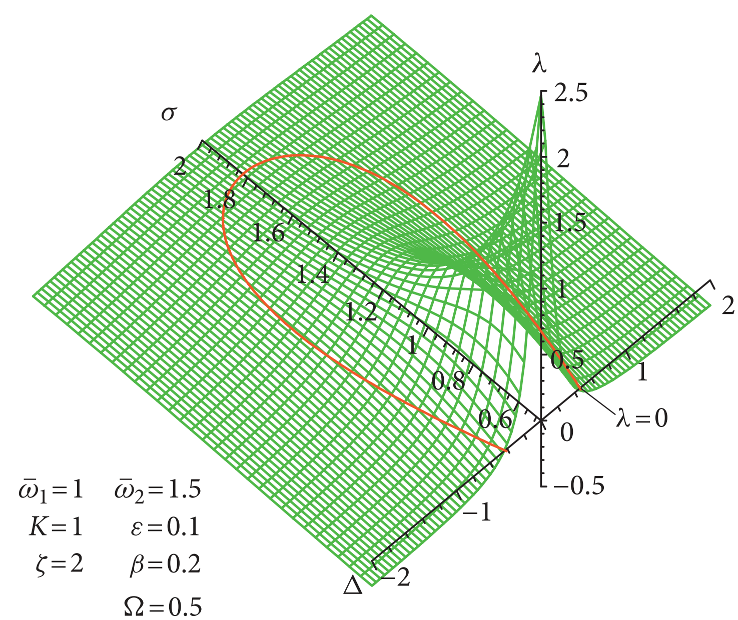

Figure 5.18 Effect of σ on Lyapunov exponents for gyroscopic systems under bounded noises with combination additive resonance

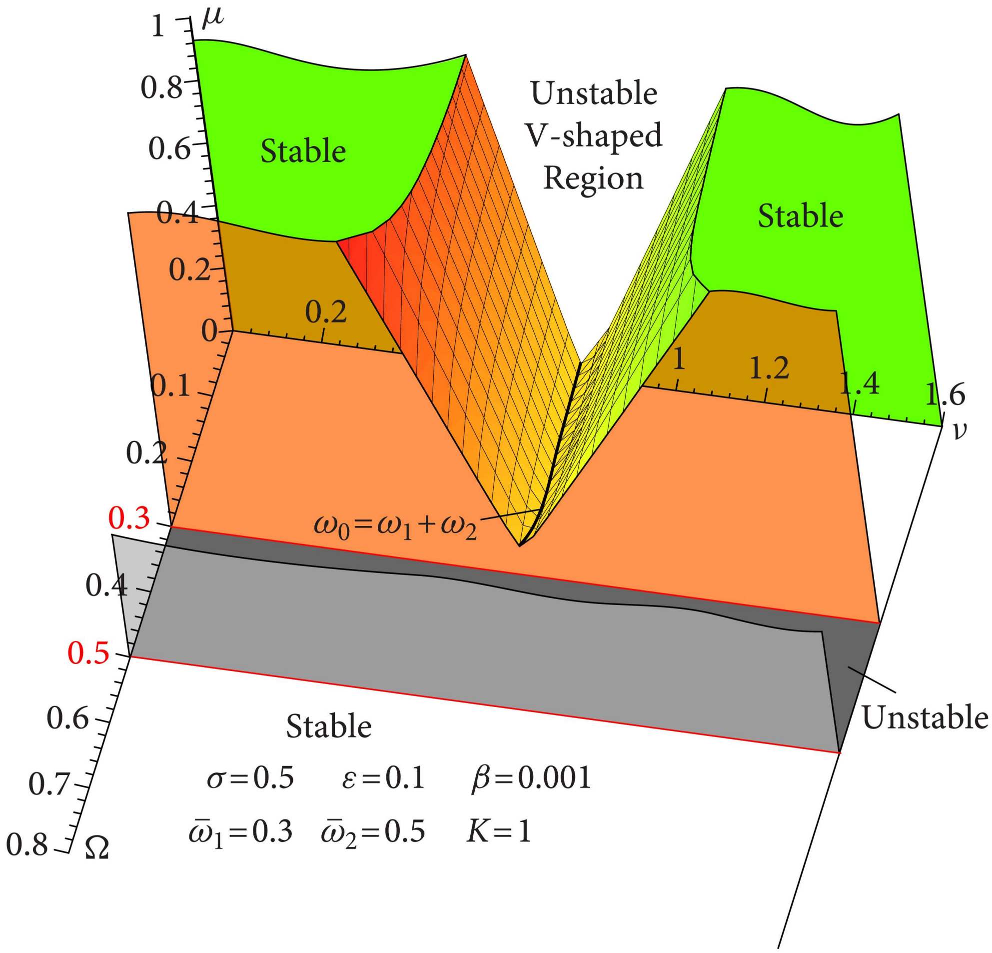

Figure 5.19 Instability regions for gyroscopic systems under bounded noises with combination additive resonance

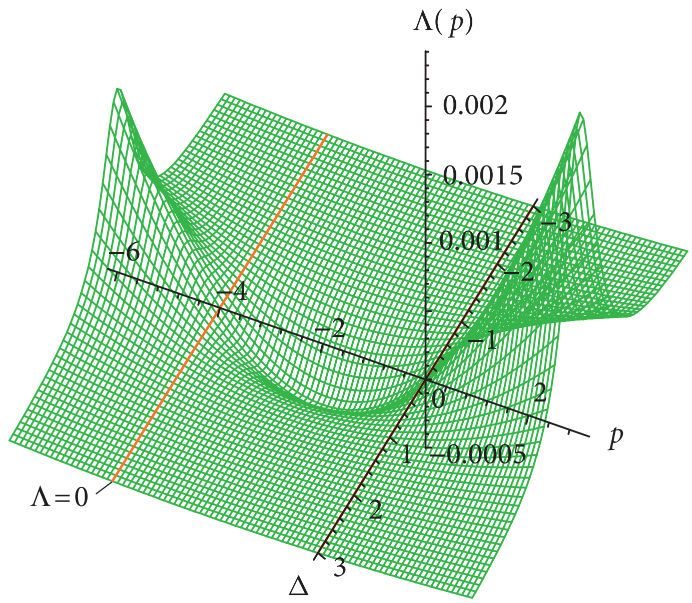

Figure 5.20 Moment Lyapunov exponents for gyroscopic systems under bounded noise with combination additive resonance

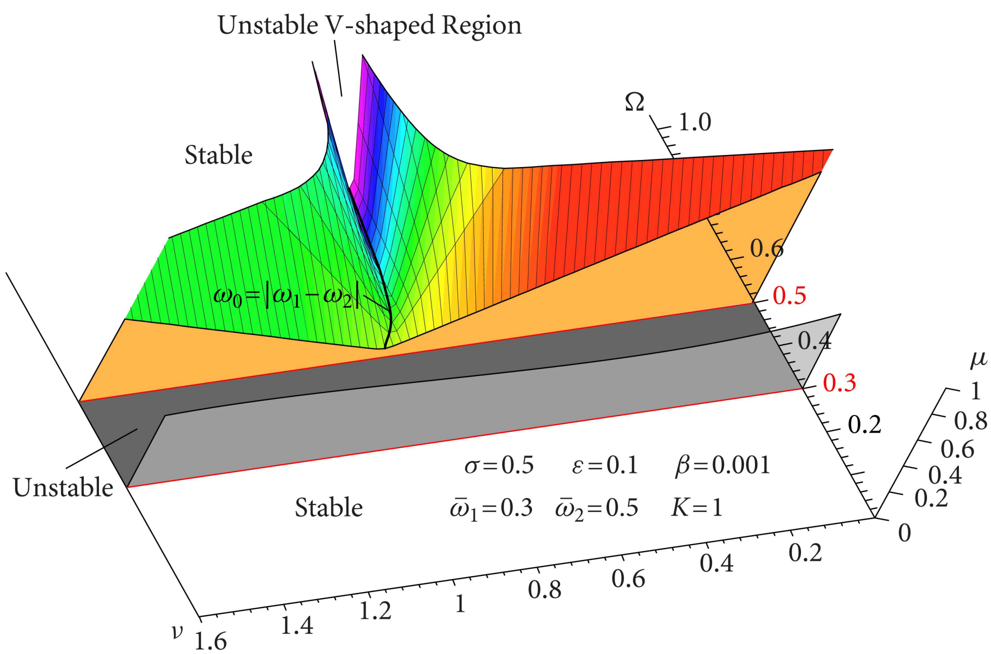

Figure 5.21 Instability regions for gyroscopic systems under bounded noise with combination differential resonance

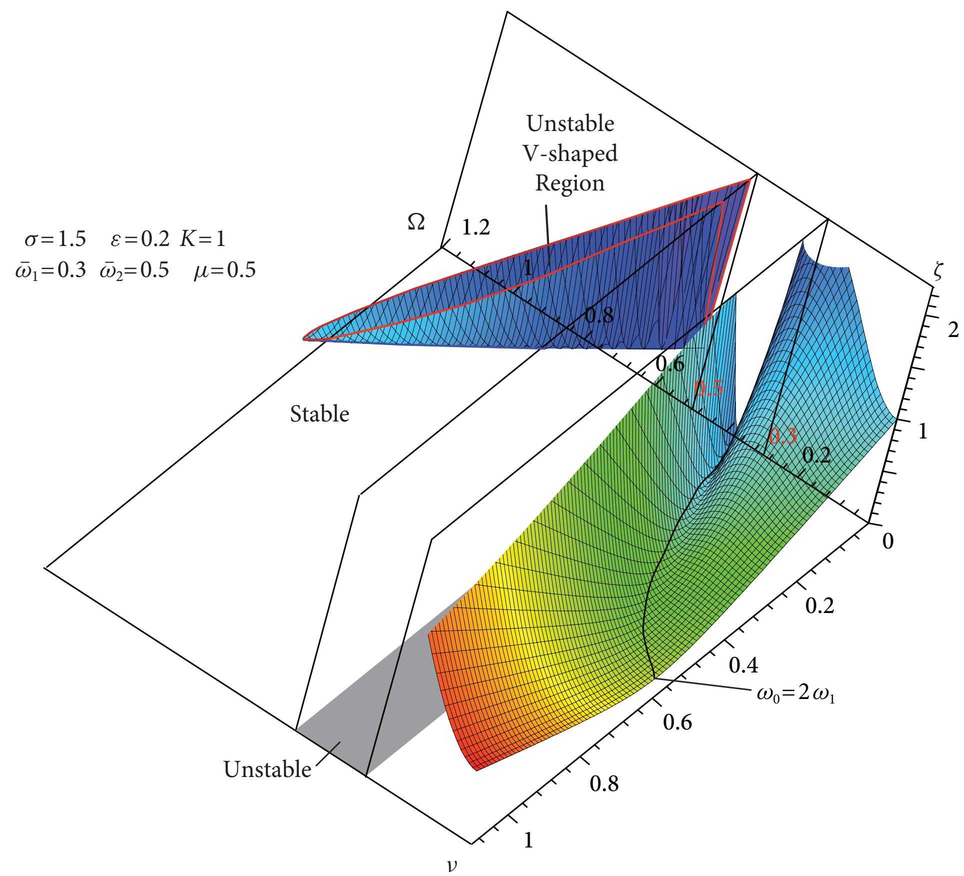

Figure 5.22 Instability regions for fractional gyroscopic systems under bounded noise for subharmonic resonance with $\omega_0 = 2\omega_1$

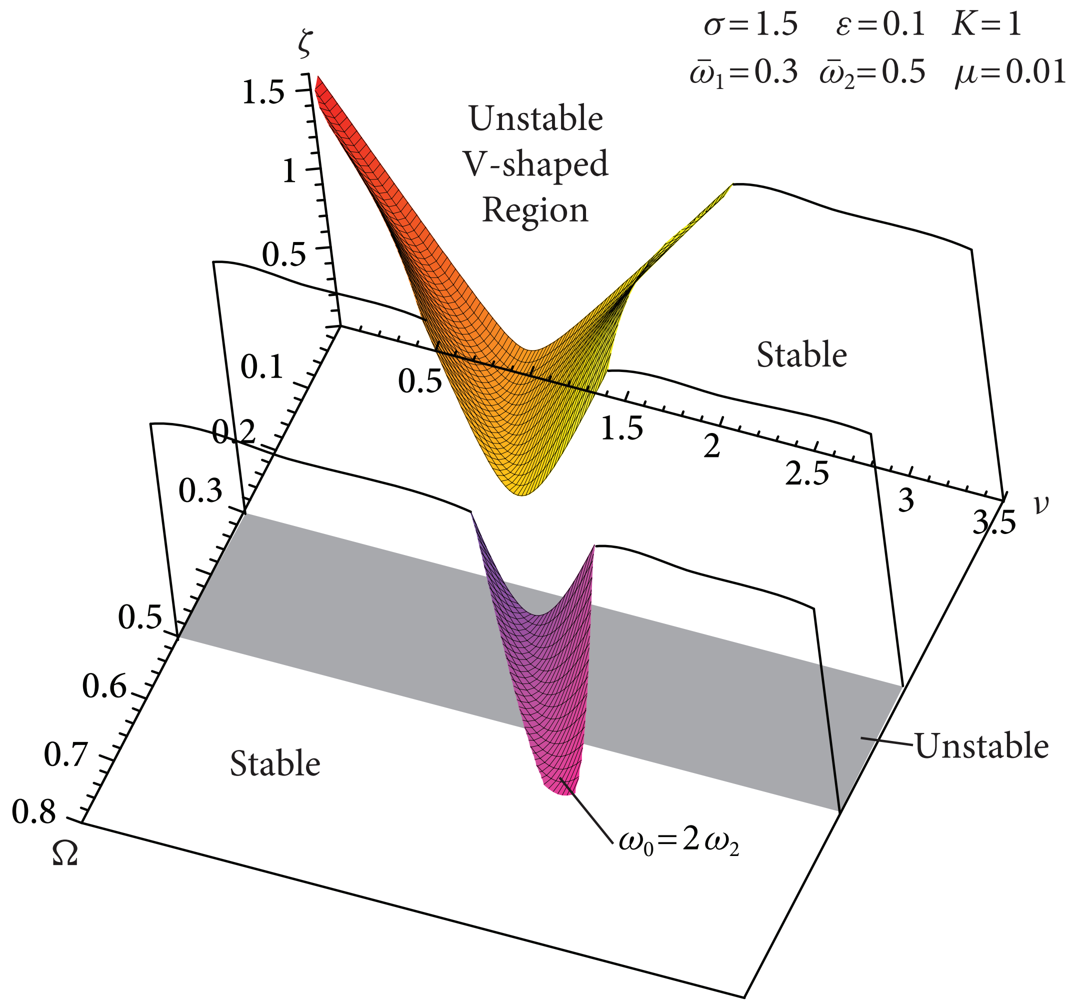

Figure 5.23 Instability regions for fractional gyroscopic systems under bounded noise for subharmonic resonance with $\omega_0 = 2\omega_2$

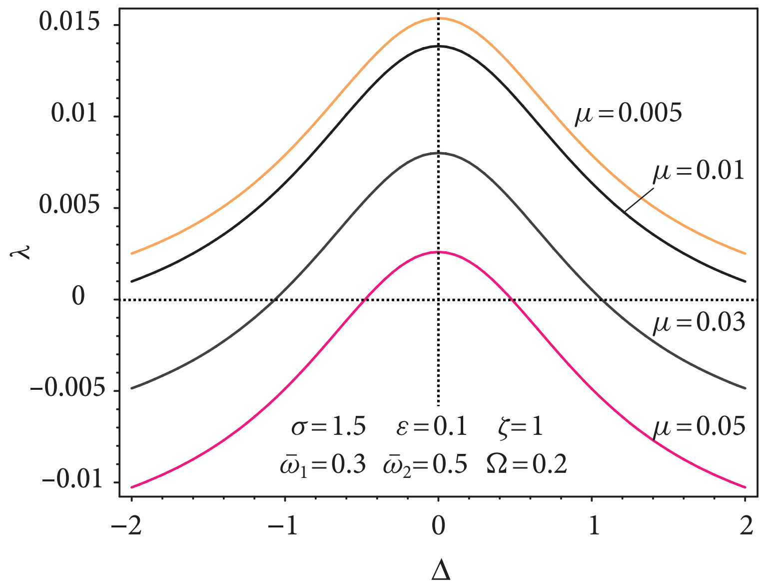

Figure 5.24 Effect of μ on fractional gyroscopic systems under bounded noise for subharmonic resonance

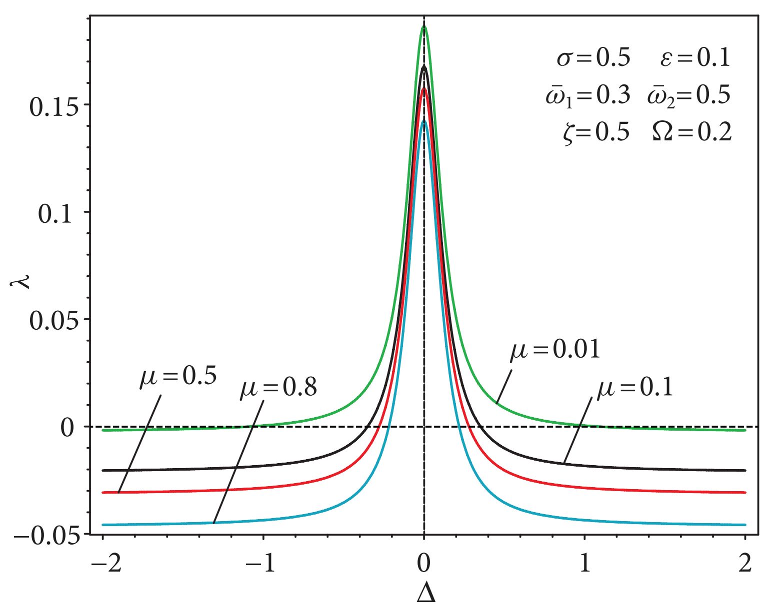

Figure 5.25 Effect of μ on fractional gyroscopic systems under bounded noise for combination additive resonance

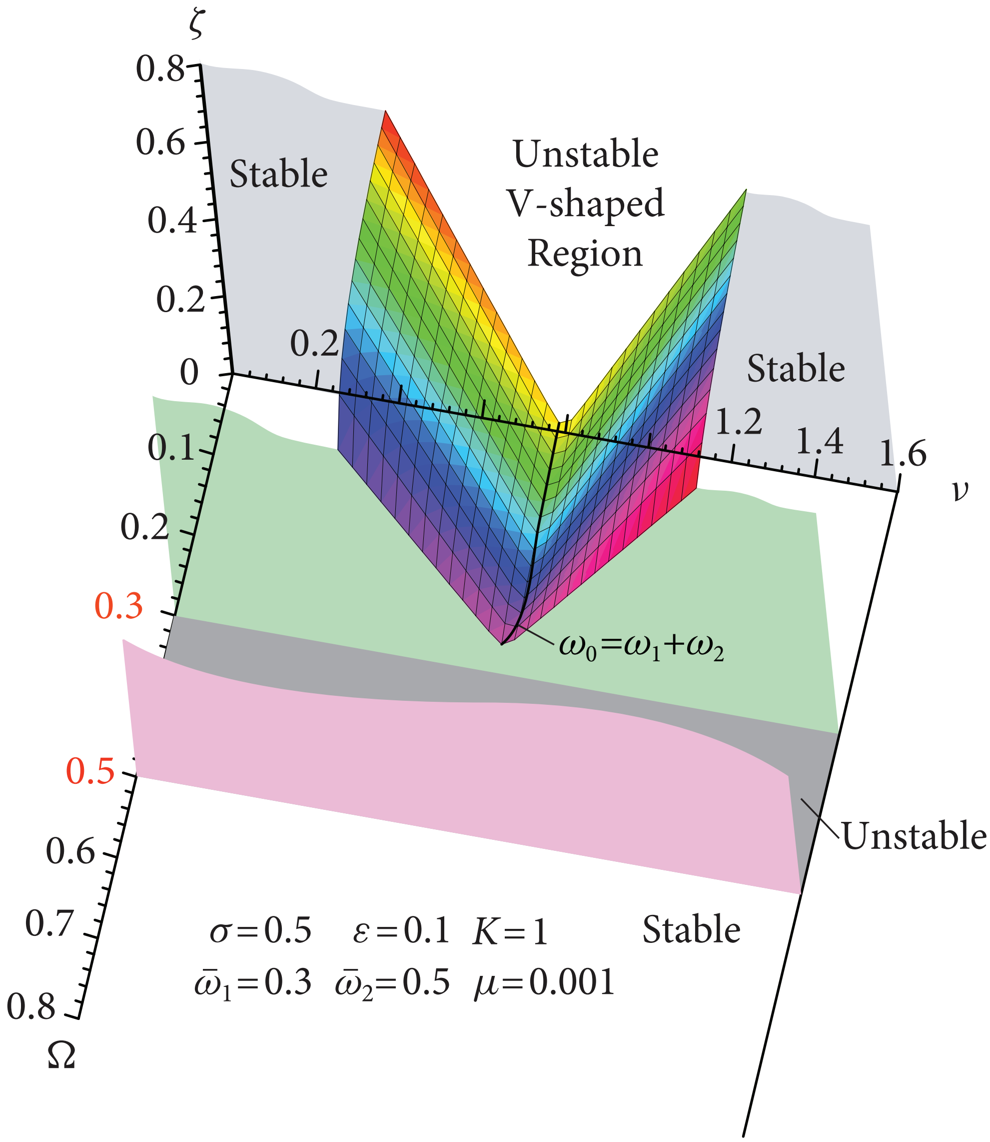

Figure 5.26 Instability regions for fractional gyroscopic systems under bounded noise with combination additive resonance

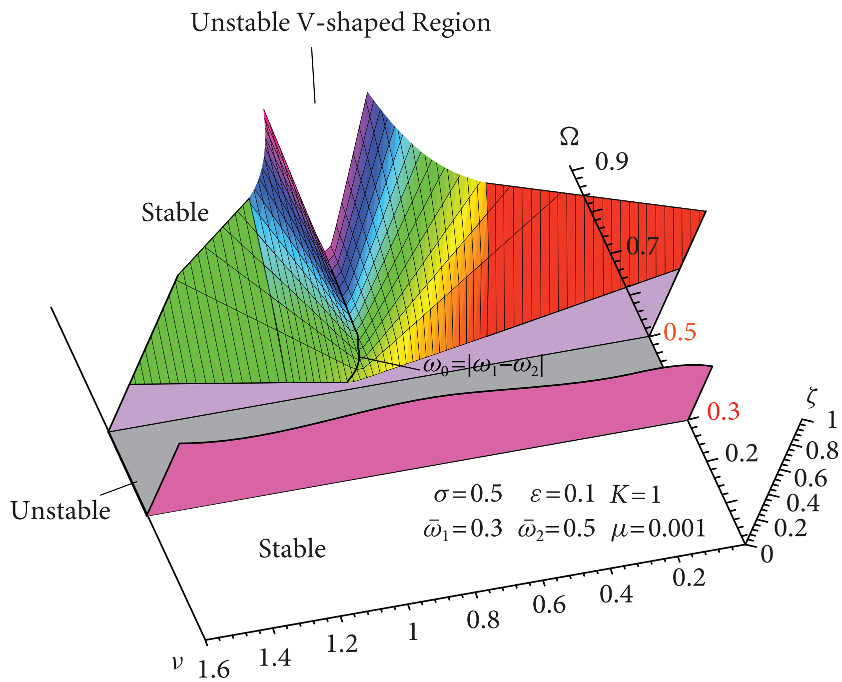

Figure 5.27 Instability regions for fractional gyroscopic systems under bounded noise with combination differential resonance

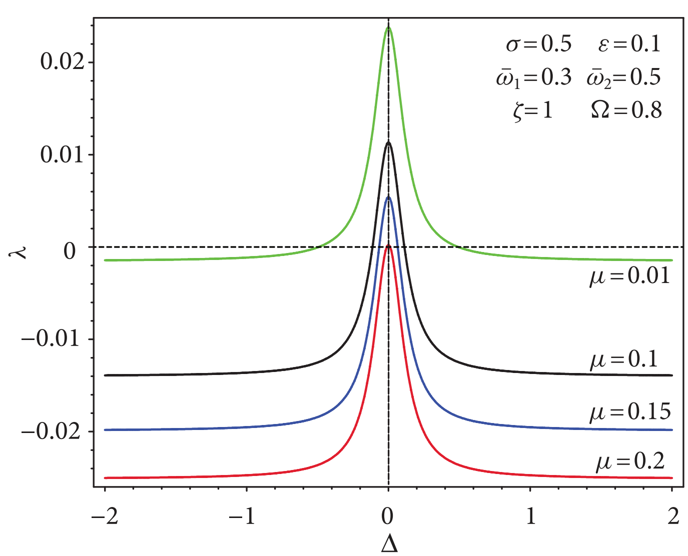

Figure 5.28 Effect of μ on fractional gyroscopic systems under bounded noise for combination differential resonance

CHAPTER 6

Conclusions and Future Research

The stochastic stability of viscoelastic structures of single-degree-of-freedom, coupled non-gyroscopic systems, and gyroscopic systems is systematically investigated in this thesis. The stochastic excitation is assumed to be white noise, real noise, and bounded noise. The viscoelastic materials are described by using fractional calculus. Lyapunov exponents and moment Lyapunov exponents, which are ideal indicators for stochastic stability, are determined by the method of stochastic averaging. Stability boundaries, critical excitations, and stability indexes are obtained. Approximate analytical results are confirmed by numerical simulations.

6.1 Contributions

Fractional stochastic differential equations of motion

Fractional calculus and viscoelastic theory are combined to formulate fractional viscoelastic constitutive relation of engineering materials. Fractional Kelvin-Voigt constitutive relation is developed, which leads to power relaxation kernel function other than conventional exponential kernel functions. The main advantage of fractional viscoelastic constitutive relation is its capability to model long-time heredity.

Equations of motion for a viscoelastic column under stochastic axial compressive load are derived by using the material's fractional viscoelastic constitutive relation, which is a single-degree-of-freedom fractional stochastic differential equation.

The flexural and torsional equations of motion of a rectangular beam under stochastic concentrated load, for both follower case and non-follower case, tend to be a system of coupled non-gyroscopic stochastic differential equations. If the first two modes are taken, the transverse flexural equations of motion of a rotating shaft under fluctuating axial thrust are derived to be a system of gyroscopic stochastic differential equations.

A new numerical method for moment Lyapunov exponents of fractional systems

The numerical algorithms to determine Lyapunov exponents and moment Lyapunov exponents usually involve periodic normalization, which appears to be inapplicable to the fractional systems, due to the fact that normalization during the iteration will lead to an error in the computation of fractional derivatives. A new numerical method for determining both the Lyapunov moments and the pth moment Lyapunov exponents of fractional stochastic systems, which governs the almost sure stability and the pth moment stability, is proposed.

The main steps of this method include discretization of fractional derivatives, numerical solution of the stochastic differential equation, and the algorithm for calculating the largest Lyapunov exponents from small data sets. The determination of both Lyapunov exponents and the pth moment Lyapunov exponents is put into the same algorithm, for both exponents are deduced from a time series data.

Higher order stochastic averaging method

The stochastic stability of a single-degree-of-freedom linear viscoelastic system under the excitation of a wide-band noise and bounded noise is investigated by using the method of higher order stochastic averaging. Higher-order stochastic averaging is able to capture the influence of such weak nonlinearities as integral stiffness nonlinearities, cubic inertia and stiffness nonlinearities, which were lost in the first-order averaging procedure.

To obtain a complete picture of the dynamic stability, asymptotic analytical expressions are derived for both the moment Lyapunov exponent and Lyapunov exponent of systems excited by wide-band noises. It is found that under wide-band noise excitation, the parameters of damping β, the parameter of retardation τ_{ε}, real noise parameter α, and the model fractional order μ have stabilizing effects on the moment stability. However, the white and real noise intensity factor σ and the elastic modulus E destabilizes the system.

Moment Lyapunov exponent and Lyapunov exponent of systems under bounded noises must be obtained by solving a eigenvalue problem. It is seen that, under bounded noise excitation, the parameters of damping β, the noise intensity σ, and the model fractional order μ have stabilizing effects on the almost-sure stability. Parametric resonance is found in systems excited by bounded noise.

Stochastic stability of coupled non-gyroscopic fractional viscoelastic systems

The two-degree-of-freedom Stratonovich equations of motion were first decoupled into four-dimensional Itô stochastic differential equations, by making use of the method of stochastic averaging for the non-viscoelastic terms and the method of Larionov for viscoelastic terms. An elegant scheme for determining the moment Lyapunov exponents is presented by only using Khasminskii and Wedig's mathematical transformations from the decoupled Itô equations. The Lyapunov exponents and moment Lyapunov exponents obtained are compared well to the Monte Carlo simulation and other analytical results in literature.

Coupled non-gyroscopic viscoelastic systems excited by bounded noise are studied. Parametric resonances is discussed in detail, which includes subharmonic resonance, combination additive resonance and combination differential resonance. Moment Lyapunov exponents are obtained from the eigenvalue problem which is solved by double Fourier series expansion. The Lyapunov exponents can be obtained from the relation with moment Lyapunov exponents. It is seen that the parametric resonance occurs around the detuning parameter $\Delta = 0$.

Stochastic stability of gyroscopic fractional viscoelastic systems excited by wide-band noise and by bounded noise

Gyroscopic viscoelastic systems excited by white noise are investigated. It is shown that the larger the noise intensity σ, the more unstable the system. When $0 \leqslant \Omega \leqslant \bar{\omega}_1$, the system becomes more and more unstable with the increase of angular velocity Ω. When

$\bar{\omega}_1 \leqslant \Omega \leqslant \bar{\omega}_2$, the system is already unstable. When $\Omega \geqslant \bar{\omega}_2$ and near $\bar{\omega}_2$, Ω plays a role of stability. The simulation results compare well with the analytical approximation results, which shows that the method based upon stochastic averaging can be used for stability analysis of gyroscopic systems.

Parametric resonances of a parametrically excited two-degree-of-freedom viscoelastic gyroscopic system are investigated by determining the moment Lyapunov exponents and the Lyapunov exponents. The partial differential eigenvalue problem governing the moment Lyapunov exponent is established using the method of stochastic averaging and mathematical transformations. Moment Lyapunov exponents are obtained from the solution of eigenvalue problems through Fourier series expansions. The Lyapunov exponent is then obtained using the relationship between the moment Lyapunov exponent and the Lyapunov exponent. The effects of noise and parameters on the parametric resonance are investigated.

6.2 Future Research

The mechanics of stochastic stability falls into two classes of problems: single-degree-of-freedom and multi-degree-of-freedom (MDOF). The present research considers only SDOF and 2-DOF systems. In the practical analysis of structural dynamics, a large structure is usually discretized by finite element method, which leads to a multi-degree-of-freedom system. Therefore, studying the stability of MDOF viscoelastic systems under stochastic perturbations is of great importance. However, for systems with degrees of freedom higher than 2, even in the elastic cases, the analysis is not easy to proceed when considering the random perturbations. Therefore, development of new theory to study MDOF systems may be a future promising research topic, both theoretically and practically. The study of stochastic stability of high-dimensional systems is still a challenging problem.

Fractional calculus and fractional differential equations are the study of an extension of derivatives and integrals to non-integer (real) orders. In statistics theory, fractional moments are moments with non-integer (real) orders. This thesis is just an attempt to introduce fractional stochastic dynamics. More investigations are expected to made in this area. For example, fractional stochastic processes is possible to be new models of excitations.

Moment stability of stochastic systems may be extended to real order moment stability, and so on.

In this study, stochastic noise process is supposed to be white noise, real noise, and bounded noise process. When stochastic stability theory is applied to practical engineering, how to determined the type of noise process is a big problem. The difficulty lies in the fact that a large sample data is needed to accurately determine the noise process model. However, large sample data cannot or even impossible to be obtained in many engineering, such as earthquake engineering, wind engineering, etc. Consequently, stochastic analysis is more theoretical than practical.

In addition to the urgent needs of theoretical modeling, experimental efforts are also indispensable. The experimental investigations can not only verify analytical results but also can explore response characteristics not predicted by the available analytical methods. The lack of experimental results are mainly attributed to the difficulties encountered in measurements of small random parameters.

In summary, large gaps still remain in the field of stochastic stability despite the fact that many efforts have been attempted in the experimental, theoretical, and numerical methods. However, since Albert Einstein perfectly solved the problem of Brown motion using the stochastic process theory, this theory finds more and more applications in science and engineering. For example, the loadings imposed on the structures are quite often random forces, such as those arising from earthquakes, wind, explosive vibration and ocean waves, which can be characterized satisfactorily only in probabilistic terms, such as white noises, real noises, or bounded noises.

Bibliography

Abdelrahman, N.M., 2002. *Stochastic Stability of Viscoelastic Dynamical Systems*. PhD thesis, University of Waterloo, Waterloo, Canada.

Ahmadi, G. and Glocker, P.G., 1983. Dynamic stability of a kelvin-viscoelastic column. *Journal of Engineering Mechanics*, **109**(4), 990–999.

Anh, N.D. and Tinh, N.D., 2001. Higher order averaging method of coefficients in fokker-planck equation. In Narayanan, S. and Iyengar, R.N., editors, *IUTAM Symposium on Nonlinearity and Stochastic Stochastic Dynamics*, 1–14, London. Kluwer Academic Publishers.

Ariaratnam, S.T. and Namachchivaya, N.Sri., 1986a. Periodically perturbed linear gyroscopic systems. *Journal of Structural Mechanics*, **14**(2), 127–151.

Ariaratnam, S.T. and Namachchivaya, N.Sri., 1986b. Periodically perturbed nonlinear gyroscopic systems. *Journal of Structural Mechanics*, **14**(2), 153–175.

Ariaratnam, S.T., Schuëller, G.I., and Elishakoff, I., 1988. *Stochastic Structural Dynamics - Progress in Theory and Application*. Elsevier applied science publishers, London.

Ariaratnam, S.T., 1977. Discussion of paper by f. kozin and s. sugimoto. In B.L Clarkson, P.J. Holmes, J.K. Hammond and Kistner, A., editors, *Stochastic Problems in Dynamics*, 34–35, London. Pitman Publishing.

Ariaratnam, S.T., 1978. Discussion on "response envelope statistics for non-linear oscillators with random excitation". *Journal of Applied Mechanics*, **45**.

Ariaratnam, S.T., 1996. Stochastic stability of viscoelastic systems under bounded noise excitation. In Naess, A. and Krenk, S., editors, *IUTAM Symposium on Advances in Nonlinear Stochastic Mechanics*, 11–18, London. Kluwer Academic Publishers.

Arnold, L., Doyle, M.M., and Namachchivaya, N. Sri, 1997. Small noise expansion of moment lyapunov exponents for two-dimensional systems. *Dynamics and Stability of Systems*, **12**(3), 187–211.

Arnold, L., Kliemann, W., and Oeljeklaus, E., 1984a. Lyapunov exponents of linear stochastic systems. In Arnold, L. and Wihstutz, V., editors, *Lyapunov Exponents (Lecture Notes in Mathematics)*, volume 1186 of *Lecture Notes in Mathematics*, p. 129–159, Germany 1984. Springer-Verlag, Berlin.

Arnold, L. and Kliemann, W., 1987. Large deviations of linear stochastic differential equations. In Engelbert, H.J. and Schmidt, W., editors, *Stochastic Differential Systems (Lecture Notes in Control and Information Sciences)*, volume 96 of *Lecture Notes in Mathematics*, p. 117–151, Germany. Springer-Verlag, Berlin.

Arnold, L., Oeljeklaus, E., and Pardoux, E., 1984b. Almost sure and moment stability for linear itô equations. In Arnold, L. and Wihstutz, V., editors, *Lyapunov Exponents (Lecture Notes in Mathematics)*, volume 1186 of *Lecture Notes in Mathematics*, p. 85–125, Germany 1984. Springer-Verlag, Berlin.

Arnold, L., 1984. A formula connecting sample and moment stability of linear stochastic systems. *SIAM Journal of Applied Mathematics*, **44**(4), 793–802.

Arnold, L., 1998. *Random Dynamical Systems*. Springer-Verlag, Berlin.

Atanackovic, T.M. and Stankovic, B., 2008. On a numerical scheme for solving differential equations of fractional order. *Mechanics Research Communications*, **35**, 429–438.

Bagley, R.L. and Torvik, P.J., 1983. A theoretical basis for the application of fractional calculus to viscoelasticity. *Journal of Rheology*, **27**(3), 201–210.

Baxendale, P.H. and Stroock, D., 1988. Large deviations and stochastic flows of diffeomorphisms. *Probability Theory and Related Fields*, **80**, 169–215.

Baxendale, P.H., 1985. Moment stability and large deviations for linear stochastic differential equations. In Ikeda, N., editor, *Proceedings of the Taniguchi Symposiun on Probabilistic Methods in Mathematical Physics*, p. 31–54, Katata and Kyoto,Japan.

Becks, L., Hilker, F.M., Malchow, H., K.Jurgens, and H.Arndt, 2005. Experimental demonstration of chaos in a microbial food web. *Nature*, **435**(30), 1126–1129.

Bogoliubov, N. and Mitropolskii, A., 1961. *Asymptotic Methods in the Theory of Non–linear Oscillations*. Gordon and Breach, New York.

Bolotin, V.V., 1964. *The Dynamic Stability of Elastic Systems*. Holden–Day, Inc, San Francisco.

Chetaev, N.G., 1961. *The Stability of Motion*. Pergamon Press, New York.

Chopra, A.K., 2007. *Dynamics of Structures–Theory and Applications to Earthquake Engineering*. Pearson Prentice Hall, New Jersey.

Clough, R.W. and Penzien, J., 2003. *Dynamics of Structures*. Computers and Structures, Incorporated, Berkeley, CA.

Coppola, V.T., 1997. Perturbation methods for strongly nonlinear oscilltors using lie transforms. In Guran, A., editor, *Nonlinear Dynamics*, p. 24–59, London. World Scientific.

Cushing, J.M., 1977. *Integrodifferential Equations and Delay Models in Population Dynamics––Lecture Notes in Biomathematics*. Springer–Verlag, Berlin.

Debnath, L., 2003. Recent applications of fractional calculus to science and engineering. *International Journal of Mathematics and Mathematical Sciences*, **54**, 3413–3442.

Deng, J., Pandey, M.D., and Gu, D.S., 2009. Extreme quantile estimation from censored sample using partial cross-entropy and fractional partial probability weighted moments. *Structural Safety*, **31**(1), 43–54.

Deng, J. and Pandey, M.D., 2008. Estimation of the maximum entropy quantile function using fractional probability weighted moments. *Structural Safety*, **30**(4), 307–319.

Dimentberg, F.M., 1961. *Flexural Vibrations of Rotating Shafts*. Butterworths, London.

Findley, W.N., Lai, J.S., and Onaran, K., 1976. *Creep and Relaxation of Nonlinear Viscoelastic Materials with an Introduction to Linear Viscoelasticity*. North–Holland, New York.

Floris, C., 2011. Stochastic stability of a viscoelastic column axially loaded by a white noise force. *Mechanics Research Communications*, **38**, 57–61.

Glockle, W.G. and Nonnenmacher, T.F., 1991. Fractional integral operators and fox functions in the theory of viscoelasticity. *Macromolecules*, **24**(24), 6426–6434.

Glockle, W.G. and Nonnenmacher, T.F., 1994. Fractional relaxation and the time–temperature superposition principle. *Rheologica Acta*, **33**(4), 337–343.

Hagedorn, P., 1978. *Nonlinear Oscillations*. Akademishe Verlagsgesellschaft, Wiesbaden. Translated By Wolfram Stadler - 1981.

Herrmann, G., 1967. *Dynamic Stability of Structures: Proceedings of an International Conference*. Pergamon Press, New York.

Heymans, N. and Bauwens, J.C., 1994. Fractal rheological models and fractional differential equations for viscoelastic behavior. *Rheologica Acta*, **33**, 210–219.

Hijawi, M., Moshchuk, N., and Ibrahim, R.A., 1997. Unified second-order stochastic averaging approach. *Journal of Applied Mechanics*, **64**(2), 281–291.

Huang, Q., 2008. *Stochastic Stability of Viscoelastic Systems*. PhD thesis, University of Waterloo, Waterloo, Canada.

Huseyin, K., 1978. *Vibrations and Stability of Multiple Parameter Systems*. Noordhoff Internatioanl Publishing, Alphen Aan Den Rijn.

Ibrahim, R.A. and Soundararajan, A., 1983. Nonlinear parametric liquid sloshing under wide band random excitation. *Journal of Sound and Vibration*, **91**(1), 119–134.

Ibrahim, R.A., 1985. *Parametric Random Vibration*. Research Studies Press/John Wiley and Sons, New York.

Inman, D.J., 2006. *Vibration with Control*. John Wiley and Sons Ltd Press, New York.

Iwan, W.D. and Spanos, P.T.D., 1978. Response envelope statistics for nonlinear oscillators with random excitation. *Journal of Applied Mechanics*, **45**, 170–174.

Janevski, G., Kozic, P., and Pavlovic, R., 2012. Moment lyapunov exponents and stochastic stability of a thin-walled beam subjected to eccentric axial loads. *Journal Of Theoretical and Applied Mechanics*, **50**(1), 61–83.

Khasminskii, R.Z. and Moshchuk, N., 1998. Moment Lyapunov exponent and stability index for linear conservative system with small random perturbation. *SIAM Journal of Applied Mathematics*, **58**(1), 245–256.

Khasminskii, R.Z., 1966a. A limit theorem for the solutions of differential equations with random right–hand sides. *Theory of Probability and Its Applications*, **11**(3), 390–406. English translation.

Khasminskii, R.Z., 1966b. On stochastic processes defined by differential equations with a small parameter. *Theory of Probability and Its Applications*, **11**(2), 211–228. English translation.

Khasminskii, R.Z., 1967. Necessary and sufficient conditions for the asymptotic stability of linear stochastic systems. *Theory of Probability and Its Applications*, **12**, 144–147. English Translation.

Khasminskii, R.Z., 1980. *Stochastic Stability of Differential Equations*. Kluwer Academic Publishers, Norwell, MA.

Kilbas, A.A., Srivastava, H.M., and Trujillo, J.J., 2006. *Theory and Applications of Fractional Differential Equations*. Elsevier Inc., New York.

Kliemann, W. and Namachchivaya, N. Sri, 1995. *Nonlinear Dynamics and Stochastic Mechanics*. CRC Press, London.

Kliemann, W., 2008. Book review for "dynamic stability of structures". *SIAM Review*, **50**, 176–179.

Kloeden, P.E. and Platen, E., 1992. *Numerical Solution of Stochastic Differential Equations*. Springer-Verlag, Berlin.

Koh, C.G. and Kelly, J.M., 1990. Application of fractional derivatives to seismic analysis of base-isolated models. *Earthquake Engineering and Structural Dynamics*, **19**, 229–241.

Kozic, P., Pavlovic, R., and Rajkovic, P., 2007. Moment lyapunov exponents and stochastic stability of a parametrically excited oscillator. *Meccanica*, **42**, 323–330.

Larionov, G.S., 1969. Investigation of the vibration of relaxing systems by the averaging method. *Mechanics of Polymers*, **5**, 714–720. English translation.

Lingala, N., 2010. *Machine Tool Chatter Suppression Using Spindle Speed Variation*. PhD thesis, University of Illinois at Urbana-Champaign, Urbana, Illinois, USA.

Lin, Y.K. and Ariaratnam, S.T., 1980. Stability of bridge motion in turbulent winds. *Journal of Structural Mechanics, ASCE*, **8**(1), 1–15.

Lin, Y.K. and Cai, G.Q., 1995. *Probabilistic Structural Dynamics: Advanced Theory and Applications*. McGraw–Hill, New York.

Lin, Y.K. and Cai, G.Q., 2000. Some thoughts on averaging techniques in stochastic dynamics. *Probabilistic Engineering Mechanics*, **15**, 7–14.

Lin, Y.K. and Prussing, J.E., 1982. Concepts of stochastic stability in rotor dynamics. *Journal of American Helicopter Society*, **27**(2), 73–74.

Lin, Y.K. and Shih, T.Y., 1982. Vertical seismic load effect on building response. *Journal of Engineering Mechanics, ASCE*, **108**, 331–343.

Lyapunov, A. M., 1892. Problème Générale de la Stabilité du Mouvement. *Comm. Soc. Math. Kharkov*, **2**, 265–272. Reprinted in *Annals of Mathematical Studies*, VOL. 17, Princeton University Press, Princeton, 1947.

Mainardi, R., 2010. *Fractional Calculus and Waves in Linear Viscoelasticity: an Introduction to Mathematical Models*. Imperial College Press, London.

McDonald, R.J. and Namachchivaya, N.Sri., 2002. Parametric stabilization of a gyroscopic system. *Journal of Sound and Vibration*, **255**(4), 635–662.

Merkin, D.R., 1956. *Gyroscopic Systems*. State publishing house, Moscow. in Russian.

Mettler, E., 1966. Stability and vibration problems of mechanical systems under harmonic excitation. In Herrmann, G., editor, *Dynamic Stability of Structures*, 169–188, New York. Pergamon Press.

Mickens, R.E., 1981. *An Introduction to Nonlinear Oscillations*. Cambridge University Press, Cambridge.

Molchanov, S.A., 1998. The structure of eigenfunctions of one-dimensional unordered structurs. *Math. USSR Izvestija*, **12**, 69–101.

Nagata, W. and Namachchivaya, N. Sri, 1998. Bifurcations in gyroscopic systems with an application to rotating shafts. *Proceedings of Royal Society A: Mathematical, physical and engineering sciences*, **454**, 543–585.

Namachchivaya, N. Sri and Ariaratnam, S.T., 1987. Stochastically perturbed linear gyroscopic systems. *Mechanics of Structures and Machines*, **15**(3), 323–345.

Namachchivaya, N. Sri., Ramakrishnan, N., Roessel, H.J. Van, and Vedula, L., 2003. Stochastic stability of two coupled oscillators in resonance. In Namachchivaya, N. Sri and Lin, Y.K., editors, *IUTAM Symposium on Nonlinear Stochastic Dynamics*, p. 167–177, Netherlands. Klumer Academic Publisher.

Namachchivaya, N. Sri and Roessel, H.J. Van, 2001. Moment lyapunov exponent and stochastic stability of two coupled oscillators driven by real noise. *ASME Journal of Applied Mechanics*, **68**(6), 903–914.

Namachchivaya, N. Sri and Vedula, L., 2000. Stabilization of linear systems by noise: Application to flow induced oscillations. *Dynamics and Stability of Systems*, **15**(2), 185–208.

Naprstek, J., 1976. Solution of random vibrations of non-linear system by means of markov process. *Acta Tech. CSAK*, **21**, 302–345.

Nolan, V. and Namachchivaya, N.Sri., 1999. Almost-sure stability of linear gyroscopic systems. *Journal of Sound and Vibration*, **227**(1), 105–130.

Onu, K., 2010. *Stochastic Averaging for Mechanical Systems*. PhD thesis, University of Illinois at Urbana-Champaign, Urbana, Illinois, USA.

Oseledec, Y.I., 1968. A multiplicative ergodic theorem. Lyapunov characteristic number for dynamical systems. *Transactions of the Moscow Mathematical Society*, **19**, 197–231. English translation.

Pandey, M.D. and Ariaratnam, S.T., 1996. Crossing rate analysis of non-gaussian response of linear systems. *Journal of Engineering Mechanics*, **122**(6), 507–511.

Pandey, M.D. and Ariaratnam, S.T., 1998. Stability analysis of wind induced torsional motion of slender bridges. *Structural Safety*, **20**(4), 379–389.

Pandey, M.D. and Ariaratnam, S.T., 1999. Stochastic stability of lateral-torsional motion of slender bridges under turbulent wind. In Narayanan, S. and Iyengar, R.N., editors, *IUTAM Symposium on Nonlinearity and Stochastic Structural Dynamics*, 185–196, London. Kluwer Academic Publishers.

Paola, M. Di and Pirrotta, A., 2009. Fractional calculus application to viscoelastic solids. *Meccanica dei Materiali e delle Strutture*, **1**(2), 52–62.

Parszewski, Z.A., 1984. Principles of rotor system instability. In Mahrenholtz, O., editor, *Dynamics of Rotors—Stability and Stiffness Identification*, 65–88, New York. Springer-Verlag.

Parzen, E., 1999. *Stochastic Processes*. Holden Day, San Francisco.

Pfitzenreiter, T., 2004. A physical basis for fractional derivatives in constitutive equations. *ZAMM – Journal of Applied Mathematics and Mechanics*, **84**(4), 284–287.

Pfitzenreiter, T., 2008. Where do fractional derivatives in stress relations come from? a structural approach. *ZAMM – Journal of Applied Mathematics and Mechanics*, **88**(7), 540–551.

Podlubny, I., 1999. *Fractional Differential Equations*. Academic Press, San Diego.

Rand, R.H. and Armbruster, D., 1987. *Perturbation Methods, Bifurcation Theory and Computer Algebra*. Springer Verlag, New York.

Rand, R.H., 2012. *Lecture Notes on Nonlinear Vibrations*. The Internet-First University Press, http://ecommons.library.cornell.edu/handle/1813/28989.

Roberts, J.B. and Spanos, P.D., 1986. Stochastic averaging an approximate method of solving random vibration problems. *International Journal of Non-Linear Mechanics*, **21**(2), 111–134.

Robinson, J.C., 2005. A topological delay embedding theorem for infinite-dimensional dynamical systems. *Nonlinearity*, **18**, 2135–2143.

Rosenstein, M.T., Collins, J.J., and Luca, C.J. De, 1993. A practical method for calculating largest lyapunov exponents from small data sets. *Physica D*, **65**, 117–134.

Rouse, Jr. P.E., 1953. A theory of the linear viscoelastic properties of dilute solutions of coiling polymers. *Journal of Chemical Physics*, **21**(7), 1272–1280.

Sachdev, P.L., 1991. *Nonlinear Ordinary Differential Equations and Their Applications*. Chapman & Hall, New York.

Sanders, J.A. and Verhulst, F., 1985. *Averaging Methods in Nonlinear Dynamical Systems*. Springer–Verlag, New York.

Sato, S., M.Sano, and Sawada, Y., 1987. Practical methods of measuring the generalized and the largest lyapunov exponent in high dimensional chaotic systems. *Progress of Theoretical Physics*, **77**(1), 1–5.

Schmidt, A. and Gaul, L., 2006. On a critique of a numerical scheme for calculation of fractionally damped dynamical systems. *Mechanics Research Communications*, **33**, 99–107.

Shlesinger, M.F. and Swean, T., 1998. *Stochastically Excited Nonlinear Ocean Structures*. World Scientific Pub Co Inc, Singapore.

Stratonovich, R.L., 1963. *Topics in the Theory of Random Noise*, volume 1. Gordon and Breach Science Publishers, Inc, New York.

Stratonovich, R.L., 1967. *Topics in the Theory of Random Noise*, volume 2. Gordon and Breach Science Publishers, Inc, New York.

Takens, F., 1981. *Detecting strange attractors in turbulence*, volume 898. Lecture Notes in Mathematics.

Vedula, L. and Namachchivaya, N. Sri., 2002. Stochastic stability of linear gyroscopic systems: Application to pipes conveying fluid. In Maidment, D.R., editor, *Proceedings of the 5th International Symposium on Fluid Structure Interaction, Aeroelasticity, and Flow Induced Vibration and Noise, IMECE2002-39024*, p. 1233–1242, New York. American Society of Mechanical Engineers.

Vedula, L., 2005. *Dynamics and Stability of Parametrically Excited Gyroscopic Systems*. PhD thesis, University of Illinois at Urbana-Champaign, Illinois, USA.

Verhulst, F., 1996. *Nonlinear Differential Equations and Dynamical Systems*. Springer–Verlag, Berlin.

Wedig, W., 1988. Lyapunov exponent of stochastic systems and related bifurcation problems. In Ariaratnam, S. T., Schuëller, G. I., and Elishakoff, I., editors, *Stochastic Structural Dynamics---Progress in Theory and Applications*, p. 315–327. Elsevier Applied Science, London.

Wolf, A., Swift, J., Swinney, H., and Vastano, A., 1985. Determining Lyapunov exponents from a time series. *Physica D*, **16**, 285–317.

Wong, E. and Zakai, M., 1965. On the relation between ordinary and stochastic equations. *International Journal of Engineering Sciences*, **3**(2), 213–229.

Xie, W.C., 2005. Monte Carlo simulation of moment Lyapunov exponents. *ASME Journal of Applied Mechanics*, **72**(2), 269–275.

Xie, W.C., 2006. *Dynamic Stability of Structures*. Cambridge University Press.

Xie, W.C., 2010. *Differential Equations for Engineers*. Cambridge University Press.

Xu, Z. and Cheung, Y.K., 1994. Averaging method using generalized harmonic functions for strongly nonlinear oscillators. *Journal of Sound and Vibration*, **174**(4), 573–576.

Yin, M., 1991. *Lyapunov Exponents and Stochastic Stability of Linear Gyroscopic Systems*. PhD thesis, University of Waterloo, Waterloo, Canada.

Yuan, L. and Agrawal, O.P., 2002. A numerical scheme for dynamic systems containing fractional derivatives. *Journal of Vibration and Acoustics*, **124**, 321–324.

Zhu, W.Q., 1988. Stochastic averaging methods in random vibration. *Applied Mechanics Review*, **41**(5), 189–199.

Zhu, W.Q., 2003. *Nonlinear Stochastic Dynamics and Control: Framework of Hamilton Theories*. Science Press, Beijing, China.